FTD-HC-23-753-71

FOREIGN TECHNOLOGY DIVISION

PRELIMINARY DESIGN OF AN AIRCRAFT

by

B. T. Goroshchenko, A. A. D'yachenko,
and N. N. Fadeyev

402

Best
Available
Copy

UNCLASSIFIED
Security Classification

DOCUMENT CONTROL DATA - R & D

(Security classification of title, body of abstract and indexing annotation must be entered when the overall report is classified)

1. ORIGINATING ACTIVITY (Corporate author) Foreign Technology Division Air Force Systems Command U. S. Air Force	2a. REPORT SECURITY CLASSIFICATION UNCLASSIFIED 2b. GROUP

3. REPORT TITLE

PRELIMINARY DESIGN OF AN AIRCRAFT

4. DESCRIPTIVE NOTES (Type of report and inclusive dates)

Translation

5. AUTHOR(S) (First name, middle initial, last name)

Goroshchenko, B. T.; D'yachenko, A. A.; and Fadeyev, N. N.

6. REPORT DATE 1970	7a. TOTAL NO. OF PAGES 391	7b. NO. OF REFS 35
8a. CONTRACT OR GRANT NO. F33657-71-D-0057 b. PROJECT NO. AAH9 604020 c. d. DIA Task No. T71-04-03	9a. ORIGINATOR'S REPORT NUMBER(S) FTD-HC-23-753-71 9b. OTHER REPORT NO(S) (Any other numbers that may be assigned this report)	

10. DISTRIBUTION STATEMENT

Approved for public release; distribution unlimited.

11. SUPPLEMENTARY NOTES	12. SPONSORING MILITARY ACTIVITY Foreign Technology Division Wright-Patterson AFB, Ohio

13. ABSTRACT

The book sets forth the fundamentals of elaboration of technical specifications for a new aircraft design, problems of the influence of geometrical and other parameters of the aircraft on its flight characteristics and stability indices (together with methods for approximate calculation of these characteristics and indices), and also the principles of layout selection, determination of the basic weight, geometrical, and structural characteristics, over-all configuration, trim, and airframe development for the preliminary design stage. In addition, the book presents an example of the application of the basic principles of preliminary aircraft design. The book is designed for engineers working in the aviation industry and may be used by students and instructors at the advanced aeronautical colleges.

DD FORM 1 NOV 65 1473

UNCLASSIFIED
Security Classification

UNCLASSIFIED
Security Classification

14. KEY WORDS	LINK A ROLE	LINK A WT	LINK B ROLE	LINK B WT	LINK C ROLE	LINK C WT
Aircraft Design						
Aircraft Stability						
Aircraft Performance						
Aircraft Reliability						

UNCLASSIFIED
Security Classification

FTD-HC-23-753-71

EDITED TRANSLATION

PRELIMINARY DESIGN OF AN AIRCRAFT

By: B. T. Goroshchenko, A. A. D'yachenko
and N. N. Fadeyev

English pages: 391

Source: Eskiznoye Proyektirovaniye
Samoleta 1970, pp. 1-332

Translated under: F33657-71-D-0057

UR/0000-70-000-000

THIS TRANSLATION IS A RENDITION OF THE ORIGINAL FOREIGN TEXT WITHOUT ANY ANALYTICAL OR EDITORIAL COMMENT. STATEMENTS OR THEORIES ADVOCATED OR IMPLIED ARE THOSE OF THE SOURCE AND DO NOT NECESSARILY REFLECT THE POSITION OR OPINION OF THE FOREIGN TECHNOLOGY DIVISION.	PREPARED BY: TRANSLATION DIVISION FOREIGN TECHNOLOGY DIVISION WP-AFB, OHIO.

TABLE OF CONTENTS

PAGE

PART II. FLIGHT CHARACTERISTICS OF THE AIRCRAFT, ITS STABILITY, AND HOW THEY ARE INFLUENCED BY ITS PARAMETERS

PAGE

FOREWORD

Normally, regardless of application, an aircraft is a component of an aerosystem. This system includes, in addition to the aircraft, facilities for engineering-technical and airport maintenance, communications systems, manufacturer-customer liaison, etc.

At the same time, an aircraft is a complex aggregate of diversified elements that have been designed to perform various functions but in a manner conducive to successful performance of the aircraft's principal tasks. Among the basic components of an aircraft, we might mention the airframe (wings, fuselage, empennage), takeoff and landing gear (undercarriage, aerodynamic and gasdynamic high-lift devices), powerplant, fuel system, equipment (piloting and navigational, monitoring and measuring, communications, crew and passenger life support), and miscellaneous systems.

The process in which a modern airplane is created is complex and lengthy. This is explained by the need to tie the airplane in with the other parts of the aerosystem and by the complexity of the aforementioned components of the airplane.

The process of developing a modern airplane can be broken up into the following stages:

- research;
- design;
- building of prototypes;

– testing and debugging;

– placing in mass production.

In turn, design can be subdivided into the following steps:

– finding the optimum combination of parameters, as ultimately embodied in the technical specifications (TS);

– preliminary design of the aircraft;

– engineering design of the aircraft on the basis of the initial data obtained during the preliminary design stage.

The work usually involved in preliminary design of an aircraft is as follows:

– the layout of the airplane, determination of its relative geometrical parameters, and estimation of its aerodynamic characteristics;

– determination of the basic weight and geometrical characteristics of the airplane, compilation of a summary of weights on the basis of more exact weight formulas and data on the powerplant, equipment, and various systems;

– layout, trim, airframe development, and refinement of the airplane's geometry;

– calculation of the airplane's polar curves, estimation of $c_{y_{ldg}}$ and $c_{y_{tko}}$ and the initial coefficients for verifying the aircraft's stability and controllability;

– determination of the technical flight performance characteristics and the takeoff and landing properties of the aircraft;

– determination of the aircraft's stability and controllability characteristics;

– estimation of the aircraft's reliability and time between overhauls;

– calculation of the cost of manufacturing and operating the airplane;

– determination of the airplane's efficiency in performing various missions;

– determination of the technical requirements to be met in engineering design of the airplane's components and subassemblies.

Performance of a number of aspects of the preliminary design work on an airplane requires knowledge of the influence of the aircraft's parameters on its flight and weight characteristics and its stability and controllability indices.

As for such aspects of the preliminary design work as evaluation of cost, reliability, and time to overhaul, as well as calculation of the airplane's efficiency, they can be completed only in the first approximation.

Accordingly, the present book consists of three parts:

– elaboration of technical specifications for the new aircraft design;

– flight characteristics of the aircraft, its stability, and how they are influenced by its parameters.

– determination of the basic weight, geometrical, and structural characteristics of the new aircraft design.

Chapters 1, 2, 3, 10, 11, 12, 13, and §14.7 were written by N.N. Fadeyev, Chapters 4, 5, 6, 7, and 14 (except for §14.7) by B.T. Goroshchenko, and Chapters 8 and 9 by A.A. D'yachenko.

Although the book uses the MKfS system of units (GOST 7664-61), the kg (instead of the kgf-s^2/m) is used arbitrarily as a unit of mass to bring the notion of weight closer to the sense in which it is usually understood.

Reader comments on the book should be addressed to Moskva, B-66, 1-y Basmannyy per., 3, Izdatel'stvo "Mashinostroyeniye,"

Part One

ELABORATION OF TECHNICAL SPECIFICATIONS FOR THE NEW AIRCRAFT DESIGN

Chapter 1

BASIS FOR GENERAL REQUIREMENTS MADE OF THE NEW AIRCRAFT DESIGN

§1.1. GENERAL REQUIREMENTS MADE OF THE NEW AIRCRAFT DESIGN

The numerous requirements made of a new aircraft design can be boiled down to the following fundamental generalized requirements:

1. most complete performance of mission;

2. production adaptability of design;

3. high operational properties, including reliability and flight safety;

4. versatility;

5. low production cost.

The new aircraft design will conform most fully to its intended purpose with proper selection of a set of flight-engineering properties (cruising speed, altitude, and range, payload, and payload bulk, takeoff and landing characteristics, etc.), as well

as its geometrical parameters (wing aspect ratio, sweepback, landing-gear laycut and data, cabin and cargo-compartment dimensions, etc.).

To impart good production adaptability to a design means to plan it in such a way that it can be built as quickly and easily as possible [6].

In the design of a component or subassembly of a product as complex as an airplane, it is insufficient to pay attention only to facilitating the manufacture of the component or subassembly. The point is that since assembly is a highly time-consuming process in the manufacture of a complicated product, considerable complication of the production of the components themselves is generally accepted if final assembly can be greatly simplified as a result. This is also the origin of the interchangeability and manufacturing-precision requirements to which the components are subject, the need to provide for various "technological compensators" that facilitate assembly, and breakdown of the design into individual panels and "prefabs" that make it possible to expand the front of the assembly operations, etc.

The following most important factors influence selection of a technological process: 1) the construction cost of the new design; 2) the skilled-workforce requirement; 3) the time needed for construction and assimilation into mass production, etc.

Operational requirements are broad and varied. Here we set forth only some of the operational principles awareness of which may be very helpful to the aviation designer:

1) failure of any component, subassembly, or instrument must be "safe," i.e., it must not result in a catastrophe. Under this principle, the most critically important components and subassemblies have come to be duplicated on the aircraft and a wide variety of emergency and backup devices have been provided;

2) it must be made certain that components can be installed on the airplane in only a single correct position. This is

normally easy to accomplish;

3) a component should be designed for the worst possible service conditions, i.e., for work with inadequate lubrication or none at all, without inspection and maintenance, being knocked against and stepped upon, shaken, subjected to high and low temperatures, moisture, etc.;

4) provision must be made for possible deformation of the component during production and use in the course of welding, cold working (and the associated internal stressing), temperature change, applied stresses, and the component's own weight.

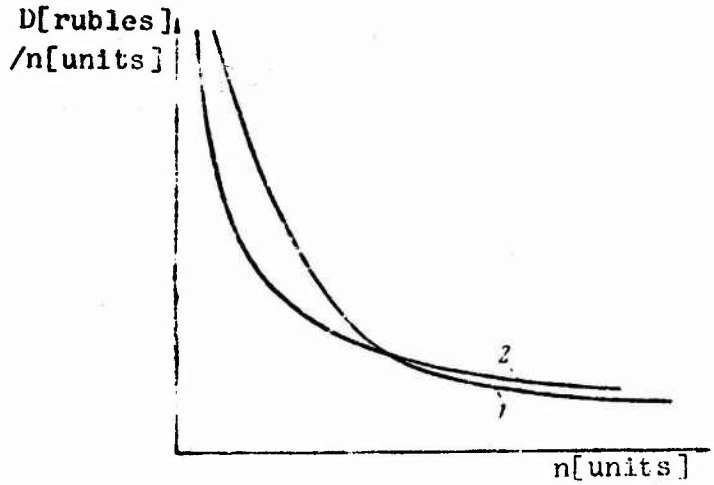

Figure 1.1. Influence of production scale on cost per unit.

The versatility (combination of functions) principle has always been applied to one degree or another at various stages in the development of civil aviation. At the present time, owing to the broader range of problems in aviation and the increasing complexity and cost of aircraft, a great deal of attention must be devoted to this principle.

Application of the versatility principle to components is even more profitable.

A component that performs several functions is usually found to be lighter in weight and simpler to produce than a set of separate components that perform the same functions. An example of versatility is found in any multiple-needle indicator, which is easier to make, requires less installation work, and occupies less space on the instrument panel than the set of single-needle indicators that it replaces.

Lowering the production cost of aircraft is one of the important design problems. Very often, other conditions the same, the selection of the optimum design of a component or part is dictated by its cost. To determine the cost of a given version of a component, the designer must have at hand reference tables giving the costs of various materials, semifinished products, and various machining methods [2]. It is also necessary to have at least a rough idea of the number of identical products to be made. The more there are of these products, the cheaper will each of them become (Fig. 1.1). The reason why this law applies for the design as a whole and for its individual components is that the cost of tooling (equipment) per unit product represents a large fraction when a small number are produced and a smaller one when more are produced. The curve makes an asymptotic approach to the cost of labor alone. As we see from Fig. 1.1, use of more expensive but more productive tooling (curve 1) in a short run increases product cost, but when the run is lengthened to include a certain number, it lowers unit cost (curve 2).

§1.2. CONTRADICTIONS BETWEEN REQUIREMENTS

The groups of requirements enumerated above frequently contradict one another. Thus, contradictions may be noted between technological and operational requirements and between versatility and specializaton of the aircraft. Essentially, the contradiction between technological and operational requirements consists in the fact that improvement of the production adaptability of the design may result in deterioration of the airplane's operational properties. The contradiction between the need for

versatility in the airplane and its specialization consists in the following. On the one hand, the more versatile the airplane, the less proficiently does it perform each of its specific tasks, but, on the other hand, if it is possible to create an airplane that, in addition to its basic function, finds numerous uses in other branches of the economy, the economy of the aircraft is improved substantially, since the larger production scale lowers the unit cost of the airplane and increases the utilization factor of each copy.

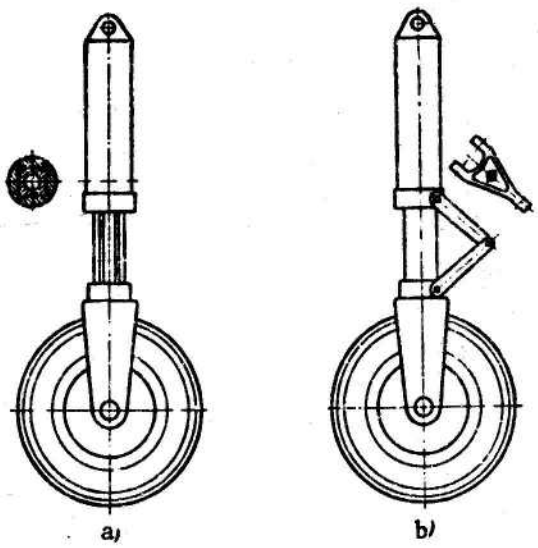

Figure 1.2. Landing-gear strut. 1) with spline; b) with torque arms.

There are also contradictions between the requirements pertaining to specific properties and characteristics in each group.

Examples of such contradictions are those between the requirements for longer times to overhaul and lower aircraft weight, for increased strength margin in a component and lower weight of the component, for increased top speed and lowered landing speed, for reduced relative weight of the wing structure and reduced drag of this structure, etc.

Because of these contradictions, no single requirement can be met to the maximum. In drawing up the technical specifications,

it is necessary to satisfy each requirement in a measure such that the contradictions are resolved and such that meeting the requirements of the set in the stated ranges will optimize the design.

On occasion, a designer will find a design solution that satisfies several contradictory requirements nicely. In such cases, this solution will obviously be the one adopted, provided that it does not stand in contradiction to some still more important requirement.

Figure 1.3. Landing flap.

A fortunate solution of this type is found in the landing gear strut shock-absorber torque arm (Fig. 1.2). At a given strength, it offers the following advantage over the spline: 1) lower weight; 2) greater simplicity of manufacture, and 3) higher operational reliability.

However, design simplification is not always sufficient basis for adopting a given solution. Thus, in spite of their simpler design, lighter weight, and high reliability, the wing landing flaps shown in Fig. 1.3 are less efficient than slotted and extension wing flaps, and use of the latter may be more sound from the standpoint of improving the airplane's takeoff and landing properties; this is confirmed by recent aeronautical engineering practice. However, it is by no means always possible to find such successful solutions.

As a rule, recourse must be taken to various expedients to resolve the contradictions.

§1.3. PROCEDURES FOR RESOLVING CONTRADICTIONS [4]

We now consider a number of procedures that the designer uses to make it easier to find optimum solutions.

1. One widely used procedure is to list the requirements made of the new design in order of their importance for the particular case [2]. In elaborating the design, an effort is made to satisfy the first, most important requirement most fully, then the second, and so forth.

An example in which this expedient is applied can be found in resolution of the contradiction between the effort to lighten the aircraft and at the same time lower its frontal drag. During the development of the high-speed airplane, this contradiction was usually resolved in favor of aerodynamic shapes with acceptance of a weight penalty. Progress moved from biplanes with struts and bracing wires and braced and semicantilever monoplanes to the cantilever wing with its thick profile, to the closed cockpit, landing-gear spats, retractable landing gear, then to the even thinner swept wing, etc.

This procedure does not help the designer extricate himself from the case – for example – in which the version that satisfies the first requirement best is inferior to other versions as regards meeting the second, third, and other requirements. In such cases, it is always possible that the designer will abandon the first variant in order not to sacrifice other secondary but numerous requirements. Note should be taken of the subjectivity inherent in this method when priorities are assigned to the requirements. If priorities are established not by the designer himself, but by his customer, the designer's task is easier, but this does not eliminate the subjectivity of the approach, since it now originates from the customer.

If the specified limits on the values of various properties are difficult to meet, it is possible that no design variant will be found in which all properties are within the specified limits,

i.e., the problem is either totally unsolvable at this time or can be solved only on the basis of a new invention or discovery.

A major invention that results in technological advance usually comes about in one of two ways: either it proceeds from a new discovery that establishes hitherto unknown relationships, or it is obtained as a result of long-term laboratory research, sometimes after many failures.

In either case, such inventions usually originate in the scientific research institutes or in other organizations with competent laboratory staffs; only in rare cases are they the result of the activity of a single inventor.

Before it is incorporated into a new design, any new invention must be checked out carefully by calculation and experiment.

Excessive promotion of inventions and the effort to invent regardless of cost, to the neglect of available experience, cannot produce good results, since too many experimental and untried elements in a prototype will lower its reliability, require increased time for testing, and may even result in total failure, despite the fundamental validity of the new ideas.

2. Another procedure for arriving at the optimum combination of properties and characteristics in the new aircraft design is to find a criterion for unifying them.

Different criteria may be selected depending on the nature of the problem.

If the contradiction between two properties stems from the fact that a change in one property will have a favorable influence on a third, more important property, while the second property changes in such a way as to change this third property in an undesirable direction, the third property becomes the criterion by means of which the contradiction can be resolved. We select the variant with the poorest value of the third property and find the optimum solution, provided that no other important properties deteriorate as a result. For example, when the

production process is made easier to the detriment of flight or operational properties, the optimum design variant may be found with the aid of a criterion that blends these properties and production adaptability. This criterion will necessarily be one of economy.

Let us examine a few examples in which this procedure is applied.

Example 1. Specific strength of material per unit weight. In selecting the material for a certain stress component that we wish to make as light as possible, it is usually found that a material with a higher strength couples this with higher specific weight. This contradiction can be resolved by selecting a material that minimizes the weight of the component at a given strength. For example, the weight of a rod of length l that must withstand a tensile force P can be expressed by the formula

$$G=\gamma Fl=\frac{\gamma}{\sigma}Pl, \tag{1.1}$$

where F is the cross sectional area of the rod and γ and σ are the specific weight and breaking stress of the material, respectively.

As we see, the weight of the rod is inversely proportional to the specific strength of the material per unit weight σ/γ; for tension, this quantity is also known as the "breaking length," since for a length $l = l_b = \sigma/\gamma$ we obtain $G = P$, i.e., the rod breaks under its own weight. If γ is in g/cm^3 and σ in kgf/mm^2, we obtain l_b in kilometers. By selecting materials on the basis of maximum specific strength per unit weight, we can, in many cases, minimize the weight of the component without detriment to strength, i.e., resolve the contradiction from the standpoint of minimum weight.

Example 2. Aviation weight* of component with respect to V_{max} [5]. It is known that a component having weight and frontal drag

*Translator's Note: This designates the weight divided by the area. See definition, page 11.

influences the top speed of an airplane through both of these properties, and that the relative decrease in V_{max} due to the presence of the component of the airplane can be expressed by the formula

$$\frac{\Delta V_{max}}{V_{max}} = -\frac{1}{\frac{3}{2}\frac{c_x \pi \lambda_{эф}}{c_y^2} - 2 - \frac{1}{2G}\left(\frac{dN_p}{dV}\right)\frac{\pi\lambda_{эф}}{c_y}} \cdot \frac{G_{a.c}}{G}, \tag{1.2}$$

where dN_a/dV is the speed derivative of the available power (in kg). Substituting $N_a = P \cdot V$ and

$$\frac{dN_p}{dV} = \frac{dP}{dV}V + P = \frac{dP}{dV}V + G\frac{c_x}{c_y},$$

we obtain the same formula for a jet aircraft:

$$\frac{\Delta V_{max}}{V_{max}} = -\frac{1}{\frac{c_x \pi \lambda_{эф}}{c_y^2} - 2 - \frac{1}{2G}\left(\frac{dP}{dV}V\right)\frac{\pi\lambda_{эф}}{c_y}} \cdot \frac{G_{a.c}}{G}, \tag{1.3}$$

where $G_{a.c}$ is the aviation weight of the component. It is known that

$$G_{a.c} = \Delta G + \frac{dc_y}{dc_x}\Delta Q. \tag{1.4}$$

Consequently, the speed loss resulting from the presence of a component with weight ΔG and frontal drag ΔQ on the airplane is proportional to the aviation weight of the component, which consists of the weight of the component and an increment proportional to its frontal drag.

Thus, the optimum variant of the component will be that which gives the smallest decrease $\Delta V_{max}/V_{max}$ or the lowest aviation weight, and selection of this version resolves the contradiction between weight and frontal drag from the standpoint of V_{max}. Similar expressions can be derived for the increment of any flight property, along with the corresponding expressions for the aviation weight.

Another definition of aviation weight proceeds from (1.2) and (1.4): the aviation weight of a component with frontal drag is the weight that the airplane could carry without any change in the given flight property if the component were removed.

The coefficient $dc_y/dc_x = \pi\lambda_{ef}/2c_y$ of the component's frontal drag ΔQ at V_{max} is so large that the aviation weight increment usually greatly exceeds the weight of the component; this explains the previously noted trend to more streamlined shapes at the expense of a weight penalty in the development of the high-speed airplane.

It must be remembered that a selection based on the aviation weight derived for a given flight property resolves contradictions only from the standpoint of this property, and will not be optimal with respect to other properties; further, for example, a selection based on V_{max} will increase the weight of tha airplane to the detriment of its takeoff and landing properties.

In the above examples, contradictory properties are unified in derived quantities – specific strength per unit weight and aviation weight – quite soundly, i.e., component weight is inversely proportional to specific strength per unit weight and the change in the flight property is proportional to aviation weight. Derived quantities are sometimes devised artificially to unify two contradictory quantities, e.g.. their product may be used when it is desired to maximize both of them (for example, the product LV combines range and speed).

If it is desirable to have one of the contradictory properties as small as possible, their ratio is taken; an example is the "speed range"

$$V_{max}\frac{1}{V_{min}} = \frac{V_{max}}{V_{min}}.$$

Combination of contradictory quantities in the form of their product implies that equal relative increments of the two are equivalent, since these relative increments result in equal relative increases in the product.

Let us now compare two relative indicators: specific strength per unit weight σ/γ and the speed range V_{max}/V_{min}. The former proceeds logically from the need to minimize the weight of the rod under tension, while we have justified the latter only in terms of the desirability of maximizing V_{max} and minimizing V_{min}; consequently, the indicator V_{max}/V_{min} will not give a reliable evaluation of the airplane in terms of these two properties. For a relative index of the form A/B to serve as an accurate criterion in evaluating the product with respect to properties A and B, it is necessary to resort to some more general requirement to prove the equivalence of a relative n-fold increase of A to a relative, also n-fold, decrease of B. Relative indicators of many kinds are used extensively both in design work and in operation of the final products, e.g., the efficiency

$$\eta = \frac{N_{useful}}{N_{consumed}},$$

the unit production cost b = B/N, the profit per ruble of investment p = P/D, productivity per machine tool N/n, etc. When such indicators are used, it is necessary to know definitely whether the indicator in question is accurately based on more general requirements and starting specifications or serves merely as an approximate criterion for evaluating the product with respect to the two contradictory quantities composing it.

Obviously, the larger the number of requirements that can be unified into a single more general criterion, the more fully will the contradictions have been resolved. We noted above that equivalence of <u>equal relative</u> increments of two contradictory properties can be expressed by the product of these two properties. This procedure can also be extended to equivalence of <u>unequal relative</u> increments, and not only of two, but of <u>any number</u> of contradictory properties.

If we know that the relative increments a, b, c, ... of the properties A, B, C, ... of the new design are equivalent, the product

$$K = A^{\frac{1}{a}} \cdot B^{\frac{1}{b}} \cdot C^{\frac{1}{c}} \ldots \tag{1.5}$$

can serve as a criterion that unifies all of these properties.

To prove the validity of this statement, it is sufficient to take logarithms in (1.5), differentiate, and convert from differentials to finite increments:

$$\ln K = \frac{1}{a} \ln A + \frac{1}{b} \ln B + \frac{1}{c} \ln C + \ldots$$

$$\frac{dK}{K} = \frac{1}{a} \frac{dA}{A} + \frac{1}{b} \frac{dB}{B} + \frac{1}{c} \frac{dC}{C} + \ldots$$

$$\frac{\Delta K}{K} = \frac{1}{a} \frac{\Delta A}{A} + \frac{1}{b} \frac{\Delta B}{B} + \frac{1}{c} \frac{\Delta C}{C} + \ldots$$

It is clear from the last expression that each of the equivalent relative increments

$\Delta A/A$ = a of property A

$\Delta B/B$ = b of property B

$\Delta C/C$ = c of property C

. . . . . .

gives the same relative increment of the criterion K, namely $\Delta K/K = 1$. Specific strength per unit weight is a particular case of this criterion.

Let us now examine a criterion that expresses equivalence not of relative, but of absolute increments.

If it is known that the absolute increments ΔA, ΔB, ΔC, ... of properties A, B, C, ... of the new design are equivalent, the abstract polynomial

$$K = \frac{A}{\Delta A} + \frac{B}{\Delta B} + \frac{C}{\Delta C} + \ldots \tag{1.6}$$

or the "reduced quantities" that are proportional to it

$$\left.\begin{aligned} A_{пр} &= K \cdot \Delta A = A + \frac{\Delta A}{\Delta B} B + \frac{\Delta A}{\Delta C} C + \ldots, \\ B_{пр} &= K \cdot \Delta B = B + \frac{\Delta B}{\Delta A} A + \frac{\Delta B}{\Delta C} C + \ldots \end{aligned}\right\} \tag{1.7}$$

$$C_{np} \quad K \cdot \Delta C = C + \frac{\Delta C}{\Delta A} A + \frac{\Delta C}{\Delta B} B + \ldots \Big\} \qquad (1.7) \text{ Cont'd.)}$$

can serve as a criterion that unifies all these properties.

Aviation weight is a particular example of this approach.

Let us consider one more example in which this procedure is applied.(1) An increase can be obtained in the speed of an aircraft with no change in load per square meter ($p = G/S = \text{const}$) by increasing engine power. Since powerplant weight per horsepower is approximately constant, increasing the power with $p = \text{const}$ results in increased flight weight and wing area. Let us suppose that calculations of this kind made for existing aircraft of the same class have shown that they all have

$$\frac{dG}{dV_{max}} = C \approx \text{cons}. \qquad (1.8)$$

while retaining their true loads per square meter.

This means that the aircraft dimensions settled upon in practice are such that a 1 km/h speed increment is bought at the cost of a C-kilogram increase in flight weight, i.e., practice itself has established equivalence of a 1-km/h speed <u>increase</u> to a C-kg <u>decrease</u> in flight weight.

Then, having a family of $G = f(V_{max})$ curves for a new aircraft design of the same class, e.g., for various $G/S = \text{const}$ (Fig. 1.4), we can find points on these curves that correspond to condition (1.8); obviously, these will be the points of tangency of straight lines drawn at an angle arc tan C to the V_{max} axis.

Using the above method, this equivalence of ΔG and ΔV_{max} can be expressed by the criterion

$$K = \frac{G}{-C} + \frac{V_{max}}{1}.$$

Footnote (1) appears on page 16.

This quantity might be referred to as the "reduced speed:"

$$V_{max_{np}} = V_{max} - \frac{G}{C}. \qquad (1.9)$$

From the maximum of this quantity, or from the minimum of the proportional "reduced weight"

$$G_{np} = -KC = G - CV_{max} \qquad (1.9')$$

Figure 1.4. Influence of speed on takeoff weight.

we can find a variant that resolves the contradiction between V_{max} and G provided that it is certain that a 1-km/h speed increment is equivalent to a weight reduction of C kilograms.

As we noted above, use of criteria of this kind requires knowledge of the equivalent values of either the relative or the absolute increments of the various properties. This investigation requires analysis of more general criteria. When the equivalence condition is not satisfied, the optimum combination of the contradictory properties and parameters is selected on the basis of a more general criterion linking these properties. Thus, the problem is reduced to one of finding general criteria. This will form the content of the next two chapters.

FOOTNOTE

Manuscript Page No.	
14	(1) Borrowed from Ye. I. Kolosov.

Chapter 2

GENERAL PREMISES FOR CRITERION USED IN EVALUATING A NEW AIRCRAFT DESIGN

§2.1. CONDITIONS FOR FINDING OPTIMUM VERSION OF DESIGN. GENERAL REQUIREMENTS FOR CRITERION FOR EVALUATION OF NEW AIRCRAFT DESIGN

In §1.3, we pointed out the need for use of a criterion that unifies the particular requirements made of the new aircraft design and its parameters in order to arrive at the optimum technical requirements for the design.

In addition, it is necessary to find limiting relationships among the pr perties and parameters of the airplane. These relationships may be determined by the real construction and use conditions of the airplane, the level of technology, and physical relationships. Given a criterion and all possible limiting relations between the airplane's properties and parameters, the following optimality condition can be formulated for the technical requirements: those technical requirements and parameters that ensure the extreme (minimum or maximum) value of the criterion with observance of the limiting relations will be optimal.

The criterion must be quantitative and express objectively the degree to which the airplane, in the particular version, serves its purpose, and it is necessary to know how the criterion depends on all of the design variables that influence it.

Since there are many variables and the criterion depends on them in a complex manner, the method used to find the optimum parameters must be such as to establish an absolute extreme of the criterion and not simply relative ones.

When it is remembered that the performance of a complicated object is influenced by an enormous number of variables and that many of these variables are interrelated in rather complex fashion, the task of finding the optimum design appears impossible. In practice, however, the work is made easier by investigating at first only the effects of the basic variables and also by the fact that many of them, including important ones, are found to be constant under the conditions of the particular assignment. In aircraft design, constant assigned quantities of this type might be, for example:

1) all engine characteristics if the engine is specified;

2) the strength according to the "Strength Norms";

3) landing speed for an airplane whose weight changes little during flight;

4) takeoff run for an aircraft with a large change in weight during flight, etc.

Those quantities whose quantitative influence on the adopted criterion cannot be determined may also be assumed constant. In consideration of the effect of comfort on the criterion, an example of this may be found in the condition of constant percentage weight of passenger equipment and space per passenger; this corresponds approximately to the condition of constant degree of comfort.

§2.2. THE GENERAL CRITERION

In many cases, the basic advantage, to be derived in the new aircraft design, is subject to quantative evaluation in terms of its "production" during a definite time span.

The development and operation of any airplane has an inevitable negative effect in the form of materials and live labor over the same period, the full variety of which can be expressed by a single indicator – the cost B expressed, for example, in rubles/year.

To add these two effects algebraically, the positive effects A must also be expressed in rubles/year. This is possible if there is a monetary equivalent a [rubles/ton-kilometer] for the unit annual production N [ton-kilometers/year]. For a transport aircraft, the average tariff for a one-ton-kilometer haul is such an equivalent. Then the positive effect A = Na [rubles/year] and the criterion K assume the form

$$K=A-B. \tag{2.1}$$

Thus, the criterion for design of a transport aircraft becomes

$$K=A-B=Na-B=P. \tag{2.2}$$

i.e., the familiar annual profit.

In addition to the two basic effects A and B, the general criterion also covers other effects with their signs if these effects admit of evaluation in rubles/year.

One of the additional effects that makes its appearance in the case of any capital outlay is the influence of this investment on the rest of the economy. The annual total of a country's capital investments is determined by its balanced budget, and an investment of D rubles for the construction of a given objective diverts this amount from the remainder of the economy. Thus, this one-time capital investment of D rubles results in annual losses to the remainder of the economy amounting to $p_{av}D$ rubles/year, where p_{av} is the average profit per ruble of investment in the entire national economy or that branch of it from which the amount is drawn. From the government's standpoint, the amount $p_{av}D$ must appear in the form of an additional minus term in the evaluation criterion for the project:

$$K = P - p_{cp} \cdot D = A - B - p_{cp}D = Na - B - p_{cp}D. \tag{2.3}$$

Thus, the cost of manufacturing the new aircraft appears twice in its criterion: the total of expenses B includes the cost of material wear and tear (depreciation) and, in addition, the loss $p_{av}D$ to the country's national economy. This must be taken into account in comparing different versions of aircraft.

Let us consider such an example. Two versions have been drafted for an airline to carry N ton-kilometers/year at the same annual profit P [rubles/year], but the second variant requires a larger capital investment. This might occur if, for example, the more expensive hardware of the second version has a service life that is longer by exactly enough so that the depreciation and all costs B and the profit P remain the same as in the first version. If judged on the basis of profit P, the two versions are equivalent. In actuality, however, the first version is superior because it gives an additional capital-investment economy, as reflected by the criterion

$$K = P - p_{cp}D.$$

The amount $p_{av}D$ [rubles/year] is sometimes called the "construction cost." Placing a completed plant in operation also requires a simultaneous investment of working capital. This capital must be added to the cost of construction, with the assumption that the sum D also includes the working capital; then $p_{av}D$ may be referred to as the "construction and start-up cost."

Another additional term in the criterion will be considered in Chapter 3.

In selecting the optimum version of a design on the basis of maximum criterion K, the conditions set forth in the plan under which the particular objective is being designed must also be observed. Such conditions include the capital investment D allocated for construction and commissioning of these objectives and their total annual product N. Two particular cases are possible:

1. D = const and N_{max}. 2. N = const and D_{min}.

Let us examine the general criterion more closely for the case in which only one element – a new airplane for an existing airline – is being designed, and not the entire carrier. The same expression for K will serve as the criterion for evaluating the aircraft-pool variants:

$$K=P-p_{cp}D=Na-B-p_{cp}D,$$

but the constant elements that are independent of changes in the airplane can be dropped from the sum B and D; B will now represent the annual costs that depend on the airplane, and D the cost of the entire aircraft pool on the line. Let us consider the first particular case, when a fixed total capital investment D = const is allocated for the line's entire aircraft pool. When the constant term $p_{av}D$ can be dropped from the criterion, leaving the annual profit P = Na - B, i.e.,

$$K=P_{(D=\text{const})}=P_1\cdot n,$$

where $P_1 = N_1a - B_1$ is the annual profit per airplane and n is the number of airplanes on the line. Since $n = D/D_1$, where D_1 is the cost of one airplane, we have

$$K=\frac{P_1}{D_1}D.$$

Since D = const we may take as our criterion in this case

$$K=p=\frac{P_1}{D_1}=\frac{N_1a-B_1}{D_1}, \qquad (2.4)$$

i.e., the profit per ruble invested. Economists have also suggested that this quantity be used as an effectiveness factor for capital investments in new technology [15]. The "1" subscripts can be dropped, since it makes no difference whether the quantities N, B, and D are considered per unit or for the entire pool.

We obtain the second particular case if a constant annual cargo volume is specified for the line. In this case, the first term in our expression for the criterion will be Na = const and

can be dropped. The criterion becomes negative, assuming the form

$$K = B' = B + p_{cp}D,$$

i.e., the criterion is now the annual cost B', in which the on-line expenses B are added to the "construction and start-up" costs $p_{av}D$. Reasoning analogous to that used in the first case endows the criterion B' with the form

$$B' = \frac{B_1'}{N_1} N,$$

but since N = const, the ratio

$$b' = \frac{B_1'}{N_1} = \frac{B'}{N}. \qquad (2.5)$$

can serve as the criterion. Here the "1" subscripts have been omitted for the same reasons as in the first example.

The quantity b' is the first cost per unit product, and this indicator is also used frequently to evaluate the effectiveness of the airline or airplane. It is only necessary to remember that the construction and start-up costs $p_{av}D$ should also be included in the cost B' to obtain a more complete evaluation.

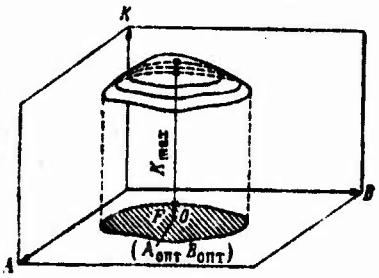

Figure 2.1. Region of near-optimum solutions.

It is clear from these two examples that criteria in the form of the ratios p = P/D and b' = = B'/N are quite correct for evaluation of a given aircraft if for the complex consisting of these aircraft we omit the fixed sum D = const (criterion p) or have a prescribed fixed annual production volume N = const (criterion b').

It must be remembered that it is not possible in all cases to estimate the basic positive effect in the same units as are used for the negative effect; in this case, reducing to equal conditions N = const, we obtain a criterion in the form of the "net cost per unit production" and

the variant selected will be optimum only for this particular condition. Certain properties do not admit of inclusion in the general criterion at all; examples are the political significance of the new design, the defense value of a nonmilitary design, the conservation or depletion of "uncharged" natural resources, comfort, aesthetic qualities, etc. In this case, there is no reason to abandon the attempt to evaluate the project on the basis of a general criterion, but the selection must be "biased" away from the criterion-optimum variant in the direction of support for properties not incorporated in the criterion. Such selection will inevitably be subjective and less precise. If, for example, the influence of the smoothly varying quantities A and B on the criterion adopted for evaluation of the objective is analyzed (Fig. 2.1), there is usually a rather extensive zone F in which the criterion K differs little from its extreme value in the neighborhood of the optimum parameter values (point O). If it was not possible to include certain important properties in the criterion K, it is advantageous in the final selection of A and B to move away from point O into the region of zone F in which the values of the imponderable properties of the objective are more favorable. Considerations involving proposed future modifications of the objective may also dictate regression from the optimum in one or another direction.

In the design of smaller parts and components, the criterion may be the increment to the total criterion that results from the presence of the particular part or component, and will be a function only of the properties of the component.

Suppose, for example, that the criterion K is a function of n variable properties of the object:

$$K=f(A, B, C \ldots N),$$

and that each part of the design influences only l of these properties, i.e., properties A, B, C, ..., L.

We write the total differential of the criterion K with respect to the 3 variables and convert from the differentials to finite increments:

$$dK=\frac{\partial K}{\partial A}dA+\frac{\partial K}{\partial B}dB+\frac{\partial K}{\partial C}dC+\ldots\frac{\partial K}{\partial L}dL;$$

$$\Delta K=\frac{\partial K}{\partial A}\Delta A+\frac{\partial K}{\partial B}\Delta B+\frac{\partial K}{\partial C}\Delta C+\ldots\frac{\partial K}{\partial L}\Delta L. \qquad (2.6)$$

In this case, the quantity ΔK can be used as a criterion for small parts. Here the partial derivatives become constant coefficients and ΔA, ΔB, ΔC, ..., ΔL become the changes in the properties of the objective resulting from the presence of the components in question.

On an airplane, for example, each part performs its function and, in addition, has a weight ΔG and a cost ΔD. If variants of a part that perform their functions equally well (have equal "functional qualities") are compared, there remains as the criterion the binomial

$$\Delta K=\frac{\partial K}{\partial G}\Delta G+\frac{\partial K}{\partial D}\Delta D.$$

If each designer has such a polynomial criterion at his disposal for selection of optimum part variants, the efforts of the entire designer staff will be oriented to acquisition of the optimum design variant.

Chapter 3

EVALUATION CRITERION FOR CIVIL AIRCRAFT

§3.1. SPEED AS "QUALITY" IN HAULING

It was shown in §2.2 that a carrier can be evaluated on the basis of its gross revenue with allowance for "construction and start-up costs" $p_{av}D$:

$$K = Na - B - p_{cp}D.$$

Let us now show that, as applied to hauling, the criterion must include another term that takes account of speed as "quality" in hauling operations.

Let a load of value K in rubles/ton belonging to an enterprise with a profit margin p_{en}[%] be hauled by a carrier at the average commercial speed V_{com} [km/h]. If one ton of such cargo remained en route for one year, it would be out of circulation for a year; similarly, storage of the cargo in a warehouse would result in a loss

$$\frac{p_{пр}\ \%}{100} \cdot K \ \frac{\text{rubles}}{\text{ton} \cdot \text{yr}}.$$

The loss incurred when the ton of cargo spends one hour en route is

$$c = \frac{K p_{пр}}{100 \cdot 365 \cdot 24} = \frac{K p_{пр}}{876\,000} \ \frac{\text{rubles}}{\text{ton} \cdot \text{yr}}, \qquad (3.1)$$

where p_{en} is in percent.

For a passenger, the coefficient C can be determined as follows:

$$C=\frac{E\cdot 12}{365\cdot 24}\cdot\frac{B_{з.п}+P}{B_{з.п}}=\frac{E}{730}\left(1+\frac{P}{B_{з.п}}\right)\frac{\text{rubles}}{\text{passenger}\cdot\text{hr}}, \qquad (3.2)$$

where E [rubles/month] is the passenger's monthly salary.

Here the factor in parentheses reflects the fact that each hour spent on the job creates value greater than the passenger's pay by the value of his production; for complete evaluation of the passenger's time, therefore, his salary must be increased by his employer's annual profit P divided by his salary B_{sal}.

Let us assume that the passenger and his baggage weigh

$$G_{pas} = 100 \text{ kg};$$

then

$$c=\frac{C}{0,1}=\frac{E_{гас}}{73}\left(1+\frac{P}{B_{з.п}}\right). \qquad (3.3)$$

The cargo or passenger spends a time $1/V_{com}$ [h/km] on each kilometer traveled and, consequently, the loss per ton-kilometer is c/V_{com} [rubles/ton-km] or, in one year,

$$N\frac{c}{V_{ком}}\ \frac{\text{ruble}}{\text{yr}},$$

where c is determined as the average for the cargo quota of the line in question.

This is the negative term that must be added to the criterion of a transport airplane to take account of speed as hauling-performance quality; then the general criterion takes the form

$$K=Na-B-p_{ср}D\cdot N\frac{c}{V_{ком}}. \qquad (3.4)$$

where $p_{av}\cdot D = B_{a.p}$.

Evaluation of cargo time en route was proposed by Prof. M.M. Protod'yakonov for selection of optimum railway routes [16]. As concerns evaluation of passenger time en route, it is encountered in the foreign literature.

The numerical value of the coefficient C for passengers and cargo can be estimated as follows.

Let us assume

$$\frac{P}{R_{з.п}}=0{,}75,$$

then

$$C=\frac{E}{73}\cdot 1{,}75=0{,}024E;$$

for

$$E=200\,\frac{\text{rubles}}{\text{month}}\quad C=0{,}024\cdot 200=4{,}8\,\frac{\text{rubles}}{\text{ton}\cdot\text{hr}}.$$

Let us now see how much one ton of cargo belonging to an enterprise operating with a profit margin of 6% must be worth for the coefficient C for the cargo to have the same value:

$$K=\frac{4{,}8\cdot 876\,000}{6}=700\,800\,\frac{\text{rubles}}{\text{т}}\approx 700\,\frac{\text{rubles}}{\text{kg}}.$$

Obviously, it will seldom be necessary to convey such expensive cargo by air, while passengers earning 200 rubles per month will be quite common.

This does not, of course, imply that air cargo is unprofitable; after all, Nc/V_{com} is only a small correcting term to the annual outlay, and the question of advantage depends on the entire criterion.

The correcting term Nc/V_{com} removes a certain element of fetishism from the notion of transport speed and permits more comprehensive and objective evaluation of the importance of speed.

This evaluation of speed does not apply to emergencies in which speed of delivery is of prime importance. Such cases also

require special delivery, e.g., by "mercy flight" for emergency medical assistance, or perhaps even a helicopter, which, although it is slower than an airplane, is not as restricted in its choice of landing sites, so that the time to move a patient by automobile is improved upon.

§3.2. AIR ROUTE EVALUATION CRITERION

To obtain an expanded expression for this criterion, an expression for the capital investment D [rubles] for the annual product N [ton-km/year] of the air route and the annual operating cost B [rubles/year] must be substituted into formula (3.4).

The capital investment may be divided into two parts:

$$D = D_{\text{н.с}} + D_{\text{с.п}}, \tag{3.5}$$

where $D_{g.s}$ is the cost of ground structures and $D_{a.p}$ is the cost of the aircraft pool; the corresponding fractions of the working capital are included in each part.

The annual product of an air route is

$$N\,\frac{\text{ton}\cdot\text{km}}{\text{yr}} = \lambda_3 G_{\text{пл}} iL = \lambda_l \overline{G}_{\text{пл}} GTV_{\text{рейс}}, \tag{3.6}$$

where λ_l is the load factor — the average payload of the aircraft expressed as a fraction of its maximum capacity G_{pl}, G is the weight of the aircraft, i is the number of hauls on the route per year, L is the nonstop distance traveled, G_{pl} is the maximum payload for a given weight of fuel (for a given range), $\overline{G}_{pl} = G_{pl}/G$ is the payload ratio (the relative weight of the payload), T is the flying time on the route per year, and V_{cruise} is the schedule or trip speed in km/h.

The trip speed is determined from the formula

$$V_{\text{рейс}} = \frac{L}{\dfrac{L_{\text{крейс}}}{V_{\text{крейс}}} + t_{\text{в.п}}} = V_{\text{крейс}} \frac{L}{L_{\text{крейс}} + t_{\text{в.п}} V_{\text{крейс}}}. \tag{3.7}$$

where V_{cruise} and L_{cruise} are the cruising speed and distance and t_{t-l} is the time to take off, climb, descend, and land.

The higher the speed and altitude of flight and the shorter the range, the greater will be the difference between trip and cruising speed.

For subsonic passenger aircraft with pressurized cabins, V_{trip} comes to 75-85% of V_{cruise}.

The annual expenses in B [17] consist of depreciation and the cost of major repairs to the aircraft (B_a) and engines (B_{en}), the cost of fuel and lubricants (B_f), paying the crews (B_{cw}), the cost of technical servicing and routine maintenance ($B_{r.m}$), and airport expenses (B_{AP}). Consequently,

$$B = B_c + B_{дв} + B_т + B_{экс} + B_{т.о} + B_{Ап}. \tag{3.8}$$

The cost of repairs to the airplane can be determined from the formula

$$B_c = \frac{n \cdot D_c}{M_c}(1 + k_c m_c)\frac{iL}{V_{рейс}}, \tag{3.9}$$

where n is the number of aircraft on the route, D_a is the cost of one airplane (dry and without engines), M_a is the total time (in hours) logged by the airplane over its entire lifetime, k_a is the cost of one major overhaul, expressed as a fraction of the cost of the airplane, and m_a is the number of major overhauls. It can be assumed that

$$D_a = d_a G_{dry\ w/o\ en} \tag{3.10}$$

where $G_{dry\ w/o\ en}$ is the weight of the dry airplane and its equipment without engines and d_a is the cost per kilogram of the dry airplane without engines; for present-day transport aircraft,

$$d_a = 10\text{-}30\ [\text{rubles/kg}].$$

The lower limit pertains to small aircraft of mixed construction, and the upper limit to all-metal aircraft with

pressurized cabins.

Statistics indicate that the lifetimes of aircraft lie in the range

$$M_c = 10000 \div 25000 \frac{\text{hr}}{\text{c-T}}.$$

The lower limit pertains to small aircraft used on local short hauls, and the upper limit to large long-haul aircraft. For medium aircraft of the LI-2 type, M_a = 15,000 h. The cost fraction accounted for by major overhauls is k_a = 0.15 for small short-haul aircraft and k_a = 0.10-0.12 for long-haul models.

If the time in flight hours between overhauls H_a [h/o'h] is known, the number of overhauls is determined from the formula

$$m_c = \frac{M_c}{H_c} - 1. \tag{3.11}$$

The next smaller whole number is taken. According to statistics,

$$H_c = 1500 \div 2000 \frac{\text{hr}}{\text{o'h}}.$$

The expenses for the engines can be determined from the formula

$$B_{\text{дв}} = \frac{nzD_{\text{дв}}}{M_{\text{дв}}}(1 + k_{\text{дв}} m_{\text{дв}}) \frac{lL}{V_{\text{рейс}}}, \tag{3.12}$$

where z is the number of engines on the airplane, D_{en} is the cost of an engine together with its propellers; M_{en} is the useful lifetime of an engine, k_{en} = 0.2 is the cost of one overhaul, expressed as a fraction of the cost of the engine, and m_{en} is the number of major overhauls per engine.

It can be assumed that for piston and turboprop engines

$$D_{\text{дв}} = d_N \cdot N, \tag{3.13}$$

where N is the rated horsepower output of the engine, d_N = 8 rubles/hp for piston engines, and d_N = 7.5 rubles/hp for turboprops. For turbojet engines,

$$D_{дв} = d_p \cdot P_0, \tag{3.14}$$

where

$$d_p = 8 \frac{\text{rubles}}{\text{kgf of thrust}};$$

P_0 is the engine's static thrust on the ground.

Statistically, the total lifetime of an engine depends on the degree of post-inception refinement of the specific engine type, lying in the range

$$M_{дв} = 2000 \div 5000 \frac{час}{дв},$$

with $M_{en} \approx 4{,}000$ for piston engines and $M_{en} \approx 2{,}000$ for turbojets and turboprops.

The number of major overhauls is determined from the formula

$$m_{дв} = \frac{M_{дв}}{H_{дв}} - 1, \tag{3.15}$$

where H_{en} is the time between overhauls and

$$H_{дв} = 600 \div 1000 \frac{\text{hr}}{\text{o'h}}.$$

If no specific data are available, it may be assumed that $H_{en} = 650$ h/o'h for piston engines and $H_{en} = 500$ h/o'h for turbojets and turboprops. The cost of fuel and lubricants is determined for turbojets by the formula

$$B_т = 1{,}1 \cdot C_{уд} \cdot P x_т \frac{L}{V_{рейс}}. \tag{3.16}$$

Here the coefficient 1.1 takes account of oil consumption and the fuel consumed in running the engines up on the ground, in the takeoff runup, and during the climb with consideration of the fuel-consumption decrease during descent and deceleration. C_{sp} [kg/kgf of thrust] and P are, respectively, the average values of

the engine's cruising specific fuel consumption and thrust, and x_f [rubles/kg] is the cost of the fuel. For kerosene, $x_f = 0.045$ ruble/kg.

In more accurate determinations of runup and climbing fuel consumption with consideration of the lower consumption during descent and deceleration, formula (3.16) takes the form

$$B_т = 1{,}05 x_т \left[C_{уд} \cdot P \frac{L}{V_{крейс}} + \frac{C_{уд.ф} G - C_{уд}(G - G_f)}{3600} \left(\frac{2H}{aM} + \frac{aM}{9.81} \right) \right] t. \qquad (3.17)$$

Here the coefficient 1.05 takes account of fuel consumed in revving the engines up on the ground, $C_{sp.M}$ is the specific fuel consumption at maximum middle-altitude climbing power, the term $C_{sp}(G - G_f)$ takes account of the fuel saved during descent and deceleration, $aM = V_{cruise}$ is the cruising speed in m/s, and H is the cruising altitude in meters.

The quantities H/aM and aM/9.81 take account of the fuel used in climbing and in the takeoff run, respectively. It can be assumed in approximation that

$$G_f \approx 0.3G.$$

The same formulas, (3.16) and (3.17), are also suitable for propeller engines, but P must be replaced by the average cruising power N_e and C_{sp} is taken in kg of fuel per horsepower-hour; the expression

$$\frac{C_{уд.ф} G - C_{уд}(G - G_f)}{3600}$$

is replaced by

$$\frac{C_{уд.ф} G - C_{уд}(G - G_f)}{3600 \cdot 75\eta} V_{крейс} \approx \frac{C_{уд.ф} G - C_{уд}(G - G_f)}{200\,000} V_{крейс},$$

where $C_{sp.M}$ is the specific fuel consumption rate at maximum middle-altitude climbing power per horsepower-hour and V_{cruise} is to

be taken in m/s.

Crew annual cost is composed of the monthly base pay of each crew member and flight pay. In addition, 7% of the total sum paid to crew members is budgeted by the line for life insurance and disability compensation.

$$B_{\text{экс}} = 1{,}07 \cdot 12n(\Sigma E) + 1{,}07(\Sigma x)iL, \tag{3.18}$$

where n is the number of aircraft on the line.

Table 3.1

Crew member	E, rubles/mo	x, rubles/km
Pilot	210	0.008
Copilot	176	0.006
Navigator	161	0.006
Flight Engineer	154	0.0048
Radar Operator	132	0.0044
Stewardess	80	0.0016

The monthly salaries E include bonuses and allowances; x is the rate of payment per kilometer flown. Values of E and x are given in Table 3.1; the sums Σ are taken for the entire crew.

The number of stewardesses is determined on the basis of one per 50 passengers.

Usually, the copilot's or navigator's seat is occupied on 50% of all flights by a higher-salaried chief pilot's representative; for this reason, 70 rubles/mo should be added to the sum ΣE and 0.0024 ruble/km to Σx.

The annual cost of technical servicing and routine maintenance (according to studies by Engineer V.P. Gal'kovskiy) per flight hour can be assumed proportional to the cost of the dry airplane with a proportionality factor of $5 \cdot 10^{-5}$, so that

$$B_{\text{т.о}} = 5 \cdot 10^{-5}(D_c + zD_{\text{дв}}) \frac{iL}{V_{\text{рейс}}}. \tag{3.19}$$

These five items of expenditure exhaust the basic so-called "direct" costs. These costs are usually increased by about another 7% to take account of the total of minor direct expenses. The cost of training, auxiliary, and service flights makes up a considerable faction of these expenses. However, these flights may be regarded as a certain number of unpaid flights, i.e., "dry runs" with the load factor $\lambda_l = 0$, and this must, in turn, be taken into account by reducing the average annual load factor λ_l of the line. We shall assume that the coefficient $\lambda_l = 0.65$ also takes account of these "unpaid" flights.

The same additional 7% also includes the cost of ground engine testing, but we have already taken them into account with the 1.05 coefficient applied to fuel cost. The remaining unaccounted minor direct costs can be discarded as insignificant.

There is one more major group of expenses — the so-called "indirect" costs, which amount to 35% or more of the "direct" costs. They include depreciation, repairs, and servicing for all ground structures and equipment, ground servicing of aircraft, passengers and cargo, administrative overhead, etc. Following the example of [17], we separate from these indirect costs the airport costs associated with servicing of the aircraft, passengers, and cargo:

$$B_{\text{АП}} = 40nG + 30i\lambda_a G_{\text{пл}}. \tag{3.20}$$

Here G and G_{pl} are in tons. The first term expresses the depreciation and cost of repairing and cleaning parking areas and cleaning the aircraft themselves, while the second term represents the cost of servicing passengers and cargo and loading and unloading cargo. The coefficients, 40 rubles/ton-year and 30 rubles/ton-flight may be lowered if cleaning and cargo handling are mechanized, but the former will be considerably higher if the aircraft are stored in hangars.

In the planning work on an air route, it is also necessary to take all remaining indirect costs into account, since they all

depend in one degree or another on the plan chosen for the route and influence its criterion K.

Thus, in planning for a new class of air route and the aircraft to service it, the takeoff and landing properties of the airplane and the corresponding runway length must be so selected that the cost of the aircraft and the runways will minimize the criterion K. Consideration of runway cost may result in selection of an airplane that costs more but uses less runway in taking off and landing.

§3.3. CRITERION FOR EVALUATING A PASSENGER AIRCRAFT

Since an extensive network of air routes already exists, the problem of designing an airplane for an existing network is of great practical importance. In this formulation of the problem, the characteristics of the air routes are the operating conditions for the new aircraft design, knowledge of which becomes one of the aforementioned conditions that are necessary for arriving at the optimum design version of the aircraft.

Air routes vary widely in length, amount of passenger and cargo traffic, airport equipment, runway length, terrain relief, climate, and other properties. There are four classes of airports as listed in Table 3.2.

Table 3.2

Airport class	Runway length	Runway width	Runway-end safety-strip length
	M		
Class 0-A	<3000	80	<400
Class I-B	2200	60	<400
Class II-C	1800	60	<400
Class III-D	1300	40	<400

The variety of air routes and airports has as a consequence that a universal aircraft designed for all routes would be far from the optimum in any particular case. It is more advantageous to design an airplane for a whole group of routes that differ little from one another in traffic flow and runway length, e.g., an intercontinental or transcontinental "liner," an aircraft for

trunk airways with 1000-2000-km nonstop distances, an airplane for 500-1,000-km local routes and, finally, an airplane for the very shortest local routes. It is necessary to specify for each of these aircraft types the appropriate airport class and the annual passenger and cargo flow N [tons-km/year], which is planned on the basis of an average N for routes of the particular type with room for future adjustment.

Having a statement of this type, we can derive a criterion for evaluation of the aircraft. Since the ground structures and equipment of air routes of an existing group remain unchanged when a new aircraft is designed for them, the cost of these items will remain practically unchanged on a change in aircraft design. As a result, all indirect costs may be assumed constant and discarded in formula (3.4) for the air-route criterion, leaving only the costs expressed by formulas (3.8)-(3.20). Moreover, as we showed earlier, the condition N = const enables us to change from the polynomial criterion of formula (3.4) to a criterion in the form of a ratio, i.e., costs per ton-kilometer.

Finally, $T = iL/V_{trip}$, i.e., the number of hours flown on the route per year, cancels in the numerator and denominator of the resulting ratio; we then obtain the criterion as the ratio of the hourly cost per single airplane to the hourly productivity of the single airplane.

For a jet aircraft, this formula takes the form

$$K = b' = \frac{D_c}{M_c}\,\frac{1+k_c m_c}{\lambda_3 G_{пл} V_{рейс}} + \frac{zD_{лв}}{M_{лв}}\,\frac{1+k_{лв} m_{лв}}{\lambda_3 G_{пл} V_{рейс}} + \frac{1{,}1 z C_{y1} P x_1}{\lambda_3 G_{пл} V_{рейс}} + \frac{1{,}07 \cdot 12\left(\sum E\right)}{\lambda_3 G_{пл} i_1 L} + \frac{1{,}07\left(\sum x\right)}{\lambda_3 G_{пл}} + \frac{5 \cdot 10^{-5}(D_c + zD_{лв})}{\lambda_3 G_{пл} V_{рейс}} + \frac{40G}{\lambda_3 G_{пл} i_1 L} + \frac{3G}{L} + \frac{p_{ср}(D_c + zD_{лв})}{\lambda_3 G_{пл} i_1 L} + \frac{c}{V_{рейс}}, \qquad (3.21)$$

where $D_a = d_a G_{dry\ w/o\ en}$, and $D_{en} = d_{en} P$.

A similar formula applies for aircraft with propeller engines, but $C_{sp}N$ must be substituted for $C_{sp}P$, with recognition of

$$D_{дв} = d_{дв} N_{ном}.$$

Let us consider a particular example:

$G = 42$ tons,	$P_0 = 6{,}000$ kgf,
$G_{dry\ w/o\ en} = 22$ tons,	$D_{en} = 8 \cdot 6{,}000 = 48{,}000$ rubles,
$G_{pl} = 4$ tons,	$M_{en} = 2{,}500$ hours,
$\lambda_l = 0.65$,	$k_{en} = 0.2$,
$V_{trip} = 790$ km/h,	$m_{en} = 3$,
$i_1 = 1/n = 200$ trips/airplane-year	$C_{sp} = 0.8$ kg/kg of thrust,
$L = 1{,}500$ km,	$P = 2{,}000$ kgf,
$d_a = 25$ rubles/kg,	$x_f = 0.045$ rubles/kg,
$D_a = 25 \cdot 22{,}000 = 550{,}000$ rubles,	$\sum = 990$ rubles/aircraft-month,
	$\sum_x = 0.033$ rubles/km-aircraft,
$M_a = 23{,}000$ hours,	$D_a + zD_{en} = 550{,}000 + 2 \cdot 48{,}000 = 646{,}000$ rubles,
$k_a = 0.12$,	
$m_a = 7$,	$P_{av} = 0.06$,
$z = 2$	$c = 4.8$ rubles/ton-hour,

$d_p = 8$ rubles/kgf of thrust.

$K = e' = b_a + b_{en} + b_f + b_{cw1} + b_{cw2} + b_{r.m} + b_{AP1} + b_{AP2} + b_{a.p} + b_{..}$ or, in figures,

$$K = e' = 0{,}0214 + 0{,}0299 + 0{,}0771 + (0{,}0163 + 0{,}0136) + 0{,}0157 + (0{,}0022 + 0{,}020) + 0{,}0496 + 0{,}0061 = 0{,}2519 \frac{\text{rubles}}{\text{ton} \cdot \text{km}} = 25{,}2 \frac{\text{kop}}{\text{ton} \cdot \text{km}}$$

With the indirect costs, this comes to

$$e' = 1{,}35 \cdot 25{,}2 = 34 \frac{\text{kop}}{\text{ton} \cdot \text{km}}.$$

It is also possible to obtain another criterion for evaluation of a passenger aircraft that is also a ratio of an advantage to cost, namely: "profit per ruble of investment," which economists recommend for evaluation of new technology and which, as we showed above, proceeds from the condition of constant total capital investment D = const. In practice, a criterion of the

form p = P/D is less suitable, since the condition D = const is usually not observed and allocations for the construction of a given version of the aircraft may continue from year to year, depending on the results from operation of the early series.

§3.4. CRITERION FOR EVALUATION OF A PART OR COMPONENT OF A PASSENGER AIRCRAFT

The properties of any part of an aircraft influence the properties of the aircraft and the criterion for its evaluation. The whole-airplane criterion may serve as the criterion for a major component of the aircraft, with exclusion of those terms of the criterion that do not change when the part being evaluated changes. For smaller parts, the increment in the airplane's criterion owing to the presence of the planned part on it may serve as the criterion.

Any part of an airplane has a cost and a weight and performs certain functions, exhibiting a certain functional quality in the process; it may also influence frontal drag, lift, safety, stability, controllability, comfort, and the like.

Let us consider a case in which a part has three inevitable properties: cost, weight, and functional quality, and, in addition, has a frontal drag or influences frontal drag. We shall assume the functional quality of the component to be constant. This must be done either because the quality must in fact remain unchanged or because the exact dependence of the aircraft criterion on the functional quality of the component is unknown. When this assumption is used, the component will influence the criterion only in virtue of its cost, weight, and frontal drag.

Examples of such components are antennas, ram air intakes, landing-gear pods, etc.

Let us assume that the type and number of the engines have been decided upon, along with the layout, parameters, and basic dimensions of the airplane; in addition, the aerodynamic design and weight calculations have been carried out and all quantities

appearing in formula (3.4) for the net cost per ton kilometer have been selected or calculated with the accuracy possible at this stage in the design work.

A number of cases will be considered, as functions of those properties of the airplane that are assumed constant.

1. Cruising Altitude and Speed Constant

Installation of a component costing ΔD rubles, weighing ΔG kgf, and having a frontal drag ΔQ kgf to perform a certain function on the airplane increases the airplane's weight by an amount ΔD_a and reduces its payload by ΔG_{pl}, which is equal to the aviation weight of the component:

$$\Delta G_{пл} = \Delta G + \frac{\pi\lambda_{эф}}{2c_y}\Delta Q.$$

The increase in b' due to the presence of the additional component (as a result of the increase in D_a and the decrease in G_{pl}) is found by the general method, by writing the total differential of b' with respect to D_a and G_{pl} and replacing the differentials with finite increments:

$$\Delta b' = \left(\frac{b_c}{D_c} + \frac{b_{экс}}{D_c} + \frac{b_{c\,п}}{zD_{ш}}\right)\Delta D - (b' - b_{экс} - b_{пр})\left(-\frac{\Delta G_{пл}}{G_{пл}}\right). \qquad (3.22)$$

Here ΔG_{pl} appears with the minus sign, since the weight ΔG and frontal drag ΔQ of the component lower the payload G_{pl} by an amount equal to the aviation weight $G_{a.c}$,

$$\Delta G_{пл} = \Delta G + \frac{dc_y}{dc_x}\Delta Q = \Delta G + \frac{\pi\lambda_{эф}}{2c_y}\Delta Q.$$

Let us evaluate the influence of the weight, cost, and frontal drag of the component.

We substitute the numbers from the example given earlier and the quantity $\pi\lambda_{ef}/2c_y = 26.4$. We obtain as a result

$$\Delta b' = 10^{-6} \cdot 0{,}14\Delta D + 0{,}0565(\Delta G + 26{,}4\Delta Q) =$$

$$= 10^{-6} \cdot 0{,}14\Delta D + 0{,}0565\Delta G + 1{,}49\Delta Q \frac{\text{rubles}}{\text{ton} \cdot \text{km}}.$$

Here ΔD is in rubles and ΔG and ΔQ in tons. To make the coefficients more commensurable, we express ΔG and ΔQ in kgf and Δb' in kopecks/ton-km.

$$\Delta b' = 0{,}000014\Delta D + 0{,}00565\Delta G + 0{,}149\Delta Q \frac{\text{kop}}{\text{ton} \cdot \text{km}}. \tag{3.23}$$

A more convenient criterion for the component is the quantity

$$K_1 = \frac{\Delta b'}{0{,}000014} = \Delta D + 400\Delta G + 10\,600\Delta Q. \tag{3.24}$$

which is proportional to Δb'.

As we see, frontal drag has the dominant influence on the increase in the net cost of cargo hauling, weight is next, and the cost of the component last. In deriving (3.24), we assumed G = const, although the weight actually appears in the term $b_{APl} = 40\ G/\lambda_l G_{pl} iL$ and G increases by 26.4ΔQ when the component is removed from the airplane. However, the ratio G/G_{pl} remains practically unchanged.

However, other circumstances related to the increase in aircraft and payloads weights are important. The former is detrimental to the airplane's takeoff and landing characteristics, while the latter requires space in the fuselage. Consequently, use of (3.22)-(3.24) presupposes the presence of available space in the fuselage and that a certain deterioration of takeoff and landing is acceptable.

2. Constant Payload and Variable Trip Speed

In this case, the presence of the component on the airplane increases D_a and lowers V_{trip}.

Using the same method, we obtain

$$\Delta b' = \left(\frac{b_c}{D_c} + \frac{b_{г.п} + b_{с.п}}{D_c + zD_{зв}}\right)\Delta D -$$

$$-(b' - b_{зк1} - b_{вк2} - b_{АП1} - b_{АП2} - b_{с.п})\frac{\Delta V_{рейс}}{V_{рейс}}. \qquad (3.25)$$

Assuming V_{trip} to be proportional to V_{cruise}, we can figure that

$$\frac{\Delta V_{рейс}}{V_{рейс}} = \frac{\Delta V_{крейс}}{V_{крейс}}.$$

We determine $\Delta V_{cruise}/V_{cruise}$ by the formula derived for $\Delta V_{max}/V_{max}$, taking instead of dP/dV

$$\frac{dP_{крейс}}{dV} = \frac{dP_{max}}{dV}\frac{P_{крейс}}{P_{max}}.$$

Assuming for the aircraft used in the example

$$\frac{c_{x_0}}{c_{x_i}} = 2{,}57, \quad \frac{dP_{крейс}}{dV} = 3{,}41,$$

$$\frac{\Delta V_{рейс}}{V_{рейс}} = -1{,}18\,\frac{\Delta G + \frac{\pi\lambda_{эф}}{2c_y}\Delta Q}{G} \qquad (3.26)$$

and substituting the quantities for the particular example into (3.25), we obtain

$$\Delta b' = 10^{-6}\cdot 0{,}14\Delta D + 0{,}152\,\frac{\Delta V_{рейс}}{V_{рейс}}\,\frac{\text{rubles}}{\text{ton}\cdot\text{km}}.$$

Here we substitute

$$\frac{\Delta V_{рейс}}{V_{рейс}} = -\frac{1{,}18}{42}\left(\Delta G + \frac{\pi\lambda_{эф}}{2c_y}\Delta Q\right) = 0{,}0281\,(\Delta G + 26{,}4\Delta Q)$$

and obtain finally

$$\Delta b' = 10^{-6}\cdot 0{,}14\Delta D + 0{,}00427\,(\Delta G + 26{,}4\Delta Q) =$$

$$= 10^{-6}\cdot 0{,}14\Delta D + 0{,}00427\Delta G + 0{,}1128\Delta Q\,\frac{\text{rubles}}{\text{ton}\cdot\text{km}}.$$

Again expressing $\Delta b'$ in kopecks/ton-km and ΔG and ΔQ in kgf, we find that the cost, weight, and frontal drag of the component

increase the net cost per ton-kilometer by

$$\Delta b' = 0{,}000014\Delta D + 0{,}000427\Delta G + 0{,}01128\Delta Q \frac{\text{kop}}{\text{ton}\cdot\text{km}}. \qquad (3.27)$$

Dividing Δb' by 0.000014, we obtain the criterion for the component, which is proportional to Δb':

$$K_2 = \frac{\Delta b'}{0{,}000014} = \Delta D + 30\Delta G + 800\Delta Q. \qquad (3.28)$$

As we see, in this case the same component has much loss effect on the net cost per ton-kilometer, because the coefficients of ΔG and ΔQ are reduced by a factor of 13. However, frontal drag is still the dominant factor in this case.

3. Payload of Trip Speed Constant

In this case, the increase in weight and frontal drag due to the presence of the component on the airplane increases the required thrust P:

$$P = c_{x_0} Sq + \frac{AG^2}{Sq}$$

by an amount ΔP:

$$\Delta P = \Delta c_{x_0} Sq + \frac{2AG}{Sq}\Delta G = \Delta Q + \frac{2Q_i}{G}\Delta G = \Delta Q + \frac{2c_y}{\pi\lambda_{эф}}\Delta G,$$

where

$$A = \frac{1}{\pi\lambda_{эф}}.$$

Increasing the thrust increases fuel consumption:

$$\Delta b_т = \frac{1.1 x_т C_{yx}}{\lambda_э G_{пл} V_{рейс}}\Delta P = b_т \frac{\Delta P}{P} = \frac{b_т}{P}\frac{2c_y}{\pi\lambda_{эф}} G_{а.д},$$

where the aviation weight of the component is

$$G_{а.д} = \Delta G + \frac{\pi\lambda_{эф}}{2c_y}\Delta Q.$$

The change in thrust also changes specific fuel consumption and engine life and, if these changes are known, they can also be taken into account. If these secondary effects of the thrust change are disregarded, the presence of the additional component and the airplane will in this case increase b':

$$\Delta b' = \left(\frac{b_c}{D_c} + \frac{b_T + b_{c.n}}{D_c + zD_{.n}}\right)\Delta D + \frac{b_T}{P}\,\frac{2c_y}{\pi\lambda_{эф}}\left(\Delta G + \frac{\pi\lambda_{эф}}{2c_y}\Delta Q\right). \qquad (3.29)$$

For our numerical example, we obtain

$$\Delta b' = 10^{-6}\cdot 0{,}14\Delta D + 10^{-6}\cdot 0{,}761\,(\Delta G + 26{,}4\Delta Q) =$$
$$= 10^{-6}\cdot 0{,}14\Delta D + 10^{-6}\cdot 0{,}761\Delta G + 10^{-6}\cdot 20{,}2\Delta Q\ \frac{\text{rubles}}{\text{ton}\cdot\text{km}}$$

(here ΔG and ΔQ are in kgf) or

$$\Delta b' = 10^{-4}(0{,}14\Delta D + 0{,}761\Delta G + 20{,}2\Delta Q)\,\frac{\text{kop}}{\text{ton}\cdot\text{km}}. \qquad (3.30)$$

Dividing by $0.14 \cdot 10^{-4}$, we get

$$K_3 = \frac{\Delta b'}{0{,}000014} = \Delta D + 5{,}44\Delta G + 144{,}3\Delta Q. \qquad (3.31)$$

4. <u>Fuel Weight Plus Payload Constant</u>

Installation of an additional component on the airplane requires that the fuel load be increased by an amount

$$\Delta G_т = \frac{C_{уд}L}{V_{рейс}}\Delta P = \frac{C_{уд}L}{V_{рейс}}\cdot\frac{2c_y}{\pi\lambda_{эф}}G_{а.д}.$$

Since the sum of the weights and the payload remains constant, it is necessary to reduce the payload by the same amount:

$$\Delta G_{пл} = \Delta G_т.$$

Then, using the coefficient of $G_{a.c}$ obtained in the first place, we determine one more term in the expression for Δb':

$$(b' - b_{АП2} - b_{вр})\frac{\Delta G_{пл}}{G_{пл}} = (b' - b_{АП2} - b_{вр})\frac{C_{уд}L}{V_{рейс}G_{пл}}\,\frac{2c_y}{\pi\lambda_{эф}}G_{а.д}.$$

For our numerical example, this term equals

$$\frac{0{,}0365\cdot 0{,}8\cdot 1500}{790\cdot 26{,}4}G_{а.д} = 10^{-6}\cdot 3{,}25G_{а.д}.$$

With allowance for this term, we obtain

$$\Delta b' = 0{,}000014\Delta D + (0{,}0000761 + 0{,}000325)\,G_{a.д} =$$
$$= 0{,}000014\Delta D + 0{,}000401\Delta G + 0{,}01059\Delta Q \frac{\text{kop}}{\text{ton}\cdot\text{km}}. \tag{3.32}$$

After dividing Δb' by the coefficient of ΔD, we obtain

$$K_4 = \Delta D + 28{,}6\Delta G + 756{,}4\Delta Q. \tag{3.33}$$

In this case, it is necessary to have space available for the additional weight of fuel; the takeoff weight and distance remain unchanged, but the landing weight and landing speed will be lowered slightly. It must also be recognized that an increase in the weight of fuel in the wing and a decrease in the fuselage payload will increase the strength margin of the wing.

5. Comparison of Cases Considered

We see from the cases considered above that the criterion for evaluation of an aircraft component varies depending on which characteristics of the airplane are assumed constant.

Now which criteria should be used? First of all, it is evident from comparison of (3.24), (3.28), (3.31), and (3.33) that the relation between the effects of weight and frontal drag is the same in all formulas, i.e., the same as in the expression for aviation weight:

$$G_{a.д} = \Delta G + 26{,}4\Delta Q$$

and a 1-kgf decrease in Q may give a weight increase up to 26 kg.

Comparing these last two terms with the cost of the component, we see that ΔG and to an even greater degree ΔQ influence the criterion b' much more strongly in the first criterion than in the others.

Selection of each aircraft component on the basis of the minimum K_1 results in the greatest lowering of the net cost per ton-kilometer.

Use of numerous similar criteria with tabulated numerical coefficients guides the efforts of the entire designer staff toward the optimum aircraft design.

The following procedure can be recommended for use of these criteria.

When the plan has been worked out with application of the criterion K_1 to all components, the design weight G_{K_2} and the frontal drag G_{0_2} are adjusted; these quantities are compared with their values G_{K_1} and Q_{0_1} from the preceding approximation. Then the change in payload weight is determined:

$$\Delta G_{пл} = G_{K_1} - G_{K_2} + \frac{\pi\lambda_{эф}}{2c_y}(Q_{0_1} - Q_{0_2}).$$

If $\Delta G_{pl} > 0$, the payload is to be increased by this amount, while the takeoff weight is increased by $\pi\lambda_{ef}(Q_{0_1} - Q_{0_2})/2c_y$.

Since there may also have been errors in the other weights in the calculation of the preceding approximation, it is better to determine ΔG_{pl} as follows:

$$\Delta G_{пл} = (G_{d_1} - G_{d_2}) + \frac{\pi\lambda_{эф}}{2c_y}(Q_{0_1} - Q_{0_2}),$$

where $G_d = (G - G_{pl})$; here we take G_{pl} from the preceding approximation.

If we obtain a $\Delta G_{pl} < 0$ (this may result from the inaccuracy of the preceding approximation), G_{pl} must be reduced by ΔG_{pl} in order to maintain the specified cruising regime. It will be recalled that $\pi\lambda_{ef}(Q_{0_1} - Q_{0_2})/2c_y$ expresses the increase in takeoff weight and that this increase is acceptable if takeoff is not affected unacceptably, while an increase in payload by ΔG_{pl} is admissible if there is space in the fuselage. If payload requires additional equipment (for example, passenger seats), some of the weight goes into the additional equipment and ΔG_{pl} will be smaller.

If there is no available space in the fuselage and the detriment to takeoff is unacceptable, the criteria K and K_3 are used; if there is space in the fuselage but the takeoff weight cannot be increased, criterion K_4 is applied.

Many of the components of the airplane have no frontal drag, but only cost, weight, and functional qualities; hence the expression for the increments of b' or the criterion K become binomial:

$$\Delta b' = C_D \Delta D + C_G \Delta G,$$

$$K = \Delta D + \frac{C_G}{C_D} \Delta G.$$

6. Cost of Weight Reduction

These binomial criteria can be used to solve the practically interesting problem of the limiting and optimum cost of a weight reduction.

Any component may carry excessive weight that can be removed at additional cost with no detriment to the functional quality of the component. The change in b' that results from component weight reduction is expressed thus:

$$\Delta b' = C_D \Delta D - C_G \Delta G.$$

Obviously, if the weight reduction is so expensive that there is no decrease in b' ($\Delta b' = 0$), the weight reduction should not be undertaken; this limiting cost per kg of weight reduction is

$$\left(\frac{\Delta D}{\Delta G}\right)_{\text{пр}} = \frac{C_G}{C_D}.$$

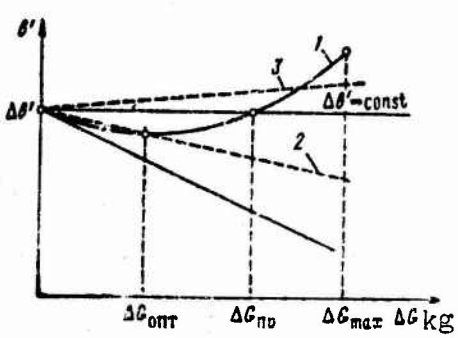

Figure 3.1. Cost of weight reduction.

When the weight reduction makes it possible to increase payload (in our example),

$$\left(\frac{\Delta D}{\Delta G}\right)_{\text{пр}} = 403 \frac{\text{руб}}{\text{кг}},$$

and in the case of a given payload and an increase in trip speed

$$\left(\frac{\Delta D}{\Delta G}\right)_{\text{гр}} = 30 \frac{\text{руб}}{\text{кг}},$$

i.e., it is much lower.

But which weight reduction should be decide upon? Let us assume that in its initial state, the component has excessive weight, but that as the weight is removed its removal becomes more expensive as the amount of remaining excessive material becomes smaller; assume, for example, that the cost ΔD of the weight reduction is an accelerating increasing function:

$$\Delta D = f(\Delta G).$$

Figure 3.1 shows the variation of $\Delta b'$ as a function of the initial state and ΔG. The term $C_G \Delta G$ causes b' to decrease linearly, while the term $C_D \Delta D = C_D f(\Delta G)$ increases b', diverting the b' curve upward from linear (curve 1). The largest decrease in the net cost per ton-kilometer is obtained at ΔG_{opt}, and the limiting weight reduction, which gives no increase in b', at ΔG_{pr}; at ΔG_{max}, all of the excess material has been removed in an operation that is now totally unproductive.

In approximation, we may assume an optimum weight reduction equal to 1/2 or the limit.

The dashed lines on the figure illustrate two more cases, in which the cost of the weight reduction is proportional to the weight removed. Line 2 corresponds to the case in which all of the excessive material must be removed, and line 3 to the case in which none of it should be removed.

§3.5. CRITERIA FOR EVALUATION OF OTHER CIVIL AIRCRAFT

The structure of the criterion for an air freighter will be the same as that for a passenger aircraft, although it may differ greatly from the latter in layout, construction, and equipment.

It will probably be necessary to change the average tariff a, the number of trips i per year, and the cost of the time to haul the cargo C [rubles/ton-h], in which it may be necessary to include losses of perishable cargo en route, and to change certain other quantities. Otherwise the analogy with the passenger aircraft will be complete.

Criteria for other civil aircraft can be drawn up in similar fashion. If, for example, the "work" or "product" N of a given airplane during a given time can be evaluated quantitatively (in hectares of treated acreage, in square kilometers of protected forest, etc.), a "net cost per unit product" criterion b = B/N can be obtained easily.

If, in addition, the cost a of processing a unit product is also known, it is possible to obtain a "profit per ruble invested" criterion p = (Na - B)/D and an "income"-type criterion for a given period:

$$K = Na - B - p_{cp}D.$$

If the advantage cannot be evaluated quantitatively, we may follow the general rule for such cases and assume it to be constant. This constancy can be ensured if all of the properties of the airplane on which this effect depends (payload, speed, altitude, range or endurance, takeoff-and-landing, and other properties) are assumed constant. This reduction to a set of constant properties is also frequently applied even when the advantage can be evaluated quantitatively. Then the criterion consists only of the negative effect

$$K = B + p_{cp}D$$

and the optimum version of the design is found by minimizing it. It must only be remembered that the preliminary design will be optimal only for the assigned values of the airplane's properties.

The optimum preliminary version based on the minimum of the negative part of the criterion is very close to the optimum variant for minimizing the cost of the entire airplane, and the cost of the airplane is approximately proportional to its takeoff weight. Thus we may use an even simpler criterion — the cost of the airplane or its takeoff weight — for a given set of aircraft properties.

The fixed values of the airplane's properties appear in the designated technical specifications. Designing from TS and from

minimum takeoff weight requires the designer not only to lighten the structural weight of the aircraft to the greatest possible degree, but also to select engine characteristics and aircraft aerodynamics such that all items in the TS are conformed to at minimum aircraft weight.

Designing from TS does not eliminate the need for the use of a criterion, but the criterion will become a narrow one of economy; it will be the cost per unit time or, more simply, the cost of the airplane, or, still more simply, its takeoff weight.

Determining the quantitative dependence of the general criterion on engine characteristics and on the geometry, weight, and other parameters of the airplane with consideration of the confining relationships between them is a complex preliminary-design task. Because of the complexity of these relationships, the problem is solved by successive approximations and comparison of the various versions with the general criterion, with selection of the variant having the optimum criterion value. For selection of the optimum parameters, the parameters are varied smoothly within their ranges, i.e., at equal intervals, and the optimum combination will be the one for which the general criterion has its extreme value. The optimum combination of the TS is found by the same manner and the same method of successive approximations. As a rule, the parameters characterizing the design are first determined statistically for each of the sets of technical specifications to be investigated, the layout of the airplane, the type of the engine and its characteristics are chosen, its dimensions and aerodynamic characteristics are evaluated, the weight, size, and operational and economy indicators of the aircraft are calculated, and the value of the general criterion is computed. Then the aerodynamic characteristics are determined for the selected layout and the dimensions found for the airplane for the various versions of the design parameters, and the flight-engineering properties, weight, geometrical, operational, and economy indicators and the general criterion are adjusted.

Approximations are computed until the value of the general criterion and, with it, the set of technical specifications ceases to change (by more than a predetermined amount). The result is one "point" on the curve of the general criterion as a function of the set of technical specifications and the aircraft parameters characterizing the design.

After thus analyzing various combinations of technical specifications and design parameters, the dependence of the general criterion on these combinations can be found. The optimum combination of technical specifications and design parameters is that for which the general criterion has its optimum value.

To perform the above task, it is necessary to know the effects of various design parameters on the flight-engineering properties of the airplane and its weight, operational, and economy characteristics. It is also necessary to know how the scheme will be affected by changes in tactical and technical properties, the principle followed in laying out, balancing, and developing the structural frame of the aircraft, and the method of determining the takeoff weight and size of the airplane.

All these steps are also necessary in designing to given technical specifications. The material is the subject of Parts II and III.

Part II

FLIGHT CHARACTERISTICS OF THE AIRCRAFT, ITS ST TY, AND HOW THEY ARE INFLUENCED BY ITS PARAMETERS

Chapter 4

EQUATIONS OF MOTION. FORCES ACTING ON THE AIRPLANE

§4.1. EQUATIONS OF MOTION

As a rule, the spatial motion of the airplane is not analyzed in preliminary design, but its motion is investigated in vertical and horizontal planes.

In analyzing the motion of the airplane in the vertical plane, it is most convenient to use equations written in the wind system of axes, in which the OX axis is directed along the velocity vector and the OY axis perpendicular to the former in the plane of symmetry of an airplane flying without slip.

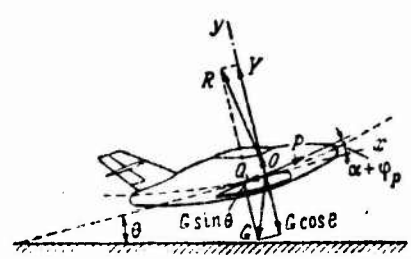

Figure 4.1. Forces acting on the airplane. System of axes.

The arrangement of the axes and the forces acting on the airplane as a material point are shown in Fig. 4.1.

Projecting the forces acting on the airplane on the axes Ox and Oy and performing simple transformations, we obtain the equations of motion

$$\frac{dV}{dt}=\frac{g}{G}[P\cos(\alpha+\varphi_P)-Q-G\sin\theta], \tag{4.1}$$

$$\frac{d\theta}{dt}=\frac{g}{GV}[Y+P\sin(\alpha+\varphi_P)-G\cos\theta], \tag{4.2}$$

where ϕ_P is the angle between the thrust vector and the wing chord.

Since the angle ϕ_P is generally small, we may set cos $(\alpha + \phi_P) = 1$ for flight at small angles of attack and neglect the term P sin $(\alpha + \phi_P)$ in (4.2). With these assumptions, expressions (4.1) and (4.2) become

$$\frac{dV}{dt}=g\left(\frac{P-Q}{G}-\sin\theta\right), \tag{4.3}$$

$$\frac{d\theta}{dt}=\frac{g}{V}\left(\frac{Y}{G}-\cos\theta\right). \tag{4.4}$$

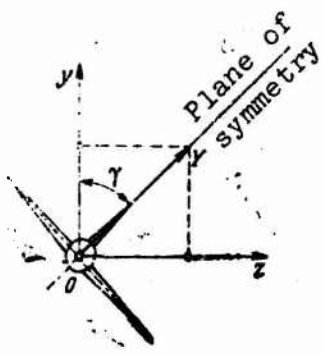

Figure 4.2. System of axes.

Since Y/G is the normal acceleration n_y and $(P - Q)/G = n_x$ Eqs. (4.3) and (4.4) can be rewritten

$$\frac{dV}{dt}=g(n_x-\sin\theta), \tag{4.5}$$

$$\frac{d\theta}{dt}=\frac{g}{V}(n_y-\cos\theta). \tag{4.6}$$

These equations must be supplemented by the obvious kinematic relations

and

$$\left.\begin{aligned}\frac{dH}{dt}&=V\sin\theta\\ \frac{dL}{dt}&=V\cos\theta.\end{aligned}\right\} \tag{4.7}$$

Since $d\theta/dt = V/r_y$, Eq. (4.6) yields an expression for the radius of curvature of the trajectory, r_y:

$$r_y = \frac{V^2}{g(n_y - \cos\theta)}. \tag{4.8}$$

To consider curvilinear motion in the horizontal plane, we take a system of axes in which Ox is directed along the velocity vector, Oy perpendicular to it and in the vertical plane, and Oz in the horizontal plane (Fig. 4.2).

With the assumptions adopted above and the coordinate system in Fig. 4.2, we obtain

$$\frac{d\varphi}{dt} = \frac{g}{V} n_y \sin\gamma \tag{4.9}$$

and

$$r_z = \frac{V^2}{g n_y \sin\gamma}, \tag{4.10}$$

where ϕ is the turn angle of the velocity vector horizontal projection and γ is the roll angle of the airplane. Since $n_y = 1/\cos\gamma$ in a horizontal term, Eqs. (4.9) and (4.10) can also be written

$$\frac{d\varphi}{dt} = \frac{g}{V} \operatorname{tg}\gamma = \frac{g\sqrt{n_y^2 - 1}}{V}, \tag{4.11}$$

$$r_z = \frac{V^2}{g\sqrt{n_y^2 - 1}}. \tag{4.12}$$

These equations of motion in the vertical and horizontal planes are used extensively in preliminary design, both to determine the flight properties of the airplane and for analysis of the effects of various parameters on them, recognizing that the aerodynamic forces and the g-factors that they determine depend on these parameters.

§4.2. LIFT

The expression for the lifting force of an airplane is familiar:

$$Y = c_y S \rho \frac{V^2}{2} = 0{,}7 c_y S p M^2. \tag{4.13}$$

If the pressure in the atmosphere is taken in mm Hg instead of kgf/m^2, we have

$$Y = 9{,}55 c_y S p M^2. \tag{4.14}$$

The dependence of c_y on angle of attack is linear for aircraft wings of large aspect ratio. Violation of linearity indicates that local flow separation has occurred on the wing. At subsonic speeds, $c_y^\alpha = dc_y/d\alpha$ is a function of the geometrical aspect ratio, sweep, and taper of the wing, while at supersonic speeds it depends basically on the Mach number M.

The smaller the wing aspect ratio and the larger M when the latter exceeds unity, the smaller is c_y and the smaller c_y^α for a given α.

Flow separation occurs on the wing at a certain angle of attack, and $dc_y/d\alpha$ decreases. In the case of unswept trapezoidal wings with aspect ratios $\lambda < 5$-7 with large Reynolds numbers (Re), a very small increase in angle of attack is sufficient to lower c_y as a result of separation. In addition, separation usually develops asymmetrically on the left and right wings for this wing type, giving rise to a strong moment that rolls the airplane onto one wing. For strongly swept wings of small aspect ratio, such as are used on supersonic aircraft, separation occurs first on small segments of the wing. It causes buffeting of the airplane, but no substantial rolling moment. A slower increase of c_y is observed as the angle of attack is increased further.

At a certain angle of attack α_{cr}, the value of c_y reaches its maximum. The c_y at which buffeting begins ($c_{y_{bf}}$) and $c_{y_{max}}$ decrease with increasing M. Buffeting at $c_y < c_{y_{max}}$ should be regarded as helpful, since it is not dangerous in itself and tells the pilot that the airplane has reached a c_y near $c_{y_{max}}$. The coefficients $c_{y_{bf}}$ and $c_{y_{max}}$ depend not only on M, but also on Re, increasing with it.

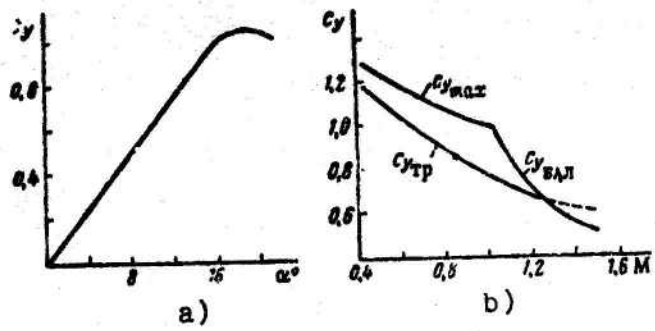

Figure 4.3. a) c_y as a function of α; b) $c_{y_{bf}}$, $c_{y_{max}}$, and $c_{y_{bal}}$ determined by maximum stabilizer deflection as functions of M.

In certain cases of flight, the maximum value of c_y is determined on the basis of longitudinal balance with the largest possible deflection of the elevators or stabilizer.

This is done because above a certain M, with the elevators or stabilizers at maximum deflection, the sum of the longitudinal moments vanishes at $c_{y_{bal}} < c_{y_{bf}}$, and $c_{y_{bf}}$ is not reached in extended steady flight.

Figure 4.3 shows the nature of c_y as a function of angle of attack and of $c_{y_{bf}}$, $c_{y_{max}}$, and $c_{y_{bal}}$ as functions of M.

Knowing $c_{y_{max}}$ as a function of M (see Fig. 4.3b), we can calculate the maximum lift that the pilot can obtain for any altitude and Mach number and find the maximum normal acceleration. Obviously,

$$Y_{max} = 0{,}7 c_{y_{max}} S p M^2, \tag{4.15}$$

$$n_{y_{max}} = \frac{0{,}7 c_{y_{max}} S p M^2}{G}. \tag{4.16}$$

For straight-line level flight, a certain speed corresponds to each value of c_y, and

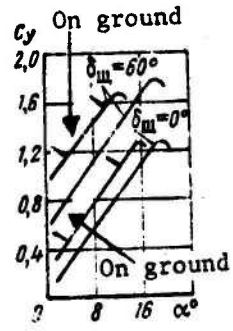

Figure 4.4. c_y as a function of α at the ground and at high altitudes.

is the larger the smaller c_y.

The lowest speed in level flight will be obtained in flight at $c_{y_{max}}$.

Low landing (V_{ldg}) and takeoff (V_{tko}) speeds are especially important for an airplane. For this reason, special high-lift devices that increase c_y at the landing and takeoff wing angles of attack are used on the wing to increase c_y during landing and takeoff.

It must be remembered that the ground effect increases c_y by another 0.15-0.20 at takeoff and landing. Figure 4.4 shows how c_y depends on α under landing and takeoff conditions ($\delta_f = 60°$).

Methods of increasing $c_{y_{ldg}}$ will be discussed in greater detail in the section on landing the aircraft.

§4.3. FRONTAL-DRAG FORCES

The frontal drag Q of an airplane depends on its frontal drag coefficient c_x, wing area, and ram pressure:

$$Q = c_x S \rho \frac{V^2}{2} = 0{,}7 c_x S p M^2. \tag{4.17}$$

The quantity

$$c_x = c_{x_0} + c_{x_i},$$

where c_{x_0} is the coefficient of profile and parasite drag at $c_y = 0$ and $c_{x_i} = Ac_y^2$ is the coefficient of induced drag.

At constant M, A = const in a broad range of angles of attack.

Thus

$$c_x = c_{x_0} + Ac_y^2. \tag{4.18}$$

The coefficient c_{x_0} is composed of frictional drag and pressure drag. The latter includes the wave drag, which makes its appearance at $M > M^*_{cr}$. M^*_{cr} is the Mach number at which a compression shock forms as a result of local supersonic velocities in the flow

past the body and c_{x_0} begins a rapid increase (c_{x_0} increases by more than 1% when M is increased 1%). c_{x_0} is a function of the Reynolds and Mach numbers Re and M. With increasing Re, the value of c_{x_0} decreases as a result of a decrease in the coefficient of friction. An increase in M above M^*_{cr} results in a sharp rise of c_{x_0}, but at an M greater than 1.1-1.4, the increase in c_{x_0} gives way to a decrease owing to a decrease in the coefficient of wave drag, which varies in approximately inverse proportion to $\sqrt{M^2 - 1}$. At M greater than 2.5, the value of $\sqrt{M^2 - 1} \approx M$ and, consequently, the wave drag becomes proportional not to M^2, but only to M. As will be shown below, this is a highly important fact.

Wave drag is proportional to the square of the profile thickness ratio $\bar{c}$. At $M < M^*_{cr}$, an increase in profile thickness also increases c_{x_0}, but not strongly.

An increase in wing sweep causes an increase in M^*_{cr}.

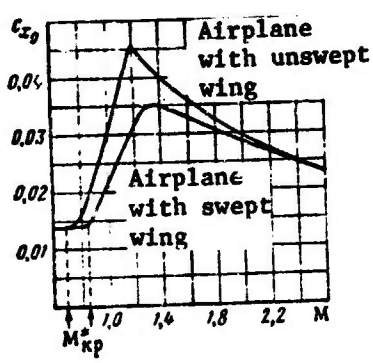

Figure 4.5. c_{x_0} of an airplane as a function of M.

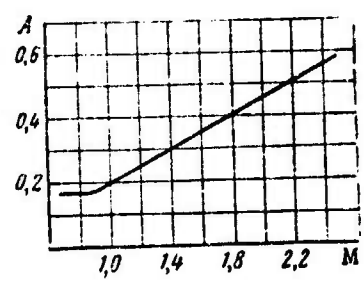

Figure 4.6. Coefficient A as a function of M.

Figure 4.5 shows the nature of c_{x_0} as a function of M for wings of various planforms with the same profile thickness.

c_{x_0} is the sum of the wing ($c_{x_{0_{wg}}}$), tail ($c_{x_{0_{tl}}}$), fuselage (c_{x_f}), and engine-nacelle ($c_{x_{e.n}}$) drag coefficients and those of other elements:

$$c_{x_0} = c_{x_{0_{wg}}} + \frac{c_{x_{0_{tl}}} S_{tl}}{S} + \frac{C_{x_f} S_f}{S} + \frac{c_{x_{n.r}} S_{n.r}}{S} + \ldots \tag{4.19}$$

We note that (4.19) implies a decrease in c_{x_0} on an increase in wing area, although the frontal drag Q_0 increases at the same time.

The coefficient A, which determines c_{x_i}, is inversely proportional for subsonic speeds to the wing effective aspect ratio:

$$A = \frac{1}{\pi \lambda_{\text{эф}}}. \tag{4.20}$$

In turn,

$$\lambda_{\text{эф}} \approx \lambda \frac{1}{1 + \frac{S_{a.f}}{S}},$$

where $S_{a.f}$ is the wing area occupied by the fuselage and engine pods and λ is the geometrical aspect ratio of the wing. At M > > 1.8,

$$A = \frac{1}{c_y^2} \approx \frac{\sqrt{M^2 - 1}}{4}. \tag{4.21}$$

Figure 4.6 shows how A depends on M. Unlike the coefficient of wave drag, which is inversely proportional to $\sqrt{M^2 - 1}$ at large M, the quantity A is directly proportional to $\sqrt{M^2 - 1}$, so that c_{x_i} increases rapidly with increasing M at a constant c_y.

The family of polar curves for the airplane for various M takes the form indicated in Fig. 4.7.

We find the expression for the maximum lift/drag ratio $K_{max} = \left(\frac{c_y}{c_x}\right)_{max}$ from the condition $\frac{d}{c_y}\left(\frac{c_{x_0} + Ac_y^2}{c_y}\right) = 0$. Hence it follows

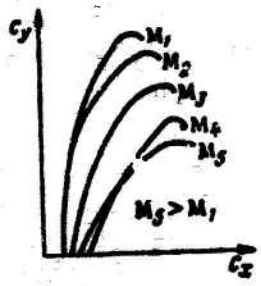

Figure 4.7. Polar curves of aircraft as function of M.

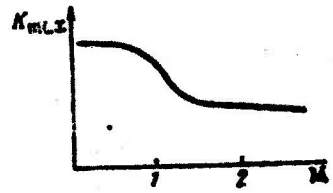

Figure 4.8. K_{max} as a function of M.

that at the optimum angle of attack

$$c_{x_0} = c_{x_i};$$

$$c_{y_{опт}} = \sqrt{\frac{c_{x_0}}{A}}; \tag{4.22}$$

$$K_{max} = \frac{1}{2}\sqrt{\frac{1}{Ac_{x_0}}}. \tag{4.23}$$

Figure 4.8 shows how the airplane's K_{max} depends on M. K_{max} = = const at small M. In the range M = 0.8-0.9 to 1.2-1.4, K_{max} decreases sharply owing to the increased A and c_{x_0}. At higher M, K_{max} changes little, since the product Ac_{x_0} remains almost constant.

Various methods are used to solve the problem of the K_{max} increase at high supersonic and subsonic speeds. At supersonic speeds, the most effective way to increase K_{max} is to lower c_{x_0}; this is done primarily by reducing the profile thickness ratio. However, the designer can adjust the coefficient A only in a narrow range. At subsonic speeds, he can not only reduce c_{x_0}, but also increase the wing aspect ratio to lower the value of A. However, a large increase in wing aspect ratio makes it necessary (in order to avoid an excessively heavy wing) to use thicker wing profiles and thus increase c_{x_0}, which ultimately reduces the effect from the increase in wing aspect ratio.

Under the conditions of horizontal straight-line flight, a definite c_y corresponds to each speed and altitude:

$$c_y = \frac{2G}{\rho S V^2} = \frac{G}{0.7 S p M^2}, \tag{4.24}$$

and, consequently, we also have $c_{x_{ih}} = Ac_y^2$. The frontal drag in level straight-line flight is

$$Q_r = (c_{x_0} + c_{x_{ir}}) S \frac{\rho V^2}{2},$$

or

$$Q_r = Q_0 + Q_{ir} = c_{x_0} S \rho \frac{V^2}{2} + \frac{2G^2 A}{S \rho V^2}, \tag{4.25}$$

or when the pressure in the atmosphere is substituted for the density

$$Q_r = Q_0 + Q_{ir} = c_{x_0} 0.7 S p M^2 + \frac{G^2 A}{0.7 S p M^2}. \tag{4.26}$$

From this we see that, while Q_0 is directly proportional to p, M^2, and S, the value of Q_{ih} is inversely proportional to these quantities. As we noted earlier, Q_0 is approximately directly proportional to M at $M \geq 2$.

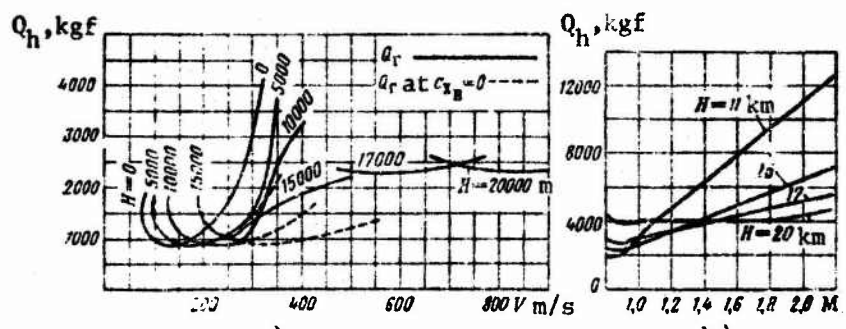

a) b)

Figure 4.9. a) Q_h as a function of speed and altitude; b) Q_h as a function of M and altitude.

The family of $Q_h = Q_h(V)$ curves for various flight altitudes is referred to as Zhukovskiy curves or required-thrust curves.

Figure 4.9 shows the characteristic trends of the $Q_h = Q_h(V)$ and $Q_h = Q_h(M)$ curves.

Since

$$Q_r = \frac{G}{K}. \tag{4.27}$$

$Q_{h_{min}}$ will occur at K_{max}, i.e., at $c_{y_{opt}}$. The flight speed at this point is also called the optimum speed. In the absence of wave drags and with constant c_y and, consequently, constant lift/drag ratio, Q_h remains constant with increasing flight altitude, and with ascent from the ground to altitude H, flight speed should be increased by a factor $\sqrt{1/\Delta}$ ($\Delta = \rho_H/\rho_0$ is the relative air density).

In the range of Mach numbers in which the maximum lift/drag ratio is independent of M, $Q_0 = Q_{ih}$ and $Q_{h\ min} = 2Q_0$ in flight at the optimum speed. On the other hand, in the M range in which lift/drag ratio decreases with flight speed in flight at $c_{y_{opt}}$ owing to deviation of the level-flight polar curves from the second-degree parabola, Q_{ih} is slightly larger than Q_0.

At any constant M in flight at the altitude at which $c_y = c_{y_{opt}}$, Q_h will equal $2Q_0$. Figure 4.9 indicates that flight at speeds greater than the optimum in the subsonic range is accompanied by a sharp increase in Q_h, while the same relative speed increase at large M results only in a small increase in Q_h. The explanation for this is that at subsonic speed, Q_0 is directly proportional to M^2 and Q_{ih} inversely proportional to M^2, while at high supersonic speeds Q_0 is proportional to M and Q_{ih} is inversely proportional to M.

For example, doubling the speed over V_{opt} increase Q_h by a factor of 2.125 in the subsonic range, but only by a factor of 1.25 in the high supersonic range. This is why it is especially important to have a large K_{max} for the supersonic airplane at high supersonic speeds, together with aircraft parameters with which high-altitude flight takes place at a lift/drag ratio near

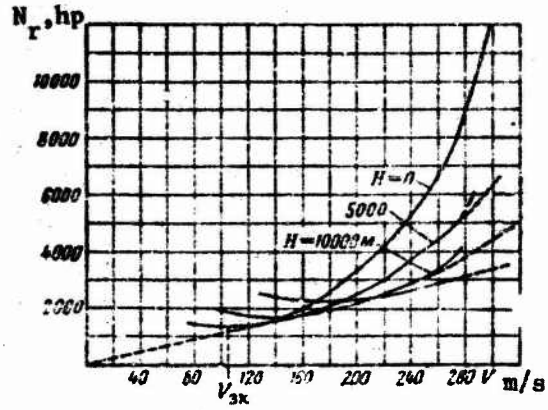

Figure 4.10. N_r as a function of speed and altitude.

the maximum.

Another characteristic flight speed apart from the optimum is the speed at which the ratio Q_h/V is minimal. This is usually known as the cruising speed.

In the absence of wave drags,

$$V_{cruise} \approx 1.31 V_{opt}.$$

At a cruising speed corresponding to $M < M^*_{cr}$, $c_{x_i} = 1/3\ c_{x_0}$, $c_x = \frac{4}{3} c_{x_0}$, $\frac{c_y^{1/2}}{c_x}$ and KV are maximal and $K = 0.86K_{max}$.

A third characteristic flight speed is the economy speed, which requires minimum power (Fig. 4.10):

$$N_n = \frac{Q_r V}{75}. \tag{4.28}$$

In the absence of wave drags, $V_{ec} = V_{opt}/1.31$. At the economy speed, $c_{x_i} = 3c_{x_0}$, $c_x = 4c_{x_0}$, $\frac{c_y^{3/2}}{c_x}$ is maximal and $K = 0.86K_{max}$.

Figure 4.11 shows the positions of the characteristic speeds on the curve of $Q_h = Q_h(V)$ and the characteristic c_y on the polar curve of the airplane. To construct a family of curves of Q_h =

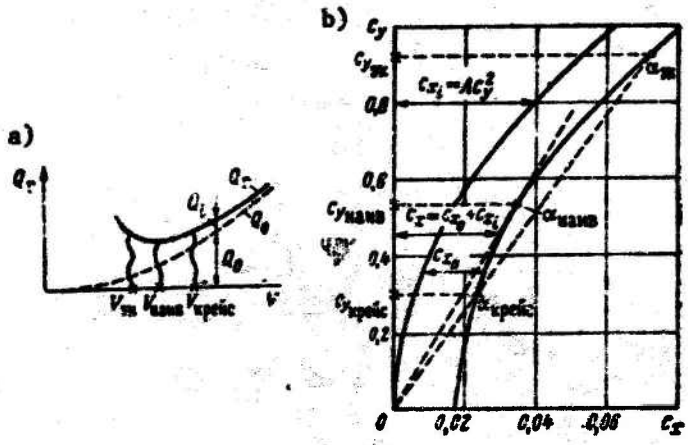

Figure 4.11. a) Positions of characteristic level-flight speed on curve of $Q_h = Q_h(V)$; b) positions of characteristic c_y on aircraft polar curve.

$= Q_h(M)$, it is necessary to have the relation $c_{x_0} = c_{x_0}(M)$ and $A = A(M)$ (see Figs. 4.5 and 4.6). Applying (4.26), we can plot Q_0, Q_{ih}, and Q_{i1} as function of M (Fig. 4.12) for a given flight altitude, e.g., H = 11,000 m. Since Q_0 is directly proportional to the atmospheric pressure p and Q_{ih} is inversely proportional to it, we obviously have for any altitude

$$Q_r = Q_{011}\frac{p}{p_{11}} + Q_{i11}\frac{p_{11}}{p}. \tag{4.29}$$

Formula (4.29) was derived without consideration of the effect of altitude on c_{x_0} through Re.

It is easy to introduce the influence of Re on c_{x_0} into the calculation. For this purpose, c_{x_0} is calculated for several altitudes and becomes dependent on the coefficient $K_{Re} = c_{x_0}/c_{x_{011}}$, which varies with altitude.

In this case, Q_h is determined from the following expression for any altitude:

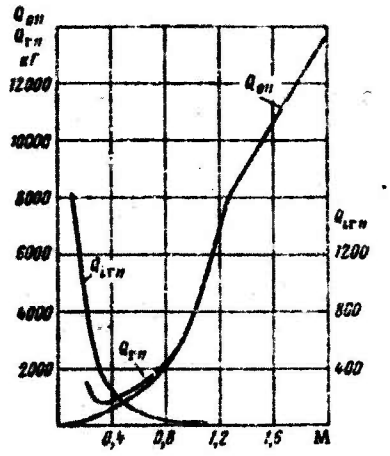

Figure 4.12. Example of Mach-number curves of Q_{011}, $Q_{i\,h11}$, and Q_{h11}.

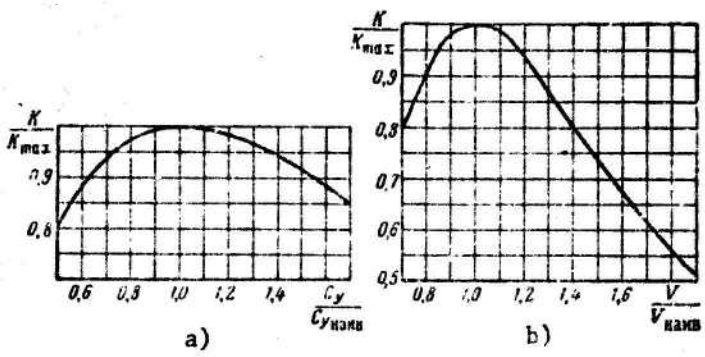

Figure 4.13. a) Plot of $\bar{K} = K/K_{max}$ vs. $c_y/c_{y_{opt}}$; b) plot of $\bar{K} = K/K_{max}$ vs. V/V_{opt}.

$$Q_{\text{г}} = Q_{011} K_{\text{Re}} \frac{p}{p_{11}} + Q_{i\,\text{г}11} \frac{p_{11}}{p}. \tag{4.30}$$

In analytical calculations of Q_{h} for subsonic speeds, it is more convenient in many cases to determine it not with (4.26), but by dividing the weight by the lift/drag ratio, which depends on the maximum lift/drag ratio and the ratio of actual speed to optimum speed.

It is easily shown that (Fig. 4.13)

$$K = K_{max} \frac{2}{\frac{c_y}{c_{y_{наив}}} + \frac{c_{y_{наив}}}{c_y}}. \tag{4.31}$$

or

$$K = K_{max} \frac{2}{\left(\frac{V}{V_{наив}}\right)^2 + \left(\frac{V_{наив}}{V}\right)^2}. \tag{4.32}$$

Thus, having calculated the optimum speed

$$V_{наив} = \sqrt{\frac{2GA^{1/2}}{\varrho S c_{x_0}^{1/2}}} \tag{4.33}$$

and K_{max} for any speed, we find the lift/drag ratio from (4.32) and, dividing the weight by it, determine Q_h. This method is highly convenient in that it permits easy allowance for the influence of changes in aircraft weight and c_{x_0} on Q_h without plotting the entire dependence of Q_h on flight speed.

Assuming for high supersonic flight speeds that Q_0 is proportional to M and that, as a result of the variation of A, Q_{ih} is inversely proportional to it, we find that

$$K = K_{max} \frac{2}{\left(\frac{V}{V_{наив}}\right) + \left(\frac{V_{наив}}{V}\right)}. \tag{4.34}$$

This relation is less exact than (4.31) or (4.32), since the maximum lift/drag ratio usually decreases, if slowly, with increasing M.

§4.4. THRUST OF TURBOJET AND TURBOFAN ENGINES (TJE AND TFE)

The thrust of a TJE depends on its thermodynamic and design parameters, its speed, the flight Mach number, and the air temperature and pressure.

A decrease in engine rpm caused by reduced fuel delivery results in a sharp drop in thrust. Near its maximum, thrust is approximately proportional to the fourth power of rpm.

With increasing M, the thrust of a TJE first drops by 12-15% at maximum rpm. A thrust minimum occurs at M = 0.2-0.4. On a

further increase in M, the thrust increases. The rapidity of the thrust buildup depends primarily on the compression ratio of the air in the compressor. The higher the compression ratio, the more rapidly does thrust increase with M. When the airplane reaches certain Mach numbers, which depend on a whole series of factors (a temperature ahead of turbine, compression ratio, air-intake characteristics, etc.), the thrust of the TJE reaches its maximum value, and a further increase in M results in a sharp thrust decrease (Fig. 4.14a).

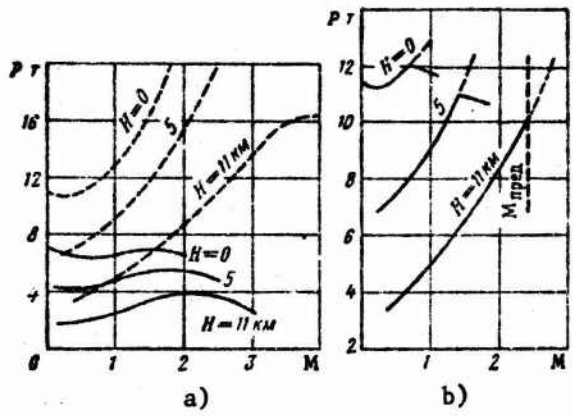

Figure 4.14. a) Thrust of TJE as function of M and altitude. Solid line: engine thrust without augmentation; dashed line: with augmentation; b) thrust of TJE with augmentation as a function of M and altitude. Solid line: strength limitations; dashed line: thrust without these limitations.

If the engine is fitted with an afterburning system, there may be no decrease in thrust in the range of small M, and the trust increase with M may take place much more rapidly (see dashed curve on Fig. 4.14a). Hence the thrust increase gained with the afterburner increases with flight speed.

For many present-day TJE's, engine thrust shows a characteristic faster-than-proportional rise with Mach number when the engine is operated at full augmentation and supersonic speeds. Use of ejector nozzles contributes greatly to fast TJE thrust

buildup with increasing speed.

For geometrically similar engines, thrust is proportional to the square of engine diameter.

The thrust of a TJE depends on the temperature and pressure of the ambient air. At constant air temperature, thrust is directly proportional to pressure. This describes the decrease in thrust with increasing altitude in the stratosphere. The law is approximate because the Reynolds number at which the compressor blades are operating decreases with increasing pressure at constant temperature, so that compressor efficiency is lower. In the presence of a regulator that ensures constant temperature ahead of the turbine this causes the thrust of the TJE to drop off somewhat more rapidly in the stratosphere than in proportion to the pressure change. This effect is disregarded in most calculations.

A decrease in air temperature increases thrust. As a result, TJE thrust decreases more slowly than air density in the troposphere at constant speeds and rpm.

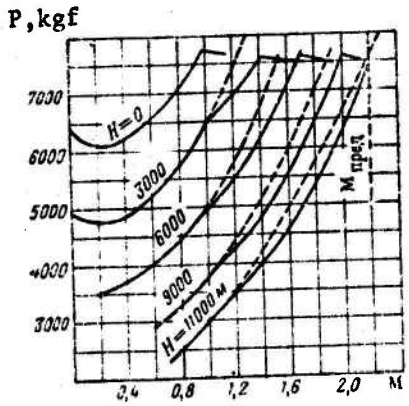

Figure 4.15. Thrust of TJE operated with augmentation as a function of M and altitude. Solid line: effective thrust; dashed line: thrust without losses at entry of air into diffuser.

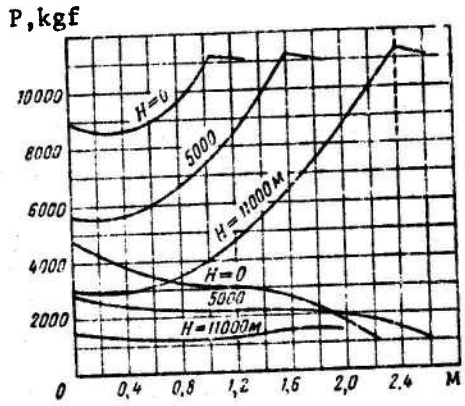

Figure 4.16. Thrust of TFE as function of M and altitude (with and without primary and duct afterburning).

The altitude curve of thrust depends on engine setting, but for most engines at V = const below H = 11 km it is closely approximated by

$$P_H = P_0 \Delta^n. \tag{4.35}$$

For TJE, n = 0.7-0.8.

At M greater than unity, the drop in thrust with altitude is slower.

As flight altitude increases to 11,000 m, the Mach number at which thrust reaches its maximum value ($M_{P_{max}}$) increases. $M_{P_{max}}$ remains unchanged in the stratosphere at constant air temperature.

Because of strength limitations, the maximum delivery of fuel to an engine operating with augmentation is limited at heights below 11,000 m at $M < M_{P_{max}}$, and the P = P(M) curve assumes the form shown in Fig. 4.14b. For most TJE's, $M_{P_{max}}$ in augmented operation exceeds the highest M at which engine performance is stable. Actually, therefore, $M_{P_{max}} = M_{lim}$ (see Fig. 4.14b).

At M below 1.1-1.3, the losses at entry of the air into the TJE are relatively small. If, however, the engine is used on an airplane capable of flight at Mach two and faster, proper profiling of the inlet diffuser becomes very important. At a given pressure recovery factor in the diffuser and the diffuser design Mach number, which usually equals M_{lim}, the thrust-lowering losses in the diffuser are small at the design altitude, which is 11,000 m for many TJE's. As M is lowered from M_{lim} to M = 1, the losses increase. They increase especially rapidly at $M > M_{lim}$. At altitudes above 11 km, they decrease in proportion to the thrust decrease. Diffuser losses increase rapidly below 11 km.

TJE augmented thrusts for several altitudes are indicated by the solid lines in Fig. 4.15, with consideration of losses in the diffuser and the restrictions on fuel delivery to the engine's afterburners.

In computing the flight characteristics of an airplane, the thrust value used should be that actually developed by the engines with consideration of the diffuser and ejector-nozzle losses. These thrust values are referred to as effective thrusts.

For some engines, maximum delivery of fuel to the afterburners at maximum rpm and $M = M_{lim}$ is permitted beginning at an altitude higher than 11,000 m. In this case, the decrease in thrust with altitude is proportional to atmospheric pressure only beginning at this altitude.

Turbofan engines (TFE) have now come into extensive use. They are more economical than TJE's in unaugmented flight at subsonic speeds. Without augmentation, the thrust of these engines decreases steadily with increasing speed in the subsonic range. It does not increase with M at large Mach numbers, as it does in the TJE, but simply drops off somewhat more slowly (Fig. 4.16).

If fuel is afterburned in both ducted and turbine air, the augmented thrust increases even more rapidly with increasing M than in the case of the TJE. On the whole, given equal temperatures ahead of the turbine and in the afterburner and equal engine weights, the augmented thrust of a TFE may exceed that of a TJE at high supersonic speeds. At the same time, the TFE has a larger frontal area than the TJE, but it is shorter.

Chapter 5

FLIGHT SPEED AND ALTITUDE RANGES, RATE OF CLIMB, AND THEIR VARIATIONS WITH AIRCRAFT AND ENGINE PARAMETERS

§5.1. TOP SPEED AND ITS VARIATION WITH ALTITUDE FOR SUBSONIC AND TRANSONIC TJE AIRCRAFT

We shall call aircraft for which $M_{max} < M^*_{cr}$ subsonic, and those for which $M^*_{cr} < M_{max} < 1\text{-}1.1$ transonic.

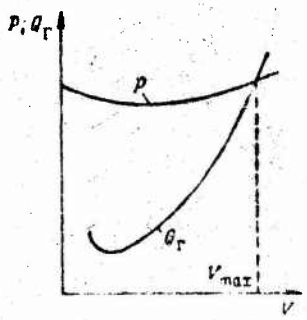

Figure 5.1. Determination of V_{max} of TJE aircraft from curves of $Q_h = Q_h(V) = P_r$ and $P = P(V)$.

Equation (4.3) implies that the frontal drag Q_h and the thrust of the engines must equal one another in level flight at constant speed.

Obviously, the greater the thrust of the engines, the higher will be the speed at which this equality is attained. Consequently, flight at V_{max} will be flight at maximum engine thrust. On the curves of available and required thrust, top speed is determined by the intersection of the curves of $Q_h = Q_h(V)$ and $P = P(V)$ (Fig. 5.1). The thrust of TJE's is taken at maximum rpm and, for augmented engine operation, also for maximum fuel delivery into the afterburner.

It follows from the above that at top speed

$$c_{x_r} S \frac{\rho V^2}{2} = c_{x_r} S \frac{\Delta V^2}{16} = P_{max}$$

and

$$V_{max} = \sqrt{\frac{16 P_{max}}{c_{x_r} S \Delta}},$$

where

$$c_{x_r} = c_{x_0} + c_{xi\,r}.$$

For present-day aircraft, however, $c_{xi\,h}$ comes to be a substantial fraction of c_{x_h} only at altitudes approaching the ceiling. At low and medium altitudes, c_{x_h} is determined by c_{x_0} at V_{max}. This means that the V_{max} for a given altitude (a given Δ) depends on the relation between P_{max} and the product $c_{x_0} S$:

$$c_{x_0} S = c_{x_{0\,exp.on}} S + c_{x_\phi} S_\phi + c_{x_{M.r}} S_{M.r}.$$

The larger P/S and the smaller c_{x_0}, the larger the value of V_{max}.

From the first airplane flight to the present day, the development of aviation has been accompanied by a continuous increase in maximum flight speed; this has been brought about both as a result of increasing P/S and decreasing c_{x_0}.

The values of P/S were increased by increasing thrust and reducing wing area. Smaller wing areas gave increased loads per square meter of wing.

Let us briefly discuss the measures that have lowered the value of c_{x_0} to a fraction on the present-day airplane — from c_{x_0} = 0.07-0.075 for the 1915/1917 biplane fighter to c_{x_0} = 0.011-0.016 for the modern interceptor operating at $M < M^*_{cr}$.

a) in the case of the modern airplane, only the wing, fuselage, control surfaces and, in a few cases, engine nacelles are swept by the free stream.

The weapons systems of many aircraft are enclosed; this applies not only to bombs, but also to guided rocket missiles.

Use of nonretracting landing gear, struts, braces, and tension bands is permissible only for aircraft for which higher top speed is less important than other requirements;

b) in virtue of its special planform, set of profiles, and high-lift devices, the wing of the modern airplane is capable of combining a small $c_{x_{0_{wg}}}$ with a relatively large $c_{y_{ldg}}$. A high-lift device consists of a singly or multiply slotted flap designed for boundary-layer blowing or a flap or turndown on the leading edge of the wing that produces the same effect. It has recently become possible to change the sweep angle of the wing in flight. This approach will undoubtedly be used with increasing frequency in the future;

c) an indispensible requirement for the modern airplane is that the wing, fuselage, and tail assembly be smooth;

d) the design and manufacturing technology of the airplane prevent the entry of air into the wings, tail assembly, or fuselage and its circulation inside them, since this would cause a substantial increase in c_x.

Let us turn to the influence of flight altitude on top speed.

We first consider a TJE airplane for which $M < M^*_{cr}$ at V_{max} regardless of altitude, so that there are no wave drags.

Since, according to (4.35), the thrust of a TJE at V = const decreases more slowly with altitude than the relative air density Δ, the ratio P/Δ will increase for V_{max}. Thus, P/Δ is approximately 1.4 times larger at 11,000 m than it is on the ground.

At the same time, c_{x_h} will also increase with increasing flight altitude, since $c_{x_{ih}}$ is inversely proportional to the square of air density.

For most TJE aircraft operating below 11,000 m, $P/\Delta c_{x_h}$ and, consequently, also V_{max} increase with altitude (Fig. 5.2); only for those aircraft that have very large c_{x_i} can V_{max} begin to decrease with altitude below 11,000 m. Above 11,000 m, V_{max} always decreases with increasing altitude, since P/Δ remains constant and c_{x_h} increases.

To calculate the change in V_{max} with altitude, Q_g is calculated and Zhukovskiy curves plotted for several altitudes. The intersection of the curves or $Q_h = Q_h(V)$ with the curves of $P = P(V)$ will determine the value of V_{max}.

Top-speed flight at $M < M^*_{cr}$ is possible only for aircraft with low thrust/weight ratios, e.g., trainers and light sport aircraft, and for multiengined jet aircraft with one or more engines out. The Mach number calculated on the assumption of zero wave drag is found to exceed M^*_{cr} for military and even passenger aircraft with TJE's and TFE's, if not on the ground, then at high altitudes at V_{max}.

In unaugmented operation of TJE's on any modern aircraft, including most interceptors, P/S is such that $M_{V_{max}}$ is only a little larger than M^*_{cr} and does not exceed unity.

Since the speed of sound decreases with increasing altitude up to H = 11,000 m, the critical flight speed $V^*_{cr} = aM^*_{cr}$ above which wave drag appears also decreases with altitude.

In addition, M^*_{cr} may be lowered slightly as a result of the increased c_y. The net result is that the V_{cr} at 11,000-m altitude will be about 15-17% below the V^*_{cr} on the ground.

If V_{max} did not vary with altitude, $M_{V_{max}}$ at H = 11,000 m would be found larger than the $M_{V_{max}}$ on the ground, also by 15-17%. If $M_{V_{max}} = M^*_{cr}$ or exceeds it on the ground, the rule is that the relative increase in the airplane's c_{x_0} owing to increased wave drag will exceed the increase of P/Δ due to higher flight

altitude. This is why V_{max} cannot remain constant, but decreases slowly with increasing altitude. At the same time, the higher the altitude of flight, the larger are $M_{V_{max}}$ and the difference $(V_{max} - V^*_{cr})$.

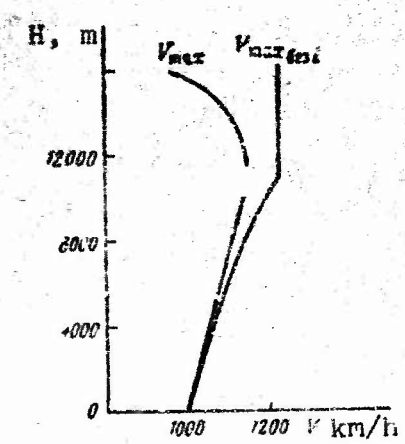

Figure 5.2. Variation of maximum flight speed with altitude for a subsonic airplane.

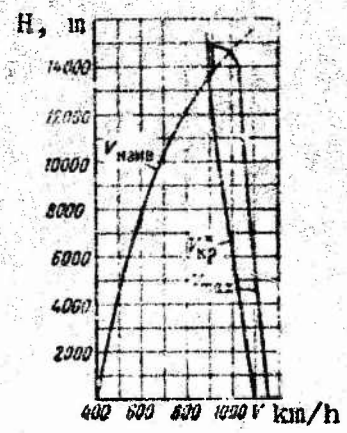

Figure 5.3. Top speed of transonic airplane as a function of flight altitude.

On the whole, transonic aircraft are characterized by the altitude curve of V_{max} shown in Fig. 5.3.

It follows from the above that the magnitude and variation of V_{max} with altitude are determined basically by V^*_{cr} for a transonic aircraft. We note that $M_{V_{max}}$ increases with altitude for all transonic aircraft because of the increase in P/Δ.

The difference $V_{max} - V^*_{cr}$ cannot be calculated analytically, since a rapid increase in c_{x_0} takes place at $M^*_{cr} < M < 1.4$. It can only be stated that the larger P/S and the thinner the wing profile, the larger will be $V_{max} - V^*_{cr}$. This difference will be smaller for an airplane with an unswept trapezoidal wing than for one with a strongly swept wing.

For the above reasons, it is necessary to abandon analytical methods for calculation of the altitude variation of V_{max} for the

transonic airplane, and to construct a family of $Q_h = Q_h(M)$ curves for several altitudes.

The above implies that the designer wishing to increase the top speed of a new transonic aircraft design must give the vehicle the largest possible M^*_{cr}.

M^*_{cr} increases as a result of:

a) a decrease in wing profile thickness;

b) use of special "M-stable" wing profiles;

c) sweeping the wing.

A decrease in profile thickness from 12% to 6% increases M^*_{cr} by about 0.08-0.10.

For a wing with a quarter-chord sweep of 35°, M^*_{cr} increases by about 15% over that for an unswept wing.

Increasing the sweep to 45°-55° produces little increase in M^*_{cr}, but the rate of increase of c_{x_0} drops off markedly at $M > M^*_{cr}$.

§5.2. TOP SPEED AND ITS ALTITUDE VARIATION FOR PARTIALLY AND FULLY SUPERSONIC AIRCRAFT

Use of thin profiles and increased sweep angles reduce the rate of increase of $c_{x_{C_{wg}}}$ at $M > M^*_{cr}$.

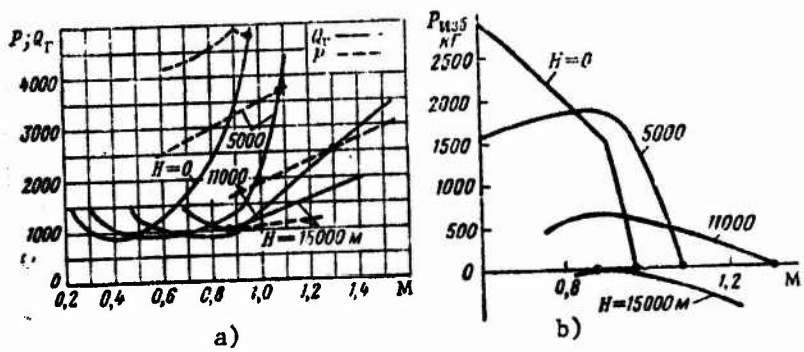

Figure 5.4. a) Typical Mach-number curves of Q_h and P for partially supersonic airplane; b) P_{exc} as a function of altitude and M for partially supersonic aircraft.

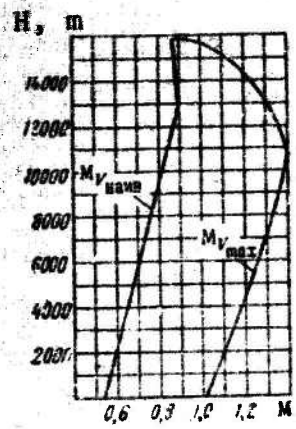

Figure 5.5. Mach number as a function of altitude at V_{max} for partially supersonic airplane.

Use of an afterburner increases P/S. The net result is that the $M_{V_{max}}$ on the ground has come to exceed M^*_{cr} by a substantial margin.

Increasing the altitude from H = 0 to H = 11,000 m increases P/Δ by a factor of about 1.4. For a thin wing profile, this increase in P/Δ can increase top speed very sharply, even into the supersonic range. Such a case is shown in Figs. 5.4 and 5.5.

For an airplane whose Zhukovskiy curves take the trend shown in Fig. 5.4 at 11,000-m altitude, there is a characteristic rapid decrease in the excess thrust $P_{exc.11} = P_{11} - Q_{011} - Q_{i\ h\ 11}$ with the approach to $M_{V_{max}}$. As altitude increases above 11 km, the difference $P - Q_0$ will decrease in proportion to the air density. Moreover, P_{exc} will also decrease owing to the larger $Q_{i\ h}$. The rapid decrease of P_{exc} with altitude (see Fig. 5.4b) causes a rapid decrease in $M_{V_{max}}$ and the airplane will be flying at transonic speed at its ceiling (see Fig. 5.4b). As a result, supersonic speeds are reached only in a certain altitude range for an aircraft characterized by the $Q_h = Q_h(M)$ and $P = P(M)$ curves shown in Fig. 5.4. However, flight at the ceiling and, as will be shown below, at maximum rate of climb must take place at M smaller than or only slightly greater than M^*_{cr}. We shall refer to such airplanes as partially supersonic.

Use of ejector nozzles and higher afterburner temperatures gives a greater increase in thrust with increasing M and, as we have noted, the thrust output of many modern TJE's increases more rapidly with speed than it would if thrust increased in proportion to M. Reducing the weight of the TJE has also made it

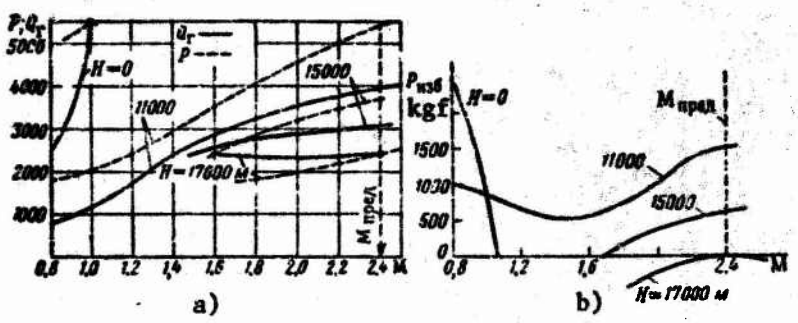

Figure 5.6. a) Typical Mach-number curves of Q_h and P for fully supersonic airplane; b) P_{exc} as a function of altitude and M for fully supersonic airplane.

possible simultaneously to increase P and the ratio P/S. As a result, TJE's came to deliver thrusts in excess of Q_h in flight at M = 1.3-1.4 at 11,000 m. At larger Mach numbers, however, Q_h varies at a rate proportional to M instead of M^2. The net result is that P_{exc} has begun to increase rather than decrease at M > 1.3-1.4 (Fig. 5.6).

With this trend of the available- and required-thrust curves, equality of P and Q_h is attained only at the Mach number at which the increase of thrust with speed begins to slow down rapidly.

For TJE's with afterburners, the rule is that these Mach numbers exceed the M_{lim} at which engine performance is stable (without surge). Hence the maximum thrust P_{max} corresponds to the limiting Mach number M_{lim} for which the inlet diffuser is designed.

In some cases, the decrease of excess thrust begins at a Mach number just below M_{lim}.

With the curves of P = P(M) and $Q_h = Q_h(M)$ shown in Fig. 5.6a, P_{exc} varies with altitude and M as shown in Fig. 5.6b, and $M_{V_{max}}$ as shown in Fig. 5.7. We see that the highest flight altitude (the ceiling) corresponds to flight at $M = M_{lim}$. It will be shown below that the per-kilometer fuel consumption will also be minimal in flight at $M = M_{lim}$. The rate of climb also reaches its

maximum at $M = M_{lim}$.

Aircraft having characteristics similar to those shown in Fig. 5.7 will be referred to as fully supersonic, since all of the most important flight regimes (top speed, maximum rate of climb, ceiling) are reached at supersonic flight speeds.

Turning to foreign aircraft-design experience, we see that all supersonic aircraft were partially supersonic during a certain period of the development of aviation, but that such aircraft are now seldom manufactured in quantity and have been replaced by fully supersonic types.

The abandonment of long-run production of partially supersonic airplanes is explained by the following factors. Such airplanes must have thin, low-aspect-ratio swept wings. As a result, they have low maximum lift/drag ratios at subsonic speeds and small $c_{y_{max}}$. At the same time, a partially supersonic aircraft, which has the disadvantages of the fully supersonic aircraft, can reach supersonic speeds only in a relatively narrow altitude range, and the value of $M_{V_{max}}$ will itself depend strongly on the temperature in the stratosphere, since even a small decrease in P_{exc} owing to a decrease in the thrust of the TJE lowers $M_{V_{max}}$ sharply (see Fig. 5.4b).

For the airplane to become fully supersonic, the relation between the TJE's thrust and $c_{x_0}S$ must be such that considerable excess thrust is available at $M = M_{lim}$ at 11,000 meters of altitude and that the product $P_{exc}V$ at $H = 11$ km and $M = 1.2$-1.3 be smaller than the product $P_{exc}V$ at the same altitude and $M = M_{lim}$.

We shall discuss the $c_{x_0}S$ relation for the fully supersonic airplane in greater detail below in our discussion of the supersonic ceiling.

For all supersonic aircraft, flight at $M_{V_{max}} = M_{lim}$ is attained with the TJE's in augmented operation. If the TJE is not

augmented, the variation of $M_{V_{max}}$ with altitude is the same for most supersonic airplanes as for transonic types.

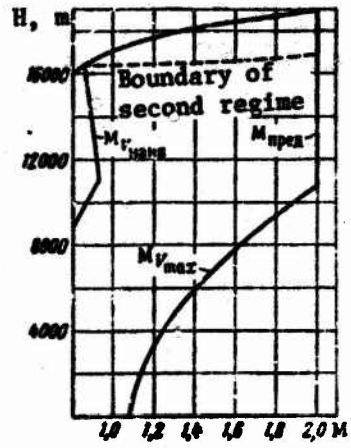

Figure 5.7. M at V_{max} as a function of altitude for a fully supersonic airplane.

For a fully supersonic airplane at altitudes below the supersonic ceiling but higher than 11,000 m, the curves of $P = P(M)$ and $P_h = Q_h(M)$ take the trends shown in Fig. 5.6a. We see that thrust equals frontal drag not only at $M = M_{lim}$ (H = 17 km), but also at $M < M_{lim}$ (H = 15 km). Thus, the thrust of the TJE determines not only the supersonic top speed, but also the lowest supersonic speed, below which horizontal flight can be executed only with deceleration, since $Q_h > P$. This speed may be referred to as the minimum supersonic speed.

The altitude variation of both the top speed and the minimum supersonic speed can be obtained by plotting a family of curves of $P = P(M)$ and $Q_h = Q_h(M)$. However, for altitudes above 11,000 m, at which the TJE's thrust varies in proportion to air pressure at constant air temperature and M = const, there is a very simple and more convenient analytical method for calculating the maximum and minimum level-flight supersonic speeds. The essentials of this method are as follows. The engine thrusts at 11,000 m and H > > 11,000 m are related by the expression $P_H = P_{11}(p_H/p_{11})$. Since the thrust P_H equals Q_{H_h} at V_{max} and the supersonic V_{min}, we have according to (4.29)

$$P\frac{p_H}{p_{11}} = Q_{011}\frac{p_H}{p_{11}} + Q_{l\,11}\frac{p_{11}}{p_H}.$$

Solving the equation for p_H, we find

$$p_H = p_{11}\sqrt{\frac{Q_{i\,h\,11}}{P_{11} - Q_{011}}}. \qquad (5.1)$$

Assigning a series of values to M, we calculate Q_{011} and $Q_{i\,h\,11}$ for them and determine the TJE's thrust at 11,000 m with consideration of diffuser losses. We use (5.1) for each M to determine p_H. Knowing the p_H, we refer to the standard-atmosphere table to find the altitudes corresponding to each of the chosen M. Thus we obtain the relation between Mach number and altitude. Mach numbers smaller than M_{clg}, which is very close to M_{lim}, will be those of flight at the minimum supersonic speeds. Mach numbers $M > M_{clg}$ will correspond to V_{max}.

In the above method of calculating the altitude variation of the steady level-flight maximum and supersonic-minimum speeds for each M, we determined the altitude at which the TJE's thrust P equals the frontal drag of the airplane in level flight (Q_h). At higher altitudes and the same M, flight at constant speed is impossible, since $Q_h > P$. Consequently, each point of the curves of $V_{max} = V_{max}(H)$ and the supersonic $V_{min} = V_{min}(H)$ is a maximum-altitude point, i.e., a point of the ceiling for the particular M.

For this reason, the altitude curves of the supersonic V_{max} and V_{min} are sometimes called ceiling curves.

If the numerator and denominator of the radicand in (5.1) are divided by the product of the ram pressure and S, the result is

$$p_{H_{\text{пол}}} = p_{11}\sqrt{\frac{Ac_{M_{11}}^2}{c_{P_{11}} - c_{x_0}}} = \frac{G_{P_{11}}}{S\,0{,}7p_{11}M^2}\sqrt{\frac{A}{c_{P_{11}} - c_{x_0}}}. \qquad (5.2)$$

If the TJE's thrust decreases more rapidly than in proportion to pressure at altitudes above 11,000 m, the altitude of flight at the supersonic $M_{V_{max}}$ and $M_{V_{min}}$ can be determined from expression (5.1) or (5.2). For this purpose, p_H is calculated or the

assumption that the TJE's thrust is proportional to air pressure. We then figure the percentage by which the thrust at the resulting ceiling altitude is smaller than that which would be developed in the pressure-proportional case, reduced P_{11} or $c_{P_{11}}$ by the same percentage, and repeat the calculation.

It must be remembered that, for certain engines, thrust becomes more closely proportional to pressure with decreasing M. While the proportionality is hardly in evidence at M = 3, it is quite important at M = 2, especially at altitudes above 15,000 m. Correct calculation of the ceiling curve therefore requires knowledge of the deviation of the thrust from what it would be if it were proportional to pressure for a series of flight speeds.

In most cases, the designer places limits on the maximum permissible flight speeds.

If the speed limits (V_{lim}) are greater than the level-flight top speeds over the entire altitude range, the values of V_{lim} will obviously be determined only by the maximum diving speed of the airplane. If the speed limit is below top speed at all altitudes or at certain altitudes, the speed limit must obviously be regarded as the practical top speed. In flying at this speed, the pilot will not make full use of the engine's thrust.

Flight-speed limits are established from strength considerations or with allowance for the influence of structural deformation on the controllability of the airplane. In this case, the designer states maximum permissible ram pressures

$$q_{\text{прел}} = \frac{\varrho V^2_{\text{прел}}}{2}. \tag{5.3}$$

Speed limits may also be established on the basis of ensuring stable engine performance or with a view to the influence of air compressibility on the stability and controllability of the airplane. In this case, a maximum permissible Mach number (M_{lim}) is established.

If the limiting ram pressure (q_{lim}) is stated, airspeed will vary with altitude in accordance with the law

$$V_{пред} = \sqrt{\frac{2q_{пред}}{\varrho}} = 4\sqrt{\frac{q_{пред}}{\Delta}} \tag{5.4}$$

and will increase with altitude in proportion to $\sqrt{1/\Delta}$.

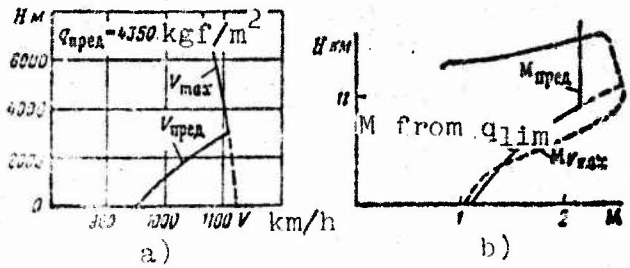

Figure 5.8. a) Speed limit of transonic airplane; b) Mach-number limit for supersonic airplane.

As a rule, the speed limit stated on the basis of q_{lim} limits the top speed from the ground to a certain altitude (Fig. 5.8a). At high altitudes, the speed is limited by M_{lim}, which does not vary with altitude (see Fig. 5.8b).

When the top speed is stated on the basis of a maximum permissible value M_{lim}, we obtain $V_{lim} = aM_{lim}$.

In this case, the top speed at the constant M_{lim} will vary with altitude like the speed of sound, i.e., it will decrease up to 11 km and then remain constant.

M_{lim} is of particular importance for modern fully supersonic TJE aircraft, since it determines more than the speed limit. As a rule, the larger M_{lim}, the higher is the ceiling, the higher the airplane's maximum rate of climb at supersonic speeds, and the lower the minimum per-kilometer fuel consumption at these speeds.

The most frequent practice is to limit speed on the basis of q_{lim} and M_{lim}. In certain cases, speed may be limited by other considerations, e.g., the heating of the airplane's skin, the permissible pressure exerted on the window glass of buildings by the sonic boom, the pressure difference across the duct supplying air to the engine, etc. We shall not dwell on these factors.

§5.3. THE AIRPLANE'S CEILING

The ceiling of an airplane is the highest altitude at which constant-speed level flight is possible.

Numerous sources refer to the "static" ceiling to draw a fine distinction between constancy of speed at the ceiling and variable-speed flight at altitudes above the ceiling. We shall not make use of this qualifier.

At ceiling altitude, the speed curves of TJE thrust and Q_h do not intersect, but touch one another. As a result, flight at the ceiling is possible only at a single defined speed.

If the airplane is subsonic and the wave drags do not influence Q_h, tangency of the curves of $P = P(M)$ and $Q_h = Q_h(M)$ occurs at the optimum speed, at which $K = K_{max}$ (Fig. 5.9) because the thrust of the TJE varies little with speed at Mach numbers considerably smaller than unity. Usually, $H_{clg} > 11{,}000$ m for TJE aircraft.

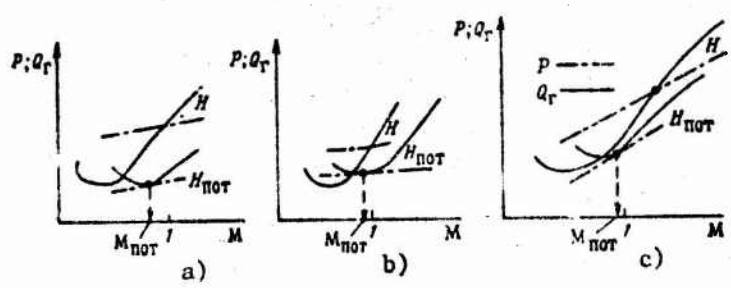

Figure 5.9. Trend of curves of drag Q_h and thrust P. a) In the absence of wave drags at ceiling altitude; b) in the presence of wave drags at ceiling altitude; c) in the presence of wave drags at ceiling altitude with TJE thrust-augmented.

At the ceiling in this case

$$P_{\text{пот}} = P_{11}\frac{p_{H_{\text{пот}}}}{p_{11}}, \quad Q_c = \frac{G}{K_{max}}.$$

Consequently,

$$P_{11}\frac{p_{H_{\text{пот}}}}{p_{11}} = \frac{G}{K_{max}},$$

whence

$$p_{H_{\text{пот}}} = \frac{p_{11}G}{P_{11}K_{max}}. \tag{5.5}$$

Averaging the thrust at 11,000 m over the M range from 0.6 to 0.9 and determining $K_{max} = (\sqrt{\pi\lambda_{ef}/c_{x_0}})/2$, we can apply (5.5) to calculate the pressure at the ceiling and thus find its altitude with almost the same accuracy as in a ceiling calculation by construction of Zhukovskiy curves or calculation of the Mach-number variation of altitude by means of (5.1).

This method of calculating the ceiling can be recommended for determination of the maximum flight altitude of a multiengined turbojet airplane in flight with one or more engines out or for airplanes with TJE's having low thrust loadings.

At the ceiling of a transonic airplane, the Mach number usually ranges from 0.7 to 0.9. At these Mach numbers, the thrust of a TJE without augmentation varies little with speed at high altitudes. As a result, the point of tangency of the thrust and frontal-drag curves is close to the optimum speed (see Fig. 5.9b). In this case, however, $K_{clg} < K_{max}$ calculated without consideration of wave drag.

Obviously,

$$p_{H_{\text{пот}}} = \frac{p_{11}G_{\text{пот}}}{P_{11}K_{\text{пот}}}. \tag{5.6}$$

The ceiling altitude of a transonic airplane can be calculated only approximately by (5.6), since the value of K_{clg} remains unknown.

It can be assumed for approximate calculations that $K_{clg}/K_{max} = 0.85\text{-}0.95$ for a transonic airplane.

Ceiling can be determined more accurately for transonic airplanes by plotting altitude as a function of M in accordance with (5.1). The ceiling for a partially supersonic airplane is computed in a similar fashion. For such an airplane, M_{clg} usually lies in the range from 0.95 to 1.1. At these M, the thrust of an augmented TJE rises rapidly with speed. As a result, the curves of $P = P(M)$ and $Q_h = Q_h(M)$ intersect at speeds greater than the optimum (see Fig. 5.9c). Under these conditions, even though formula (5.6) remains valid, we cannot use it to calculate the ceiling of a partially supersonic airplane, since P_{11} and K_{clg} are unknown.

As expressions (5.5) and (5.6) imply, the ceilings of subsonic, transonic, and partially supersonic airplanes are determined primarily by the thrust/weight ratio of the airplane, P_{11}/G, and the lift/drag ratio in flight at the ceiling, which is equal or nearly equal to K_{max}.

As a result, increases in thrust/weight ratio and K_{max} obtained by increasing the wing aspect ratio and reducing c_{x_0} are highly effective in raising the ceiling. If wave drags that lower the maximum lift/drag ratio occur at ceiling altitude, it becomes advantageous to lower the load per square meter of wing, since it lowers the optimum flight speed and, consequently, the ceiling speed, with the result that the wave drag vanishes.

Accordingly, a high-altitude transonic airplane must have a high thrust/weight ratio, a small load per square meter, and a large wing aspect ratio.

As we indicated above, flight of a fully supersonic airplane at its ceiling takes place at the largest permissible Mach number (M_{lim}) or at an M close to it, with maximum thrust from the TJE. This is because the thrust of the TJE increases rapidly with increasing M, while Q_h changes little with increasing M at the

altitude of the supersonic ceiling. The relative positions of the curves of $P = P(M)$ and $Q_h = Q_h(M)$ at the ceiling of a fully supersonic airplane are indicated in Fig. 5.6a ($H = 17{,}000$ m). It is found that, as thrust decreases or increases, M_{clg} remains almost constant, beginning to decrease only on a sharp decrease in thrust. We shall return again to the question of the value of M_{clg}.

At the ceiling,

$$P_{11M_{\text{пред}}}\frac{p_{H_{\text{пот}}}}{p_{11}}=Q_r=\frac{G}{K_{\text{пот}}},$$

whence

$$p_{H_{\text{пот}}}=\frac{p_{11}G}{P_{11M_{\text{пред}}}K_{\text{пот}}}. \tag{5.7}$$

The value of P_{11} is taken for $M_{clg} \approx M_{lim}$.

Let us discuss the value of K in flight at the ceiling.

As P_{11} increases, $P_{H_{clg}}$ decreases, flight altitude increases, and, consequently, $c_{y_{clg}}$ increases at constant M. At a certain value of P_{11}, which we shall arbitrarily call the optimum, flight at the ceiling will take place at the optimum c_y and K_{clg} will become equal to K_{max}. Let us show that $P_{11_{opt}}$ equals twice the profile and parasite drags in flight at an altitude of 11,000 m:

$$P_{11_{\text{opt}}}=2Q_{011}.$$

Under the conditions of flight at the ceiling with $M = M_{clg}$:

$$P_{H_{\text{пот}}}=c_{x_{\text{пот}}}0{,}7Sp_{H_{\text{пот}}}M^2_{\text{пот}}.$$

But $P_{H_{clg}} = P_{11}p_{H_{clg}}/p_{11}$. Using this, we get

$$P_{11}\frac{p_{H_{\text{пот}}}}{p_{11}}=c_{x_{\text{пот}}}0{,}7Sp_{H_{\text{пот}}}M^2_{\text{пот}}$$

and the conditions of flight at the ceiling imply the equality

$$P_{11} = c_{x_{пот}} 0{,}7\, S p_{11} M^2_{пот}. \tag{5.8}$$

If flight at the ceiling takes place with

$$c_{y_{пот}} = c_{y_{крейс}}, \qquad \text{we have} \qquad c_{x_{пот}} = 2c_{x_0}$$

and

$$P_{11_{opt}} = 2c_{x_0} 0{,}7\, p_{11} M^2_{пот} = 2Q_{011}. \tag{5.9}$$

Q.E.D.

Dividing left by left and right by right members of (5.8) and (5.9), we obtain a highly important parameter:

$$\bar{P} = \frac{P_{11}}{P_{11_{opt}}} = \frac{P_{11}}{2Q_{011}} = \frac{c_{x_{пот}}}{2c_{x_0}}. \tag{5.10}$$

If the airplane's polar curve is a second-degree parabola, then no matter what the values of c_{x_0} and A, the same ratio K/K_{max} will correspond to a given value of the ratio $c_x/2c_{x_0}$. Thus, for example, in flight at $c_{y_{cruise}}$, irrespective of c_{x_0} and A,

$$c_x = \frac{4}{3} c_{x_0}; \quad \frac{c_{x_{крейс}}}{2c_{x_0}} = \frac{2}{3}; \quad \frac{K_{крейс}}{K_{max}} = 0{,}86.$$

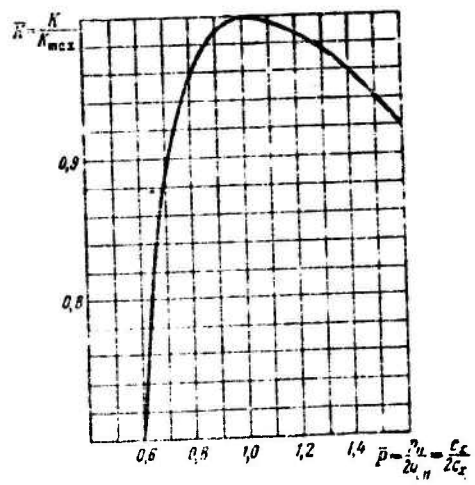

Figure 5.10. $\bar{K} = K/K_{max}$ as a function of $\bar{P} = \frac{P_{11}}{2Q_{011}} = \frac{c_x}{2c_{x_0}}$

The universal dependence of K/K_{max} on $c_x/2c_{x_0} = \bar{P}$ appears in Fig. 5.10. It is convenient for use in calculation of K_{clg} and determination of the ceiling altitude from expression (5.7). To this end, we compute the values of K_{max} and Q_{011} for $M = M_{clg} \approx M_{lim}$. Doubling Q_{011}, we find the ratio $\bar{P}$. Knowing $\bar{P}$, we refer to Fig. 5.10 to obtain the ratio K_{clg}/K_{max} and multiply the latter by K_{max} to obtain the unknown K_{clg}. Knowing K_{clg} and applying (5.7), we determind $p_{H_{clg}}$ and the altitude of the supersonic ceiling.

This method of calculation is quite accurate. It is possible to calculate $p_{H_{clg}}$ in the same manner by using (5.1) and taking the values of P_{11}, Q_{011}, and $Q_{i\ h\ 11}$ at $M_{clg} \approx M_{lim}$.

Let us consider the factors on which the supersonic-ceiling altitude depends.

It follows from (5.7) that an increase in thrust lowers $p_{H_{clg}}$ and raises the ceiling altitude. As long as $P_{11} < 2Q_{011}$, increasing the thrust moves $c_{y_{clg}}$ closer to $c_{y_{opt}}$ and increases K_{clg}.

At P_{11} greater than $2Q_{011}$, flight at the ceiling takes place with $c_{y_{clg}} > c_{y_{opt}}$. Under these conditions, an increase in P_{11} will lower K_{clg} instead of increasing it.

Substituting $c_{x_0} + Ac_y^2$ for $c_{x_{clg}}$ in (5.8), we get

$$c_{y_{пот}} = \sqrt{\frac{1}{A}\left(\frac{P_{11}}{0.7Sp_{11}M_{пот}^2} - c_{x_0}\right)} = \sqrt{\frac{c_{P_{11}} - c_{x_0}}{A}}. \qquad (5.11)$$

It follows from (5.11) that $c_{y_{clg}}$ and, consequently, K_{clg} do not depend on the weight of the airplane, but are determined primarily by P_{11}/S.

Likewise, it is easily found that

$$c_{y_{пот}} = c_{y_{наив}}\sqrt{2\left(\frac{P_{11}}{2Q_{011}}\right) - 1} = c_{y_{наив}}\sqrt{2\bar{P} - 1}. \qquad (5.12)$$

We have shown that at the supersonic ceiling, $c_{y_{clg}}$ may be either smaller or larger than the optimum, i.e., $c_{y_{clg}} < c_{y_{opt}}$ when $P_{11} < 2Q_{011}$ and $c_{y_{clg}} > c_{y_{opt}}$ when $P_{11} > 2Q_{011}$.

If $\bar{P} = P_{11}/2Q_{011} < 0.8$, it will be possible for M_{clg} to differ appreciably from M_{lim}.

In this case, it is recommended that the ceiling altitude be

determined by calculating the ceiling curve by expression (5.1) or (5.2).

It follows from (5.2) that a given ceiling altitude for $M = M_{lim}$ can be obtained with a large wing area (small G/S and small $c_{P_{11}}$) or with a small wing S (large G/S and large $c_{P_{11}}$).

Foreign aircraft-engineering experience has shown that the second alternative is preferable to the first. This, in turn, is explained by the fact that an increase in S reduces the difference $c_P - c_{x_0}$. When this difference is small, it decreases sharply even in response to a small decrease in thrust, such as might result from a rise in air temperature. As a result, the airplane's summer supersonic ceiling is found to be much lower than the winter ceiling altitude.

Further, as will be shown below, a small value of $c_{P_{11}} - c_{x_0}$ lengthens the time needed to reach supersonic speeds and increases fuel consumption.

According to (5.2), the pressure at ceiling altitude is directly proportional to the airplane's weight G at constant P_{11}, S, and M.

An increase in M_{lim} is accompanied by an increase in the altitude of the airplane's supersonic ceiling. This is understandable. As we have indicated, an increase in M_{lim} leads only to a slight decrease in the maximum lift/drag. At the same time, the thrust of a TJE with afterburning always rises rapidly with flight speed. At a large M_{lim}, therefore, it is easier to obtain a larger value of the product $P_{11}K_{clg}$ and thereby lower $p_{H_{clg}}$ than it is at small M_{lim}.

§5.4. CLIMBING. FLIGHT WITH ACCELERATION

Rate of climb is an important characteristics of an airplane. High rates of climb are especially important for interceptors.

It follows from (4.3) that

$$\frac{P-Q_r}{G}=\frac{1}{g}\frac{dV}{dt}+\sin\theta, \tag{5.13}$$

and, consequently, in the presence of a thrust excess $(P - Q_h) > 0$, the pilot can accelerate $(dV/dt > 0)$ or climb $(\theta > 0)$ or accomplish both simultaneously.

Multiplying the right and left sides of (5.13) by V, we find that at constant speed on a trajectory $(dV/dt = 0)$

$$V_y^*=V\sin\theta=\frac{(P-Q_r)V}{G}=n_xV. \tag{5.14}$$

The rate of climb at V = const has been denoted by V_y^*. It is easy to obtain an expression for V_y when speed changes along the trajectory from (5.13):

$$V_y=\frac{V_y^*}{1+\frac{V}{g}\frac{dV}{dH}}. \tag{5.15}$$

Hence we see that the more rapid increase in speed on the trajectory with altitude and the higher the trajectory speed V itself, the greater will be the difference between V_y and V_y^*.

A flying airplane possesses an energy E composed of its kinetic $E_k = mV^2/2$ and potential $E_p = GH$ energies. The energy per kilogram of aircraft weight is characterized by the energy altitude H_e:

$$H_e=H_k+H=\frac{V^2}{2g}+H. \tag{5.16}$$

Multiplying the right and left sides of (5.13) by ds, where s is the path length, and recognizing that $\sin\theta ds = dH$, we get

$$\frac{dV^2}{2g}+dH=n_xds=dH_e,$$

which implies that

$$\frac{dH_e}{dt}=n_xV=V_y^*. \tag{5.17}$$

Thus, V_y^* characterizes the rate of change of the airplane's energy altitude.

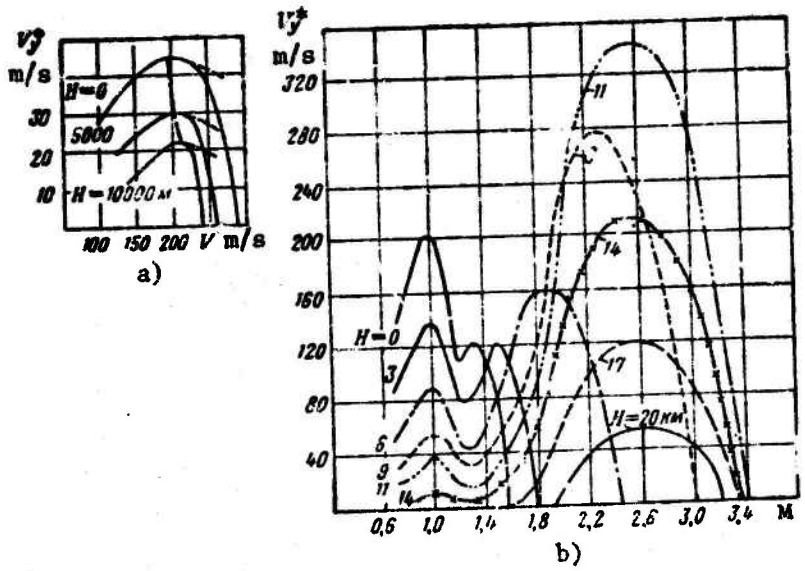

Figure 5.11. a) V_y^* as a function of altitude and speed for transonic and subsonic aircraft; b) V_y^* as a function of altitude and M for a fully supersonic airplane.

The energy altitude concept is extremely helpful in all cases in which flight speed changes simultaneously with a change in altitude.

It follows from (5.16) that

$$V=\sqrt{2gH_e-H}. \tag{5.18}$$

Knowing H and H_e, we can always find the flight speed by applying (5.18).

It follows from (5.17) that the energy altitude increases in the presence of a thrust excess ($n_x > 0$) and decreases when thrust is deficient. At $V_y^* = 0$, H_e is constant, but this does not mean that flight altitude is also constant. The latter may increase on a decrease in speed or decrease when speed increases.

The importance of the dependence of V_y^* on altitude and speed is evident from all of the foregoing. The nature of this dependence (Fig. 5.11a) is approximately the same for subsonic and

transonic aircraft. V_y^* is shown in Fig. 5.11b as a function of M and altitude for a fully supersonic airplane. The speed at which V_y^* is maximal is of particular interest for each altitude.

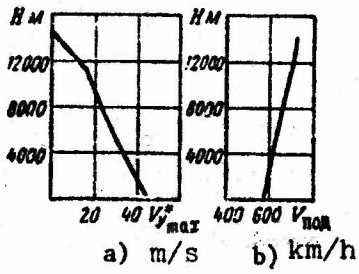

Figure 5.12. a) $V_{y_{max}}^*$ as a function of altitude for a subsonic airplane; b) V_{clb} as a function of altitude for a subsonic airplane.

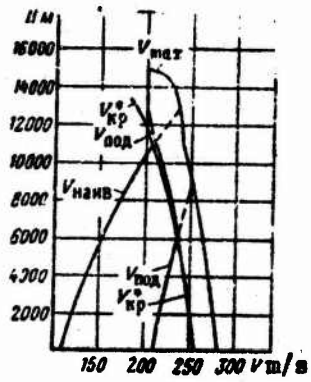

Figure 5.13. V_{clb} as a function of altitude for a transonic airplane.

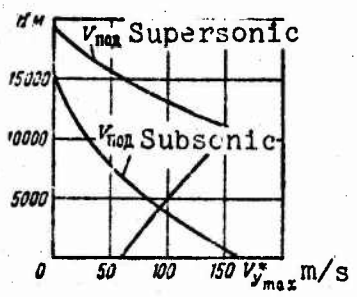

Figure 5.14. $V_{y_{max}}^*$ as a function of altitude for a fully supersonic airplane.

For subsonic, transonic, and partially supersonic aircraft, $V_{y_{max}}^*$ decreases with altitude owing to the decrease in $P - Q_h$ (Fig. 5.12a). The rate of climb V_{clb} corresponding to $V_{y_{max}}^*$ rises with altitude for the subsonic airplane (see Fig. 5.12b). For the transonic and partially supersonic aircraft, it increases to a point near V_{cr}^*. At high altitudes, the speed on a climbing trajectory with $V_{y_{max}}^*$ makes a close approach to V_{cr}^* (Fig. 5.13).

For a fully supersonic airplane, the increase in augmented engine thrust with speed becomes more rapid beginning at certain values of M, and Q_h begins to increase approximately in proportion to V

rather than V^2. As a result, V_y^* stops decreasing with increasing M and begins to rise. The result is a second maximum of V_y^*, which corresponds to $M = M_{lim}$ or to Mach numbers close to M_{lim} at altitudes above 11,000 m (see Fig. 5.11b).

At the second maximum, V_y^* has its largest value at 11,000 m. Above this altitude, it decreases with increasing altitude (see Fig. 5.11b). The net result is that V_y^* has its subsonic maximum at the ground and its supersonic maximum at an altitude of 11,000 m (Fig. 5.14).

If full fuel delivery to the afterburner is permitted beginning not at 11,000 m, but at a higher altitude, it is at precisely this altitude that V_y^* reaches its maximum.

For most modern aircraft capable of climbing at high speed, the climbing-trajectory speed should be determined with consideration of the influence of dV/dH on V_y and, consequently, on the time to climb.

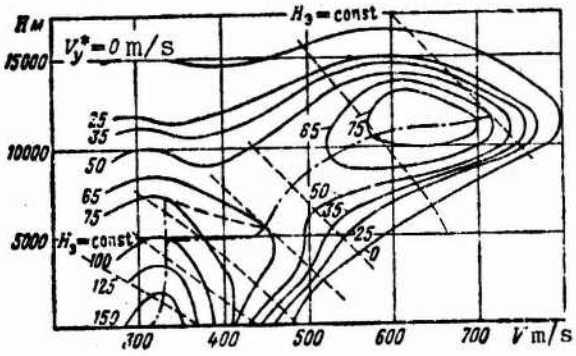

Figure 5.15. Diagram for calculation of V_{clb} as a function of altitude to ensure fastest climb to energy altitude.

It follows from (5.17) that the time (t) to climb to the energy altitude is

$$t = \int_{H_{э\,нач}}^{H_{э\,кон}} \frac{1}{V_y^*} dH_э. \qquad (5.19)$$

Determination of the altitude variation of speed along the trajectory that minimizes t is a complex variational problem. However, it is not necessary to solve it in preliminary design of the aircraft. Prof. I.V. Ostoslavskiy and A.A. Lebedev proposed an approximate method for computing time to climb. It assumes conventionally that the acceleration $n_y = 1$ during the climb. In this case, the variational problem becomes degenerate and reduces to determination of the speed and altitude at which V_y^* has its maximum value at each energy altitude (H_e).

If a family of $V_y^* = \text{const}$ curves [2.3] is plotted on the $V = V(H)$ diagram for constant H_e, the points of tangency of the $V_y^* = \text{const}$ curves with the curves of $H_e = \text{const}$ give the altitude variation of speed for which the maximum of H_e will be reached in the shortest time (Fig. 5.15). For a fully supersonic airplane, the diagram similar to that shown in Fig. 5.15 will always have a segment of motion with acceleration and descent at $H_e = \text{const}$. It is reasonable to replace it by acceleration along an approximately level trajectory, since no great altitude loss will occur on exact solution of the problem with consideration of n_y. Plotting of the lines $V_y^* = \text{const}$ requires many calculations; another method for computing the minimum time to climb and accelerate can therefore be recommended. The speed variation of $1/V_y^*$ is computed for a series of altitudes. H_e is determined for each speed, and the plots of $1/V_y^* = 1/V_y^*(H_e)$ are plotted on the same diagram for all altitudes. Then the envelope is drawn to these curves as indicated by the dot-dash line in Fig. 5.16.

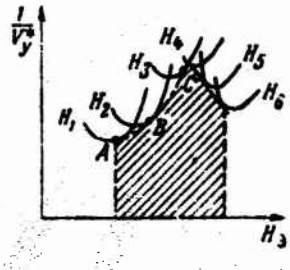

Figure 5.16. Diagram for calculation of shortest time to climb to energy altitude.

The shaded area on Fig. 5.16 gives the time required to change H_e from $H_{e_{ini}}$ to $H_{e_{fin}}$. Calculating the speeds corresponding to points A, B, C, ... on the curves, we obtain the altitude variation of the speed V along the climbing trajectory.

This method must be used to calculate the time to climb for fully supersonic airplanes.

For transonic and partially supersonic aircraft climbing with augmented thrust, it is permissible to assume the climbing speed constant and close to V^*_{cr} for the 11,000-meter altitude. If the airplane has a modest thrust/weight ratio, it can be recommended that V be calculated for $V^*_{y_{max}}$ at the ground and that the speed V_{clb} on the trajectory be taken as the mean between V_{clb} from the $V^*_{y_{max}}$ at the ground and the V^*_{cr} at 11,000-meter altitude. V^*_y is calculated for speeds computed by this method for several altitudes. Its altitude curve is plotted, and the time to climb is determined, adding to it the time to accelerate after takeoff to the ground value of V_{clb}. Since the variation of V_y with altitude is nearly linear from the ground to H = 11,000 m and beyond 11,000 m (but with a different slope), and $V_y = 0$ at the ceiling, it is quite permissible to find V_y at the ground and at 11,000 m in plotting this relationship.

If we assume a linear variation of V_y from the ground to the ceiling altitude H, the time to climb from the ground to altitude can be calculated with the expression

$$t_{наб} = \frac{2{,}3H_{пот}}{V_{y_{max0}}} \lg \frac{1}{1 - \frac{H}{H_{пот}}}. \qquad (5.20)$$

If it is necessary to make only rough calculations of the time to climb and the rate of climb for a fully supersonic airplane, the following procedure is admissible.

The time to climb to 11,000 m is calculated by the method described above. Then the time to accelerate from V^*_{cr} to the speed corresponding to M_{lim} is determined, and this is followed by calculation of the time to climb to the required altitude at $M = M_{lim}$.

Chapter 6

FLIGHT RANGE AND ITS VARIATION WITH AIRCRAFT AND ENGINE PARAMETERS

§6.1. ENGINE FUEL CONSUMPTION

We shall consider first the influence of altitude and Mach number on the specific fuel consumption C_{sp} for turbojets and turbofans operated at maximum rpm without augmentation (Figs. 6.1 and 6.2). The specific consumption in this case will be denoted by C'_{sp} to distinguish it from the value for a throttled-back TJE. At all Mach numbers, increasing the altitude to 11,000 m results in a lower C'_{sp}. The altitude change from 11,000 to 15,000 m has almost no effect on C'_{sp}. It increases appreciably on a further increase in altitude. Increasing the Mach number of flight causes specific fuel consumption to rise.

Figure 6.3 shows C'_{sp} as a function of M and altitude for augmented operation of turbofan and turbojet engines. Up to 11,000 m, altitude increase at constant M lowers C'_{sp}. Above 11,000 m, climbing increases C'_{sp} appreciably, especially above 15,000 m, and this increase is stronger at low Mach numbers than at high ones. All TJE's are characterized by a weaker dependence of C'_{sp} on Mach numbers $M > 1.2$-1.5.

It must be remembered that C'_{sp} depends appreciably on the parameters of the TJE. In unaugmented operation, turbofans have lower specific fuel consumptions than turbojets at subsonic speeds.

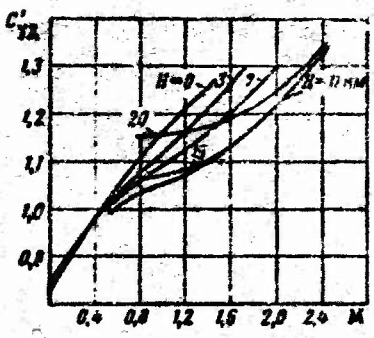

Figure 6.1. Specific fuel consumption of unaugmented turbojet as a function of M and altitude.

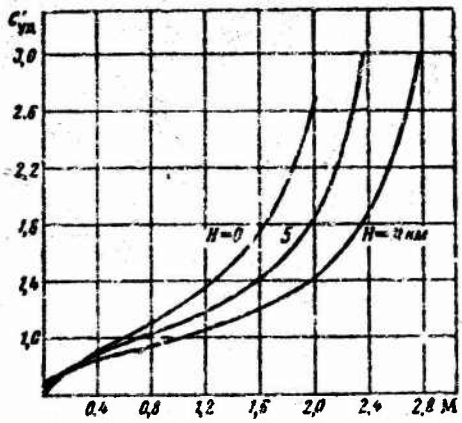

Figure 6.2. Specific fuel consumption of unaugmented turbofan as function of M and altitude.

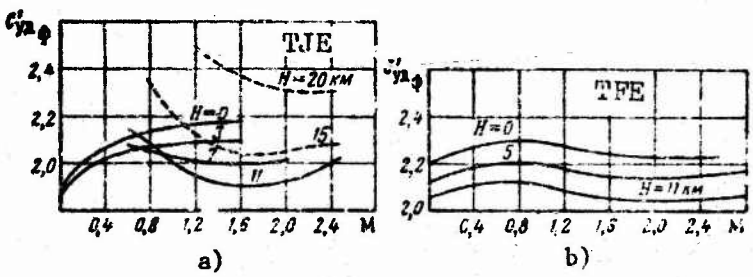

Figure 6.3. Augmented specific fuel consumption as a function of M and altitude: a) TJE; b) TFE.

The per-hour fuel consumption C_h equals the product of the thrust by C_{sp}: $C_h = C_{sp}P$. Since thrust decreases with increasing altitude and increases with increasing M, the per-hour fuel consumption will decrease rapidly with increasing altitude and increase with M. This is particularly strongly manifest in augmented operation of TJE's.

In supersonic flight at altitudes below the design altitude of the engine air inlet diffuser, the effective thrust P_{ef} of the engine is much smaller than the engine thrust obtained without consideration of the additional entry losses, while the per-hour

consumption remains unchanged. Hence the effective specific consumption referred to the effective thrust will be larger than the original specific consumption.

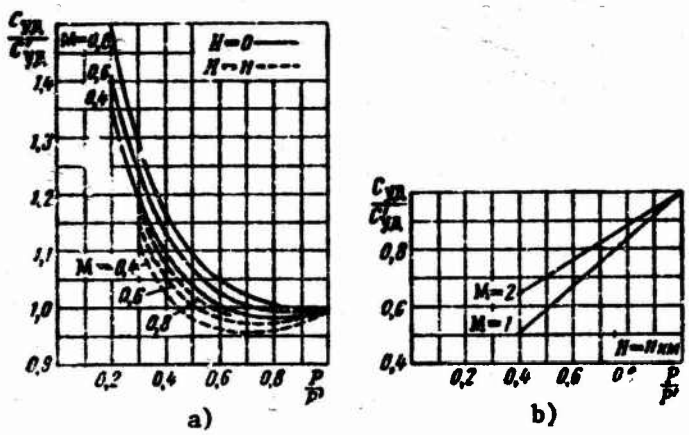

Figure 6.4. Influence of engine throttling on specific fuel consumption in operation: a) without augmentation; b) with augmentation.

In the quite frequent cases in which a definite thrust smaller than the maximum must be obtained from the engine at given M and altitude, fuel delivery is reduced (the engine is throttled back), whereupon engine speed decreases in unaugmented flight and even in augmented flight for certain TJE's. The throttling ratio is characterized by P/P' (the ratio of the thrust of the throttled-back engine P to its thrust P' at full delivery of fuel at the same altitude and Mach number).

We shall denote the specific consumption of the throttled-back TJE by C_{sp}. Then the influence of throttling of the TJE on C_{sp} will be given by the dependence of $\bar{C}_{sp} = C_{sp}/C'_{sp}$ on P/P'. Figure 6.4a shows the nature of this curve in unaugmented engine operation; it is determined to a substantial degree by the parameters of the TJE, the altitude, and the Mach number. The effect of throttling of the TJE on C_{sp} is small for many TJE's at high altitudes, Mach numbers from 0.8 to 0.95, and P/P' greater than 0.6, and it may be assumed that $C_{sp} = 0.95\text{-}0.97C'_{sp}$. If the TJE

is throttled far back ($P/P' = 0.25$-0.35), as may be required for level flight at low altitudes with $M = 0.5$-0.7, C_{sp} will exceed C'_{sp} substantially and may reach values of 1.4-1.5 or even larger ones.

Figure 5.4b shows $\bar{C}_{sp} = C_{sp}/C'_{sp}$ as a function of P/P' in augmented flight. We see that in this case throttling the TJE back causes a substantial decrease in specific fuel consumption. This decrease will be larger at lower Mach numbers.

§6.2. PER-KILOMETER AND PER-HOUR FUEL-CONSUMPTION RATES OF TJE AND TFE AIRCRAFT AT SUBSONIC AND TRANSONIC SPEEDS

The amount of fuel consumed during the time taken by the airplane in flying a distance of one kilometer with respect to the ground at constant altitude and speed is called the per-kilometer fuel consumption q.

When the wind is calm and the true speed V (the airplane's airspeed) equals its ground speed, the per-kilometer consumption is

$$q = \frac{C_h}{3{,}6V}. \tag{6.1}$$

In (6.1), speed is expressed in meters per second. In steady-speed level flight, the rpm of a TJE must be that at which the thrust developed by the engine equals the level-flight frontal drag Q_h of the airplane. Then, since $Q_h = G/K$, the per-hour and per-kilometer fuel consumption rates will be

$$C_h = \frac{GC_{yn}}{K}, \tag{6.2}$$

$$\left.\begin{aligned} q &= \frac{GC_{yn}}{3{,}6VK}, \\ q &= \frac{GC_{yn}}{3{,}6aMK}. \end{aligned}\right\} \tag{6.3}$$

If substantial thrust losses occur at the engine intake, the effective specific consumption should be used in expressions (6.2) and (6.3).

We shall first consider the influence of speed on the per-kilometer consumption in unaugmented flight at M below M^*_{cr}.

In high-altitude flight, the engine is run at almost full throttle, and at $P/P' > 0.6$, the influence of P/P' on C_{sp} is insignificant (see Fig. 6.4a). Under these conditions, we may assume with a certain approximation that C_{sp} is independent of flight speed.

Since $q = C_h/3.6V = C_{sp}Q_h/3.6V$, it is obvious that at constant C_{sp}, q will change with speed in the same way as the ratio Q_h/V.

It was shown in §4.3 that Q_h/V is minimal at the so-called cruising speed, which exceeds the optimum speed by a factor of 1.31. At this speed, the product KV is smallest and $K = 0.86K_{max}$.

Consequently, the airplane should be flown at cruising speed under conditions such that C_{sp} depends little on speed and the throttling of the TJE in order to obtain the lowest per-kilometer fuel consumption. This speed is easily found graphically on the Zhukovskiy curve of $Q_h = Q_h(V)$ by drawing a tangent to it from the origin.

For low-altitude flight, the engine must be throttled down considerably at cruising speed. Under these conditions, there is a rapid increase in C_{sp}. Thus, at the cruising speed, the ratio C_{sp}/KV is not minimal because of the larger C_{sp}, even though the product KV is maximal. Hence the minimum per-kilometer consumption will be obtained in flight near the ground at a speed higher than cruising. Obviously, the more rapid the increase in C_{sp} as the TJE is throttled back (as P/P' is reduced), the greater the margin by which the speed of minimum per-kilometer consumption will exceed cruising speed.

With increasing altitude, cruising flight will occur at steadily increasing values of P/P'. This is because the thrust of the TJE in maximum-rpm operation decreases with increasing altitude, while Q_h remains constant at a constant c_y. With

increasing altitude, therefore, the difference between the speed for minimum per-kilometer consumption and cruising speed will diminish.

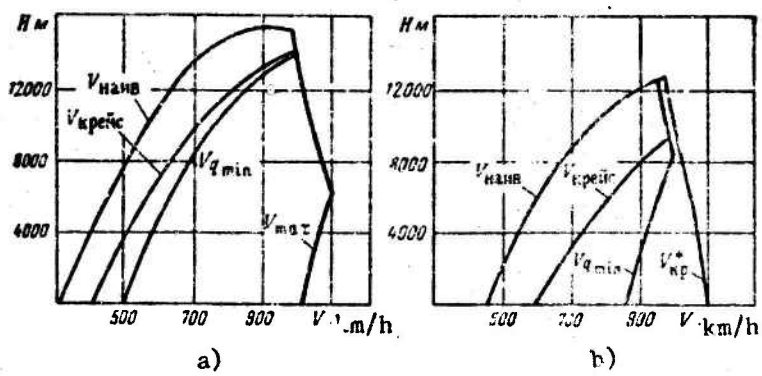

Figure 6.5. Flight speed for minimum per-kilometer fuel consumption as a function of altitude in unaugmented flight. a) Transonic airplane with wing aspect ratio larger than 6; b) supersonic airplane with wing aspect ratio smaller than 3-4.

The cruising speed is a speed with constant c_y. It therefore increases with altitude in proportion to $\sqrt{1/\Delta}$. The speed for minimal per-kilometer fuel consumption increases somewhat more slowly with altitude (Fig. 6.5a).

The cruising speed will be higher, the larger the load per square meter of wing and the smaller the wing aspect ratio. As a result, the cruising speed calculated on the assumption of constant c_{x_0} is found to exceed V^*_{cr} even at altitudes of the order of 6,000-10,000 m for transonic aircraft with large wing loads per square meter and small wing aspect ratios. It will be recalled that c_{x_0} increases rapidly at V^*_{cr} owing to the appearance of wave drag. An excess of speed over V^*_{cr} lowers the lift/drag ratio and increases per-kilometer consumption. For this reason, V^*_{cr} should be taken as $V_{q_{min}}$ (see Fig. 6.5b). Since V^*_{cr} decreases with altitude, the speed for minimal per-kilometer consumption does not increase with altitude at the altitudes for

which $V_{q_{min}} \approx V^*_{cr}$, but decreases slowly, becoming nearly constant above 11,000 m.

For supersonic aircraft in cruising flight at low altitudes, the engine must be throttled back very sharply, so that $V_{q_{min}}$ is considerably larger than V_{cruise}; at high altitudes, $V_{q_{min}} \approx V^*_{cr}$ and stops increasing with altitude (see Fig. 6.5b).

Let us consider the effect of flight altitude on per-kilometer fuel consumption. With increasing altitude, the speed at which the per-kilometer consumption is minimal increases. The lift-drag ratio at $V_{q_{min}}$ increases with altitude, since the closer the approach to cruising speed, the larger does this ratio become. Specific fuel consumption decreases primarily owing to increased throttle given the TJE and, consequently, the smaller $\bar{C}_{sp}$. On the other hand, the increase of C'_{sp} due to the increase in speed with altitude is offset by a decrease resulting from the altitude increase. On the whole, the higher the altitude, the greater the decrease in per-kilometer consumption.

For modern aircraft, a change in altitude from zero to 10,000-12,000 m results in a decrease in per-kilometer consumption by about half. It might be assumed that, owing to the relatively small change in $V_{q_{min}}$ for aircraft with small aspect ratio wings, an increase in altitude should not lower the per-kilometer consumption so sharply. However, this is not the case, since per-kilometer consumption rises considerably at low altitudes as a result of the larger C_{sp}, and flight at a speed far above cruising lowers the value of KV.

Obviously, the minimum per-kilometer fuel consumption will occur at the altitude at which C_{sp}/KV is minimal. This altitude is slightly higher than that at which $V_{q_{min}}$, determined at constant c_{x_0}, becomes equal to V^*_{cr}. The smaller the load per square meter of the airplane's wing, the larger its wing aspect ratio

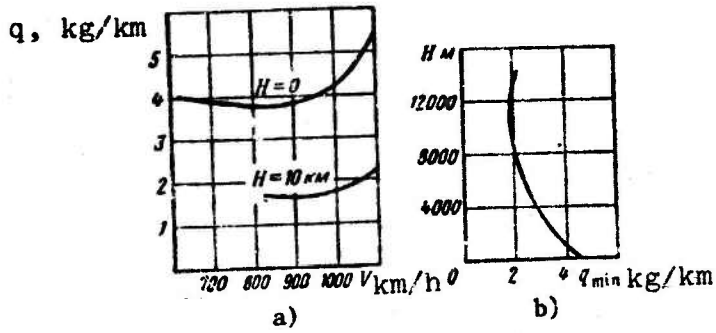

Figure 6.6. a) Influence of speed and altitude on per-kilometer fuel consumption in unaugmented flight; b) variation of minimum per-kilometer consumption with altitude in unaugmented flight.

and the larger V^*_{cr}, the closer is the altitude of minimum per-kilometer consumption to the airplane's ceiling.

The per-kilometer fuel consumption cannot be minimal in flight at the ceiling because a) C'_{sp} at full throttle is larger than the C_{sp} of a slightly throttled-back engine; b) at the ceiling in flight at V near V^*_{cr}, the product of lift/drag ratio by speed is smaller than it is at altitudes below the ceiling.

Modern aircraft have minimum-q altitudes 2,000-3,000 meters below ceiling.

Figure 6.6a shows the variation of per-kilometer fuel consumption with altitude and speed in unaugmented flight, and Fig. 6.6b the altitude variation of q_{min}.

Aircraft for which low-altitude flight takes place with the engine throttled far back and $V_{q_{min}}$ much higher than V_{cruise} owing to large thrust/weight ratios have a characteristically indistinct speed minimum of q. This is because both the product VK and C_{sp} in (6.2) decrease simultaneously on an increase in speed in the speed range above V_{cruise}, so that the dependence of q on flight speed becomes weaker.

Let us consider the influence of speed and altitude on the per-hour fuel consumption in flight. Per-hour consumption reaches a minimum at a speed very close to that at which the airplane flies at minimum rpm and, consequently, with the TJE throttled farthest back. The ratio C_{sp}/K is minimal at $V_{C_{h_{min}}}$ in expression (6.2) for C_h.

Since $V_{C_{h_{min}}}$ is close to V_{opt}, $V_{C_{h_{min}}}$ increases with altitude in proportion to $\sqrt{1/\Delta}$. The higher the altitude of flight, the less is the engine throttled back at $V_{C_{h_{min}}}$ and the smaller is $\bar{C}_{sp}$; since, despite the speed increase, C'_{sp} decreases with altitude, $C_{sp} = \bar{C}_{sp}C'_{sp}$ will also be smaller.

At a constant lift/drag ratio very close to K_{max}, the decrease in C_{sp} will lower the minimum per-hour consumption as altitude increases. C_h reaches its minimum value at about the altitude at which the engine is throttled back to the point at which C_{sp} reaches its minimum. This statement will hold provided that at this altitude the $V_{C_{h_{min}}}$ calculated for constant c_{x_0} is smaller than V^*_{cr}, which is true in most cases. This altitude is just below the airplane's ceiling.

For present-day airplanes, per-hour fuel consumption near the ceiling is lower than the minimum per-hour consumption at zero altitude by a factor of 1.5-1.8.

If $V_{q_{max}} \approx V^*_{cr}$ at high altitude, as is typical for modern supersonic airplanes with small aspect ratio wings, the speeds with minimum per-hour and per-kilometer fuel consumption will be closely similar and flight at $V_{q_{min}}$ will not greatly increase the per-hour consumption. For the same airplanes, the speed $V_{q_{min}}$ at the ground will be more than 1.8 times $V_{C_{h_{min}}}$, and flight with $V_{q_{min}}$ will take place with a C_h considerably larger than $C_{h_{min}}$.

The per-kilometer fuel consumption at flight speeds below V^*_{cr} is most conveniently calculated as follows.

The values of the optimum lift/drag ratio and the optimum flight speed are determined. The ratio V/V_{opt} is found for the speed V of interest. Expression (4.32) is used to calculate K, followed by determination of $Q_h = G/K$ and $P/P' = Q_h/P'$.

Using the relation $\bar{C}_{sp} = \bar{C}_{sp}(P/P')$ (see Fig. 6.4a), we find $\bar{C}_{sp}$, $C_{sp} = \bar{C}_{sp}C'_{sp}$ and the per-kilometer consumption

$$q = \frac{Q_h C_{sp}}{3,6V}.$$

For low-altitude flight, knowledge of the relation $\bar{C}_{sp} = \bar{C}_{sp}(P/P')$ is indispensable for calculation of q, since C_{sp} may be several tens of percent higher than C'_{sp}. In computing the per-kilometer consumption at altitudes greater than 8-10 km, it may be assumed in the first approximation that $\bar{C}_{sp} \approx 0.95\text{-}0.97C'_{sp}$.

Calculation of q_{min} is complicated by the fact that we do not know the speed at which q assumes its minimum value. For flight at low and zero altitudes, it is necessary to calculate q for several speeds, i.e., for $V_{cruise} = 1.31V_{opt}$ and higher. We find q_{min} and $V_{q_{min}}$ by plotting q as a function of speed.

For high-altitude flight, it is necessary to calculate V_{cruise} and inspect to determine whether it exceeds V^*_{cr}. If not, $V_{q_{min}}$ and q_{min} are found as described above, but if $V_{cruise} > V^*_{cr}$, the speed of minimum per-kilometer fuel consumption will be practically equal to V^*_{cr}. It is for this speed that q_{min} should be calculated, assuming zero wave drag.

As we indicated, the lowest per-kilometer fuel consumption is obtained at an altitude 2,000-3,000 m below ceiling. Per-kilometer consumption varies slowly with altitude in this altitude range. If q_{min} has been calculated for an altitude 2,000 m below ceiling, it need not be calculated for other altitudes.

The maximum range of flight at subsonic speeds is proportional to fuel weight and inversely proportional to the average value of the minimum per-kilometer consumption. Per-kilometer consumption at $V_{q_{min}} < V^*_{cr}$ will be lowered to some degree by increasing the cruising speed and K_{max}, since $K_{cruise} = 0.86K_{max}$. It follows from the analytical expression for $c_{y_{cruise}}$ and K_{max} that V_{cruise} is inversely proportional to $\lambda_{ef}^{1/4}$, and that K_{max} is directly proportional to $\lambda_{ef}^{1/2}$ and inversely proportional to $c_{x_0}^{1/2}$. Thus, given equal increases in lift/drag ratio through c_{x_0} and through λ_{ef} for subsonic airplanes, it will be more advantageous from the standpoint of q_{min} to increase K_{max}, which lowers c_{x_0}, rather than increasing λ_{ef}.

If $V_{q_{min}} \approx V^*_{cr}$, then λ_{ef} will not influence $V_{q_{min}}$, leaving only the effect of λ_{ef} on lift-drag ratio. Then

$$q = \frac{GC_{y_1}}{3.6KV^*_{cr}}. \tag{6.4}$$

At $V_{q_{min}} < V^*_{cr}$, an increase in the load per square meter of wing at K = const increases $V_{q_{min}}$ and reduces q_{min}. At $V_{q_{min}} \approx$ $\approx V^*_{cr}$, it will be more advantageous from the standpoint of lowering q to have a wing load at which V^*_{cr} flight occurs with $K \approx K_{max}$ at an altitude 2,000-3,000 m below ceiling. At the same time, it is obvious that if $V_{q_{min}} \approx V^*_{cr}$, per-kilometer consumption will be lowered as a result of all of the measures that increase V^*_{cr} and do not lower K_{max} appreciably. For example, this explains why 30°-35° swept wings (at 1/4 chord), which have a large V^*_{cr} at wing aspect ratios from 6.5 to 7.5 and a $M_{q_{min}} = M^*_{cr}$ around 0.82-0.84, have come into extensive use on modern transonic passenger aircraft.

Per-kilometer consumption is directly proportional to C_{sp}. At high altitudes, as we indicated, C_{sp} is nearly equal to C'_{sp}.

Thus, lowering specific consumption in engines operated at maximum power helps increase range. For many types of military aircraft, it is important to secure low per-kilometer consumptions in zero-altitude flight. In flight at cruising speed at these altitudes, fuel consumption per kilometer is very high, chiefly because the engine is throttled far back under these conditions and C_{sp} is very high. As a result, not only small values of C_{sp}, but also the smallest possible increase in C_{sp} on throttling far back are important for low-flying airplanes.

The turbofan engine is particularly suited for zero-altitude flight. This is because the TJE has a smaller C'_{sp} and a smaller increase in C_{sp} when throttled down. Moreover, the thrust of a TFE operated without augmentation does not increase with speed, but decreases. As a result, it does not have to be throttled back as far in zero-altitude flight at $V_{q_{min}}$.

Aircraft that have high rates of climb and high ceilings as a result of large thrust/weight ratios in unaugmented flight have higher values of q_{min} at the ground. This is because of the need to fly at a speed considerably higher than cruising (to permit opening the throttle to lower C_{sp}), and this results in a smaller KV.

Low-level range at high speeds rather that at $V_{q_{min}}$ is important for many airplanes, such as fighters.

In this type of flying, a rapid rise of per-kilometer consumption begins at a Mach number higher than M^*_{cr}. As a result, an increase in M^*_{cr} will help lower consumption per kilometer. If the airplane must fly at 1,200-1,300 km/h at zero altitude, per-kilometer consumption can also be lowered by using the thinnest possible profile on strongly swept wings.

In zero-altitude flight at the speed of sound, induced drag is very small. As a result, a reduced wing area will lower Q_h and thus q. At high zero-altitude speeds approaching V_{max}, the ratio P/P' is large and C_{sp} close to C'_{sp}. The smaller C'_{sp},

therefore, the lower will be the consumption per kilometer per ton of weight.

§6.3. PER-KILOMETER FUEL CONSUMPTION OF TJE AND TFE AIRCRAFT AT SUPERSONIC SPEEDS

For the overwhelming majority of aircraft, supersonic flight involves augmenting the thrust of the TJE. In this case, throttling the engine back results in a substantial decrease in C_{sp}, something that is not observed, as we noted above, in unaugmented operation of TJE's.

The transition to supersonic speeds is accompanied by changes in c_{x_0} and A that result in a sharp decrease in maximum lift/drag ratio.

As a result, the speed and altitude variations of the per-kilometer and per-hour fuel consumptions at supersonic speeds exhibit a number of highly important peculiarities that must be taken into account.

In Fig. 4.9b, we showed typical Zhukovskiy curves covering a broad range of altitudes and Mach numbers. We saw that the higher the altitude of flight, the slower is the increase of Q_h with increasing speed (Mach number). This is because induced drag, whose contribution to Q_h increases with altitude, decreases with increasing speed.

The higher is M in the range from unity to 1.4-1.6 at an altitude of 11,000 m, the smaller is the degree to which the engine of a modern supersonic airplane must be throttled back to make P equal to Q_h. This results in an increase in C_{sp} with increasing M of level flight. This dependence of Q_h and C_{sp} on M is due to the fact that the increase of the product $Q_h C_{sp}$ is faster than proportional to M at 11,000 meters, so that $q = Q_h C_{sp}/3.6aM$ usually increases with increasing M. The higher the altitude, the smaller the increase in Q_h. At a certain altitude, Q_h varies with speed more slowly than M or in proportion to it, so that the fuel consumption per kilometer decreases with increasing M.

In high-altitude flight, the lowest consumption per kilometer is obtained at the speed corresponding to the limiting Mach number. By way of illustration, Fig. 6.7 shows per-kilometer consumption as a function of M and altitude in thrust-augmented flight.

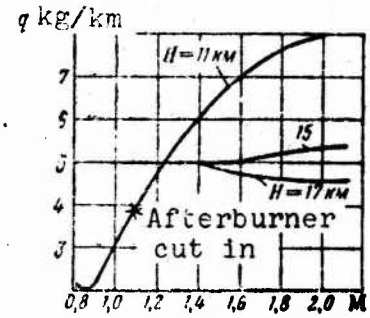

Figure 6.7. Influence of Mach number and altitude on fuel consumption per kilometer in augmented-thrust flight.

At high altitudes, the minimum per-kilometer consumption is obtained, as we indicated, at $M \approx M_{lim}$.

The question arises as to the altitude at which, in flight at M_{lim} = = const, the per-kilometer fuel consumption will be minimal.

According to (6.3), this will be the altitude at which the ratio C_{sp}/K is minimized at M = const. In flight at constant M, the higher the altitude, the larger must c_y become. Here, Q_h = = G/K will decrease up to the altitude at which $c_y = c_{y_{opt}}$ and $K = K_{max}$. Q_h will increase with altitude above this level.

$Q_h = P$ in level flight at constant speed. Equality of thrust to frontal drag is obtained at $M = M_{lim}$ by throttling the TJE back. At the ceiling, the engines are operating at full fuel delivery. If P_{11}/S is large and $\bar{P} = P_{11}/2Q_{011} > 1$, the equality $Q_h = P$ will be obtained at the ceiling with $c_{y_{clg}} > c_{y_{opt}}$. For lower thrust values, when $\bar{P} = 1$, ceiling flight will occur with $c_{y_{clg}} = c_{y_{opt}}$ and $K = K_{max}$. A further decrease in the airplane's thrust/weight ratio ($\bar{P} < 1$) will result in flight at the ceiling with $c_{y_{clg}} < c_{y_{opt}}$ and $K < K_{max}$.

If c_{y_0} were independent of altitude and TJE throttle setting, which would presumably be possible in unaugmented-thrust supersonic flight, the altitude of minimum per-kilometer fuel

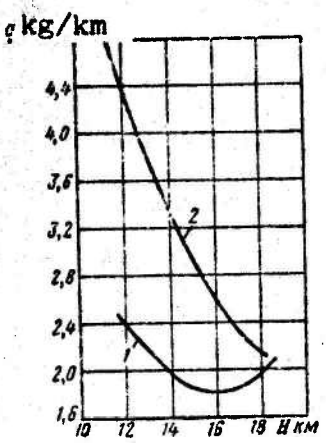

Figure 6.8. Influence of altitude on per-kilometer fuel consumption in thrust-augmented flight. Curve 1 – at ceiling $c_{y_{clg}} > c_{y_{opt}}$; curve 2 – at ceiling $c_{y_{clg}} < c_{y_{opt}}$.

consumption would be the ceiling altitude, or, for airplanes having $\bar{P} > 1$, the altitude at which $c_y = c_{y_{opt}}$ and $K = K_{max}$.

In augmented-thrust flight, throttling the TJE back lowers C_{sp} sharply. It is therefore advantageous to fly not at the altitude of maximum lift/drag ratio, but at a lower altitude, at which the engine is throttled back and the ratio C_{sp}/K is at minimum.

In constant-M flight, the farther the airplane is below its ceiling, the farther must its engine be throttled back, and hence the smaller will C_{sp} become. Lowering altitude at M = const lowers c_y and, consequently, influences lift/drag ratio. At the altitudes at which $c_y < c_{y_{opt}}$, a decrease in altitude will lower the lift/drag ratio the more sharply the greater the difference between c_y and $c_{y_{opt}}$ (see Fig. 4.13a). At the altitude at which the relative decrease in C_{sp} with altitude equals the relative decrease of lift/drag ratio with altitude, per-kilometer fuel consumption will be minimal, since C_{sp}/K assumes its smallest value. This altitude will always be lower than that at which $c_y = c_{y_{opt}}$. If $\bar{P} > 1$, we have according to (5.12) $c_{y_{clg}} > c_{y_{opt}}$, and therefore a lowering of altitude from the ceiling with M = const will first lower per-kilometer consumption (Fig. 6.8, curve 1). At $\bar{P}$ smaller than 0.70-0.85, $c_{y_{clg}}$ is much smaller than $c_{y_{opt}}$, and a decrease in flight altitude will result in a very sharp decrease in lift/drag. In this case, the minimum per-kilometer fuel consumption is obtained in flight at the

ceiling (see Fig. 6.8 curve 2). The altitude curves of per-kilometer fuel consumption compared in Fig. 6.8 illustrate the advantage of a larger $\bar{P}$ in respect to the magnitude of q, especially for altitudes below the ceiling.

For modern supersonic aircraft, the minimum per-kilometer fuel consumption in augmented flight around Mach two is 1.5-2.5 times the minimum per-kilometer fuel consumption in unaugmented flight at M = 0.8-0.9.

Increasing M_{lim} to three brings the supersonic minimum consumption per kilometer close to the consumption per kilometer of the same airplane at subsonic speeds, or even lower.

It must be remembered that in most cases the supersonic flight range will nevertheless be shorter than the range at subsonic speeds, since much less fuel is expended in reaching M = = 0.85-0.9 and altitudes of 11-13 km than in climbing to 18-20 km and accelerating to $M \geq 3$.

A more remote prospect is a decrease in q at $M \geq 3$ when further development of the TJE permits high supersonic speeds without thrust augmentation. Then the per-kilometer fuel consumption at supersonic speeds will be much lower than the consumption at M = 0.85-0.95, and the supersonic flight range may even exceed the range at transonic speeds.

Let us now turn to calculation of the minimum per-kilometer fuel consumption at supersonic speeds.

If the dependence of $\bar{C}_{sp} = \bar{C}_{sp}(P/P')$ is nonlinear in the range of P/P' from unity to 0.6, we proceed as follows. We assign several altitudes. For $\bar{P} = P_{11}/2Q_0 > 1$, we take the altitude with $c_y = c_{y_{opt}}$ and three to four lower altitudes. The calculation for $\bar{P} \leq 1$ is carried out for the ceiling and three or four lower altitudes. Q_h is calculated from (4.29) for $M = M_{lim}$ and the altitudes indicated above; the ratio $Q_h/P' = P/P'$ is determined. $\bar{C}_{sp}$ is determined and $C_{sp} = \bar{C}_{sp}C'_{sp}$ is found.

Next, q is calculated:

$$q=\frac{Q_{\text{г}}C_{\text{ул}}}{3{,}6aM_{\text{прех}}}.$$

The altitude curve of q is plotted and used to determine the altitude with the lowest per-kilometer consumption and the consumption itself.

If the curve of $\bar{C}_{sp} = \bar{C}_{sp}(P/P')$ is nearly linear, as it is in most cases (see Fig. 6.4b), calculation of q_{min} and $H_{q_{min}}$ is vastly simplified [33].

If $\bar{C}_{sp}$ depends linearly on P/P', the variation of $\bar{C}_{sp}$ as the TJE is throttled down can be characterized by the $\bar{C}_{sp}$ with P/P' = = 0.6. We shall proceed accordingly.

We transform the expression for consumption per kilometer by introducing $\bar{K}_q = K/K_{max}$ and $\bar{C}_{sp} = C_{sp}/C'_{sp}$:

$$q=\frac{GC_{\text{ул}}}{3{,}6aM_{\text{прел}}K}=\frac{GC'_{\text{ул}}}{3{,}6aM_{\text{прел}}K_{\max}}\left(\frac{\bar{C}_{\text{ул}}}{\bar{K}_q}\right). \tag{6.5}$$

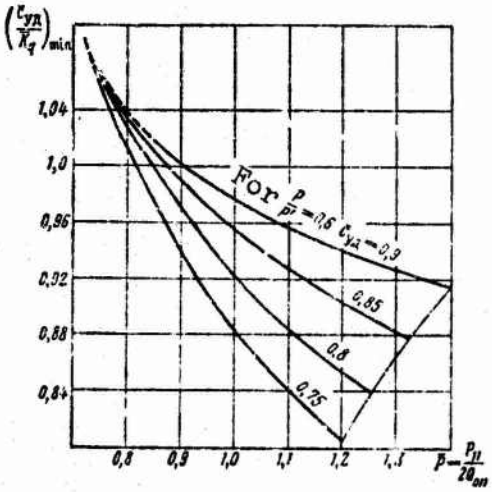

Figure 6.9. Curves of $(\bar{C}_{sp}/\bar{K}_q)_{min}$.

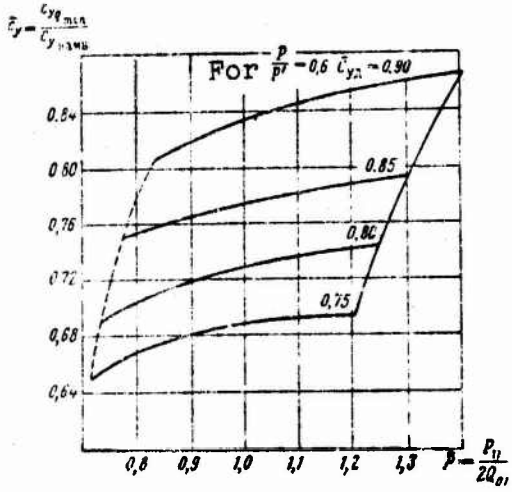

Figure 6.10. Curves of $\bar{c}_y = c_{y_{q_{min}}}/c_{y_{opt}}$ vs. $\bar{P}$.

If it is assumed that C'_{sp} and K_{max} are independent of altitude, it is obvious that at M_{lim} = const, q varies with altitude in proportion to $\bar{C}_{sp}/\bar{K}_q$. The minimum of the $\bar{C}_{sp}/\bar{K}_q$ is what determines the minimum of q. The minimum value of the ratio $\bar{C}_{sp}/\bar{K}_q$ is a function, on the one hand, of the degree of the decrease in C_{sp} when the TJE is throttled back, which is characterized, by hypothesis, by the value of $\bar{C}_{sp}$ at P/P' = 0.6, and, on the other hand, of $\bar{P} = P_{11}/2Q_{011}$. Figure 6.9 shows $(\bar{C}_{sp}/\bar{K}_q)_{min}$ as a function of $\bar{P}$ for various $\bar{C}_{sp}$ and P/P' = 0.6.

The altitude with q_{min} is characterized by the ratio of the pressure at the altitude with $c_y = c_{y_{opt}}$ to the pressure at the altitude with q_{min}. It is a function of $\bar{P}$ and the value of $\bar{C}_{sp}$ at P/P' = 0.6.

Figure 6.10 presents curves of the ratio of the pressure in the atmosphere at the altitude of flight with $c_{y_{opt}}$ to the pressure at the altitude of flight with q_{min}.

Calculation of q_{min} and $H_{q_{min}}$ is greatly simplified by use of the diagrams in Figs. 6.9 and 6.10.

The $\bar{C}_{sp}$ for P/P' = 0.6 is found from the engine's fuel-consumption curves. K_{max} and $\bar{P} = P_{11}/2Q_{011}$ are calculated for M = = M_{lim}. Their values are usually known before range is calculated. We refer to the diagram of Fig. 6.9 to find $(\bar{C}_{sp}/\bar{K}_q)_{min}$ for $\bar{P}$ and $\bar{C}_{sp}$ at P/P' = 0.6 and use expression (6.5) to find q_{min}.

We calculate $c_{y_{opt}}$ and the pressure at the flight altitude with $c_y = c_{y_{opt}}$:

$$p_{c_{y_{\text{опт}}}} = \frac{G}{S \cdot 0{,}7\, M^2_{\text{крит}}\, c_{y_{\text{опт}}}}. \qquad (6.6)$$

The ratio $p_{c_{y_{opt}}}/p_{q_{min}} = c_{y_{q_{min}}}/c_{y_{opt}}$ and the altitude of flight with minimum consumption per kilometer are determined from the diagram of Fig. 6.10 for the $\bar{P}$ and $\bar{C}_{sp}$ at P/P' = 0.6. If C'_{sp}

increases rapidly with altitude and its curve is known, the above calculation procedure requires preliminary determination of the altitude of flight with q_{min} by assigning a C'_{sp}, taking the new value of C'_{sp} for it, and then recalculating q_{min} and $H_{q_{min}}$.

The altitude and q_{min} obtained in this way will be slightly on the high side, because the effects of the decrease in C'_{sp} on $H_{q_{min}}$ were not considered.

Let us turn to the influence of the airplane's design parameters and the characteristics of the TJE on the minimum fuel consumption per kilometer at supersonic speed.

It follows from (6.5) that all measures that increase the maximum lift/drag ratio reduce the specific consumption C'_{sp} and increase M_{lim}, thus helping lower the per-kilometer consumption at supersonic speeds.

As is indicated by the curves of $\bar{C}_{sp}/\bar{K}_q = (\bar{C}_{sp}/\bar{K}_q)(\bar{P})$ (see Fig. 6.9) with $\bar{C}_{sp}$ a linear function of P/P', the larger $\bar{P}$, the smaller is $(\bar{C}_{sp}/\bar{K})_{min}$ and, consequently, q_{min}. However, C_{sp} is usually observed to decrease more slowly with decreasing P/P' when P/P' < 0.6. Therefore the minimum per-kilometer fuel consumption will occur at a $\bar{P}$ near the value at which the engine is throttled back enough so that P/P' ≈ 0.6 in flight with q_{min}. This condition is indicated in Fig. 6.9 by the dot-dash curve. We see that the less rapid the decrease in C_{sp} as the TJE is throttled down (the larger $\bar{C}_{sp}$ at P/P' = 0.6), the larger is the $\bar{P}$ at which the same minimum of $\bar{C}_{sp}/\bar{K}_q$ is reached.

It follows from the above that to lower per-kilometer fuel consumption at supersonic speeds, it is advantageous to take a P_{11} such that $\bar{P} = P_{11}/2Q_{011}$ exceeds 1.0-1.1. We note that the altitude of flight with Q_{min} will then be below the supersonic ceiling.

As we noted above, larger values of $\bar{P}$ help lower per-kilometer fuel consumption at altitudes far below ceiling (see Fig. 6.8).

§6.4. CRUISING-CLIMB FLIGHT

Returning to the expressions for per-kilometer consumption, we see that at constant V and c_y, the value of q is directly proportional to the weight G of the airplane, since the lift-drag ratio and C_{sp} are then constant. Since a certain Mach number corresponds to each speed above 11,000 m, and the lift-drag ratio depends on this Mach number, the above proposition is valid for these altitudes even in the presence of wave drag; on the other hand, if wave drag is zero, it holds for all altitudes.

In flight at altitudes above 11,000 m at constant speed and at an angle θ to the horizontal such that G/p remains constant as the weight of the airplane decreases owing to fuel depletion, the airplane's angle of attack and, consequently, its lift-drag ratio will be constant. In this case, Q_h and P' vary equally during flight, and at constant rpm the throttling of the engine and, consequently, also C_{sp} will remain unchanged. Owing to the constancy of C_{sp}/KV, the per-kilometer consumption comes to diminish in proportion to the decrease in the airplane's weight owing to fuel depletion.

The climbing angle θ at which G/p is constant is a very small one. It amounts to a few minutes of arc. This climb is known as the cruising climb or "flight along the ceilings." It owes the latter name to the following considerations. If, after the airplane has reached its practical ceiling, the pilot holds to the same angle of attack and the same speed, he will be flying at all times at the altitude corresponding to the ceiling. This altitude will increase steadily owing to the decreasing weight of the airplane.

However, the cruising climb at constant speed, constant angle of attack, and constant TJE rpm can be performed starting at any speed and the c_y corresponding to it. All that is necessary is that the air temperature remain constant in the altitude range in which the flight is executed, so that the thrust of the TJE will vary in proportion to the pressure.

The cruising climb saves fuel, since the average value of c is lower for this flight mode. If the speed and altitude at the beginning of flight corresponds to flight with q_{min}, this condition will be preserved at all times during the cruising climb, but if the pilot holds to a constant altitude, the difference between the ceiling and the actual altitude will increase as the airplane becomes lighter. The larger this difference, the greater will be the increase in per-kilometer fuel consumption.

The decrease in fuel consumption on transition to the cruising time as compared to level flight will be larger the greater the weight of fuel burned. If fuel weighing 40-45% of the airplane's weight is consumed and V^*_{cr} does not influence the speed of minimum per-kilometer fuel consumption, the average q can be lowered by about 10% or even more in cruising-climb flight.

If q_{min} was reached at about the altitude at which the product $V^*_{cr}K$ reached its minimum, the speed of flight with minimum per-kilometer fuel consumption is usually close to V_{opt}. In this case, the decrease in c_y due to lightening of the airplane will, in flight at constant speed and altitude, lead to an insignificant decrease in lift-drag ratio and the advantage of going over from level flight to the cruising climb will not be as appreciable.

For many modern supersonic aircraft in unaugmented flight, it is 2-4% of the average consumption per kilometer.

Everything that we have said concerning the cruising climb also applies to "flight along the ceilings" at supersonic speed with q_{min}. If the altitude is not increased as fuel is burned at supersonic speeds, C_{sp}/K will increase. Obviously, this increase will be larger, the more rapid the increase in per-kilometer fuel consumption as the airplane descends from that at which it is minimal. For this reason, "flight along the ceilings" is especially advantageous for supersonic aircraft having $\bar{P}$ = 0.7-0.8. For airplanes with $\bar{P} \geq 1$, such flight saves less fuel.

§6.5. FUEL CONSUMPTION IN ACCELERATING CLIMB AND DECELERATING DESCENT

The amount of fuel burned by a modern supersonic airplane in reaching M_{lim} and near-ceiling altitudes amounts to 10-15% of the airplane's takeoff weight. This means that 40-50% of the entire normal fuel load may be burned during the climb. Serious attention must therefore be given to correct calculation of fuel consumption and possible ways of lowering it. In climbing at maximum engine power

$$dG_{\text{топл}} = \frac{C_h dt}{3600} = \frac{P' C'_{sp}}{3600} dt.$$

According to (5.17)

$$dt = \frac{dH_э}{V_y^*},$$

whence

$$dG_{\text{топл}} = \frac{P' C'_{sp}}{3600 V_y^*} dH_э. \tag{6.7}$$

When the energy altitude changes from H_{e1} to H_{e2}, the amount of fuel burned will be

$$G_{\text{топл}} = \int_{H_{э1}}^{H_{э2}} \frac{P' C'_{sp}}{3600 V_y^*} dH_э. \tag{6.8}$$

To obtain the shortest time to climb and reach speed, it would be necessary to fly at trajectory speeds at which $1/V_y^*$ is minimal at each energy altitude (see §6.2). To obtain minimum fuel consumption at each H_e, on the other hand, the speed must be such as to minimize the ratio $P'C'_{sp}/3600V_y^*$. Since P' and C'_{sp} vary with changing altitude and speed, flight for minimum time to climb will not be the climbing mode with minimum fuel consumption.

Figure 6.11 shows $3600V_y^*/P'C'_{sp}$ as a function of speed for various constant altitudes for a supersonic airplane, and Fig.

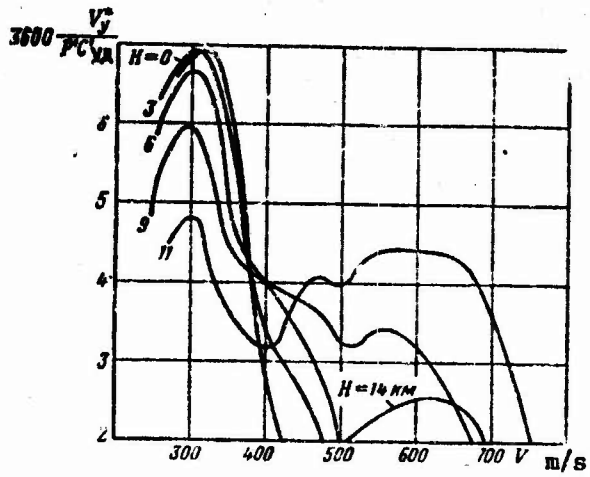

Figure 6.11. Typical dependence of $3600V_y^*/P'C'_{sp}$ on speed and altitude.

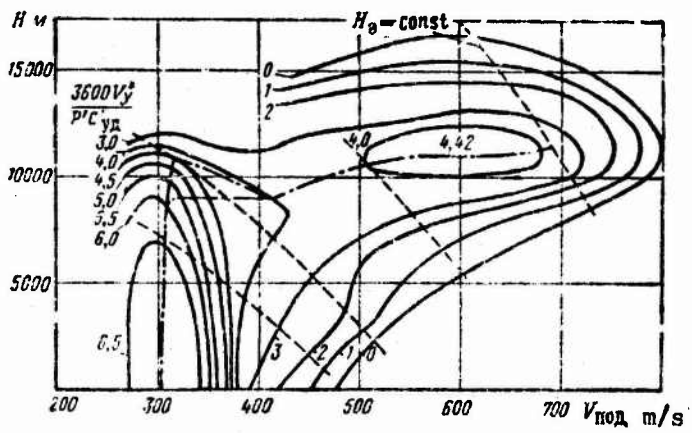

Figure 6.12. Diagram for determining rate of climb that ensures reaching energy altitude with minimum fuel consumption.

6.12 presents a diagram for determining the V_{clb} with minimum fuel consumption.

We see that at high altitudes, the speed at which the ratio $3600V_y^*/P'C'_{sp}$ is maximal and fuel consumption is minimal becomes supersonic. Calculations indicate that the climbs with $V_{y\,max}^*$ and those with minimum fuel consumption are very closely similar at

subsonic speeds and, above 11-13 km, at M near M_{lim}. There is a difference in the altitudes of accelerating to M near M_{lim}. To obtain minimum fuel consumption, it is more advantageous to accelerate at a slightly higher altitude. However, the accelerating altitude difference is not very large and a single mean altitude is often indicated for interceptors.

Expression (6.7) can be transformed by introducing the value of V_y^*:

$$\delta G_{\text{подъ}} = \frac{P' C'_{y\text{д}} \delta H_э}{3600 V_y^*} = \frac{P' C'_{y\text{д}} G \delta H_э}{3600 V (P' - Q_r)} = \frac{G C'_{y\text{д}}}{3600 V \left(1 - \frac{Q_r}{P'}\right)} \delta H_э.$$

The resulting expression for $\delta G_{f_{clb}}$ is conveniently used in resolving the question as to whether it is advantageous to go to the afterburner to reduce climbing fuel consumption.

If the increased C'_{sp} in the augmented-thrust climb offsets the increase in the difference $1 - (Q_h/P')$, climbing with the afterburner may save fuel. It should be noted that for most transonic airplanes, with the exception of heavily overloaded ones, climbing without the afterburner is more economical.

The calculation of fuel consumed in climbing and accelerating is quite similar to the calculation described in §5.4 for the time to climb and accelerate. The only difference is that in the time calculation, we plotted the H_e curve of $1/V_y^*$ for a series of altitudes, while in calculating $G_{f_{clb}}$ we construct the H_e curve of $P'C'_{sp}/3600V_y^*$ for a series of altitudes and then draw the envelope. The area between the envelope and the axis of abscissas gives the $G_{f_{clb}}$ needed to change H_e from $H_{e_{ini}}$ to $H_{e_{fin}}$.

It is often necessary in preliminary design of an airplane to determine the climbing and accelerating fuel consumption referred to takeoff weight even when the weight of the airplane, the wing area, and the thrust of the TJE are unknown. In this case, it is convenient to use an approximate method proposed by N.N. Fadeyev. With this method, determination of $G_{f_{clb}}/G$ requires only knowledge

of the average C_{sp} over the climbing and accelerating stage and the energy altitude $H_{e_{fin}}$ at the end of the acceleration and climb.

If during the climb the frontal drag is zero and the thrust is μG, where $\mu = P/G$, we have $V_y^* = \mu V$, since

$$\frac{dH_э}{dt} = V_y^* = \frac{(P-Q)V}{G} = \mu V.$$

The time to accelerate and climb will be

$$t = \frac{H_{э_{кон}}}{V_{y_{ср}}^*} = \frac{H_{э_{кон}}}{\mu V_{ср}} \approx \frac{H_{э_{кон}}}{0{,}5\mu V_{кон}},$$

and the fuel consumed in climbing and accelerating

$$G_{т_{пол}} = \frac{C_{h_{ср}}}{3600} t = \frac{\mu G C_{уд_{ср}}}{3600} t$$

and

$$\frac{G_{т_{пол}}}{G} = \frac{C_{уд_{ср}} H_{э_{кон}}}{1800 V_{кон}} = \frac{C_{уд_{ср}}}{1800}\left(\frac{V_{кон}}{2g} + \frac{H_{кон}}{V_{кон}}\right). \qquad (6.9)$$

It is clear from the above that at $Q = 0$, the relative fuel consumption $G_{f_{clb}}/G$ is independent of thrust, depending only on $C_{sp_{av}}$, F_{fin}, and $H_{e_{fin}}$. Expression (6.9) does not take account of the fuel consumed in overcoming frontal drag in motion on the climbing and accelerating trajectory. In approximate calculations, it is permissible to assume that this part of the fuel consumed in motion on the climbing trajectory is equal to the fuel consumed in level flight at the final altitude and speed over a distance equal to the length of the climbing and accelerating trajectory.

With these assumptions, and having reduced the weight of the airplane at the beginning of flight by the $G_{f_{clb}}$, calculated from (6.9), we calculate the range of cruising-climb flight. The range of value obtained here will also include the length of the climbing

and accelerating trajectory.

For transonic airplanes, it is usually necessary to calculate $G_{f_{clb}}/G$ for an unaugmented-thrust climb to 10,000-11,000 m with acceleration to M = 0.85-0.9, since flight with minimal per-kilometer fuel consumption ($q = q_{min}$) takes place at these H and M. In this case, we exaggerate the time to climb to $H_{e_{fin}}$ and $G_{f_{clb}}/G$ by assuming that $V_{av} = 0.5V_{fin}$, as was done in deriving (6.9). To adjust the calculation, we introduce the correction factor k_{clb} into (6.9):

$$\frac{G_{T_{пол}}}{G} = \frac{k_{пол} C_{y_{ср}} H_{э_{кон}}}{1800 V_{кон}}. \qquad (6.10)$$

Comparison of the calculated results for M_{fin} = 0.85-0.90 indicates that $k_{clb} \approx 0.8$. $C_{sp_{av}}$ is determined as the mean between the C_{sp} at M = 0.85-0.9 at the ground and at 11,000 m. If afterburners are used during the climb and $M_{lim} = 2$, k_{clb} should be taken equal to 1.2 in determining $G_{f_{clb}}/G$ and using (6.10); C_{sp} should be determined at 11,000 m as the mean between the C_{sp} for M = 0.9 and M = 2.

At this stage in the design, when the thrust at M_{lim} and 11,000 m, the weight of the airplane, and its wing area are already known, we recommend another approximate, but more exact method of calculating the total climbing and accelerating fuel consumption, distance, and time.

We recommend this method for supersonic aircraft, which have large $G_{f_{clb}}/G$. It is based on the results of processing a large number of calculated climb-and-acceleration fuel-consumption figures for various P_{11}/G and $\bar{P} = P_{11}/2Q_{011}$.

To determine $G_{f_{clb}}/G$, it is necessary to calculate

$$H_{э_{кон}} = \frac{V^2_{кон}}{2g} + H_{кон}, \quad \text{find } Q_{011} = 0{,}7 p_{11} M^2_{кон} c_{x_0} S,$$

and calculate the values of P_{11}/G and $\bar{P} = P_{11}/2Q_{011}$ for M_{fin}. (For a supersonic airplane, M_{fin} is usually equal to the Mach-number limit.) Then, referring to Fig. 6.13, we find the initial value $\bar{G}_{f_{clb.ini}} = G_{f_{clb.ini}}/G$ for $H_{e_{fin}}$ and calculate

$$\bar{G}_{\text{т под}} = \bar{G}_{\text{т под. исх}} K_1 K_2 K_3. \tag{6.11}$$

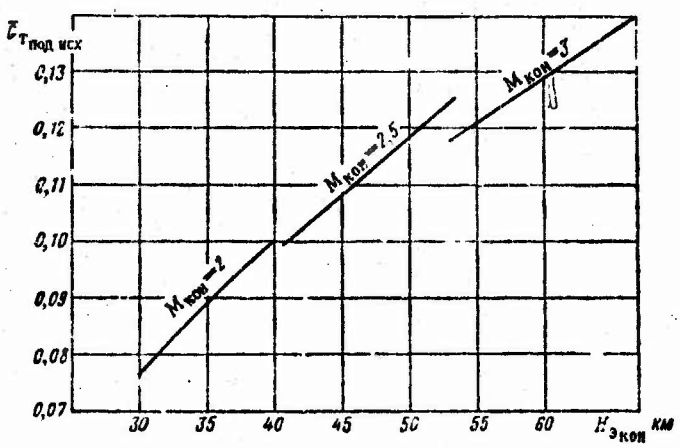

Figure 6.13. Relative climbing and accelerating fuel consumption as a function of final energy altitude $H_{e_{fin}}$ and M_{fin}.

The coefficient K_1, which allows for $\bar{P}$, is taken from the diagram of Fig. 6.14, and the coefficient K_2 for P_{11}/G is taken from Fig. 6.15.

The coefficient

$$K_3 = 0{,}5\left(\frac{C_{y_{\text{л}M=0,9}} + C_{y_{\text{л}M_{\text{кон}}}}}{2}\right) = 0{,}25\left(C_{y_{\text{л}M=0,9}} + C_{y_{\text{л}M_{\text{кон}}}}\right)$$

is calculated for H = 11 km. In determining $G_{f_{clb}}$ by (6.11), we incur an error no greater than 1.5% of the airplane's takeoff weight.

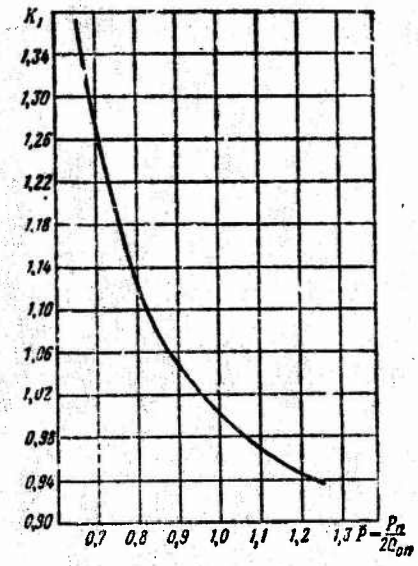

Figure 6.14. Coefficient X_1 of approximate dependence of $\bar{G}_{f_{clb}}$ on $\bar{P} = P_{11}/2Q_{011}$.

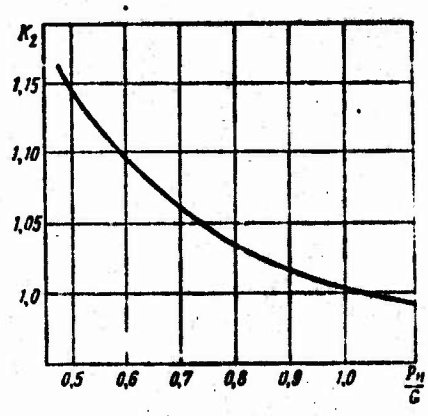

Figure 6.15. Coefficient K_2 of approximate dependence of $\bar{G}_{f_{clb}}$ on thrust/weight ratio P_{11}/G.

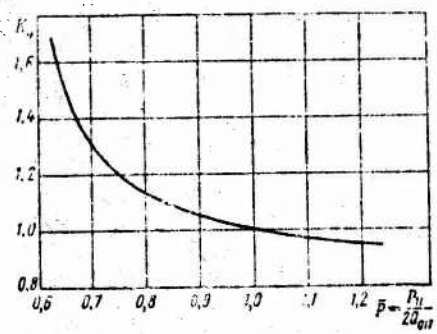

Figure 6.16. Coefficient K_4 of approximate dependence of climbing and accelerating trajectory length in augmented-thrust operation on $\bar{P} = P_{11}/2Q_{011}$.

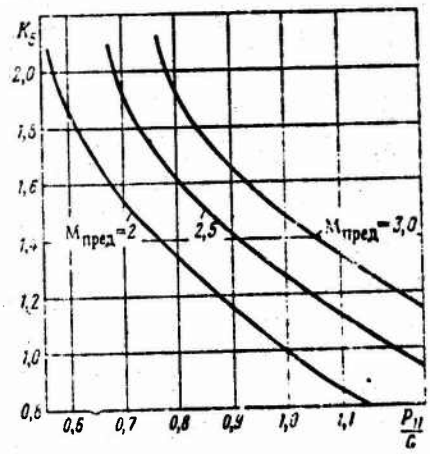

Figure 6.17. Coefficient K_5 of approximate dependence of climbing and accelerating path length in augmented-thrust operation on thrust/weight ratio P_{11}/G.

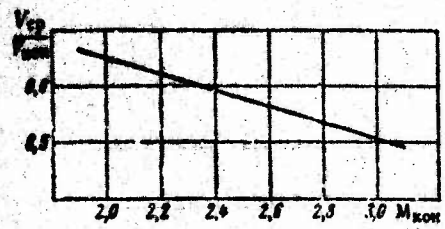

Figure 6.18. V_{av}/V_{fin} in climb and acceleration as a function of M_{fin}.

The accelerating and climbing distance is determined from the expression

$$L_{\text{нол}} = 2{,}2H_{e_{\text{кон}}} K_4 K_5, \qquad (6.12)$$

$H_{e_{fin}}$ is calculated from the values of H_{fin} and V_{fin}, while the coefficients K_4 and K_5, which allow for the influence of $\bar{P}$ and P_{11}/G on the climbing and accelerating distance, are taken from the diagrams of Figs. 6.16, and 6.17).

The time to accelerate and climb is

$$t_{\text{нол}} = \frac{L_{\text{нол}}}{V_{\text{ср}}}. \qquad (6.13)$$

V_{av} is determined from V_{fin} and the dependence of V_{av}/V_{fin} on M_{fin} that appears in Fig. 6.18.

Since this method gives the total fuel consumption during the acceleration and climb, as well as the accelerating-path length, the flight distance "along the ceilings" will no longer include the length of the climbing and accelerating trajectory, as it does in N.N. Fadeyev's method. In this case

$$L = L_{clb} + L_{lvl} + L_{des}.$$

If the airplane has M_{lim} = 2.5-3 and the limiting ram pressure q_{lim} is much smaller than 10,000 kgf/m^2, a considerable part of the acceleration and climb will be flown at the limiting trajectory speed determined by the maximum permissible ram pressure q_{lim}. In this case, (6.11) may be used to calculate $G_{f_{clb}}/G$, but determination of L_{clb} by expression (6.12) will result in a substantial error.

For a rough estimate of L_{clb}, it may be assumed that with q_{lim} = 4,000 kgf/m^2 at M_{lim} = 3, the value of L_{clb} will be twice that obtained when L_{clb} is determined from (6.12).

In a decelerating glide with the engine operating at minimum rpm and H_e changing from 30-35 km to zero, the weight of fuel consumed equals about 0.01 of the airplane's weight. This consumption may be assumed proportional to the change in H_e.

§6.6. FLIGHT RANGE AND ITS CALCULATION

The technical range L_{tec} is the ground distance covered by an airplane during climbing and acceleration, level flight at q_{min} or cruising climb, and gliding descent using all fuel on board.

Thus,

$$L_{tec} = L_{clb} + L_{lvl} + L_{des}. \tag{6.14}$$

In level flight or, more precisely, cruising climb, the amount of fuel consumed equals the fuel reserves less the amounts consumed in climbing $G_{f_{clb}}$ and descending $G_{f_{des}}$:

$$G_{f_{lvl}} = G_f - (G_{f_{clb}} + G_{f_{des}}). \tag{6.15}$$

In reality, an airplane cannot reach its technical flight range, since a certain fuel reserve must remain in the tanks after landing for use in testing the engines prior to takeoff and in taxiing, as well as during the landing. In addition, there is practically always a certain amount of fuel left in the tanks that cannot be burned. However, the tactical-technical specifications for the airplane usually state a technical range, and this range is calculated in the course of preliminary design.

With aircraft having $M_{lim} < 2.5$-3, maximum range is obtained with unaugmented operation of the engine in cruising-climb flight with $q = q_{min}$.

In some cases, e.g., interception of an aerial target by a fighter, it is necessary to obtain a higher average flight speed and, simultaneously, the longest possible range. Under this requirement, the airplane must be flown with the afterburner on at M_{lim} at the altitude at which per-kilometer fuel consumption is minimal.

A certain range at supersonic speed with $M = M_{lim}$ may be required of supersonic bombers and reconnaissance and passenger aircraft.

In thrust-augmented supersonic flight, a 180° turn involves considerable consumption of fuel owing to its large radius. This consumption must be taken into account.

Let us turn to calculation of the maximum range of an airplane.

In cruising-climb flight, per-kilometer consumption is directly proportional to weight. In flying a distance dL the weight of the airplane decreases by $dG = qdL$, so that $dL = dG/q$, and the distance covered during a change in flight weight from G_1 to G_2 will be

$$L = \int_{G_1}^{G_2} -\frac{dG}{q} = \int_{G_2}^{G_1} \frac{dG}{q}.$$

Substituting the expression for q, we get

$$L_{\text{гор}} = \int_{G_2}^{G_1} \frac{3{,}6aMK}{C_{y2}} \cdot \frac{dG}{G} = \frac{2{,}3 \cdot 3{,}6aMK}{C_{y2}} \lg \frac{G_1}{G_2} = \frac{2{,}3G}{q} \lg \frac{G_1}{G_2}. \qquad (6.16)$$

In the expression for range, G is the weight of the airplane for which the per-kilometer fuel consumption q was calculated. Since $G_1 - G_2 = G_f$, we have

$$\frac{G_1}{G_2} = \frac{G_1}{G_1 - G_f} = \frac{1}{1 - \frac{G_f}{G_1}}$$

and, consequently,

$$L_{\text{гор}} = \frac{2{,}3}{\frac{q}{G}} \lg \frac{1}{1 - \frac{G_f}{G_1}}. \qquad (6.17)$$

It follows from (6.17) that, in order to calculate the distance covered on the cruising-climb segment of the flight, it is necessary to know the initial and final weights of the airplane, which

differ by the weight of the fuel burned. In the preceding section, we described a method for computing the fuel consumed during climbing and accelerating, $G_{f_{clb}}$, and the level-flight initial weight will obviously be $G - G_{f_{clb}}$. The level-flight final weight is $G - G_f + G_{f_{des}}$, where G_f is the fuel reserve and $G_{f_{des}}$ is the fuel consumed during descent. Applying (6.17), we find the cruising-climb range and, adding it to the distances covered during the climb and glide, we find the technical flight range of the airplane.

If a bomb or a load accommodated inside the fuselage is dropped over the target in cruising-climb flight, and this bomb or load weighs more than 2-3% of the weight of the airplane, use of formula (6.17) to compute the cruising-climb distance covered will result in appreciable underestimation of the flight range, since the airplane will be lighter after leaving the target. In this case, it is necessary to determine the cruising-climb distance from the expression

$$L = \frac{4,6}{\frac{q}{G}} \lg \frac{1}{0,5\frac{G_{cg}}{G_1} + \sqrt{1 + \frac{G_T + G_{cg}}{G_1}}}, \tag{6.18}$$

where G is the weight for which the per-kilometer fuel consumption Q was calculated, G_1 is the weight of the airplane at the beginning of cruising-climb flight, G_{cg} is the weight of the cargo or bomb dropped over the target, and G_f is the weight of the fuel burned in cruising-climb flight.

The range of cruising-climb flight or flight at constant altitude (L_{lvl}) may be determined by calculating the average per-kilometer fuel consumption on the level-flight segment instead of by use of (6.17). To this end, we find the average flight weight of the airplane:

$$G_{cp} = G - G_{T_{пол}} - 0,5(G_{T_{гор}} + G_{T_{сц}}). \tag{6.19}$$

We find the altitude and speed of minimal per-kilometer fuel consumption and the value of $q_{av_{min}}$ for G_{av}.

The cruising-climb range is determined from the expression

$$L_{rop} = \frac{G_{rop}}{q_{cp_{min}}}. \tag{6.20}$$

If $G_{f_{lvl}}/G < 0.3$, the error in the calculation of L_{lvl} from the average per-kilometer consumption is negligible. For $G_{f_{lvl}}/G$ of 0.4 and 0.5, it lowers L_{lvl} by comparison with the value obtained from (6.17) by 2.3 and 3.5%, respectively.

If the airplane flies part of the distance with underwing tanks, which increase its frontal drag appreciably, it is necessary to calculate the fuel consumed during climbing with the underwing tanks. Procedure: determine the weight of the fuel remaining in the underwing tanks for level flight and make separate calculations of the level-flight range with the underwing tanks and after they are dropped. If an externally stored bomb or missile that increases the airplane's frontal drag appreciably is released over the target, q_{min} should be calculated with the mean between the values of c_{x_0} with and without the external load. If the flight is made at low altitude and the frontal drag during the flight away from the target differs appreciably from the frontal drag during flight to the target, it is recommended that the minimum per-kilometer fuel consumptions be found for the weight of the airplane at the beginning of level flight from the target ($q_{min_{ini}}$) and at the end of level flight from the target ($q_{min_{fin}}$), with the approximate assumption that $q_{min_{av}} = 0.5(q_{min_{ini}} + q_{min_{fin}})$. Simultaneously, this calculation will give $V_{q_{min}}$ for flight to and from the target.

As expression (6.20) implies, the cruising-climb range is inversely proportional to $q_{min_{av}}$ and depends in large part on the relative weight $G_{f_{lvl}}/G$ of the fuel burned in the cruising climb.

If we are concerned with the supersonic flight range, $G_{f_{lvl}}$ will be strongly influenced by the climbing and accelerating fuel consumption. In subsonic flight, the climbing fuel consumption is relatively small and $G_{f_{lvl}}$ is determined basically by the weight of the fuel placed in the airplane's tanks.

Methods for lowering the per-kilometer fuel consumption and the amount of fuel consumed in climbing and accelerating were examined above.

Opportunities for increasing flight range by increasing the relative fuel weight G_f/G involve decreases in the relative weights of the airframe, powerplants, equipment, and payload of the airplane.

Chapter 7

TAKEOFF AND LANDING CHARACTERISTICS OF THE AIRPLANE AND THEIR VARIATION WITH AIRPLANE AND ENGINE PARAMETERS

§7 1. TAKEOFF

Takeoff consists of the following stages (Fig. 7.1): runup along the ground to liftoff speed and climbing acceleration.

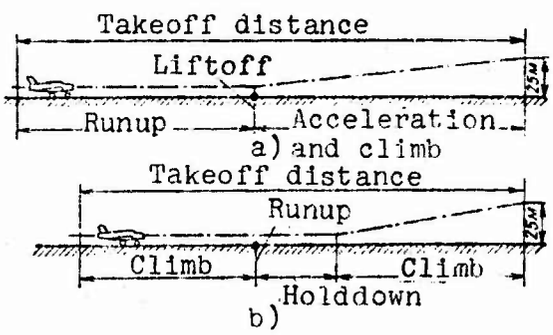

Figure 7.1. Diagrams of takeoff: a) turbojet airplane; b) propeller-driven airplane (with low power/weight ratio).

On reaching a height of 25 meters, a turbojet airplane is moving at a speed approximately 30% above that at liftoff. After liftoff, piston-engined and light turbojet aircraft may use most of their excess thrust for acceleration only while covering a certain distance. This stage in the takeoff is then known as

holddown (see Fig. 7.1b).

The distance from the start of the takeoff run to the point over which the airplane passes at an altitude of 25 meters is known as the takeoff distance. Abroad, the altitude at the end of the takeoff distance is conventionally set at 15 rather than 25 meters. Takeoff distance naturally depends strongly on the flight speed developed at the end of this distance. The higher this speed, the smaller will be the fraction of the thrust excess used to gain altitude on the climbing and accelerating segment and the flatter and longer will this trajectory become. The takeoff distance defined by attainment of h = 25 m is 1.6-2 times longer than the runup for TJE airplanes.

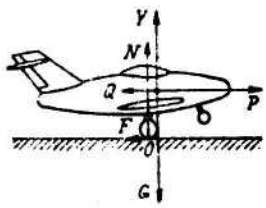

Figure 7.2. Diagram of forces acting on airplane during takeoff runup.

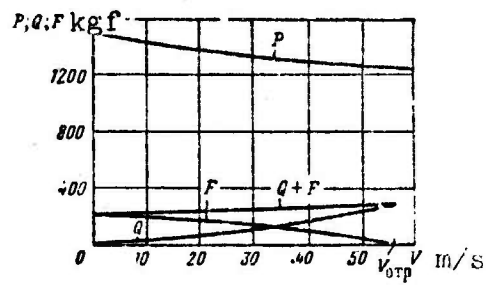

Figure 7.3. Forces acting on airplane during runup as functions of runup speed.

The speed of a modern jet airplane on the climbing trajectory with $V_{y_{max}}$ is considerably greater than its speed at the end of the takeoff distance. Before climbing to gain altitude, therefore, the pilot executes a climb combined with rapid acceleration.

In most cases, the technical specifications for an airplane state specific requirements as to the lengths of the takeoff and landing distances or the runup and rollout distances. It is therefore important that the designer be able to relate the runup and takeoff distances with the characteristics of the airplane and its engines.

This book will consider the problems of takeoff solely from this point of view.

Let us first consider the runup. During runup, the forces indicated in Fig. 7.2 act on the airplane. Projecting them onto the Ox axis, we write the equation of motion for runup:

$$\frac{dV}{dt}=\frac{g}{G}(P-Q-F); \tag{7.1}$$

$$F=fN=f(G-Y), \tag{7.2}$$

where f is the friction coefficient and N is the ground-reaction force.

The higher the speed, the greater will be the frontal drag Q and, since lift is stronger, the smaller will be the friction F. As a result, the sum Q + F varies little during runup (Fig. 7.3). In the case of jet airplanes, the thrust of the TJE during runup decreases slowly in a takeoff without afterburner and increases slightly in an afterburner takeoff. The acceleration varies in the same fashion during the runup. An expression for the runup distance L_{run} follows from (7.1):

$$L_{\text{раз}}=\frac{1}{2}\int_{0}^{V^2_{\text{отр}}}\frac{G}{g(P-Q-F)}dV^2. \tag{7.3}$$

Since the acceleration changes insignificantly during runup and its variation with speed is near linear, errors no greater than 5% are incurred in computing runup distance from an average acceleration that does not vary during the runup. Here the average acceleration must be determined as the acceleration at a speed equal to 0.72 of the liftoff speed for turbojet airplanes and for 0.75 of liftoff speed for airplanes with turboprop engines.

Let us derive an analytical expression for the average runup acceleration:

$$j_{cp}=\frac{g}{G}[P_{cp}-(Q+F)_{cp}].$$

$$(Q+F)_{cp}=\left(c_{x_{0_{раз}}}+\frac{1}{\pi\lambda_э}c^2_{y_{раз}}\right)S\frac{\varrho V^2_{cp}}{2}+$$

$$+f\left(G-c_{y_{раз}}S\frac{\varrho V^2_{cp}}{2}\right)=\left(c_{x_{0_{раз}}}+\frac{1}{\pi\lambda_э}c^2_{y_{раз}}-\right.$$

$$\left.-c_{y_{раз}}f\right)S\frac{\varrho V^2_{cp}}{2}+fG.$$

Transforming, we have

$$S\frac{\varrho V^2_{cp}}{2}=\frac{S\varrho V^2_{отр}}{2}\frac{c_{y_{отр}}}{c_{y_{отр}}}\left(\frac{V_{cp}}{V_{отр}}\right)^2.$$

but at liftoff speed $Sc_{y_{1/o}}\rho V^2_{1/o}/2 = G$, and the ratio $(V_{av}/V_{1/o})^2 \approx 0.5$, so that $S\rho V^2_{av}/2 = 0.5G/c_{y_{1/o}}$. Substituting the expression for $S\rho V^2_{1/o}/2$, we obtain

$$(Q+F)_{cp}=G\left[\frac{0,5}{c_{y_{отр}}}\left(c_{x_{0_{раз}}}+\frac{1}{\pi\lambda_э}c^2_{y_{раз}}-c_{y_{раз}}f\right)+f\right].$$

The sum in the square brackets will be referred to as the reduced coefficient of friction f_{red}:

$$f_{пр}=f+\frac{0,5\left(c_{x_{0_{раз}}}+\frac{1}{\pi\lambda_э}c^2_{y_{раз}}-c_{y_{раз}}f\right)}{c_{y_{отр}}}. \tag{7.4}$$

Then $j_{av} = g[(P_{av}/G) - f_{red}]$ and the runup distance can be determined from the expression

$$L_{раз}=\frac{V^2_{отр}}{2g\left(\frac{P_{cp}}{G}-f_{пр}\right)}. \tag{7.5}$$

As we indicated, P_{av} should be taken at a speed of $0.72V_{1/o}$ for turbojet-engine airplanes. Analysis of the runup distances of modern airplanes indicates that for takeoff from a concrete runway, in which case $f \approx 0.02$, the reduced coefficients of friction are 0.056, 0.045, and 0.039 for wing aspect ratios of 2-3.5 and $c_{y_{1/o}}$ = 0.7, 1.0, and 1.3, respectively, and 0.037, 0.031, and

0.0285 for aspect ratios larger than six and $c_{y_{1/o}}$ of 1.0, 1.5, and 2.0.

It follows from(7.5) that the runup distance is proportional to the square of liftoff speed, while the latter is

$$V_{отр} = 4\sqrt{\frac{G}{Sc_{y_{отр}}}}. \tag{7.6}$$

In determining the liftoff speed of aircraft with large thrust/weight ratios, it is recommended that the projection of the thrust onto the y axis at the liftoff angle of attack $\alpha_{1/o}$ be taken into account. In this case,

$$V_{отр} = 4\sqrt{\frac{G - P\sin(\alpha_{отр} + \varphi_T)}{c_{y_{отр}} S}}, \tag{7.7}$$

where ϕ_t is the angle between the chord and the thrust vector. Expressions (7.5) and (7.6) imply that the runup distance is approximately proportional to the load per square meter of wing and inversely proportional to $c_{y_{1/o}}$.

The lift coefficient at liftoff should be determined with consideration of flap deflection, which increases it. It must be remembered that the proximity of the ground at the landing angle of attack increases $c_{y_{1/o}}$ (for a low-wing design) by 0.15-0.20 (see Fig. 4.4). The wing attack angle of an airplane at liftoff must always be 3°- 4° smaller than the critical attack angle (α_{cr}), at which c_y falls off, since reaching $c_{y_{cr}}$ causes one-sided flow separation from the wing and sharp rolling onto that wing for many aircraft, and especially those with unswept trapezoidal wings.

For small airplanes with unswept wings, the landing angle of attack was determined by the critical-angle value. As a result, $c_{y_{1/o}}$ and $c_{y_{1dg}}$ depended on $c_{y_{max}}$. The critical attack angles became larger for airplanes with small-aspect-ratio wings. The value of $\alpha_{cr} > 16°$ for aspect ratios of 2-3 on airplanes with

wings swept more than 45°. With decreasing aspect ratio and increasing sweep, the distance from the airplane's CG to the end of the fuselage increased simultaneously. As a result, landing gear that would have permitted takeoff with liftoff angles of attack 3°-4° smaller than α_{cr} would have been very tall and, consequently, heavy. Retraction would also be extremely difficult. For these reasons, the liftoff attack angle of an airplane with small-aspect-ratio wings is determined not by α_{cr}, but by landing-gear height. This height also determines the liftoff attack angles of many heavy airplanes having wings with aspect ratios of 6-8 and 25°-35° sweep. The liftoff attack angles of such airplanes are approximately 8°-11°. If the undercarriage height of an airplane with a 35° swept wing permits $\alpha_{ldg} \geq 13°$, it is necessary to find the wing's α_{cr} in the presence of the ground and the value of the difference $\alpha_{cr} - \alpha_{ldg}$.

In determining $c_{y_{1/o}}$, it must be remembered that the propwash over the wing from turboprop engines (when the engines are housed in wing nacelles) increases $c_{y_{1/o}}$ by 15-25%.

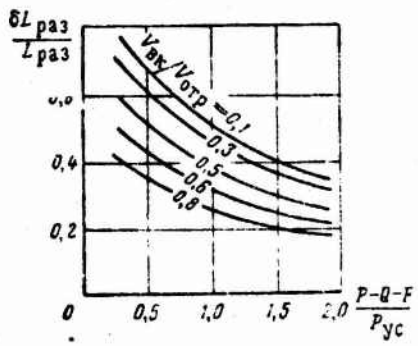

Figure 7.4. Runup distance reduction as affected by booster thrust and speed at which booster is cut in.

It follows from expressions (7.5) and (7.6) that the best ways to shorten the runup distance are to increase the airplane's thrust/weight ratio P_0/G, which equals the ratio of zero-altitude engine thrust to the airplane's takeoff weight, to increase $c_{y_{1/o}}$, and to reduce the load per square meter of wing, G/S.

A highly effective means of shortening runup distance is to switch in the engine's afterburner during takeoff and use rocket takeoff boosters.

Augmenting the thrust of a modern turbojet engine on the ground increases its output by 40-60%. Without afterburning, P_{av} during the runup is also about 5% smaller than P_0, while $P_{av} \approx P_0$ in augmented operation.

On the whole, the runup distance is much shorter with augmentation than without it.

The shortening of the runup distance that results from using booster thrust depends first on the ratio of booster thrust P_{bo} to the average accelerating force during takeoff without boosters $(P - Q - F)$, and second on the ratio of the runup speed at which the boosters are cut in to the liftoff speed $V_{ci}/V_{l/o}$.

It can be shown that the relative decrease $\delta L_{run}/L$ of the runup distance is approximately [2.4]:

$$\frac{\delta L_{\text{раз}}}{L_{\text{раз}}} = \left(1 - \frac{V_{\text{вк}}^2}{V_{\text{отр}}^2}\right) \frac{P_{\text{ус}}}{P_{\text{ус}} + (P - Q - F)_{\text{ср}}}. \tag{7.8}$$

Figure 7.4 shows $\delta L_{run}/L_{run}$ as a function of relative booster thrust and the speed at which the booster is cut in.

A solid booster can be dropped after takeoff, and its use has almost no effect on the design weight of the airplane. Thus, although the use of takeoff boosters increases the cost and complexity of operating the airplane, it has no effect on its other flight characteristics.

§7.2. LANDING

An airplane lands in the following characteristic stages (Fig. 7.5):

a) the glide, in which flight altitude is lowered from 25 m to 8-12 m;

b) flattening out - curvilinear motion during which altitude is reduced to 0.5-1 m and the glide-speed vector angle θ is reduced to zero;

c) the flare - flight parallel or nearly parallel to the

ground, during which the angle of attack is steadily increased from the value at the end of flattening to the landing angle of attack, while speed is reduced;

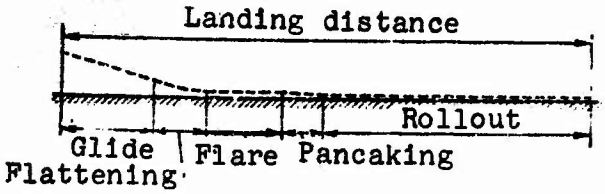

Figure 7.5. Diagram of airplane landing.

d) pancaking - curvilinear motion at constant angle of attack with loss of 0.5-1 m of altitude;

e) the rollout, during which speed varies from the landing speed at the instant of touchdown to zero or to the runway-end taxiing speed.

Not every landing can be broken up into the above five steps. In many cases, altitude is lost during flattening out and the airplane's wheels touch down without a pancaking stage. In some landings, the airplane touches the ground at the end of flattening-out; then the angle of attack may be either smaller than or equal to the landing attack angle.

Modern jet airplanes with small aspect ratio wings have moderate maximum lift/drag ratios. If, therefore, the glide were flown with little or no engine thrust the glide-path angle would be large and the airplane would be descending at a high rate in the glide. In this case, it will be necessary to increase the initial altitude of the flattening maneuver and the pilot would find it very difficult to start this maneuver at the proper time. For this reason, the landing glide of a modern airplane is flown with the engines developing considerable thrust. Many airplanes are very hard to land dead-stick. This does not imply that dead-stick landing of the jet is impossible, but its execution is complicated by the fact that the landing glide must be flown with a speed reduction, at which the glide angle decreases. It follows from the above that all measures that increase the maximum lift/drag ratios of subsonic aircraft under landing conditions aid in simplifying

the modern aircraft and are highly desirable.

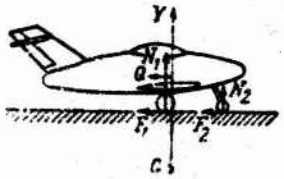

Figure 7.6. Diagram of forces acting on airplane during rollout.

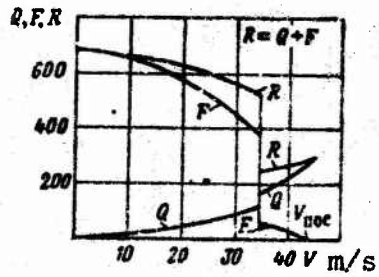

Figure 7.7. Forces acting on airplane during rollout as functions of rollout speed.

The landing glide is flown with the gear down and with use of the wing flaps, which increase the wing's $c_{y_{ldg}}$. Therefore, especially for airplanes with small aspect ratio wings, the high-lift devices must increase $c_{y_{ldg}}$, but must lower the maximum lift/drag ratio to the smallest possible degree.

Airplanes with tricycle landing gear run on their main wheels during the first part of rollout and do not use the wheel brakes. Then, steering the airplane, the pilot brings down the nose wheel and begins to brake sharply. Here the airplane is acted upon by the forces indicated in Fig. 7.6. Their changes with speed during rollout are shown in Fig. 7.7, and the equation of motion is written thus:

$$\frac{dV}{dt} = -\frac{g}{G}(Q + F). \tag{7.9}$$

It follows from the above that the braking force F changes abruptly during rollout and that its average value depends on the time at which braking is started and to an even greater degree on the coefficient of friction at the wheel-brake shoes. All of this makes it very difficult to calculate the rollout distance:

$$L_{пр} = \frac{1}{2} \int_{V^2_{пос}}^{0} \frac{G}{g(Q+F)} dV^2. \tag{7.10}$$

The main braking force in operation during rollout is the frictional force determined by the wheel-brake mechanism. It may therefore be assumed that variations from the average negative acceleration during rollout are small.

Working out of the relation between L_{ro}, V_{ldg}, and j_{av} with the rollout considered as uniformly decelerating motion during which

$$L_{пр}=\frac{V^2_{пос}}{2j_{ср}}. \tag{7.11}$$

has shown that j_{av} = -2.3 - 2.6 m/s^2 for modern jet airplanes with 45°-60° swept wings; j_{av} = 2.0-2.3 m/s^2 during rollout for heavy airplanes with 25°-35° wing sweep.

When drag parachutes are used, j_{av} is increased to -3.0-3.5 m/s^2.

When thrust is reversed, the absolute values of the j_{av} given above must be increased by $9.81P_{rev}/G$ [m/s^2].

Using the above average values of the rollout acceleration and knowing the landing speed, we can determine the rollout distance accurate to about 10%. The landing distance is 2.0-2.5 times the rollout distance.

Since the values of j_{av} during the rollout differ little from one another for modern aircraft, the rollout distance is obviously determined basically by the airplane's landing speed.

During pancaking from a height of about 0.5 meters, the flight speed drops by about 5%. Thus we obtain the following expression for the landing speed:

$$V_{пос}=0{,}95\cdot 4\sqrt{\frac{G}{Sc_{y_{пос}}}}. \tag{7.12}$$

It follows from expressions (7.11) and (7.12) that the rollout distance is directly proportional to the load per square meter of wing under landing conditions and inversely proportional to $c_{y_{ldg}}$.

Analysis of the landing speed of modern aircraft indicates that their $c_{y_{ldg}}$ range from 0.5 to 3. Aircraft of the flying-wing type with wing aspect ratios of 1.9-2.2 and leading-edge sweep angles around 60° have the smallest $c_{y_{ldg}}$, from 0.5 to 0.6. The small $c_{y_{ldg}}$ of these wings is explained by the absence of the horizontal stabilizer and hence the impossibility, dictated by the need for longitudinal balance, of using flaps.

In aircraft having the same type of wing but also horizontal tails, flaps increase $c_{y_{ldg}}$ to 0.7-0.8. Increasing the wing aspect ratio to 2.5-3.5, reducing the sweep angle to 45°, and blowing the boundary layer off the flap and turned-down wing leading edge increase $c_{y_{ldg}}$ to 1.15-1.4. The landing attack angles of all these aircraft are determined not by α_{cr}, but by landing-gear height, and vary from 9° to 12°.

For transonic airplanes with wing sweeps around 35° and aspect ratios of 6.5-8, $c_{y_{ldg}}$ varies over a very broad range, from 1.2 to 3.0. The value of $c_{y_{ldg}}$ is determined basically by the effectiveness of the wing high-lift devices and, in addition, by landing-gear height. Transonic airplanes have landing angles of attack between 8° and 13°. At α_{ldg} equal to or greater than 13°, $c_{y_{ldg}}$ comes to depend not only on landing angle of attack (landing-gear height), but also on $c_{y_{max}}$ (α_{cr}). Thus the designer must use high-lift devices that increase α_{cr}, e.g., by providing the outer wing with leading-edge slats. Thus, the wings of the Boeing 707 and 720 passenger airplanes, which have $\alpha_{ldg} \approx 10.4°$, do not have wingtip leading-edge flaps, while the Boeing 737 wing, for which $\alpha_{ldg} \approx 12.8$, does have them.

The impossibility of obtaining large $c_{y_{ldg}}$ with small wing aspect ratios and large sweep angles gave a great deal of impetus to the development of variable-sweep aircraft capable of supersonic flight with the wing swept far back and with a small aspect

ratio and landing with the wing at a small sweep angle and large aspect ratio.

The problem of the relation between the runup and rollout distances of aircraft is of great interest. In military supersonic aircraft, the rule is that the runup distance is shorter than the rollout distance even without takeoff boosters.

For transonic aircraft, the runup and rollout distances are closely similar, and the runup distance of a heavy airplane may even exceed its rollout distance.

Chapter 8

METHODS OF ENSURING STABILITY AND CONTROLLABILITY OF AIRCRAFT

§8.1. GENERAL REQUIREMENTS FOR STABILITY AND CONTROLLABILITY OF AIRCRAFT

Irrespective of whether an airplane is controlled by a pilot or by automatic devices, good stability and controllability are necessary for guidance of the airplane along a given trajectory. Thus, problems of the aerodynamic layout of the airplane that will endow it with the necessary stability and controllability characteristics under all flight conditions occupy an important position in the over-all problem of synthesizing the closed-loop control system in the preliminary design stage.

To obtain satisfactory stability and controllability characteristics in the airplane in all flight situations, its aerodynamic-design characteristics must meet certain requirements:

– the control-surface deflections that are possible and acceptable on the basis of design or other considerations, as well as the forces fed back to the control levers, must ensure all flight regimes required of the aircraft in question;

– the airplane must be stable in its own disturbed motion. The parameters of the disturbed motion must damp as quickly as possible;

– the airplane's response to manipulation of the controls must be such that the transition is not accompanied by overshoots of the parameters of the airplane's motion (especially of the normal acceleration) beyond established limits;

– the lag in the airplane's response to operation of the controls (its response time) must remain within established limits;

– the airplane's control system must perform with high reliability.

Because of the rather broad altitude and speed ranges of flight, a given set of aerodynamic-design features cannot satisfy all of the requirements stated above. The resulting gap between the required stability and controllability characteristics and the possibilities inherent in the airplane's aerodynamic-design layout must be filled by automatic devices designed to improve the airplane's stability and controllability. Rational aerodynamic-design layout of the airplane and selection of the proper automatic systems are two inseparable parts of the coordinated process of synthesizing the closed-loop control system.

The present work is concerned basically only with the first department of closed-control-system development. In other words, we are concerned basically with problems in the selection of advantageous – from the standpoint of stability and controllability – aerodynamic shapes for the airplane, tail-section and control-surface dimensions, wing dihedral, and aerodynamic devices that improve stability and controllability characteristics.

In addition, we shall submit a technique for checking the correctness of the choice of basic tail- and control-surface parameters based on the airplane's trim in the design flight modes. It is assumed in the latter case that the geometrical shape and dimensions of the airplane have been arrived at in the first approximation and that the takeoff weight, moments of inertia, and standard aerodynamic characteristics are known.

The class of airplanes considered here will be limited to

transonic and supersonic types that take off and land conventionally.

Before proceeding to the elaboration of a rational aerodynamic-design layout of the airplane (from the viewpoint of stability and controllability), it is necessary to form a clear conception of the basic stability and controllability problems that arise in modern transonic and supersonic airplanes.

§8.2. ENSURING STABILITY AND CONTROLLABILITY OF TRANSONIC AIRPLANES

Analysis of statistical data on modern transonic aircraft indicates that the overwhelming majority have swept wings and tails. Use of swept wings has disadvantages as well as advantages. The former consist in deterioration of stability and controllability characteristics. The following problems arise:

– when the airplane is set at large attack angles, it loses some or all of its normal-acceleration stability. This phenomenon is known as "grabbing" in aviation practice, since the airplane increases its angle of attack spontaneously and bends the trajectory of its motion upward.

The normal-acceleration instability at large angles of attack is compounded by "floating" of the ailerons, i.e., when both ailerons are deflected upward simultaneously on an increase in attack angle. Upward deflection of both ailerons is made possible by deformation of the control rods (cables), taking up of slack, and deformation of the wing structure at the attachment points of the aileron control-line rockers;

– longitudinal normal-acceleration stability is lowered at critical flight speeds owing to the appearance of shock-stall effects (formation of local compression shocks);

– the lateral stability and controllability characteristics of the airplane deteriorate in low-speed flight at large attack angles, which cause the airplane to wobble from wing to wing. This effect is governed largely by the transverse stability m_x^β,

the decrease in aileron effectiveness, and the directional stability m_y^β;

– the effectiveness of the control surfaces, and that of the ailerons in particular, decreases substantially in flight at Mach numbers equal to or greater than critical. Aileron effectiveness is also lowered sharply in the presence of bending-torsional deformations of the wing. These deformations become especially large toward the wingtip.

Let us consider what measures must be taken in laying out a transonic airplane to eliminate some or all of the above stability and controllability deficiencies.

a) Aerodynamic-Design Measures to Reduce "Grabbing" of the Airplane on Going to Large Attack Angles

First of all, let us briefly examine the essential physical nature and causes of the decrease in the normal-acceleration stability of swept-wing aircraft on going to large attack angles. It is known that this phenomenon is basically due to features of the flow past the swept wing and the horizontal tail surface behind it in the airplane system, i.e., when the entire airplane as a whole is considered instead of just the isolated tail surface.

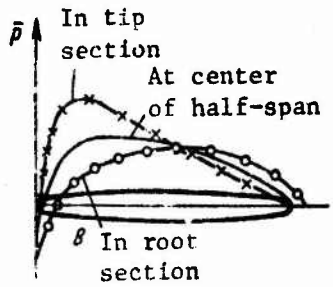

Figure 8.1. Distribution of pressure over chord in root, midlength, and tip sections of swept wing.

The presence of the midlength and tip effects in the airflow over a swept wing changes the pressure-distribution pattern along the span and chord of the wing, with the root sections differing from the tip sections basically in the amount of vacuum at the front of the profile. The vacuum on the upper surface of the front of the profile ($\alpha > 0$) is smaller in the root sections than in the tip sections. Figure 8.1 indicates that at small attack angles and subcritical speeds, the tip

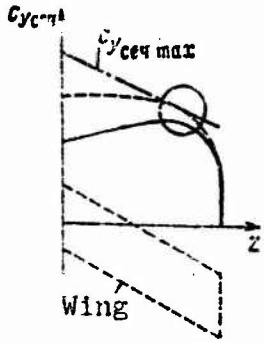

Figure 8.2. Changes in spanwise distribution of lift coefficient $c_{y_{sec}}$ on swept wing. ——$c_{y_{sec}}$; ---variation of $c_{y_{sec}}$ on increase of wing angle of attack; -·-·-$c_{y_{sec\,max}}$; o is the point at which flow separation begins.

sections of the wing are more heavily loaded than the root sections. This means that the section lift coefficients $c_{y_{sec}}$ will be larger on the tip sections of a swept wing (even for unity taper) than in the root sections (Fig. 8.2, solid line). When the airplane's angle of attack increases, the lift coefficients increase on all sections of the wing (dashed line in Fig. 8.2), with c_y increasing more rapidly on the root sections of the swept wing than on the tip sections.

At a large enough wing angle of attack, $c_{y_{sec}}$ may reach its maximum on certain sections of the wing (see dash-dot line in Fig. 8.2). This means that flow detachment will occur in these sections as the angle of attack increases and begin to spread along the wing. Consequently, flow detachment begins on that part of the wing on which the section lift coefficient $c_{y_{sec}}$ reaches its maximum first.

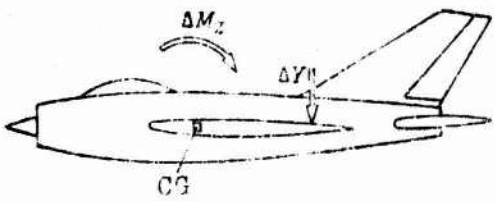

Figure 8.3. Origin of pitchup moment on flow separation at tips of swept wing.

To find the point at which flow separation begins on the wing, it is necessary to know the spanwise variation of the lift coefficients $c_{y_{sec}}$ and $c_{y_{sec\,max}}$. For an unwarped wing with the same profile over the span, the variation of $c_{y_{sec\,max}}$ along the span depends on wing planform. The influence of planform on $c_{y_{sec\,max}}$ is associated

principally with the taper and sweep of the wing.

The taper lowers the Reynolds numbers of the tip sections and reduces $c_{y_{sec\ max}}$. The sweep of the wing causes crossflow of the boundary layer from the root toward the tips of the wing and its accumulation and premature separation at these points. As a result, $c_{y_{sec\ max}}$ decreases along the half-span of a tapered swept wing even when the taper is unity (see Fig. 8.2).

This figure indicates that, as the angle of attack of the swept wing increases, the lift coefficient $c_{y_{sec}}$ reaches its maximum $c_{y_{sec\ max}}$ earliest near the tips of the span. Thus, flow separation begins at the tips of a swept wing at large angles of attack. This means that at large c_y, an increase in wing angle of attack lowers the lift at the wing tips and sets up a pitchup moment (Fig. 8.3). An over-all increase in lift occurs as a result of the increased lift at the root and at midlength of the wing, and this also tends to increase the pitchup moment originating from wing lift.

In addition, the pitchup moment acquired by the airplane on going to larger attack angles is further increased by a decrease in the lifting properties of the horizontal tail, since the lift of the wing root sections is increased, leading to an increase in the downwash angles in the vicinity of the horizontal tail and a decrease in its true angles of attack.

As a consequence, the airplane loses longitudinal stability with respect to normal acceleration. Graphically, this is represented by an upward bend of the $m_z = f(\alpha)$ curve — a so-called "spoon" appears at large angles of attack (Fig. 8.4).

Figure 8.4. Pitching-moment-coefficient variation of a swept-wing airplane as a function of angle of attack.

It follows from this analysis of the aerodynamic problems of swept-wing

aircraft that the loss of normal-acceleration stability at large attack angles can, in principle, be eliminated by:

– changing the spanwise distribution of the maximum section lift coefficient $c_{y_{sec\ max}}$ (dot-dash curve in Fig. 8.2);

– changing the spanwise distribution of $c_{y_{sec}}$ (Fig. 8.2, solid curve) in such a way that $c_{y_{sec}}$ will be smaller at the tips of the wing at a given angle of attack than in the root section;

– preventing accumulation of boundary layer on the wing tips;

– rational placement of the horizontal tail on the airplane to minimize the downwash at the tail.

Accordingly, there are several aerodynamic-design measures directed toward improvement of longitudinal normal-acceleration stability at large attack angles.

The first of these, whose purpose is to adjust the spanwise distribution of $c_{y_{sec\ max}}$, is to build up the wing with a variety of profiles instead of identical ones: profiles wich less lift at the root and profiles with higher lift at the wing tips, with the possibility of using symmetrical profiles in the root of the wing or even profiles with negative centerline curvature, the so-called "inverted" profiles. Use of lower-lift profiles with negative centerline camber has practically no detrimental effect on the total lifting ability of the wing, since the root section of a swept wing is not fully loaded because of the spanwise redistribution of the lift, as we see from Fig. 8.2. It then becomes possible to use root profiles with larger relative thickness (12-15%) wich no appreciable increase in the frontal drag at near-critical Mach numbers.

It appears that the Boeing firm was guided by this principle in modifying the type 707 to the type 720, when it introduced a buildup on the leading edge of the wing root sections to give the profile centerline a negative curvature and reduce its thickness

ratio (Fig. 8.5). The value of $c_{y_{sec\ max}}$ was lowered on the built-up segment at the root of the wing (Fig. 8.6).

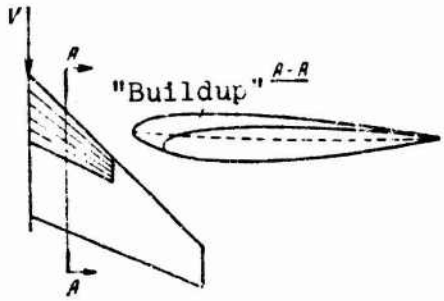

Figure 8.5. Schematic representation of "a buildup" on swept wing of Boeing 720 aircraft.

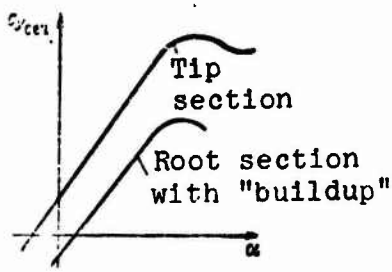

Figure 8.6. Variation of lift coefficients vs. angle of attack of root sections with "a buildup" and tip sections without "a buildup" on swept wing.

Thus, by placing higher-lift profiles at the tips and lower-lift profiles at the root of the wing, it is possible, in principle, to distribute $c_{y_{sec\ max}}$ spanwise in such a way as to prevent flow separation from the wing tips at large attack angles.

In addition, $c_{y_{sec\ max}}$ can also be increased at the wing tips by the use of leading-edge slats at the tips to deflect the wing nose sections.

A second measure for improvement of the normal-acceleration stability of swept-wing aircraft is to impart an aerodynamic twist to the wing. It consists in twisting the wing sections progressively away from the root sections, to an angle of -3° to -5° at the wing tips. This adjusts the spanwise distribution of $c_{y_{sec}}$ in such a way that the wing root section is loaded more heavily and the wing tips are relieved. Since there is no change in $c_{y_{sec\ max}}$ on the tip sections, a wing twisted in this way can reach large attack angles (with respect to root chord) before separation begins on the tip sections of the wing.

In designing a swept wing twisted in this manner, it is necessary to take account of bending-torsional deformation of the wing tips, which also twists the tip sections of the wing to a negative angle with respect to the root sections. The more flexible the wing, the greater will be the twist acquired as a result of its deformation.

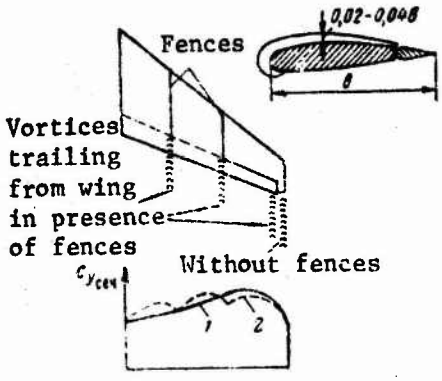

Figure 8.7. Effect of mounting stall fences* on upper surface of swept wing on spanwise distribution of the lift coefficient $c_{y_{sec}}$: 1) without fences; 2) with fences.

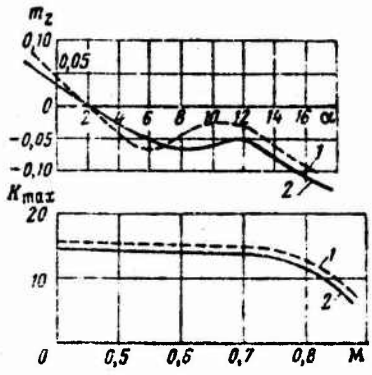

Figure 8.8. Variation of aerodynamic characteristics of swept wing (χ = 35°) on installation of stall fences: 1) without fences; 2) with fences.

A third way to improve longitudinal normal-acceleration stability at large attack angles consists in the use of devices that reduce boundary-layer pileup at the wing tips. They include use of stall fences on the upper surface of the wing, use of pylons to suspend the engines under the wings, and the use of "doglegs" on the leading edge of the swept wing.

Usually, one or two, and less often three stall fences are mounted on the wing. They must be oriented in the direction of symmetrical flow over the wing. The height of the stall fences represents 2-4% of the local wing chord. The fences mounted on the wing divide it into separate sections. Flow of the boundary

*Translator's Note: A stall fence is a barrier running over the wing chord to prevent crossflow over the wing.

layer toward the wing tips then occurs only within the limits of the particular wing segment. Vortices form at the fences, and the boundary layer accumulated at these points flows off with them (Fig. 8.7). We see that the use of two stall fences on the wing upper surface has not only eliminated accumulation and detachment of the boundary layer at the wing tips, but has at the same time improved the spanwise distribution of lift.

As an example, Fig. 8.8 shows the variation of the pitching-moment coefficient m_z with the angle of attack α and that of the maximum lift/drag ratio K_{max} as a function of M for a swept wing with sweep angle $\chi = 35°$ when two stall fences are mounted on it (their heights are $\bar{h} = 0.04$; $z_1 = 0.41l/2$ and $z_2 = 0.66l/2$). We see that while the stall fences improve normal-acceleration stability, they also lower the airplane's lift/drag ratio, since they increase its frontal drag.

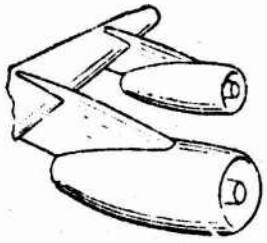

Figure 8.9. Wing of Boeing 707 airplane showing engine nacelles on pylons.

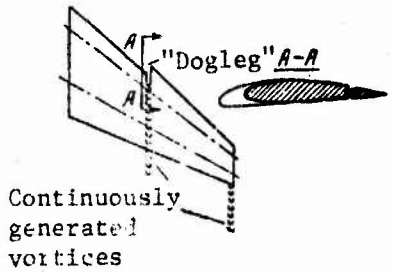

Figure 8.10. Diagram of "dogleg" on leading edge of swept wing.

The effect of using pylons to suspend the engines under the wing is similar to that of stall fences. However, these pylons act as stall fences on the lower surface of the wing, where the boundary-layer crossflow is considerably smaller than it is on the upper surface. The gain from use of such pylons is therefore small. For this reason, the engine pylons of certain airplanes (for example, the Boeing 707) are mounted in such a way that they also extend onto the wing upper surface (Fig. 8.9). In this case,

the pylons work as stall fences.

A "dogleg" in the leading edge of a swept wing, as shown in Fig. 8.10, functions in much the same way as a stall fence. The "dogleg" forms a steady vortex on the wing surface and this vortex acts as a stall fence, pulling the accumulating boundary layer along with it and preventing it from flowing across to the wing tip. It should be noted that, unlike stall fences, "doglegs" are effective over the entire speed range. They are therefore used by military aircraft with swept and delta wings capable of flight not only at subsonic, but also at supersonic speeds. Sometimes the use of the "dogleg" alone does not give the desired result. In this case, the "dogleg" may be used with a buildup on the wing leading edge (see Fig. 8.10, section A-A). This enhances the effect.

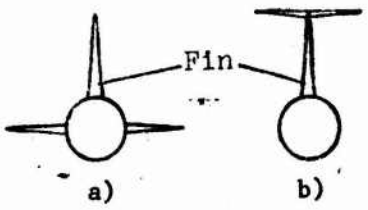

Figure 8.11. Diagrams showing two placements of horizontal tail to obtain minimum downwash in the symmetry plane of the airplane: a) horizontal tail on fuselage; b) horizontal tail on vertical fin.

It is not recommended that the "dogleg" be made very deep, since this would weaken the wing.

A fourth way to improve longitudinal normal-acceleration stability at large attack angles is to place the horizontal tail at a position relative to the wing and fuselage in which the downwash in the tail region is minimized. It is known that, disregarding the influence of the stream of gases from the TJE's, the least downwash at small attack angles is obtained when the horizontal tail is placed on the fuselage below its axial line (see Fig. 8.11a) or on top of the fin (see Fig. 8.11b). At large attack angles, a horizontal tail atop the fin enters a region of strongly stagnated flow. This lowers its effectiveness. The horizontal tail below the fuselage axis does not have this deficiency.

However, it should be noted that the choice of the horizontal-tail mounting point on a conventionally configurated airplane depends very strongly on where the engines are mounted on the airplane. The tail may not be placed where it is struck by the stream of gases from the engines or in a position such that this jet passes too far from the surface of the horizontal tail.

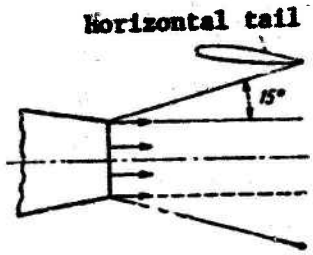

Figure 8.12. Diagram showing position of horizontal tail relative to engine exhaust-gas jet.

When the jet of gases from the engines passes close to the surface of the tail, a suction force will be applied to it. This force will vary in magnitude as a function of engine setting. Accordingly, the longitudinal moment that tends to throw the airplane out of trim will vary with the power being developed by the TJE. This makes control more difficult.

It has been established experimentally that the horizontal tail must be placed relative to the stream of gases from the engines in such a way that it does not intrude across the boundary of the jet, i.e., into the surface of the jet, on which the speed of an air particle equals the speed of flight. In approximation, this surface may be assumed to be that formed by a cone with a generatrix inclined 15° to the axis of the TJE and described about the engine's exhaust nozzle (Fig. 8.12).

If the TJE's have no effect on the tail, then of the two schemes shown in Fig. 8.11, the one with the lower position of the horizontal tail on the fuselage is superior from the design and weight standpoints and also as regards vibrational strength (immunity to flutter).

We note that this placement of the horizontal tail is better not only for transonic aircraft, but also for supersonic types.

A fifth measure taken to improve longitudinal normal-acceleration stability at large attack angles is concerned with countering aileron "float." The phenomenon of simultaneous upward deflection of ailerons at the wing tips when the airplane's angle of attack increases is known as aileron "float." It is caused by deformation of the control rods or cables and the taking up of slack under the influence of the aileron hinge moment $M_{h.a}$.

The hinge moment that causes aileron "float" can be computed by the formula

$$M_{h.a} = m^{\alpha}_{h.a} q \cdot S_a b_a \Delta\alpha, \tag{8.1}$$

where $m^{\alpha}_{h.a}$ is the derivative of the aileron hinge moment coefficient with respect to angle of attack, q is the ram pressure, S_a is the aileron area, and b_a is the aileron mean chord. We see that, other conditions the same, the amount of aileron "float" depends on the derivative $m^{\alpha}_{h.a}$. Thus, by reducing $m^{\alpha}_{h.a}$, the designer reduces aileron "float." We note that one way to reduce the derivative $m^{\alpha}_{h.a}$ is to compensate aerodynamically by blunting the trailing edge of the aileron.

Aileron "float" can also be reduced at a given $m^{\alpha}_{h.a}$ by routing the aileron control lines so as to minimize the deformation of the control rods and reduce the amount of slack. For example, aileron "float" can be reduced substantially by placing the hydraulic boosters in the immediate vicinity of the ailerons.

For unswept-wing aircraft, aileron "float" has no substantial influence on pitching moment. For swept-wing aircraft with ailerons at the wing tips, simultaneous upward deflection of the ailerons on an increase in angle of attack gives rise to a secondary pitchup moment (since the tip sections of the wing are behind the airplane's center of gravity), which lowers normal-acceleration stability. This makes it understandable why the following design measures must be taken to reduce the influence of aileron "float" on normal-acceleration stability if the effect cannot be eliminated altogether:

– eliminate (to the extent possible) the ailerons at the tips of the wing and provide lateral control by means of ailerons placed at the center of the wing and interceptors on the upper surface of the wing. These measures are used, for example, on the American Convair 880 and 990 passenger aircraft;

– mount two ailerons on the wing: an inboard aileron that operates at all times during flight and an outboard aileron that is switched in under flight conditions such that the inboard ailerons alone are not sufficient to provide lateral control (for example, during takeoff, landing, flight with the flaps down, etc.). This principle is exemplified in the Boeing 707.

b) Measures to Improve Longitudinal Normal-Acceleration Stability at Critical Flight Speeds

It is known that a substantial decrease in the lift coefficient occurs on a swept wing[1] at a certain attack angle at $M \geq M_{cr}$ (Fig. 8.13). Other conditions the same, the critical M

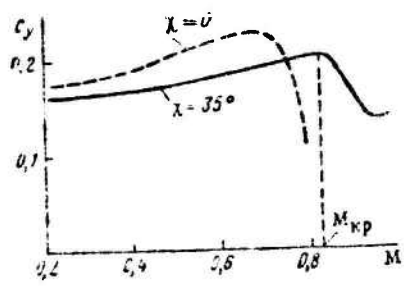

Figure 8.13. Coefficient c_y as a function of M (at $\alpha = 2°$) for swept and unswept wings built up from identical profiles.

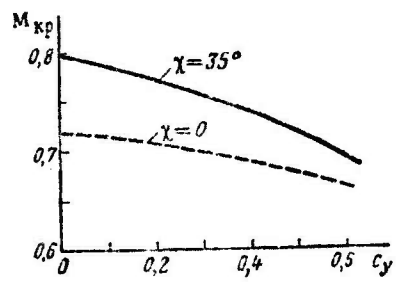

Figure 8.14. M_{cr} as a function of c_y for swept and unswept wings.

decreases with increasing coefficient c_y (Fig. 8.14). Remembering that the spanwise distribution of $c_{y_{sec}}$ along a swept wing is nonuniform (see Figs. 8.1 and 8.2), we conclude that the development

Footnote (1) appears on page 188.

of shock stall on a swept wing begins at the wing tip. Since the tip sections of the wing are aft of the center of gravity, the decrease in lift caused by an increase in angle of attack at $M \geq M_{cr}$ results in an increase in the pitchup moment, i.e., it reduces longitudinal normal-acceleration stability. This phenomenon can be eliminated or controlled by the following procedures:

— by raising the critical Mach number of the wing tip sections by reducing their thickness ratio (use of buildups, etc., see Fig. 8.10), by changing the coordinate of maximum profile

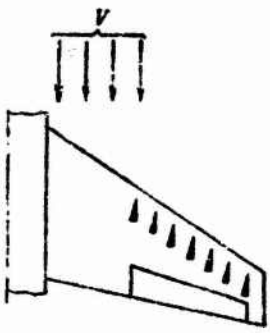

Figure 8.15. Diagram showing placement of wedge-shaped boundary-layer trips on wing of airplane.

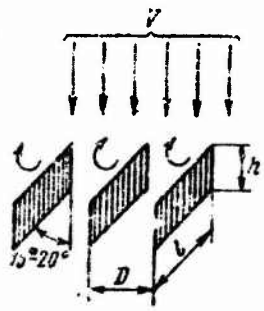

Figure 8.16. Diagram showing placement of trips in the form of vanes on the right wing; height $h = 0.01b$, length $l = (0.015-0.03)b$; spacing $D = (0.04-0.08)b$.

thickness (in the tip sections, the profile should have maximum thickness at about mid-chord), and by imparting aerodynamic twist to the wing;

— by preventing premature separation of the boundary layer behind the local compression shock. This is done by reducing the profile thickness ratio (thereby lowering the intensity of the shock) and by increasing the energy of the boundary layer by mounting various types of leading-edge slats, by boundary-layer blowing and suction, and by installing boundary-layer trips. The latter take the form of a row of wedge-shaped projections (Fig. 8.15) or a row of profiled vanes mounted on the upper surface of the wing perpendicular to it to form an angle of 15°-20° with the

direction of the flow (Fig. 8.16). The air stream acquires a twist in a certain direction as it flows over the trip. The result is formation of a series of vortices that act parallel to the washed surface of the wing along the upper surface of the boundary layer. This causes strong mixing of the boundary layer with the external flow. The boundary layer acquires an influx of energy from the external flow, and this prevents it from being separated from the compression shock. This is essentially a kind of boundary-layer blowing.

Trips functioning in this manner also prevent premature detachment of the boundary layer during flight at large attack angles. Placed in the immediate vicinity of the control-surface (aileron, rudder) axles, they remain effective up to large attack angles.

Rule-of-thumb dimensions for trips made in the form of rectangular vanes are as follows: height above surface $h \approx 0.01b$; length $l = (0.015-0.03)b$; spacing (distance between vanes) $D = (0.04-0.08)b$; b is the wing chord (see Fig. 8.16).

Naturally, the generation of vortices by the trips requires an expenditure of energy, so that the airplane's drag is increased. The drag of the trips can be reduced by adjusting their shape. Thus, the rectangular vanes may be replaced by wedge trips (see Fig. 8.15). A radical solution of the trip-drag problem consists in retracting them into the surface on which they are mounted and deploying them as needed during flight. Such trips are used, for example, on the deHavilland Trident.

c) Aerodynamic Design Measures Taken to Improve Lateral Stability and Controllability Characteristics at Large Angles of Attack

A peculiarity of swept-wing aircraft is that their lateral stability increases with increasing attack angle (as long as the airstream remains smooth). At the same time, the airplane's directional stability m_y^β decreases sharply at attack angles α greater than 10°. Hence it follows that the relation between lateral and directional stability varies as a function of flight

condition for swept-wing aircraft (this applies equally to delta-wing aircraft), and, consequently, so do its lateral stability characteristics. If a normal relation between lateral and directional stability prevails at medium and high speeds (comparatively small angles of attack), lateral stability may become excessive and directional stability deficient at low speeds and large attack angles. This usually results in excessive fluctuation of the parameters of lateral divergent motion, making it difficult to fly the airplane in critical takeoff and landing situations.

In flight at large angles of attack, it also becomes very difficult to ensure normal lateral controllability of the airplane. This is due basically to three factors: a decrease in the effectiveness of the ailerons (which usually work in a flow-detachment zone at the tips of a swept wing), a decrease in directional stability, and an increase in the lateral stability m_x^β. In fact, even a small slip angle in the presence of high lateral stability sets up a substantial rolling moment. It becomes difficult to counter this moment by deflecting the ailerons since the ailerons are not sufficiently effective ($m_x^{\delta_a}$ is small).

The above implies, that in order to improve the lateral stability and controllability of an airplane at large attack angles, it is necessary to take aerodynamic-design measures directed toward reduction of the lateral stability m_x^β and increasing the airplane's controlling moments in roll and its static directional stability m_y^β.

The lateral stability m_x^β of an airplane can, in principle, be reduced by:

- placing the wing lower on the fuselage;
- giving the wing a negative dihedral (of the order of 2° - 5°);
- mounting a fence under the fuselage

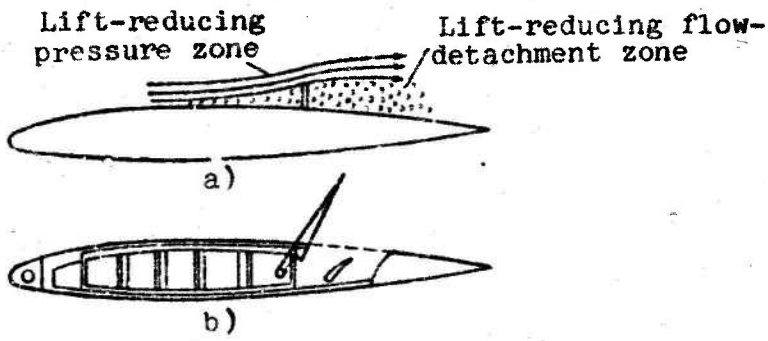

Figure 8.17. Aerodynamic (a) and design (b) schemes of spoilers.

The roll controlling moment can be increased by two methods: increasing aileron effectiveness [by taking measures to prevent flow separation from the wing tips (see §8.2a)] and by mounting additional lateral control surfaces on the airplane in the form of what are known in the foreign literature as "spoilers."

A spoiler is a plate (more precisely, a flap whose dimensions may be comparable to those of the aileron) that is extended from the upper surface of the wing (Fig. 8.17). Raised above the wing surface, the spoiler raises the pressure in front of it by ramming the airstream, while the pressure behind it also increases as a result of flow detachment. Thus, the lift on the upper surface of the wing is reduced at a certain distance from the airplane's longitudinal axis. The resulting moment causes the airplane to roll.

Spoilers are highly efficient controls even in flight at Mach numbers above critical.

The spoilers can also be used as air brakes when they are deployed simultaneously on both wings.

Spoilers are usually hydraulically controlled. When spoilers are used together with ailerons, the lateral-control system is designed in such a way that when the aileron has reached a certain deflection angle (say, 8°-10°), the spoiler control is activated

and opens the spoiler[2] on the side of the wing on which the aileron has been deflected upward. Such spoilers need not be used in the basic flight situations (those prevailing for most of the time). This greatly reduces the detrimental effect of the spoilers, which consists in an increase in the airplane's frontal drag.

d) Measures Designed to Improve Control-Surface Effectiveness, Primarily That of the Ailerons, in Flight at $M \geq M_{cr}$

A substantial decrease in elevator, rudder, and especially aileron effectiveness is observed in flight at high speeds corresponding to $M \geq M_{cr}$. The decrease in aileron effectiveness at high speeds is due to the compressibility of the air, on the one hand, and to elastic deformations of the wing on the other.

Let us consider the effect of the compressibility of air. The operation of the ailerons, like that of the elevators and rudder, is based on the fact that deflecting them through an angle δ changes the curvature of the profile and increases its lifting or lateral force.

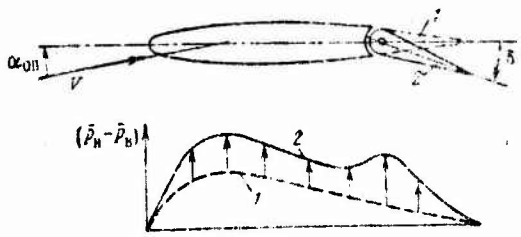

Figure 8.18. Schematic drawing of change in aerodynamic load on tail surface in subsonic flow. 1) Surface undeflected; 2) surface deflected.

Figure 8.18 shows schematically the variation of aerodynamic load $(\bar{p}_l - \bar{p}_u)$ along the chord of a tail (wing) at a small angle

Footnote (2) appears on page 188.

of attack in subsonic flow ($M < M_{cr}$) for two positions of the control surface: 1) undeflected and 2) deflected through an angle δ. We see that at subcritical flight speeds, deflection of the tail control surface (or aileron) causes a change in the pressure distribution not only in the region of the control-surface chord, but also over the entire profile. The result is a substantial increase in the lift of the tail surface or wing.

Thus, the force increase depends basically not on the change in the pressure distribution over the control surface, but for the most part on the pressure-distribution change over the entire tailplane or wing profile.

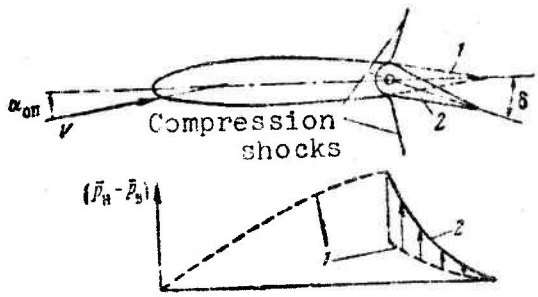

Figure 8.19. Schematic drawing of change in aerodynamic load on tail surface in transonic flow ($M > M_{cr}$): 1) Surface undeflected; 2) surface deflected.

A different picture forms in flight at above-critical speeds, when rather large zones of locally supersonic speed terminating in compression shocks form on the wing or tailplane. The formation of supersonic zones reduces the effect of deflecting the control surface on the chordwise distribution of pressure on the tailplane.

It may be found at a certain $M > M_{cr}$ that the distribution of pressure over the profile on the segment from the nose to the compression shock no longer depends on control-surface position (Fig. 8.19). We see that at above-critical flight speeds, deflection of the control surface has practically no effect on the

pressure distribution over the profile from the nose to the compression shock. The pressure changes only on the chord of the control surface. This results in a smaller change in the controlling force and, consequently, reduced effectiveness of the controls: ailerons, elevators, and rudder.

Since smaller thickness ratios are usually used on the tailplane than on the wing, and since the tail is usually swept back more sharply than the wing, the ailerons lose effectiveness in flight before the elevator and rudder.

The decrease in control-surface effectiveness means that larger deflections are needed to turn the airplane at a given angular velocity, and this results in a substantial increase in the effort at the controls. In modern aircraft flying at high speeds, these efforts may be far beyond the physical capabilities of the pilot. It therefore becomes necessary to lighten the airplane's controls (reduce the required effort).

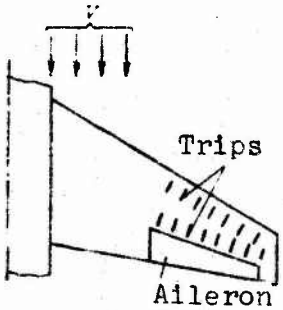

Figure 8.20. Diagram showing placement of trips on swept wing to counter tip separation and improve aileron effectiveness.

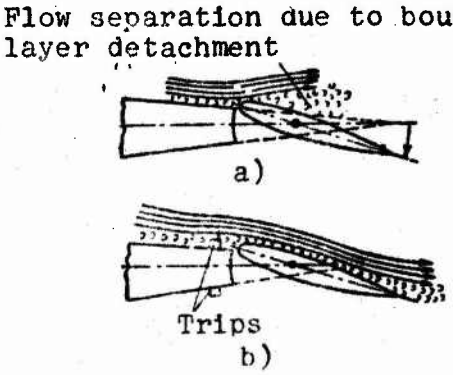

Figure 8.21. Diagram showing effect of trips on flow past rudder at large rudder deflections: a) flow without trips; b) flow with trips.

The following measures are taken to improve control-surface effectiveness and reduce the effort required at the control:

– in longitudinal control, the elevator is abandoned in favor of the all-moving stabilizer, a measure that increases longitudinal

control effectiveness substantially;

– aileron effectiveness at above-critical speeds is improved by measures whose effect is to improve longitudinal stability at $M > M_{cr}$ (see §8.2b);

– trips (vortex generators) are used directly to ensure aileron and rudder effectiveness at large deflection angles; they are mounted ahead of the aileron (Fig. 8.20) and rudder (Fig. 8.21) leading edges. Figure 8.21a shows the flow around a cross section of a rudder deflected at large angles without the use of trips, and Fig. 8.21b the corresponding flow when trips are used. We see that this improves not only the effectiveness of the rudder, but also its hinge moment, since the use of trips actually eliminates the possibility of rudder overcompensation at large δ.

Various types of compensation (aerodynamic, "internal," servotabs, servorudders) and hydraulic boosters, usually in reversible operation, are used to reduce the effort required at the controls. However, there are also cases in which boosters operating on the irreversible principle are used on transonic aircraft (e.g., the Boeing 727).

Let us analyze the influence of wing elastic deformations on aileron effectiveness.

Elastic deformations of the wing may also lower aileron effectiveness substantially in flight at high speeds. This applies in particular to swept wings with straight leading edges, relatively small profile thickness ratios, and comparatively large aspect ratios.

When the ailerons are deflected on such a wing, they set up a rolling moment M_x. Simultaneous deflection of the ailerons causes a shift of the wing center of pressure in the part of the wing serviced by the ailerons. This shift in the center of pressure gives rise to twist of the wing sections. Thus, when the aileron is deflected downward, the profile nose sections will also dip to smaller angles of attack. For this reason, the

increment in wing lift produced by downward deflection of the aileron becomes smaller (as compared with its value on an absolutely rigid wing). The resistance to twisting depends on the rigidity of the wing. It is a constant for a given airplane (a given wing). In this case, the wing twist angle $\Delta\alpha$ increases in proportion to ram pressure at a given aileron deflection. Consequently, the change in lift and rolling moment due to deformation of the wing is approximately proportional to the fourth power of speed. The rolling moment stemming directly from the aileron deflection is proportional to the square of speed.

The twist of the tip sections of a swept wing also helps the downward-deflected aileron to flex the wing by increasing the lift at its tip. Upward bending of a swept wing causes a further decrease of the angles of attack of the wingtip sections and, consequently, a further decrease in the lift and the rolling moment imparted to the airplane.

As flight speed increases, therefore, the increment in the lift and rolling moment due to deformation of the wing increases more rapidly than the rolling-moment increment due directly to the aileron deflection. This means that a speed may be reached at which deflection of the ailerons will not set up rolling moments, since the rolling moment due directly to the aileron deflection will be cancelled by the rolling moment due to deformation of the wing, i.e.,

$$M_{x_a} - M_{x_{def}} = 0, \tag{8.2}$$

where M_{x_a} is the moment set up about the x axis by the aileron deflection alone; $M_{x_{def}}$ is the rolling moment due to deformation of the wing.

The speed at which these moments become equal (at which the ailerons have become totally ineffective) is known as the aileron-reversal speed. At flight speeds greater than the reversal speed, a deflection of the ailerons produces the opposite of the usual effect. Quite understandably, the more rigid the wing, the higher

is the reversal speed. The greater the wingspan or, consequently, the greater its aspect ratio, and the greater the sweep of the wing, the lower will be the reversal speed.

Reducing the length of the aileron and moving it toward the tip of the wing (for example, with the object of increasing flap span) lowers the aileron-reversal speed, since the aileron is moved to the least rigid part of the wing, which is most susceptible to twisting in the direction opposite to the direction of aileron deflection.

Thus, qualitatively, aileron-reversal speed depends on the rigidity, sweep, and aspect ratio of the wing.

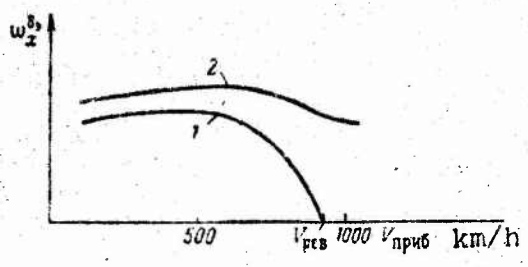

Figure 8.22. Illustrating effectiveness of variation of ailerons (1) and ailerons with spoilers (2) as a function of indicated airspeed.

Reliability of the airplane requires that the maximum permissible flight speed be about 100 km/h below the reversal speed.

To move the aileron-reversal speed farther from the operational speed range, the following measures are taken on modern aircraft:

- wing rigidity is increased, as by using profiles with larger relative thickness at the root of the wing, by reducing the sweep of the wing, by reducing its aspect ratio. We see that these measures run counter to those taken to improve takeoff and landing characteristics (aspect ratio) or to reduce the influence of shock stall on stability and controllability characteristics;

– the ailerons are moved (as far as possible) toward the root sections. This eliminates the actual cause of aileron reversal and represents a radical measure for heavy aircraft;

– spoilers are used together with ailerons for lateral control of the airplane. We note that the use of spoilers does not twist the wing and, consequently, does not contribute to reversal.

Figure 8.22 gives an idea of the effectiveness of lateral control with ailerons and ailerons used together with spoilers. We see that the parameter $\omega_x^{\delta_a}$, which characterizes aileron effectiveness, varies differently as a function of indicated airspeed when ailerons are used alone (curve 1) and when they are used together with spoilers (curve 2).

§8.3. ENSURING STABILITY AND CONTROLLABILITY OF SUPERSONIC AIRCRAFT

The need to increase flight speeds and altitudes required changes in the aerodynamic shapes of aircraft, their inertial characteristics, and the characteristics of their powerplants As compared to subsonic and transonic aircraft, modern supersonic aircraft have the following design features:

– for the most part, they use thin ($\bar{c}$ = 3.0-5%) swept and delta wings of small aspect ratio and fixed sweep angle, as well as swept wings whose sweep is variable in flight;

– their fuselages have large slenderness ratios ($\lambda_f = L_f/d_f$ = 8-12);

– the relative dimensions $\bar{S}_{v.t} = S_{v.t}/S$ of their vertical tailplanes have increased considerably, with some decrease in the arm ratio $\bar{L}_{v.t} = L_{v.t}/l$;

– the powerplants of the aircraft and their altitude-speed characteristics changed substantially. This applies in particular to the thrust characteristics of the engines in augmented operation. The result has been that the airplane may have lower stability in cruising supersonic flight at high altitudes.

The small relative thickness of the wing profile of interceptor-type supersonic aircraft prohibits use of the wing to accommodate basic loads. This sharply lowers the moment of inertia I_x (as compared with subsonic aircraft) about the airplane's longitudinal axis, with simultaneous substantial increases in the moments of inertia I_y and I_z owing to the fact that the basic loads are accommodated in the long fuselage.

Analysis of statistical data on aircraft of similar types indicates that in supersonic aircraft, the ratio of the moments of inertia I_y/I_x has increased by a factor of 4-7. This has a definite influence on stability and controllability characteristics.

In designing a supersonic airplane, the designer must take measures that will ensure the necessary stability and controllability characteristics both in flight at subsonic speeds (at small and large angles of attack) and in flight at supersonic speeds at high and medium altitudes.

This problem cannot be solved by aerodynamic-design measures alone, since it is usually necessary to deal with a number of problems the requirements for solution of which are contradictory. Further, certain problems of stability and controllability cannot be solved at all without automatic devices.

If we proceed from the assumption that the supersonic airplane will have a wing of swept or delta planform, with fixed sweep angle, the basic effort directed at improvement of its stability and controllability will reduce to the following:

– providing the necessary longitudinal normal-acceleration stability, aileron effectiveness, and ratio m_x^β/m_y^β in flight at low speeds and large angles of attack;

– ensuring practically constant normal-acceleration stability $(\bar{x}_F - \bar{x}_{cg})$ on transition from subsonic to supersonic flight;

– ensuring the required effectiveness of longitudinal control at $M \geq 1$ and stick (control-column) effort for the particular

flight situation;

– providing the necessary damping of rotational and translational divergent motion in pitch. The latter is vital for aircraft that cruise at supersonic speeds at high altitude;

– providing the necessary directional stability m_y^β and yaw damping $m_y^{\bar{\omega}_y}$ in flight at $M > 1.5$;

– ensuring effectiveness of the directional and lateral controls at large M.

Let us dwell briefly on the aerodynamic-design measures taken to solve these problems.

a) Measures Taken to Improve Longitudinal and Lateral Stability and Lateral Controllability of the Airplane in Flight at Large Angles of Attack

When a supersonic airplane flies at low subsonic speed and large angles of attack, it encounters the same problems as a subsonic or transonic airplane with a fixed-sweep wing. For this reason, the design measures taken to eliminate longitudinal- and lateral-stability and lateral-controllability deficiencies in the supersonic airplane will be the same in principle as those for transonic aircraft (see §8.2, a, c).

It is appropriate to note here that use of a variable-sweep wing is an effective measure against the decrease in normal-acceleration stability and the increase in the airplane's lateral stability m_x^β at large attack angles. This is provided that the wing is swung to the minimum-sweep position before going over to large angles of attack. In this case, flow detachment from the wing tips does not produce a strong pitchup moment, since the tip sections of the wing are only a short distance aft of the airplane's center of gravity.

It is known that the lateral stability m_x^β of an airplane with a small wing sweep angle varies little with increasing angle of attack. The small lateral stability m_x^β of the airplane and its constancy in practice as the lift coefficient c_y increases has a

favorable influence on the ratio m_x^β/m_y^β and, consequently, also on the lateral stability and controllability characteristics. Research has shown that better lateral stability and controllability characteristics are obtained in the airplane at large angles of attack in low-speed flight when a small value of the ratio m_x^β/m_y^β is obtained by reducing m_x^β and increasing the static directional stability m_y^β, which is generally inadequate.

b) <u>Measures Taken to Ensure Practical Constancy of Normal-Acceleration Stability over the Entire Range of M</u>

It is known that when an airplane goes from flight at M < 1 to flight at M > 1, a large increase in its normal-acceleration stability ($\bar{x}_F - \bar{x}_{cg}$) takes place owing to a tailward shift of the

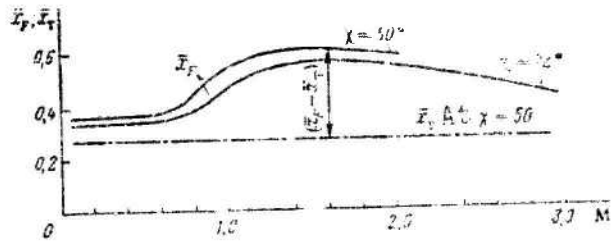

Figure 8.23. Variation of aerodynamic-center position of airplane with lifting fuselage as a function of M for two wing sweep angles $\chi = 50$ and 72°.

airplane's aerodynamic center in the range M = 0.9-1.4. Use of conventional swept and delta wings with large sweep angles and a conventional low-lift fuselage makes it possible to reduce the tailward shift of the aerodynamic center and make it smoother in this M range. Use of a fuselage with greater lift together with a conventional strongly swept wing also results in a smoother tailward shift of the aerodynamic center in the range M = 0.9-1.4 and, in addition, shifts the center forward at M = 2.0 (Fig. 8.23). This has a favorable effect on the airplane's longitudinal stability in supersonic flight. However, the displacements of the aerodynamic center due to restructuring of the flow past the airplane nevertheless remain large in the case of the conventional

fuselage and conventional swept wings with sweep angles up to 60°. This means that these aircraft will also have high normal-acceleration stability $[(x_F/b_a) - (x_{cg}/b_a)]$ at supersonic speeds. High normal-acceleration stability is undesirable because it reduces the maneuverability of the airplane at supersonic speeds considerably, increases the sacrifice of lift/drag ratio that must be made to trim the airplane, and lowers the altitude of trimmed nonsteady level flight in the dynamic-altitude range.

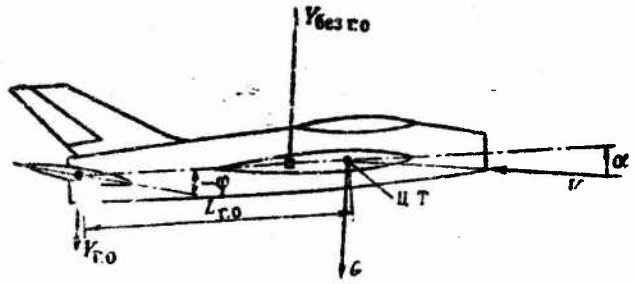

Figure 8.24. Longitudinal balance of airplane of conventional configuration.

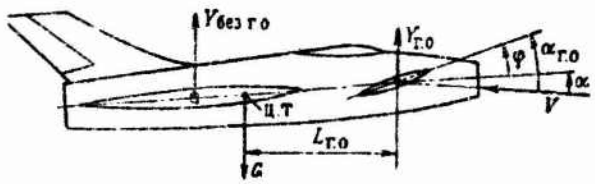

Figure 8.25. Longitudinal balance of airplane of "canard" configuration.

The decrease in maneuverability occurs because the high normal-acceleration stability $(\bar{x}_F - \bar{x}_{cg})$ requires large stabilizer (elevator) deflections to trim the airplane in level flight. Since the available stabilizer (elevator) deflections are always limited, the increased use of the stabilizer to trim the airplane in level flight at $M > 1.5$ means that the stabilizer-deflection margin for maneuvering is reduced.

Let us consider the influence of $(\bar{x}_F - \bar{x}_{cg})$ on the lift/drag ratio in level flight.

For this purpose, we shall compare two supersonic-aircraft configurations: the conventional layout with the horizontal tail positioned aft of the wing and the "canard" configuration. We shall consider their longitudinal-balance conditions in level flight on the assumption that m_{x_0} (i.e., the moment at $c_y = 0$) and the moment from the powerplants are zero (Figs. 8.24, 8.25). The figures show that the trimming force of the horizontal tail (or elevons) is directed downward in the case of the conventional (and "tailless") aircraft and upward for the "canard." It must also be remembered that in the case of the "canard," the arm $L_{h.t}$ of the horizontal "tail" is slightly larger by virtue of the layout than it is for the conventional airplane and much larger than in the "tailless" airplane. This means that the trimming forces will be larger in absolute value for the "tailless" layout and smallest for the "canard." Since the tail (elevon) trimming force of the "tailless" and conventional aircraft requires increasing the lift of the airplane without the horizontal tail (i.e., it lowers the lifting property of the airplane), and the tail trimming force increases the lifting properties of the airplane in the case of the "canard," this means that, other conditions the same, the sacrifice of L/D to trim the airplane will be smallest for the "canard" and largest for the "tailless" airplane.

Calculation indicates that for a conventional-layout airplane in supersonic flight (at $M \geq 1.5$), the loss of maximum lift/drag ratio K_{max} involved in trimming may run to 10% or more. This follows, for example, from formula (8.3) for determination of the maximum lift/drag ratio with allowance for trimming the airplane:(3)

$$K_{max} = \frac{1}{2}\sqrt{\frac{c_y^2}{c_{x_0}(1+a)}}, \qquad (8.3)$$

where a is a quantity that allows for the trimming drag of the airplane:

Footnote (3) appears on page 188.

$$a = \frac{n}{\bar{S}_{r.o}} \frac{(\bar{x}_F - \bar{x}_T)^2}{\bar{L}^2_{r.o}}; \tag{8.4}$$

n is a coefficient that takes account of the peculiarities of the configuration. For a conventionally configurated airplane n ≈ 1.7, and for the "canard" it is about 0.8:

$$\bar{S}_{r.o} = \frac{S_{r.o}}{S}; \ \bar{L}_{r.o} = \frac{L_{r.o}}{b_a}.$$

We see that to reduce the loss of the maximum lift/drag ratio of the airplane that is involved in trimming it, normal-acceleration stability must be reduced at supersonic speeds.

It follows from the expression for normal-acceleration stability that it can be controlled in two ways:

– by changing the trim (the coordinate x_{cg}) in accordance with the change in the aerodynamic-center coordinate x_F of the airplane;

– by stabilizing the position of the longitudinal aerodynamic center while the CG position of the airplane is left unchanged.

In practice, it is quite difficult to adjust the trim of the airplane in accordance with the changes in the position of its aerodynamic center because this requires development of special automatic systems that determine and adjust the position of the CG on a shift of the aerodynamic longitudinal center. It is also necessary to install powerful pumps to transfer a large amount of fuel during the short time that it takes the airplane to accelerate from M = 0.9 to M ≈ 1.4, special trimming fuel tanks mounted at considerable distances from the airplane's CG, and the associated fuel plumbing. This means that the airplane must carry extra equipment. However, each extra kilogram of equipment involves a 5-8-kg increase in takeoff weight.

Despite these difficulties, this method of maintaining approximately constant static normal-acceleration stability over the entire range of M is nevertheless used in practice on certain modern supersonic airplanes. For example, the American B-58A "Hustler" and French "Mirage IV" supersonic bombers have special trimming tanks in the tail section of the fuselage for transfer of fuel. By thus ensuring constancy of the minimum $(\bar{x}_F - \bar{x}_{cg})$ with respect to Mach number, the designers have reduced the loss of lift/drag ratio that is involved in longitudinal trimming of the airplane.

Another method of maintaining constant longitudinal static stability with respect to normal acceleration at subsonic and supersonic speeds is to stabilize the position of the airplane's longitudinal aerodynamic center against Mach-number changes.

In principle, this can be done in any of several ways:

- changing the aerodynamic configuration of the airplane in flight;

- changing the horizontal-tailplane area in flight. This is not accompanied by a change in configuration;

- by selecting a fixed wing-and-fuselage shape, i.e., a configuration of the airplane, that ensures a more advantageous shift of the aerodynamic center as a function of M.

Let us briefly discuss the problem of stabilizing the position of the airplane's aerodynamic center against M by changing the aerodynamic layout of the airplane in flight.

By mounting a horizontal foreplane on a normally configurated or "tailless" airplane, retracting it into the fuselage in subsonic flight and extending it with the transition to supersonic speeds as the coordinate of the airplane's aerodynamic center without the foreplane increases, the position of the aerodynamic center of the entire vehicle can be kept practically constant. We see that the conventionally configurated airplane becomes a combination type, while the "tailless" airplane becomes a "canard."

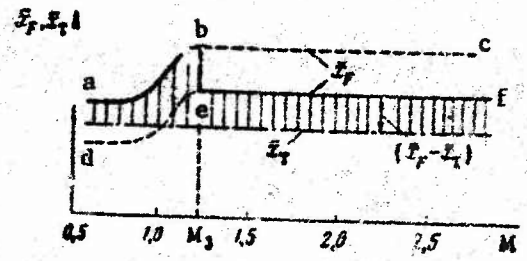

Figure 8.26. Variation of position of airplane's aerodynamic center as a function of M.

On "canard" aircraft, stabilization of the position of the longitudinal aerodynamic center against Mach number requires that the horizontal noseplane be designed to feather in flight at subsonic speeds ("free-floating foreplane") and be locked in position by a special device at a certain supersonic speed. At subsonic speeds, the "free-floating foreplane" will have no influence on aerodynamic-center coordinate, because, even though the airplane is a "canard" in external configuration, it is essentially a "tailless" airplane by the manner in which the aerodynamic forces are generated. When the foreplane has been locked, it becomes a true "canard," since the foreplane influences the position of the vehicle's longitudinal aerodynamic center. In this case, the tailward shift of the aerodynamic center of the airplane without horizontal stabilizer due to an increase in M must be offset by a forward shift of the aerodynamic center obtained by actuating the foreplane.

In Fig. 8.26. the solid line abef indicates the variation with M of the position of the longitudinal aerodynamic center of the airplane with the foreplane "free-floating" at subsonic speeds and locked at supersonic speeds. We see that the foreplane is locked at $M = M_l$. Curve abc indicates the Mach-number variation of the aerodynamic-center position with the "free-floating foreplane" at subsonic and supersonic speeds. Curve def shows the variation of airplane's aerodynamic-center coordinate when its horizontal fore-

plane is locked in position. In other words, curves ABC and DEF indicate the Mach-number variation of the longitudinal aerodynamic center position for aircraft of two configurations: "tailless" and "canard," respectively. The shaded area in Fig. 8.26 indicates the variation of the airplane's normal-acceleration stability with Mach number when it has a forward stabilizer feathered at $M < M_l$ and locked at $M > M_l$. We see that the $(\bar{x}_F - \bar{x}_{cg})$ of such an airplane varies little on the transition from subsonic to supersonic flight and back, and can therefore be adjusted to ensure the necessary controllability characteristics.

We note that a "free-floating stabilizer" can, in principle, also be used with a servotab at subsonic speeds to set up a longitudinal controlling (trimming) moment. This may be found helpful for improvement of the takeoff and landing characterists of "canard" aircraft.

To reduce the influence of downwash from the foreplane on the wing, it is advisable to mount the foreplane above the plane of the wing chord on the fuselage.

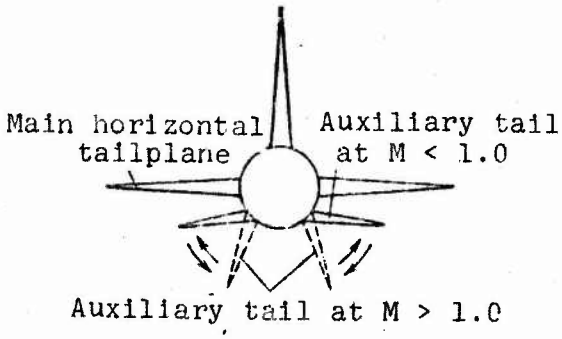

Figure 8.27. Diagram of tailplane whose area is varied in flight as a function of M.

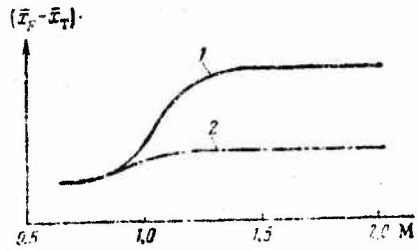

Figure 8.28. Mach-number curves of normal-acceleration stability of aircraft with fixed (1) and in-flight-variable (2) tailplanes.

The position of the airplane's longitudinal aerodynamic center can also be stabilized against Mach number in the case of a conventional configuration, by mounting a horizontal stabilizer

whose area can be varied in flight. It is known that use of the conventional horizontal tailplane causes a tailward shift of the airplane's aerodynamic center. At a given M, the extent of this displacement depends on $A_{h.t} = S_{h.t}L_{h.t}/S_{b_a}$. By varying $A_{h.t}$ in flight, e.g., by adjusting $S_{h.t}$, the position of the aerodynamic center can be regulated and, consequently, so can $(\bar{x}_F - \bar{x}_{cg})$. High normal-acceleration stability at supersonic speeds means, among other things, that the airplane has a large $A_{h.t}$.

If two horizontal tailplanes (main and auxiliary) are mounted on the airplane in a biplane scheme, and in such a way that at $M > 1$ the planes of one auxiliary horizontal tail can be rotated with respect to the longitudinal axis, the total horizontal-tail area will be reduced and the total vertical-tail area increased. Figure 8.27 is a schematic representation of such an in-flight-variable tailplane.(4) When the airplane decelerates from supersonic to subsonic speeds, the auxiliary tailplane must be returned from the vertical to the horizontal position in accordance with the change in M. To obtain smooth variation of the airplane's aerodynamic-center coordinate with changes in M, it is necessary to couple the servomotor that controls the position of the auxiliary tailplane with a Mach-number sensor. It is then possible to provide a variation of the normal-acceleration stability approximately as shown by the dash-dot line in Fig. 8.28.

The next way to reduce the aft displacement of the aerodynamic center as M rises from 0.9 to 1.4 and promote forward displacement of this center during flight at $M > 2.0$ is to use the optimum fixed-in-flight configuration of the airplane. It is assumed that one such configuration might be a "tailless" airplane with a double-delta wing. On such a wing (which consists of two triangles), the sweep of the root section may range up to 70°-75°, while the tip section may be swept back at around 60°. The fuselages are designed to give increased lift. To reduce the lift

---

Footnote (4) appears on page 188.

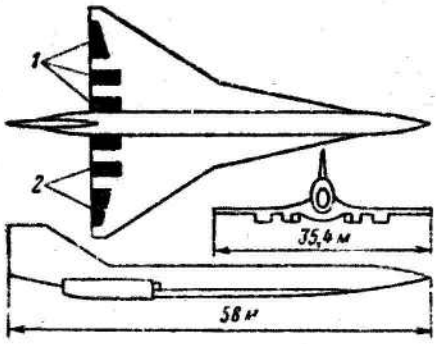

Figure 8.29. Diagram of supersonic airplane with double-delta wing. 1) Elevons along entire span; 2) outboard and midwing elevon sections.

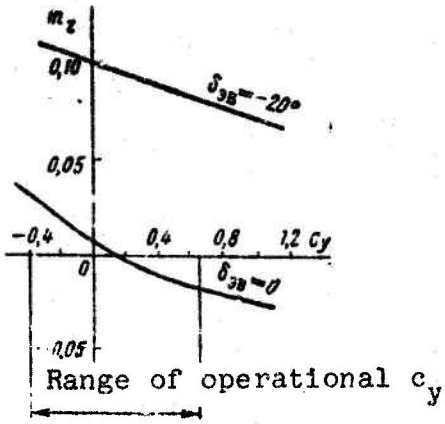

Figure 8.30. Variation of longitudinal-moment coefficient m_z as a function of c_y of double-delta-wing airplane model.

from the wing tip sections, an aerodynamic twist is imparted to the wing. This increases the load on the root sections and the fuselage, which are more strongly swept and have lower lifting properties (c_y^α). This results in a more favorable displacement of the aerodynamic center in the range M = 0.9-1.4.

This wing form is used on the Swedish Draken supersonic fighter and on the supersonic transport under development in the USA, a diagram of which appears in Fig. 8.29.

By selecting the proper relation between the areas of the fore and aft deltas and giving an aerodynamic twist to the double-delta wing, it is possible to obtain not only a small displacement of the airplane's aerodynamic center in the range M = 0.9-1.4, but also good longitudinal normal-acceleration stability at large angles of attack. This is fully consistent with what was said in §8.2a. This statement is also supported by the data given in Fig. 8.30 for a model of a double-delta airplane. We see that this airplane suffers no appreciable decrease of normal-acceleration stability at large c_y. In other words, the so-called "spoon" does

not appear at large c_y. This is an advantage of the double-delta wing over the conventional swept wing. We see that elevon effectiveness is retained up to large angles of attack (large c_y). It is appropriate to mention that elevons, which act as elevators, can be used to set up a controlling moment during takeoff such that the angular acceleration in pitch is approximately 13-14 deg/s^2. Statistical data indicate that the pitch angular acceleration at takeoff may reach 10-12 deg/s^2 for a subsonic jet airliner of conventional configuration.

c) Measures Taken to Ensure the Required Effectiveness of Longitudinal Control and the Required Stick Forces

It was indicated in the preceding section that an elevator loses its effectiveness as a longitudinal-control surface when a transonic airplane flies at $M > M_{cr}$. This statement also applies to the supersonic airplane.

Elevator effectiveness also remains low on an increase in M above 1, since the aerodynamic load changes only on the deflected control surface, i.e., the effect of the elevator does not extend to the stabilizer in this case. For this reason, an all-moving stabilizer is used for longitudinal control of almost all supersonic airplanes of conventional layout (except for the "tailless" configuration). Use of the all-moving stabilizer improves the maneuverability of fighters appreciably at supersonic flight speeds. It also reduces the pitchup moment of the aircraft (and the surge of the normal acceleration n_y) as it decelerates from supersonic to subsonic speed with the stick forward (the pitchup moment arises as a result of the forward shift of the aerodynamic center). This is explained by the fact that the effectiveness of the all-moving stabilizer does not vary as much with M as does that of the elevator.

Use of an all-moving stabilizer in longitudinal control requires the designer to place its pivot axis properly. This is complicated by the fact that the flow around the stabilizer is restructured when the Mach number moves from $M < 1$ to $M > 1$. At

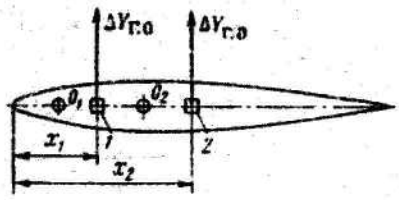

Figure 8.31. Illustrating overcompensation of stabilizer in subsonic flight when the pivot axis passes through point O_2.

M > 1, the aerodynamic load is more uniformly distributed chordwise over the stabilizer. As a result, the point of application of the lift increment $\Delta Y_{h.t}$ of the stabilizer (Fig. 8.31, point 2) lies at about 50% aerodynamic chord. In subsonic flight, on the other hand, the stabilizer lift increment $\Delta Y_{h.t}$ is placed at about 25% chord (Fig. 8.31, point 1). To reduce the hinge moment at supersonic speeds, it would be desirable to place the stabilizer axle at O_2 rather than O_1. Then, however, the stabilizer would be overcompensated in flight at subsonic speeds. Such a stabilizer cannot be controlled manually or by means of a reversible hydraulic booster. In such cases, therefore, it is necessary to provide supersonic aircraft with irreversible hydraulic boosters capable of taking up all of the aerodynamic load acting on the stabilizer, i.e., the stabilizer is controlled not directly by the pilot, but through an irreversible booster.

When the pilot deflects the stick in this case, he has to overcome only the friction in the control line from the stick to the booster, and holding the stick in a given position requires no effort of him. This is not acceptable, since the pilot cannot fly the airplane without "feel" at the controls. The designer is therefore obliged to insert special loading systems corrected for stick travel, speed (Mach number), and flight altitude into the longitudinal-control system. In other words, the use of irreversible boosters requires installation of power assists and automatic devices that regulate control-lever force in accordance with the airplane's flight situation and the physiological capabilities of the pilot.

d) Ensuring Required Damping of Rotational and Translational Longitudinal Motion

Supersonic airplanes are designed to fly in a broad range of altitudes and speeds (Mach numbers). Their static ceilings may range above 20 km. This means that flight at altitudes of 18-20 km at supersonic speeds is nothing out of the ordinary for supersonic airplanes.

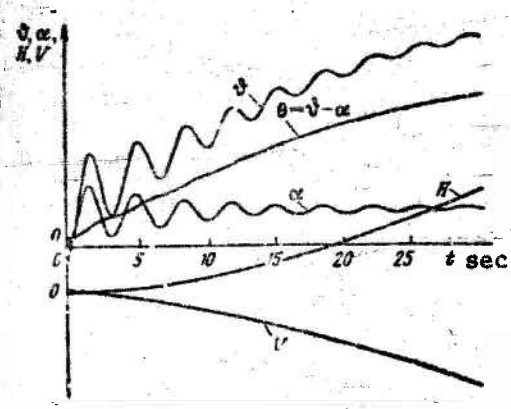

Figure 8.32. Variation of longitudinal-motion parameters of airplane after an instantaneous deflection of the stabilizer by a constant amount $\Delta\phi_{st} = -1°$.

An increase in flight altitude is accompanied by a sharp decrease in the density of the air, which results in a decrease in the damping moments of the airplane in general and the pitch damping moment in particular.

It is known that a decrease in the damping moments of an airplane weakens the damping of its angular motions and increases the peak values of the airplane's angular coordinates (for example, its attack and pitch angles) and the period of the oscillations. The settling time at new airplane-motion parameters after deflection of the stabilizer by a constant amount is then found to be rather long. This can be seen from the calculated data shown in Fig. 8.32 for a hypothetical airplane flying (before the stabilizer deflection) at supersonic speed and an altitude of 20 km. We see that the stability and controllability characteristics with respect to the angles of attack α and pitch θ are poor. The transients of the angles α and θ can be improved by artificially increasing the airplane's damping moment. This is usually done by installing damping devices (dampers) which, for example, by deflecting the stabilizer in proportion to the pitch angle rate $d\vartheta/dt = \omega_z$, artificially increase the damping moment in pitch and thereby improve the angular (rotational) motion of the airplane.

The translational motion of the airplane (variation of speed V and altitude H) is not improved, since there is practically no change in its damping.

Calculations indicate that cruising supersonic flight of a TJE airplane at high altitudes will often involve level-flight modes in which the longitudinal stability and controllability of the airplane with respect to speed and altitude are much poorer than they are in flight at low and medium altitudes. This is basically because high-altitude flight is accompanied by a substantial decrease in the damping of the airplane's translational motion (speed damping), which is characterized by the quantity

$$\frac{Q^V_{\alpha=\text{const}} - P^V_P}{m}, \tag{8.5}$$

where $Q^V_{\alpha=\text{const}}$ is the partial derivative with respect to speed of the frontal drag calculated for a constant angle of attack α, P^V_P is the partial derivative of the available thrust with respect to speed, and $m = G/g$ is the mass of the airplane.

It is impossible to eliminate the shortcoming by reconfigurating the airplane.

A radical solution to the problem consists in providing the airplane with an engine-type flight-speed control (thrust control) whose operation is coordinated with that of the automatic pilot. To this end, the autopilot must stabilize pitch angle. This thrust control must regulate flight speed by varying powerplant thrust output. To accomplish this, the engines must have a thrust reserve amounting to about 25-30% of the maximum thrust in the given flight situation.

It is appropriate to note that if the powerplant thrust vector passes through or above the airplane's center of mass, the thrust control can solve this problem by itself. If, however, the placement of the engines on the airplane causes the thrust vector to pass below the center of mass, use of the engine thrust control alone causes oscillations of the airplane to build up; here, at

the beginning of the transient response, the speed and altitude oscillations decrease, but then increase with increasing time. This phenomenon is unacceptable. In this case, the engine thrust control (flight-speed control) must work in harmony with an automatic pilot that stabilizes pitch angle. These measures are sufficient to ensure good flight-situation stability and normal controllability of the airplane with good speed and altitude control response.

e) Ensuring the Necessary Directional Stability m_y^β and Yaw Damping in Flight at M > 1.5

It is known that acceleration of an airplane from subsonic speeds to M > 1.5 results in changes for the worse in such important lateral stability characteristics as the directional

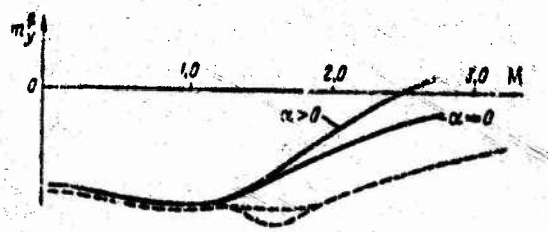

Figure 8.33. Mach-number curves of directional stability m_y^β of a hypothetical airplane with conventional tail (solid curve) and with in-flight-variable tail (dashed curve) (see Fig. 8.27).

stability m_y^β and the related yaw damping of the airplane. This can be seen from the data presented in Fig. 8.33. This figure indicates, for example, a typical Mach-number variation of the directional stability of an airplane without an auxiliary horizontal tail at two angles of attack α. We see that increasing the angle of attack at supersonic speeds (M > 1.5) causes a substantial decrease in m_y^β. This is because an increase in the angle of attack α at this M causes an increase in the crosswash angles in the area of the fin atop the fuselage. An increase in the crosswash angles at the top fin means a decrease in its true slip

angles, the lateral force of the vertical tail, and the yawing moment generated by this force.

A fin or fence mounted under the fuselage is in a superior position (as regards crosswash at positive attack angles) than a fin mounted atop the fuselage.

A decrease in the directional stability m_y^{β} and the damping $m_y^{\bar{\omega}_y}$ with increasing M (at M > 1.5) implies, among other things, that at these Mach numbers the airplane does not have a large enough static movement of the vertical tail area $B_{v.t} = S_{v.t}L_{v.t}/Sl$ and that this tail is not sufficiently effective.

Aerodynamic-design measures taken to improve the directional stability m_y^{β} and yaw damping $m_y^{\bar{\omega}_y}$ are as follows:

- increasing the area of the vertical tail with little change in its aspect ratio;

- increasing the area and aspect ratio of the vertical tail;

- increasing the effectiveness of the vertical tail by locating it at the optimum position with respect to the horizontal tail.

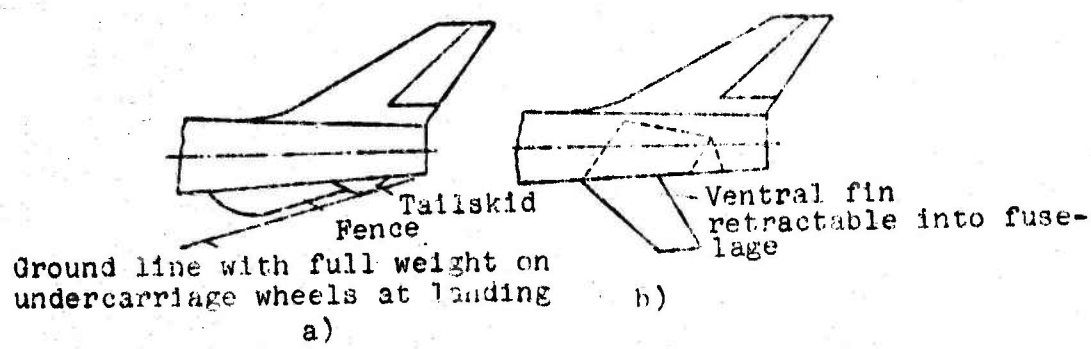

Figure 8.34. Diagram showing mounting of ventral fences (a) and fins that retract when landing gear is lowered (b).

The first measure – increasing the area of the vertical tail with practically no change in its aspect ratio – involves parallel

mounting of two and sometimes even three fins, or a fairing fin on the segment of fuselage between the cabin and the main fin. These measures increase m_y^β and yaw damping for the most part by increasing the area of the vertical tail while leaving its effectiveness unchanged. The results are an increase in the lateral stability m_x^β, since the planes of the vertical tail are situated to one side of the airplane's longitudinal axis (i.e., asymmetrically). The increase in lateral stability must be regarded as undesirable.

The second measure is to increase the area and aspect ratio of the vertical tail. This is conveniently done by installing ventral fences, auxiliary ventral fins that are dropped at landing or retracted into the fuselage when the landing gear is lowered (Fig. 8.34), or an auxiliary-horizontal tail that becomes an auxiliary i. at $M > 1.5$ (see Fig. 8.27) or by using wingtip sections that rotate downward at supersonic speeds to function as ventral fins. This last design solution was used on the North American B-70 Valkyrie bomber. Figure 8.33 gives an idea of how the directional stability of an airplane with in-flight-variable tail varies with Mach number.

Such aerodynamic-design measures increase the moment-area ratio $B_{v.t}$ of the vertical tail and increase its effectiveness appreciably, since the auxiliary vertical-tail surfaces below the fuselage utilize the fuselage also and thus increase the effective aspect ratio of the vertical tail considerably. The latter results in a substantial increase in its lifting properties and, consequently, an increase in the directional stability m_y^β and yaw damping $m_y^{\bar{\omega}_y}$. We note that the measures enumerated above also lower the lateral stability m_x^β. This is also a desirable effect.

Naturally, such designs produce a substantial increase in the weight of the airplane, but this is dictated by the need to improve its most important lateral stability and controllability characteristics.

The third aerodynamic-design measure consists essentially in placing the vertical and horizontal tails relative to one another in such a way as to optimize the effectiveness of the vertical tail. Research has shown that for this purpose, the horizontal tail must be placed on the fuselage as far as possible below the airplane's longitudinal axis, with $1/4\ b_{a_{h.t}}$ aft of $1/4\ b_{a_{v.t}}$, i.e., to make the arm $L_{h.t}$ longer than $L_{v.t}$.

It is also possible to place the horizontal tail atop the fin.

The increase in vertical-tail effectiveness when the horizontal tail is placed in the above positions is due to the plate effect.

We note that in addition to the desirable increase in vertical-tail effectiveness obtained by mounting the stabilizer high (on the fin), there is also an undesirable increase in the airplane's lateral stability m_x^β and a decrease in its effectiveness at large attack angles owing to movement into a region of strongly stagnated flow. When the horizontal tail is mounted lower on the fuselage, the increase in vertical-tail effectiveness is accompanied by a decrease in m_x^β. For these reasons, and also in view of the structural difficulties of ensuring rigidity of the tail when the horizontal tailplane is placed atop the fin, it is more advantageous to use the lower horizontal-tail position.

When the lower stabilizer position is used, the effectiveness of the vertical tail can then be increased even further by using a large stabilizer negative dihedral. This is because the stabilizer produces a plate effect in this case and increases the area and aspect ratio of the vertical tail. Stabilizers of this type are used on the modern French supersonic aircraft Trident II and Nord 1500 Griffon and the American Phantom II.

The above methods of increasing directional stability and yaw damping do not always ensure the necessary value of these characteristics, especially in high-altitude flight. Acceptable

m_y^{δ} and $m_y^{\bar{\omega}_1}$ characteristics can be obtained in all of the airplane's flight situations only by rational selection of the airplane's aerodynamic configuration and by the use of semiautomatic (or automatic) damper-type devices. Here it must be remembered that the possibilities inherent in automation are also limited.

f) Ensuring Effective Directional and Lateral Control of the Airplane at Large Mach Numbers

It was pointed out above that control-surface effectiveness decreases in flight at supersonic speeds. This applies not only to the elevator, but also to elevons, ailerons, and rudders. The effectiveness of the control surfaces decreases steadily as M increases above 1.5.

Aileron effectiveness depends not only on the forces set up on them, but also on wingspan. For swing-wing aircraft, the transition to high supersonic flight speeds is accompanied by backward rotation of the wing. This results in a substantial reduction of the wingspan and the rolling moment from the ailerons.

To increase directional-control effectiveness at $M > 2.0$, it is advisable to use all-moving vertical fins with conventional profiles. In flight at $M > 4$, all-moving fins with wedge profiles are quite effective and are used, for example, in the vertical-tail design of the experimental hypersonic North American X-15 aircraft.

Elevons with blunt trailing edges can be used (for "tailless" type aircraft) to increase lateral-control effectiveness at high speeds. This measure to improve lateral and longitudinal controllability is used in the Convair F-106, SAAB-35 Draken, and other interceptor-type aircraft.

The lateral-control effectiveness of an airplane of conventional configuration can also be increased by the use of stabilizer halves (elevons) capable of differential deflection. This has been done on the F-111, the North American X-15, the British TSR-2, and other aircraft.

We note that the differential stabilizer may be inadequate as the sole lateral-control component on the airplane at low speeds, and especially at landing. In such cases, it is necessary to use combinations of lateral controls on the airplane as follows:

- ailerons together with the differential stabilizer;
- spoilers together with the differential stabilizer.

FOOTNOTES

Page No.	
155	(1) We refer here to wings with sweep angles no larger than 45° and profile thickness ratios of the order of 8-14%.
160	(2) The spoilers on the Convair 880 can be opened to their full deflection of 60° in about 2 seconds. The time to retract spoilers is usually shorter than the time to deploy them.
171	(3) Formula (8.3) is valid for a flat, untwisted wing; see A.A. Badyagin, "The maximum lift/drag ratio of an airplane with consideration of trim," Aviatsionnaya tekhnika," No. 1, 1963, "Vysshaya shkola,"
176	(4) This tailplane design is used on the American Change-Vought or F8U-3 Crusader.

Chapter 9

SELECTION OF GEOMETRY OF TAILPLANES AND WING DIHEDRAL

§9.1. SELECTION OF GEOMETRICAL PARAMETERS OF THE AIRPLANE'S HORIZONTAL TAILPLANE

Generally, the horizontal tailplane of an airplane consists of a stabilizer and an elevator. "Tailless" aircraft are an exception. In this type of airplane, the wing performs its own functions and those of the stabilizer, while the elevons take over the elevator function.

The basic requirement made of a horizontal tail is that it provide the necessary stability and controllability characteristics in all operational flight situations. However, it is not necessary in the preliminary-design stage to calculate these characteristics for all flight regimes. It is sufficient to estimate the longitudinal stability and controllability characteristics in the design flight modes.

The design regimes chosen are as follows:

- takeoff;
- landing with gear down at maximum flap deflection;
- flight in the regime most characteristic for the particular airplane;
- flight at the speed limit or Mach-number limit.

The parameters of the horizontal tail must be such as to ensure the required trim margin ($\bar{x}_F - \bar{x}_{cg}$) and adequate controllability in these regimes. We note that the ground effect must be taken into account in plotting trim diagrams for takeoff (at the instant of liftoff) and for landing with gear and flaps down.

On the basis of the requirements made of the horizontal tail, the following parameters of this surface must be selected during preliminary design:

- planform and placement on the airplane;

- the relative values of the area $\bar{S}_{h.t} = S_{h.t}/S$ and the moment-area ratio $A_{h.t} = \bar{S}_{h.t} \cdot \bar{L}_{h.t}$ of the horizontal tail. $A_{h.t}$ must be such as to provide the airplane with the necessary normal-acceleration stability at low speeds in maximum tailheavy trim;

- the relative elevator area $\bar{S}_{ele} = S_{ele}/S_{h.t}$, the type of elevator compensation, and the maximum elevator deflection angles.

The dimensions of the elevator (all-moving stabilizer, elevons) are considered adequate if they leave an elevator-deflection margin of at least 10% of the maximum deflection angle for a nose-wheeled airplane trimmed at its landi.., angle of attack with gear and flaps down. For aircraft with tail skids, this margin must be increased to approximately 15-20%. We note that trim is checked with the airplane in its maximum operational nose-heavy state.

If the airplane has a moving stabilizer and an elevator (elevons), it is expedient to use the stabilizer to trim the airplane and the elevator for finer pitch-angle corrections. The dimensions of the stabilizer are then selected for the landing trim of the airplane, and those of the elevator (elevons) on the basis of the pitch controllability needed in level flight.

In selecting the planform of the horizontal tail, we begin from the requirement that it is desirable to have a large $\bar{L}_{h.t} = L_{h.t}/b_a$ at any given horizontal-tailplane area. One way of accomplishing this is to sweep the tailplane back. The tailplane

sweep should be about the same as the wing sweep. For transonic aircraft, the sweep angle of the tail is usually adjusted so that the M_{cr} of the tail will be slightly higher than the M_{cr} of the wing, i.e., so that the phenomena associated with the compressibility of air will appear on the tail after they have appeared on the wing. This ensures retention of good controllability of the airplane even when its flight speed has reached the value corresponding to the wing M_{cr}. If the tail profile thickness ratio exceeds 10%, it is recommended that the sweep of the tail be made greater than that of the wing by 3°-5°. These considerations apply equally to the vertical tailplane.

Table 9.1

Approximate Over-All Parameters of Horizontal Tailplanes of Transonic Aircraft

Parameters \ Type of aircraft	Light turbo-jets	Heavy turbo-jets	Heavy prop-jets
$A_{h.t} = \bar{S}_{h.t}\bar{L}_{h.t}$	0.30-0.45	0.52-0.76	0.8-1.1
$\bar{S}_{h.t} = S_{h.t}/S$	0.12-0.20	0.15-0.25	0.2-0.28
$\bar{S}_{ele} = S_{ele}/S_{h.t}$	0.25-0.30	0.20-0.30	0.2-0.4

The taper of the tailplane can be arrived at on the basis of statistical data for existing aircraft of the same type. Usually, horizontal tails are tapered in the range $\eta_{h.t} = 1.5-3.0$.

The position of the horizontal tail was discussed in §8.2a, from which it follows, for example, that the horizontal tail of a conventionally configurated airplane is placed to advantage, other conditions the same, on the fuselage below its longitudinal axis with the largest possible $\bar{L}_{h.t}$. Aircraft with engines mounted on the fuselage behind the wing are an exception.

In first approximation, the moment-area ratio $A_{h.t} = \bar{S}_{h.t}\bar{L}_{h.t}$ of the horizontal tail, as well as $\bar{S}_{h.t}$ and the relative elevator area $\bar{S}_{ele} = S_{ele}/S_{h.t}$, can be taken from statistical data on existing similar aircraft.

Analysis of the horizontal-tailplane geometries of modern transonic aircraft indicates that they lie for the most part in the ranges indicated in Table 9.1. For transonic aircraft, the horizontal-tailplane area $S_{h.t}$ includes the center section in the fuselage.

Modern supersonic aircraft of normal configuration have the following horizontal-tail parameters:

$$A_{г.о_{обмыв}} = \frac{S_{г.о_{обмыв}}}{S} \cdot \frac{L_{г.о_{обмыв}}}{b_a} = 0.15 - 0.25;$$

$$S_{г.о_{обмыв}} = \frac{S_{г.о_{обмыв}}}{S} = 0.1 \div 0.2,$$

where $S_{h.t_{wash}}$ is the area of the horizontal tail washed by the airstream. Very often, it is equal to the area of the moving stabilizer; $L_{h.t_{wash}}$ is the distance from 1/4 b/a of the washed part of the horizontal tail to the airplane's center of gravity.

Calculations indicate that for "canard"-type supersonic transports, the relative area of the horizontal foreplane washed by the flow, $\bar{S}_{h.f.p}$, depends on the function of the foreplane. If the horizontal foreplane is designed basically to trim the airplane (i.e., in the case in which control of the airplane in pitch is the job of the stabilizer and elevons), then $\bar{S}_{h.f.p} = 0.02$-0.04 and the elevon area $\bar{S}_{ev} = 2S_{ev}/S = 0.06$-$0.12$.

If, on the other hand, the horizontal foreplane is to serve as a destabilizer, i.e., to lower normal-acceleration stability $(\bar{x}_F - \bar{x}_{cg})$ at supersonic flight speeds, its relative area $\bar{S}_{h.f.p} = S_{h.f.p}/S$ washed by the flow depends on the required decrease in normal-acceleration stability at $M > 1.5$. It can be assumed for approximate calculations that one percent of washed horizontal-foreplane area displaces the longitudinal center forward by 1.7-2.0% of wing mean aerodynamic chord when the foreplane has an arm ratio $\bar{L}_{h.f.p}$ of 1-1.3.

After selection of the planform, profile, and tentative geometry of the horizontal tail and its deflection angles, it is necessary to determine the position of the airplane's longitudinal aerodynamic center and the maximum tailheavy $\bar{x}_{cg_t}$ and the maximum noseheavy $\bar{x}_{cg_n}$ operational trims for the selected tailplane parameters. If it is then found that the range of variation of the airplane's operational trims ($\bar{x}_{cg_t} - \bar{x}_{cg_n}$) does not conform to requirements, this means that the parameters of the tailplane must be changed.

§9.2. APPROXIMATE CALCULATION OF LONGITUDINAL AERODYNAMIC CENTER POSITION AND EXTREME TRIMS OF AIRPLANE

As we know, the point about which the pitching moment is independent of attack angle is known as the longitudinal aerodynamic center of a body. The most widely used definition is different: the longitudinal aerodynamic center is the point of application of the increment to the body's total aerodynamic force that results from a change in attack angle.

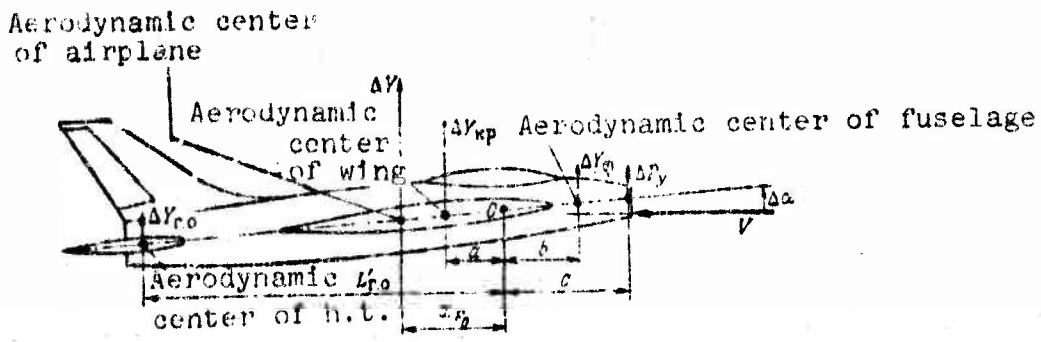

Figure 9.1. Diagram for determining aerodynamic center of a turbojet-engined airplane.

In steady flight, the position of an airplane's longitudinal aerodynamic center ($\bar{x}_p = x_p/b_a$) depends on the aerodynamic-center positions and lifts of its individual parts: wing, fuselage, engine pods, horizontal tail. The position of an airplane's longitudinal aerodynamic center is also strongly influenced by

interference of the wing with the fuselage, engine pods, and horizontal tail. The engines and flap, tab, and airbrake deflections may also influence the position of the airplane's longitudinal aerodynamic center.

Recommendations will be given below for approximate determination of the airplane's aerodynamic center position and those of its component parts on the assumption that landing flaps, tabs, and airbrakes are retracted.

If the positions of the longitudinal aerodynamic centers are known separately for each design component of the airplane, the aerodynamic-center coordinate of the airplane as a whole with respect, for example, to point O (Fig. 9.1) can be determined from the relation

$$\Delta Y \cdot x_{F_0} = \sum \Delta Y_i x_{F_i}, \tag{9.1}$$

where $\Delta Y = \Sigma \Delta Y_i$ is the total lift increment for the airplane due to the increment in angle of attack, x_{F_0} is the coordinate of the airplane's longitudinal aerodynamic center relative to point O. Positive values of x_{F_0} are reckoned in the direction of flight speed (see Fig. 9.1); ΔY_i is the lift increment of the i-th design component of the airplane due to the attack-angle increment, and x_{F_i} is the coordinate of the point of application of the lift increment of the i-th design component, i.e., the coordinate of the center reckoned from the point O of the particular design component of the airplane.

As applied to a single-turbojet airplane (see Fig. 9.1), expression (9.1) is written

$$\Delta Y \cdot x_{F_0} = \Delta P_y c + \Delta Y_\Phi b - \Delta Y_{\text{кр}} a - L_{\text{г.о}} \Delta Y_{\text{г.о}};$$

whence we obtain after transformations

$$\bar{x}_{F_0} = \frac{x_{F_0}}{b_i} = \frac{c_{P1}\bar{c} + c^a_{y_\Phi}\frac{F_\Phi}{S}\bar{b} - (c^a_{y_{\text{кр}}})^{\text{кр}} \cdot \bar{a} - (c^a_{y_{\text{г.о}}})^{\text{г}} A_{\text{г.о}} K_{\text{г.о}} \left(1 - \frac{d\varepsilon}{d\alpha}\right)}{c_{P1} + c^a_{y_\Phi}\frac{F_\Phi}{S} + (c^a_{y_{\text{кр}}})^{\text{кр}} + (c^a_{y_{\text{г.о}}})^{\text{г}} \bar{S}_{\text{г.о}} K_{\text{г.о}} \left(1 - \frac{d\varepsilon}{d\alpha}\right)}. \tag{9.2}$$

where

$$c_{pi} = \frac{P}{qS}\frac{1}{\frac{V_e}{V}-1}; \quad \frac{V_e}{V} = 1 + \frac{9.81 P_{sp}}{V}; \tag{9.3}$$

q is the ram pressure, P_{sp} is the specific thrust, S is the wing area including the part in the fuselage, $c^{\alpha}_{y_f}$ is the derivative of the fuselage lift coefficient referred to the midships-section area, F_f is the midships-section area of the fuselage, $(c^{\alpha}_{y_{wg}})^{**}$ is the derivative of the wing lift coefficient with respect to angle of attack with consideration of its interference with the fuselage and engine pods, $(c^{\alpha}_{y_{h.t}})^{*}$ is the derivative of the horizontal-tailplane lift coefficient with respect to attach angle, referred to tailplane area with consideration of fuselage interference, $\bar{S}_{h.t} = S_{h.t}/S$ is the relative area of the horizontal tail including the part in the fuselage, $A'_{h.t} = (S_{h.t}/S)(L'_{h.t}/b_a)$ is the moment-area ratio of the horizontal tail with the part in the fuselage about the selected point O (see Fig. 9.1), $K_{h.t}$ is the flow-stagnation coefficient at the horizontal tail, ε is the downwash at the horizontal tail in the airplane's plane of symmetry, and $\bar{a} = a/b_a$, $\bar{b} = b/b_a$, and $\bar{c} = c/b_a$ are, respectively, the arm ratios of the forces ΔY_{wg}, ΔY_f, and ΔP_{sp}.

It is evident from (9.2) that in order to determine the coordinate of the new airplane's longitudinal aerodynamic center, it is necessary to know, in addition to its geometrical parameters, the position of the center on each design element, the value of c^{α}_{y} for this element, and, for a horizontal tail placed aft of the wing, the downwash gradient $d\varepsilon/d\alpha$ (or $d\varepsilon/dc_y$) and the stagnation coefficient $K_{h.t}$ in the region of the horizontal tail. Below we present material that can be used as a basis for approximate determination of the longitudinal-center position and the lifting properties of the airplane's basic design components.

a) Determination of Longitudinal Aerodynamic Center Positions and Lifting Properties of Fuselages and Engine Nacelles

As a rule, the fuselages and engine nacelles of modern aircraft and their weapons pods and underwing tanks are given shapes closely approaching those of axisymmetric solids of revolution. In approximate calculations, it is therefore quite acceptable to assume that the aerodynamic characteristics of the fuselages and engine nacelles are identical to those of axisymmetric solids of revolution.

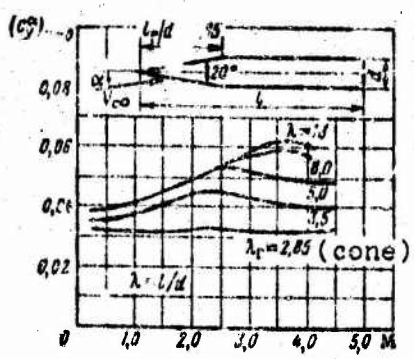

Figure 9.2 Mach-number variation of the derivative $(c_y^\alpha)_{\alpha=0}$ of solids of revolution with conical nose sections.

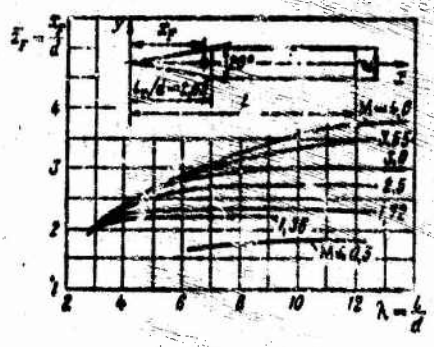

Figure 9.3. Slenderness-ratio curves of aerodynamic-center position $\bar{x}_F = x_F/d$ of solids of revolution with conical nose sections.

A wide variety of solid-of-revolution shapes are used in aviation. A simple body can be divided into two parts: a forward (nose) section and a stern (tail) section. The boundary separating the tail and nose sections of a solid of revolution is the cross section with the largest diameter d, which is known as the midships- (maximum-)section diameter. In general, the tail section of the solid of revolution may have a curved generatrix (in the form of a parabola), but it is usually made cylindrical or with cylindrical and conical segments, terminating in a base plane.

The most common nose-section shapes are sharp-pointed with conical and ogival generatrices.

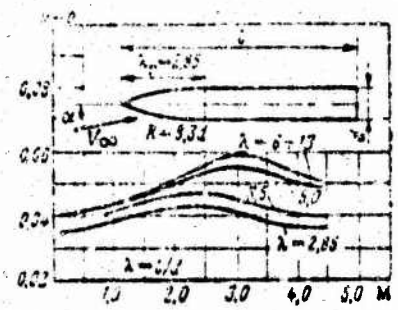

Figure 9.4. Mach-number variation of the derivative $(c_y^\alpha)_{\alpha=0}$ for axisymmetric solids of revolution with ogival nose sections.

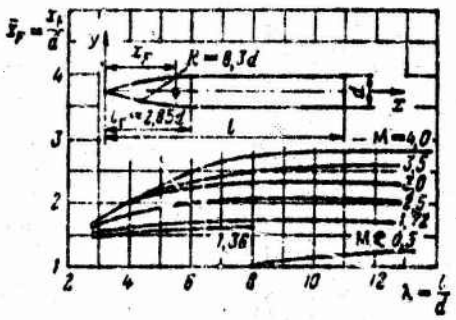

Figure 9.5. Slenderness-ratio variation of aerodynamic center relative coordinate $\bar{x}_F = x_F/d$ of solids of revolution with ogival nose sections.

The aerodynamic characteristics of sharp-nosed axisymmetric solids of revolution with cylindrical tail sections are represented graphically in Figs. 9.2 and 9.3. These figures give the aerodynamic characteristics $c_y^\alpha = f_1(M; \lambda)$ and $\bar{x}_F = x_F/d = f_2(M, \lambda)$ for solids of revolution with conical nose sections. The slenderness ratio of the conical nose section is $\lambda_n = l_n/d = 2.85$. It is assumed that the slenderness ratio of the body as a whole is changed by changing the slenderness ratio of the cylindrical section.

Figures 9.4 and 9.5 give the aerodynamic characteristics $c_y^\alpha = f_3(M, \lambda)$ and $\bar{x}_F = x_F/d = f_4(M, \lambda)$ for axisymmetric solids of revolution with ogival nose sections. The generatrix radius of the ogival nose section is $R = 8.3d$.

The experimental results presented in Figs. 9.4 and 9.5 pertain to axisymmetric solids of revolution whose slenderness is varied by varying that of the cylindrical section, while the slenderness of the ogival nose section remains constant at $\lambda_n = l_n/d = 2.85$.

In Figs. 9.2 and 9.4, the derivative (c_y^α) is referred to a midships-section area of $\pi d^2/4 = F_f$.

If the fuselage or engine nacelle of the vehicle being designed has a conical or ogival nose section with a slenderness $\lambda_n \approx 3$-5, while the tail section consists of cylindrical and conical segments and the taper angle of the conical segment is small, the aerodynamic characteristics of the fuselage or engine nacelle will then be closely similar to the solid-of-revolution aerodynamic characteristics given in Figs. 9.2-9.5.

The data given in these figures can also be used as approximate data for solids of revolution with paraoolic nose-section generatrices.

b) Determination of Longitudinal Aerodynamic Center Position and Lifting Properties of Wings

The derivative $c^\alpha_{y_{wg}}$ for isolated delta wings can be determined from the diagram in Fig. 9.6. The position of the longi-

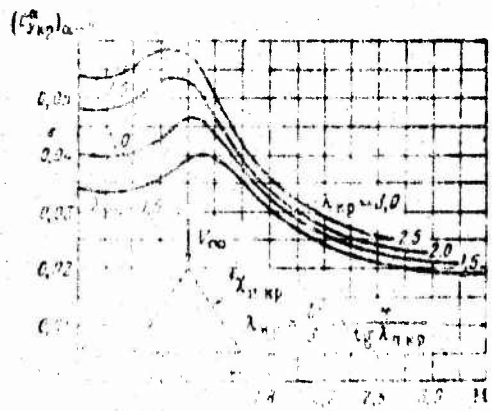

Figure [illegible] Semi-empirical variation of the derivative $(c^\alpha_{y_{kp}})_{\alpha=0}$ of isolated delta wings.

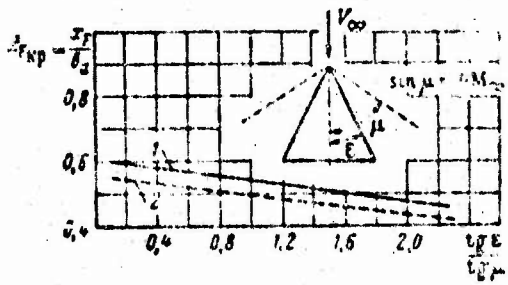

Figure 9.7. Plot of relative coordinate of aerodynamic center $\bar{x}_{F_{wg}} = x_F/l_a$ of isolated delta wings against tan c/tan μ: 1) with wedge-shaped leading edge; 2) with elliptical leading edge.

tudinal aerodynamic center with respect to the forward end of the mean [illegible] can be determined approximately from the following [illegible] isolated delta wing at $M \leq$ [illegible]

$$\bar{x}_{F_{кр}} = 0{,}37 + 0{,}01\lambda_{кр}, \qquad (9.4)$$

where

$$\lambda_{кр} = \frac{l^2}{S} = \frac{4}{\operatorname{tg}\chi_{п.кр}}.$$

Expression (9.4) can be used to determine aerodynamic-center coordinates for delta wings with aspect ratios of 1.5 to 3.0.

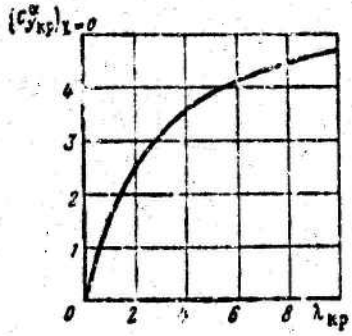

Figure 9.8. The derivative $(c^{\alpha}_{y_{wg}})_{\chi=0}$ for straight (unswept) wing as a function of aspect ratio λ_{wg} at $M \leq 0.5$.

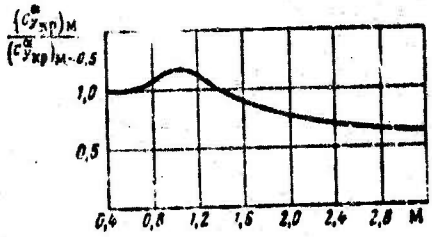

Figure 9.9. Mach-number plot of the ratio $(c^{\alpha}_{y_{wg}})_M/(c^{\alpha}_{y_{wg}})_{M\leq 0.5}$.

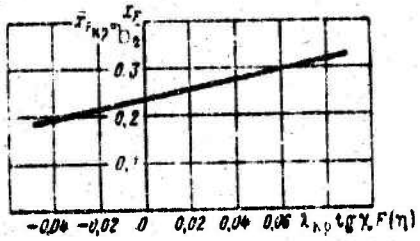

Figure 9.10. Relative coordinate of aerodynamic center $\bar{x}_{F_{wg}} = x_F/b_a$ of isolated swept wing as a function of $\lambda_{wg}\tan\chi F(\eta)$ at $M \leq 0.5$.

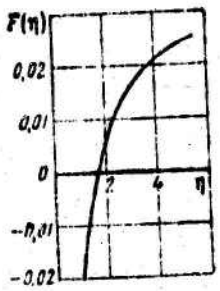

Figure 9.11. Plot of the function $F(\eta)$ against the taper η of a swept wing.

The position of the longitudinal aerodynamic center of an isolated delta wing can be determined for $M > 1$ from the diagram

in Fig. 9.7. Here, curve 1 pertains to delta wings with wedge-shaped leading edges, and curve 2 to wings with elliptical leading edges.

For isolated swept wings, the derivative $c^{\alpha}_{y_{wg}}$ is determined approximately from the expression

$$(c^{\alpha}_{y_{wg}})_{\chi\neq 0}=(c^{\alpha}_{y_{wg}})_{\chi=0}\sqrt{\cos\chi}, \qquad (9.5)$$

where $(c^{\alpha}_{y_{wg}})_{\chi\neq 0}$ is the derivative characterizing the lifting properties of the straight wing. It is determined for $M \leq 0.5$ from Fig. 9.8 (where α is in radians).

If the derivative $(c^{\alpha}_{y_{wg}})$ of a swept wing is known for small Mach numbers $M \leq 0.5$, its values for $M > 1.0$ are easily determined from the data of Fig. 9.9. This figure presents a plot of the ratio $(c^{\alpha}_{y_{wg}})_M/(c^{\alpha}_{y_{wg}})_{M\leq 0.5}$ against Mach number, where $(c^{\alpha}_{y_{wg}})_M$ is the derivative for the isolated swept wing at any $M < 3.0$ and $(c^{\alpha}_{y_{wg}})_{M\leq 0.5}$ is the derivative for the isolated swept wing at small $M \leq 0.5$.

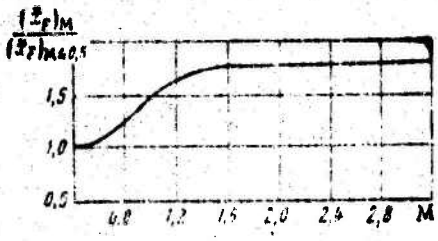

Figure 9.12. Variation of the ratio $(\bar{x}_F)_M/(\bar{x}_F)_{M\leq 0.5}$ with M for swept wings with sweep angles larger than 45°.

The relative coordinate of the longitudinal aerodynamic center $\bar{x}_{F_{wg}}$ for an isolated swept wing can be determined for small $M \leq 0.5$ from Fig. 9.10, where λ_{wg} tan $\chi \cdot F(\eta)$ is the abscissa. Here, χ is the leading-edge sweep angle of the wing, $F(\eta)$ is determined from the diagram in Fig. 9.11, and $\eta = b_0/b_e$ is the wing taper ratio.

The position of the aerodynamic center of a swept wing relative to the forward point of its mean aerodynamic chord can be determined for $M > 1.0$ from Fig. 9.12 if its position at small $M \leq 0.5$ has been determined.

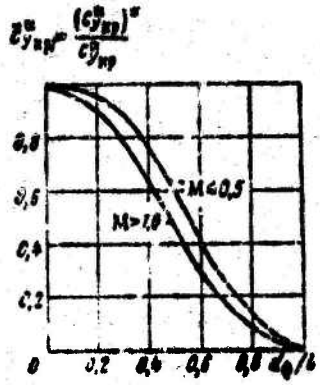

Figure 9.13. Plot of $\bar{c}^{\alpha}_{y_{wg1}} = (c^{\alpha}_{y_{wg}})^{*}/c^{\alpha}_{y_{wg}}$ as a function of fuselage relative diameter $\bar{d}_f = d_f/l$.

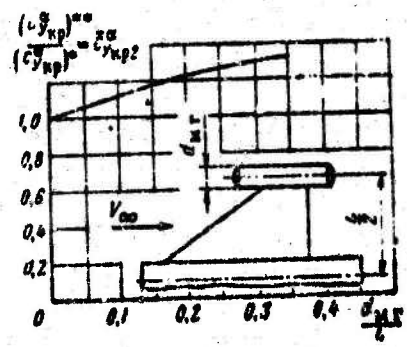

Figure 9.14. Plot of $\bar{c}^{\alpha}_{y_{wg2}} = (c^{\alpha}_{y_{wg}})^{**}/(c^{\alpha}_{y_{wg}})^{*}$ against relative diameter of engine nacelle d_{en}/l.

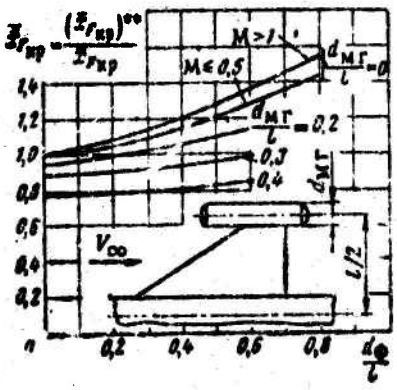

Figure 9.15. Influence of engine nacelles on position of wing aerodynamic center.

Interference of a wing of any planform with the fuselage lowers the lifting properties of the wing ($c^{\alpha}_{y_{wg}}$) and shifts its longitudinal aerodynamic center toward the trailing edge. The extent of this interference depends chiefly on the ratio of the maximum fuselage diameter to the wingspan, i.e., on d_f/l.

If fuel tanks or engine nacelles are mounted on the wing tips, their influence on the wing reduces to an increase in the derivative $c^{\alpha}_{y_{wg}}$ and a forward shift of the longitudinal aerodynamic center on delta and swept wings. This effect of wing tip nacelles on the wing is manifested in the presence and in the absence of a fuselage. The quantitative characteristics of these effects are presented in diagram form in Figs. 9.13-9.15.

Figure 9.13 shows $\bar{c}^{\alpha}_{y_{wg1}} = (c^{\alpha}_{y_{wg}})^{*}/c^{\alpha}_{y_{wg}}$ as a function of fuselage relative diameter for $M \leq 0.5$ and $M > 1.0$.

Here $(c^{\alpha}_{y_{wg}})^{*}$ is the derivative of the wing lift coefficient with respect to angle of attack when the wing is mounted on the airplane's fuselage and $c^{\alpha}_{y_{wg}}$ is the derivative of the isolated-wing lift coefficient with respect to angle of attack.

Theory and experiment have shown that the results given in Fig. 913 can be used for delta, trapezoidal, straight, and swept wings mounted on a cylindrical airplane fuselage section in the Mach-number range $M = 0.2$-5.0 and at angles of attack $\alpha = 0$-$6°$.

Figure 9.14 shows $\bar{c}^{\alpha}_{y_{wg2}} = (c^{\alpha}_{y_{wg}})^{**}/(c^{\alpha}_{y_{wg}})^{*}$ as a function of the relative diameter d_{en}/l of the engine nacelle.

Here $(c^{\alpha}_{y_{wg}})^{**}$ is the derivative of the wing lift coefficient with respect to angle of attack in the presence of a fuselage and wing tip engine nacelles, i.e., when the wing with the nacelles is mounted on the fuselage, and $(c^{\alpha}_{y_{wg}})^{*}$ is the derivative of the wing lift coefficient with respect to angle of attack when the wing is mounted on the fuselage without the engine nacelles.

Theory and certain experimental data indicate that the results shown graphically in Fig. 9.14 can be used for delta and swept wings mounted on a cylindrical fuselage section in such a way that their center chords coincide with the fuselage (solid-of-revolution) axis, while the axes of the wing tip engine nacelles lie in the plane of the wing. These results are valid in the Mach-number range from 0.2 to 3.0 if the fuselage relative diameter is in the rahge $d_f/l = 0$-0.35.

Figure 9.15 shows how the longitudinal aerodynamic centers of delta and swept wings are shifted as a result of their interference with the fuselage and wing tip engine nacelles at subsonic and supersonic speeds. We see that an increase in the fuselage relative diameter d_f/l increases $\bar{\bar{x}}_{F_{wg}} = (\bar{x}_{F_{wg}})^{**}/\bar{x}_{F_{wg}}$, i.e.,

shifts the longitudinal center toward the wing trailing edge. Here $(\bar{x}_{F_{wg}})^{**}$ is the relative coordinate of the wing longitudinal center with consideration of wing interference with the fuselage and engine nacelles and $\bar{x}_{F_{wg}}$ is the relative coordinate of the longitudinal aerodynamic center of the isolated wing.

An increase in the engine-nacelle relative diameter d_{en}/l causes a decrease in $\bar{\bar{x}}_{F_{wg}}$, and this means that placing wing tip engine nacelles on delta and swept wings shift their longitudinal foci forward.

We note that the data given in Figs. 9.13-9.15 were calculated in such a way that the entire effect of mutual interference of the wing with the fuselage and with the wing tip fuel tanks and engine nacelles would apply only to the wing, i.e., it is unnecessary to consider the influence of the wing in determining the lifting properties and longitudinal-center positions of the fuselage and nacelles.

c) Determination of Lifting Properties and Position of Longitudinal Aerodynamic Center for the Horizontal Tail

The coordinate of the longitudinal aerodynamic center of the horizontal tail relative from the forward point of its mean aerodynamic chord must be determined in the same way as for wings, with consideration of the fuselage effect; fuselage diameter is to be measured at the $1/2\ b_{a_{h.t}}$ level of the horizontal tailplane.

In determining the lifting properties of a horizontal tail mounted aft of the wing, it is necessary to consider how they are influenced not only by the section of fuselage on which the horizontal tail is mounted, but also by the part of the fuselage forward of the horizontal tail. It is also necessary to allow for the influence of the wing on the lifting properties of the horizontal tail. These two effects on the lifting properties of the horizontal tail are taken into account by determining the downwash gradient at the tail, $d\varepsilon/d\alpha = c_y^{\alpha} d\varepsilon/dc_y$, and the flow stagnation coefficient $K_{h.t.}$ in the region of the horizontal tail.

Consequently, the lift increment $\Delta Y_{h.t}$ of the horizontal tail due to a change in the airplane's angle of attack is determined with consideration of the fuselage and wing effects by the familiar expression

$$\Delta Y_{г.о} = (c^{\alpha}_{y_{г.о}})^{*} \Delta\alpha \left(1 - \frac{d\varepsilon}{d\alpha}\right) S_{г.о} K_{г.о} \frac{\rho V^2}{2}, \tag{9.6}$$

where $\Delta\alpha$ is the attack-angle increment, $(c^{\alpha}_{y_{h.t}})^{*}$ is the derivative of the horizontal-tail lift coefficient with respect to attack angle. It is determined in the same way as for the wing, with consideration of the fuselage effect; $S_{h.t}$ is the area of the horizontal tail counting the part in the fuselage, if the horizontal tail is mounted directly on the latter.

If the horizontal tail of an airplane with a wing having an aspect ratio $\lambda_{wg} < 3.0$ is mounted on the fin far above the fuselage, we can take a $K_{h.t} = 0.9$. If the horizontal tail is in the immediate vicinity of the fuselage, $K_{h.t} \approx 0.85$.

If the airplane has a large wing aspect ratio, i.e., $\lambda_{wg} > 3.0$, then $K_{h.t}$ is determined by the expression

$$K_{г.о} = 0{,}95 - 0{,}4 \frac{S_{ф_{г.о}}}{S_{г.о}}. \tag{9.7}$$

where $S_{f_{h.t}}$ is the area of the horizontal tailplane covered by the fuselage.

The derivative $d\varepsilon/d\alpha = c^{\alpha}_{y_{wg}}\, d\varepsilon/dc_y$, which characterizes the variation of the downwash at the horizontal tailplane as a function of attack angle, is easily determined if $d\varepsilon/dc_y$ is known. For <u>delta-wing</u> aircraft flying at subsonic speeds, this quantity can be determined from the formula

$$\frac{d\varepsilon}{dc_y} = \frac{0{,}63}{\lambda_{wg}} K_x K_y. \tag{9.8}$$

where

$$K_x = 0{,}96 + \frac{0{,}04}{\bar{L}^*_{r.o}};$$

$$\bar{L}^*_{r.o} = \frac{2L_{r.o}}{l};$$

l is the wingspan, $L_{h.t}$ is the distance between the center of gravity and the aerodynamic center of the horizontal tail;

$$K_y \approx 1 - \frac{\bar{y}^*_{r.o}}{0{,}75} + 0{,}5\bar{y}^{*2}_{r.o},$$

where $\bar{y}^*_{h.t} = 2y_{h.t}/l$ and $y_{h.t}$ is the distance between the wing root chord line and the longitudinal aerodynamic center of the horizontal tail.

Table 9.2

$\bar{L}^*_{r.o}$	∞–2	1	0,5	η	1	0,6	0,4	0,2
K_L	0,61	0,52	0,43	K_η	1	0,63	0,7	0,53

For swept-wing aircraft, the derivative $d\varepsilon/dc_y$ is given by

$$\frac{d\varepsilon}{dc_y} = \frac{1}{\lambda_{кр}} x_1 x_2 x_3 x_4, \tag{9.9}$$

where

$$x_1 = (0{,}45 - 0{,}02\lambda_{кр})\left(2 - \frac{1}{\eta}\right),$$

η is the relative taper of the wing,

$$x_2 = 0{,}75 + \frac{0{,}2}{\bar{L}^*_{r.o}};$$

$$x_3 = 1 - 0{,}7(2 - \bar{y}^*_{r.o})\bar{y}^*_{r.o},$$

$$x_4 = 1 + 0{,}15\sin^2\chi.$$

For supersonic speeds, the derivative $d\varepsilon/dc_y$ for delta wings and trapezoidal wings with straight leading edges can be determined from the formula

$$\frac{d\varepsilon}{dc_y} = \frac{K_\varepsilon}{\lambda_{кр}} K_\eta (1 - \bar{y}_{h.t}), \tag{9.10}$$

where $\bar{y}_{h.t} = 2y_{h.t}/l$ is the distance[1] of the horizontal tailplane above or below the wing vortex sheet, expressed as a fraction of wing half-span, K_ε is a coefficient indicating the dependence of $d\varepsilon/dc_y$ on $\bar{L}^*_{h.t}$ (see Table 9.2), and K_η is a coefficient indicating the dependence of the derivative $d\varepsilon/dc_y$ on the taper of a cropped delta wing (see Table 9.2).

We note that formula (9.10) can also be used to determine the downwash behind swept wings with trailing-edge sweep angles no greater than 25°.

Having determined the position of the airplane's longitudinal aerodynamic center, we can proceed to determination of the extreme trims.

d) Determination of Extreme Tailheavy and Extreme Noseheavy Trims of the Airplane.

If the coordinate of the airplane's longitudinal aerodynamic center relative to the forward point of the mean aerodynamic chord $\bar{x}_F = x_F/b_a$ is known, the maximum tailheavy operational trim of the airplane $\bar{x}_{cg_t}$ is easily determined if the maximum permissible normal-acceleration stability at subsonic speeds is also known. The smallest acceptable normal-acceleration stability $(\bar{x}_F - \bar{x}_{cg_t})$ depends on the type of airplane. Thus, for interceptors $(\bar{x}_F - \bar{x}_{cg_t}) = 0.02$-$0.4$; for bombers $(\bar{x}_F - \bar{x}_{cg_t}) = 0.04$-$0.06$, and for passenger aircraft $(\bar{x}_F - \bar{x}_{cg_t}) \approx 0.08$-$0.10$.

The maximum noseheavy trim $\bar{x}_{cg_n}$ is determined from the airplane's landing-trim conditions:

Footnote (1) appears on page 235.

$$Y + P\alpha_{\text{пос}} \approx G, \tag{9.11}$$

$$M_{z_0} + M_z^{\alpha}\alpha_{\text{пос}} + M_z^{\varphi}\varphi + M_z^{\delta_{\text{эл}}}K_1\delta_{\text{эл}_{\max}} + M_{z_P} = 0, \tag{9.12}$$

where Y is the lift of the airplane with landing flaps down and with consideration of the ground effect; P is powerplant thrust, M_{z_0} is the pitching moment at $\alpha = \phi = \delta_{el} = 0$, M_z^{α}, M_z^{ϕ}, and $M_z^{\delta_{el}}$ are the derivatives of the airplane's pitching moment with respect to angle of attack and the deflection angles of the stabilizer and elevator, respectively, K_1 is a coefficient that takes account of the required elevator-deflection margin available at landing, ϕ is the stabilizer deflection angle (a defined quantity), $\delta_{el_{max}}$ is the maximum elevator deflection, α_{ldg} is the airplane's landing angle of attack. It can be assumed in first approximation that $\alpha_{ldg} \approx 10°-12°$; $M_{z_P} = Py_P$ is the moment of the thrust P, which passes at a distance y_P from the airplane's center of gravity; $M_{z_P} > 0$ if the thrust sets up a pitchup moment.

After simple transformations, we obtain expressions for the maximum noseheavy position $\bar{x}_{cg_n}$ of the center of gravity and the lift-trim coefficient to land the airplane with maximum noseheavy trim:

$$\bar{x}_{\tau_n} = \bar{x}_F - \frac{(m_{z_0} + m_{z_P} + m_z^{\varphi}\varphi + m_z^{\delta_{\text{эл}}}K_1\delta_{\text{эл}_{\max}})}{c_{y_{\text{пос.доп}}}}; \tag{9.13}$$

$$c_{y_{\text{пос.доп}}} = c_y^{\alpha}\alpha_{\text{пос}} + c_y^{\varphi}\varphi + c_y^{\delta_{\text{эл}}}K_1\delta_{\text{эл}_{\max}} + c_y\alpha_{ldg} + \Delta C_{y_{\text{доп}}} + \Delta C_{y_{\text{зем}}} \tag{9.14}$$

where $m_{z_P} = \frac{Py_P}{q S_{\text{ов}} b_{\text{ов}}}$ is the thrust moment coefficient;

$$m_z^{\varphi} = \pm (c_{y_{\text{г.о}}}^{\alpha})^{*} A_{\text{г.о}} K_{\text{г.о}} \eta_{\text{г}};$$

$$m_z^{\delta_{\text{эл}}} = \pm (c_{y_{\text{г.о}}}^{\alpha})^{*} A_{\text{г.о}} K_{\text{г.о}} \eta_{\text{эл}}.$$

(In these expressions, the minus sign is used when the tail is situated aft of the center of gravity); m_{z_0} can be assumed equal to zero in first approximation, n_{st} and n_{el} are the

effectiveness coefficients of the stabilizer and elevator, respectively; at subsonic speeds, it can be assumed that $n_{el} = \sqrt{S_{el}/S_{h.t}}$, while at supersonic speed $n_{el} = S_{el}/S_{h.t} = \bar{S}_{el}$. n_{st} is defined similarly; $S_{h.t}$ is the total area of the horizontal tailplane, including the elevator;

$$c_y^{\alpha} = (c_{y_{r.t}}^{\alpha})^{\alpha} + (c_{y_{r.o}}^{\alpha})^{\alpha} \bar{S}_{r.o} \left(1 - \frac{d\varepsilon}{d\alpha}\right) K_{r.o} + c_{y_{\Phi}}^{\alpha} \frac{F_{\Phi}}{S} + c_{y_{Mr}}^{\alpha} \frac{F_{Mr}}{S};$$

$$c_y^{\delta} = (c_{y_{r.o}}^{\alpha})^{\alpha} \bar{S}_{r.o} K_{r.o} n_{rr};$$

$$c_y^{\delta_n} = (c_{y_{r.o}}^{\alpha})^{\alpha} \bar{S}_{r.o} K_{r.o} n_n;$$

$c_P = 2P/\rho V^2 S$ is the thrust coefficient, $\Delta c_{y_{fl}}$ is the lift-coefficient increment due to lowering the landing flaps. This quantity can be taken from statistical data in first approximation; $\Delta c_{y_{grd}}$ is the lift-coefficient increment due to the ground-proximity effect. It can be taken from the statistics in first approximation.

§9.3. SELECTION OF VERTICAL-TAILPLANE PARAMETERS, WING DIHEDRAL ANGLE, AND AILERON PARAMETERS

a) Selection of Vertical-Tailplane Parameters

The vertical tail of an airplane usually consists of a fin (fins) and a rudder. They are subject to the following requirements:

- they must provide the airplane with the required lateral stability and controllability characteristics in all operational flight conditions;

- they must make it possible to trim the airplane in the event of failure of one outboard (critical) engine during take-off at $c_y = c_{y_{1/o}}$ with the flaps up;

- they must make it possible to trim the airplane in the event of failure of two engines on one side in flight in the condition most characteristic for the particular aircraft type;

- they must make it possible to land the airplane without

crabbing in a side wind with a speed of no less than 15 m/s.

It is possible to conform fully to all these requirements made of the vertical tailplane of a modern aircraft only when both the vertical tailplane itself and the entire aircraft are properly configurated and automatic devices are used.

During the preliminary-design process, it is necessary to select the following vertical-tail parameters:

– planform and position with respect to the fuselage and with respect to the horizontal tailplane;

– the relative value of the area $\bar{S}_{v.t} = S_{v.t}/S$ and the moment-area ratio $B_{v.t} = S_{v.t}L_{v.t}/Sl$ of the vertical tailplane;

– the rudder relative area $\bar{S}_{rud} = S_{rud}/S_{v.t}$, the type of compensation, and the maximum rudder deflection angles.

Table 9.3

Over-All Dimensions of the Vertical Tailplanes of Modern Transonic Aircraft

Parameter \ Aircraft type	Light turbo-jets	Heavy aircraft	
		Turbojet	Propjet
$B_{v.t} = S_{v.t}L_{v.t}/Sl$	0.06-0.10	0.040-0.065	0.050-0.080
$\bar{S}_{v.t} = S_{v.t}/S$	0.15-0.20	0.10-0.17	0.13-0.19
$\bar{S}_{rud} = S_{rud}/S_{v.t}$	0.20-0.28	0.22-0.35	0.28-0.50
$\delta_{r_{max}}$	±(20°-25°)	±(20°-25°)	±(20°-25°)

The planform and profile of the vertical tail are selected on about the same basis as the planform and profile of the horizontal tail. The reader is referred to §8.3e concerning the position of the vertical tail with respect to the fuselage and horizontal tail.

The relative values of the areas $\bar{S}_{v.t}$ and $\bar{S}_{rud}$ and the moment-area ratio $B_{v.t}$ of the vertical tail are taken in first

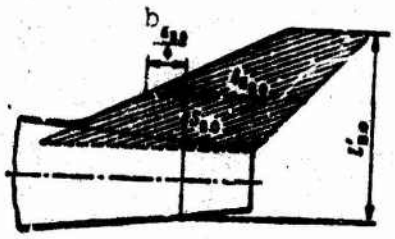

Figure 9.16. Illustrating determination of vertical tailplane area $S_{v.t}$ and its span $l'_{v.t}$.

approximation from statistical data. Analysis of statistics on the geometrical parameters of vertical tailplanes as used on modern transonic airplanes indicates that $\bar{S}_{v.t}$, $B_{v.t}$, and $\bar{S}_{rud}$ are in the ranges indicated in Table 9.3.

In determining the parameters listed in this table, only the part of the fin above the fuselage was included in the vertical-tailplane area. Ventral-fence areas were not included. Figure 9.16 schematizes the determination of the area of the vertical tail, the position of its mean aerodynamic chord $b_{a_{v.t}}$, etc.

Modern supersonic aircraft have the following vertical-tailplane parameters:

$$B_{в.о} \approx 0{,}07 \div 0{,}11; \quad \bar{S}_{в.о} \approx 0{,}16 \div 0{,}20;$$
$$\bar{S}_{р.н} = 0{,}20 \div 0{,}26; \quad \delta_{н_{max}} \pm 25°.$$

We note that large values of $B_{v.t}$ are characteristic for supersonic interceptors. Analysis of statistical data indicates that the effective aspect ratios of the vertical tailplanes of modern supersonic aircraft lie in the range $1.5 \leq \lambda_{v.t} < 3.5$.

Here the effective aspect ratio of the vertical tail is a relative quantity equal to the ratio of the square of the effective span of the vertical tail $l'_{v.t}$ (see Fig. 9.16) to the area of the vertical tail:

$$\lambda_{в.о} = \frac{(l'_{в.о})^2}{S_{в.о}}$$

The vertical tailplanes of modern transonic and supersonic aircraft are tapered in the range $1.5 \leq \eta_{v.t} \leq 3.3$. However, vertical tails with tapers of 2.5-3.0 are most frequently encountered.

The area of the ventral fences used to improve lateral stability and controllability characteristics represent 2-5% of wing area. The effectiveness of ventral fences per unit of fence area is approximately 1.5-1.8 times the effectiveness of the main dorsal tailplane surface.

Following tentative selection of the vertical-tailplane and rudder dimensions, it is necessary to establish the wing dihedral and aileron parameters.

b) Selection of Wing Dihedral and Aileron Geometry

The designer can adjust the lateral stability m_x^β of the airplane by varying the dihedral of its wing. Modern transonic and supersonic aircraft with swept and delta wings are given a negative dihedral to lower lateral stability, which becomes excessively high in flight at large angles of attack (i.e., at large c_y). Statistical data indicate that modern transonic and supersonic aircraft generally have negative wing dihedrals from zero to -5°. However, there are also known aircraft configurations with negative wing dihedrals of minus ten degrees. A large wing negative dihedral results in a substantial decrease in the distance between the ground and the wingtips. This distance must be sufficient to prevent the airplane from striking its wings on the ground during takeoff and landing in cross winds up to 15 m/s. For this purpose, the negative wing dihedral is sometimes imparted not to the entire wing, but only to its tip sections. It is appropriate to note that the airplane's lateral stability can, in principle, be lowered by imparting a negative dihedral to the horizontal tailplane [and] by placing the wing lower on the fuselage. However, the latter measure lowers the airplane's lift/drag ratio and increases the fuselage-to-ground distance, which makes it difficult to use, for example, on transport airplanes.

It is expedient to begin by assigning a wing dihedral on the basis of statistical data, with subsequent hypothetical testing and adjustment.

Aileron geometry is arrived at on the basis of lateral-control requirements. Basic among the latter are the following:

- providing for trimming of the airplane at zero slip angle in the event of failure of an outboard engine during takeoff with $c_y \approx c_{y_{1/o}}$ (wing flaps up);

- making it possible for the airplane to execute its landing glide and landing (gear and flaps down) in a 15-m/s crosswind blowing at 90° to the runway;

- providing for trim of the airplane in the event of in-flight failure of two engines on the same side in the flight situation most characteristic for the particular airplane;

- aileron efficiency must be such that when they are fully deflected during takeoff and landing at speeds $V = (1.1\text{-}1.3)V_{min}$, the dimensionless steady-state roll angular velocity $\bar{\omega}_x = \omega_x l/2V$ will be greater than or equal to 0.07;

- the ailerons of maneuverable aircraft must be able to set up a roll angular rate of

$$1 \text{ rad/s} \leq \omega_x \leq 1.6 \text{ rad/s}$$

in flight at the speed limit;

- the stick effort per unit of roll angular velocity at the flight-speed limit must not exceed a certain value.

Statistical data on modern aircraft and calculations indicate that these requirements can generally be satisfied by using conventional ailerons. Their dimensions should be in the following ranges:

- aileron relative area $2S_a/S \approx 0.036\text{-}0.085$; the smaller figure is more pertinent to interceptor-type aircraft, and the larger to heavy aircraft;

- the chord of the ailerons (to the aileron hinge axis) should be 20 to 30% of the wing chord;

– the span of the ailerons is often limited by the span of the landing flaps, usually representing 30-40% of the wing half-span.

The maximum aileron deflection angle depends on the type of balancing employed and, according to statistical data, ranges from 20° to 30°. We note that the relative span and chord of the ailerons are selected simultaneously with the dimensions of the balancing tabs and the maximum aileron deflection angle.

Having arrived at the geometry of the vertical tailplane, the ailerons, and the wing dihedral, it is necessary to make an approximate calculation of the airplane's lateral-stability derivatives and its axial moments of inertia, and then to check the selection of the vertical-tailplane and aileron geometries and the wing dihedral against them.

§9.4. APPROXIMATE CALCULATION OF THE AIRPLANE'S LATERAL STABILITY AND CONTROLLABILITY DERIVATIVES

a) Calculation of the Airplane's Lateral Stability

The lateral stability m_x^β of the airplane is determined basically by the wing, the vertical tailplane, and wing-fuselage interference. The lateral stability due to the fuselage, the horizontal tail, and their interference is usually small and can be disregarded in preliminary design. On this basis, the airplane's lateral stability can be written

$$m_x^\beta \approx m_{x_{wg}}^\beta + \Delta m_{x_{int}}^\beta + m_{x_{v.t}}^\beta; \qquad (9.15)$$

where $m_{x_{wg}}^\beta$ is the lateral stability due to the airplane's wing, $\Delta m_{x_{int}}^\beta$ is the lateral-stability increment due to interference of the wing with the fuselage, and $m_{x_{v.t}}^\beta$ is the lateral stability due to the vertical tailplane. Let us consider the calculation of each term in (9.15).

It is known that when a sweptback or delta wing acquires a slip angle, the forward half-wing has a smaller effective sweep

angle, while the sweep angle of the other wing half increases by the amount of the slip angle β. This results in changes of the c_y of the right and left wings in slip and in the formation of a wing rolling moment characterized by its coefficient m_x^β. It has been established theoretically and experimentally that the lateral stability of a swept (delta) wing with zero dihedral increases as the lift coefficient of the wing increases up to a certain point.

If a wing of any planform has a dihedral angle ψ (formed by the chord planes), the angle of attack of the forward wing half increases at a slip angle β, while it decreases on the other half of the wing by an amount

$$\Delta\alpha \approx \psi\beta.$$

This results in changes in the lift of the left and right wings and the appearance of a wing rolling moment at any angle of attack α.

The airplane's lateral stability is strongly influenced by the heightwise position of the wing on the fuselage. Thus, a high wing increases lateral stability as a result of wing-fuselage interference. A low wing, on the other hand, lowers lateral stability.

It follows from the above that the wing lateral stability can be determined, without consideration of its interference with the fuselage, from the formula

$$m_{x_{wg}}^{\beta} = (m_{x_{wg}}^{\beta})_{\chi} + (m_{x_{wg}}^{\beta})_{\psi}, \qquad (9.16)$$

where $(m_{x_{wg}}^{\beta})_{\chi}$ is the lateral stability due to the sweep of the wing and $(m_{x_{wg}}^{\beta})_{\psi}$ is the lateral stability due to the wing dihedral angle ψ. At small m, $(m_{x_{wg}}^{\beta})_{\chi}$ and $(m_{x_{wg}}^{\beta})_{\psi}$ can be determined approximately from formulas (9.17)-(9.22).

For delta wings with relative tapers $\infty \geq n \geq 5$, these derivatives can be determined from the expressions

$$(m^3_{x_{кр}})_\chi = -0{,}125\,\mathrm{tg}\,\chi_{п.кр}\,\frac{\eta+2}{\eta+1}\,c_y; \tag{9.17}$$

$$(m^3_{x_{кр}})_\psi = -0{,}167 c^a_{y_{кр}}\,\frac{\eta+2}{\eta+1}\,\psi, \tag{9.18}$$

where $\eta = b_0/b_e$ is the wing relative taper and b_e is the length of the tip chord.

Table 9.4

η	5	3	2	1
K_0	0.73	0,87	1.0	1,2

For sweptback wings with relative wing tapers $\eta \leq 5$,

$$(m^3_{x_{кр}})_\chi = -0{,}15\,\mathrm{tg}\,\chi_{\frac{1}{4}}\,\frac{\eta+2}{\eta+1}\,c_y; \tag{9.19}$$

$$(m^3_{x_{кр}})_\psi = -0{,}13 c^a_{y_{кр}}\,\frac{\eta+2}{\eta+1}\,\psi. \tag{9.20}$$

For unswept wings

$$(m^3_{x_{кр}})_{\chi=0} = -\left[\frac{K_\lambda}{\lambda_{кр}}\,\frac{(1{,}15\eta-0{,}15)}{(\eta+1)} - 0{,}05\right] c_y. \tag{9.21}$$

where λ_{wg} is the wing aspect ratio, K_0 is a coefficient that depends on wing taper (see Table 9.4), and

$$(m^3_{x_{кр}})_\psi = -0{,}16 c^a_{y_{кр}}\,\psi. \tag{9.22}$$

Table 9.5

$\lambda_{кр}$	0	1	2	2,5	3,0	4	5	6	8	10
K_λ	0	0,38	0,5	0,69	0,75	0,86	0,95	1,0	1,[illegible]	[illegible]

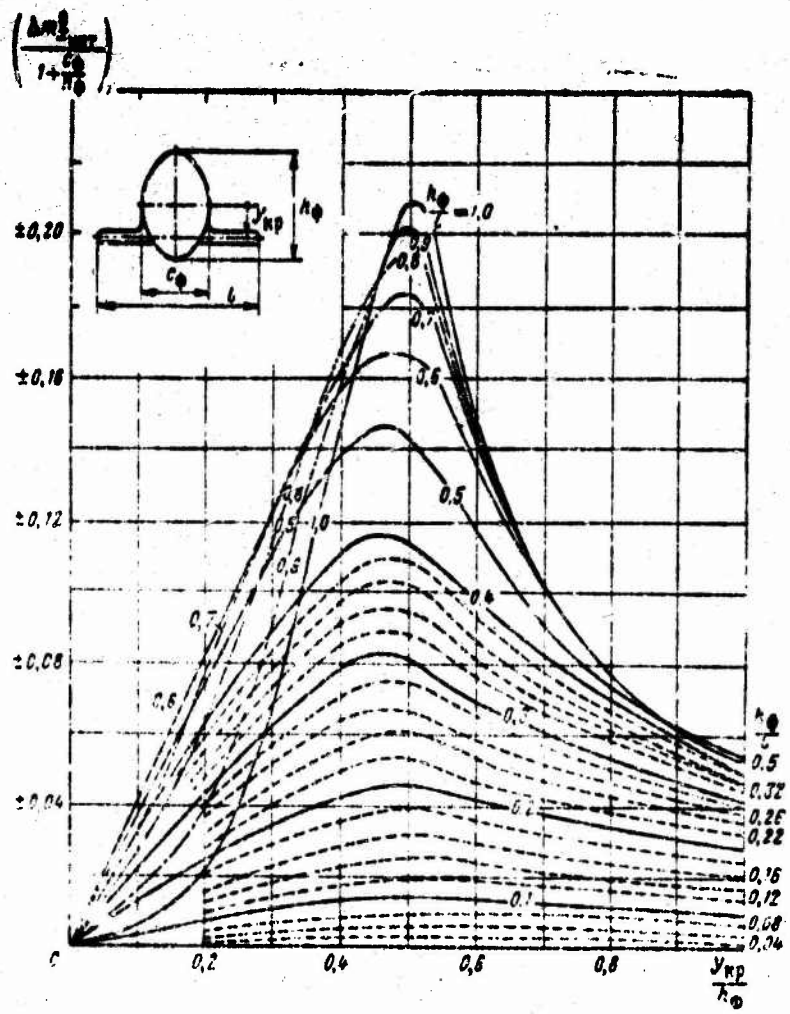

Figure 9.17. Plot of $m_{x_{int}}/[1 + (c_f/h_f)]$ against heightwise position of wing on fuselage y_{wg}/h_f at small $M \leq 0.5$.

The increment to the airplane's lateral stability due to the interference of any wing planform with the fuselage can be determined from the formula

$$\Delta m^{\beta}_{x_{int}} = \left(\frac{\Delta m^{\beta}_{x_{int}}}{1 + \frac{c_\Phi}{h_\Phi}}\right) \left(1 + \frac{c_\Phi}{h_\Phi}\right) K, \qquad (9.23)$$

where c_f and h_f are the width and height of the fuselage, respectively, and β is in radians.

The quantity $(\Delta m^{\beta}_{x_{int}}/[1 + (c_f/h_f)])$ is taken from the diagram in Fig. 9.17. We note that the results are valid for a wing with an aspect ratio of 6. For wings with other aspect ratios, the figure obtained from Fig. 9.17 must be multiplied by a correction factor K_λ. Table 9.5 shows how K_λ depends on wing aspect ratio. We note that for a low-wing monoplane, $(m^{\beta}_{x_{int}}/[1 + (c_f/h_f)])_1$ is taken from Fig. 9.17 with the plus sign, while the minus sign is used for a high-wing monoplane.

We know that use of a vertical tailplane changes the airplane's lateral stability. This is because the total lateral force $Z_{v.t}$ that arises from the vertical tailplane in slip is generally applied at a certain distance from the longitudinal axis of the airplane, thus generating a rolling moment of the aircraft. The vertical-tailplane lateral stability $m^{\beta}_{x_{v.t}}$ can be determined for small M from the formula

$$m^{\beta}_{x_{в.о}} = c^{\beta}_{z_{в.о}} \bar{S}_{в.о} \bar{y}_{в.о} \left[\left(1 - \frac{\partial\sigma}{\partial\beta}\right) K_{в.о}\right]_{ф+кр}, \qquad (9.24)$$

where $c^{\beta}_{z_{v.t}}$ is the derivative of the lateral-thrust coefficient of a vertical tail mounted on the fuselage (in the absence of the wing) with respect to the slip angle β, $\bar{y}_{v.t} = y_{v.t}/l$ is the arm ratio of the vertical-tail lateral force, l is the wingspan, σ is the average crosswash angle at the vertical tailplane, $K_{v.t} = q_{v.t}/q$ is the flow-stagnation coefficient, $[(1 - \partial\sigma/\partial\beta)K_{v.t}]_{f+wg} = K_{f+wg}$ is a coefficient that takes account of the change in the effectiveness of a vertical tailplane mounted on the fuselage due to the influence of the wing, the interference of the wing with the fuselage, and stagnation of the flow by the wing and fuselage.

With the airplane at a given angle of attack, σ is a practically linear function of the slip angle β (for $\beta < 10°$), i.e., it can be assumed that

$$\sigma = \frac{\partial\sigma}{\partial\beta}\beta.$$

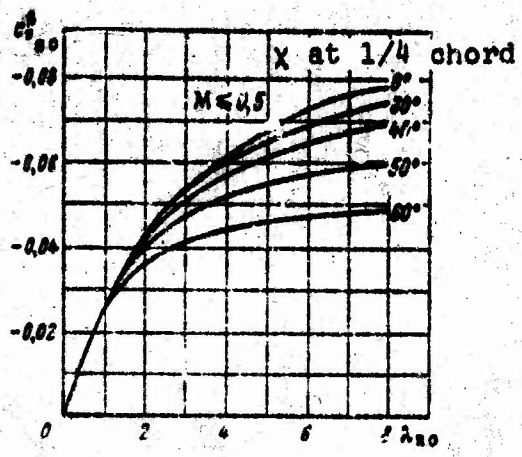

Figure 9.18. Derivative $c^{\beta}_{z_{v.t}}$ of vertical tail as a function of its aspect ratio and 1/4-chord sweep at small $M \leq 0.5$.

At $M \leq 0.5$, the derivative $\partial\sigma/\partial\beta$ depends on angle of attack and the configuration of the airplane. In the preliminary-design stage, the dependence of $\partial\sigma/\partial\beta$ on angle of attack can be disregarded, using its average value in the range $c_y = 0$-0.4. In this case, the derivative $\partial\sigma/\partial\beta$ will depend only on the airplane's configuration, i.e., on how high the wing is placed on the fuselage. As compared with the midwing configuration, a high position of the wing on the fuselage increases the crosswash at the vertical tailplane, thereby lowering its effectiveness. A low position of the wing on the fuselage, on the other hand, reduces the crosswash angle σ at the vertical tail, thereby increasing its effectiveness.

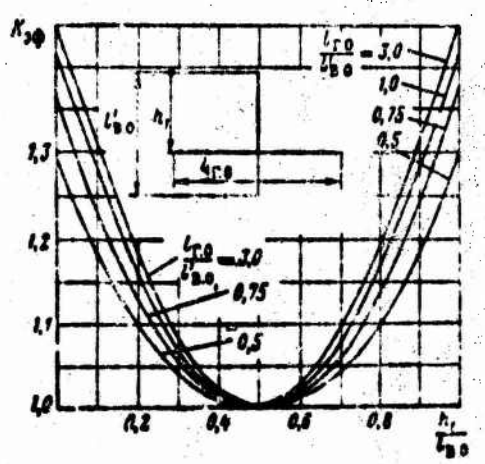

Figure 9.19. Variation of effective aspect ratio coefficient K_{ef} of vertical tailplane due to its interference with the horizontal tail at $M \leq 0.5$.

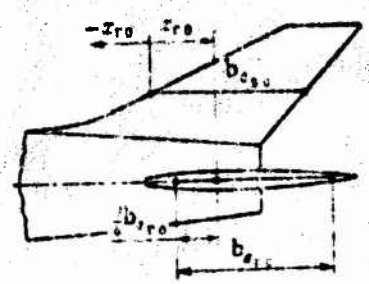

Figure 9.20. Scheme illustrating determination of the coordinate $x_{h.t}$.

The derivative $c^{\beta}_{z_{v.t}}$ referred to the area of the vertical tailplane can be determined from Fig. 9.18, which shows the variation of vertical-tailplane effectiveness $c^{\beta}_{z_{v.t}}$ as a function of the effective aspect ratio $\lambda_{v.t} = (l'_{v.t})^2/S_{v.t}$ for various sweep angles at 1/4 chord. If a horizontal tailplane is mounted on the fin or fuselage, the derivative $c^{\beta}_{z_{v.t}}$ should also be determined from Fig. 9.18 for small M, but for a different vertical-tailplane aspect ratio $\lambda^{*}_{v.t}$:

$$\lambda^{*}_{v.t} = \lambda_{v.t} K_{ef} R, \tag{9.25}$$

where K_{ef} is a coefficient that takes account of the heightwise position of the horizontal tail on the vertical tail. This coefficient can be obtained from the diagrams in Fig. 9.19; R is a coefficient that takes account of the relative positions of the horizontal and vertical tails along the longitudinal axis Ox (Fig. 9.20). Table 9.6 shows how R depends on $x_{h.t}$, i.e., on the distance of 1/4 $b_{a_{h.t}}$ from the leading edge $b_{a_{h.t}}$.

Table 9.6

$\frac{x_{h.t}}{b_{a_{h.t}}} = \bar{x}_{h.t}$	−1,0	−0,5	0	0,5	1,0
R	0,2	0,5	1,0	1,4	1,65

If 1/4 $b_{a_{h.t}}$ is aft of the forward end of the vertical-tailplane mean aerodynamic chord, we have $x_{h.t}/b_{a_{h.t}} > 0$.

The quantity $[(1 - (\partial\sigma/\partial\beta))K_{v.t}]_{f+wg} = K_{f+wg}$ can be determined approximately from the formula

$$K_{\phi+wp} = 0.95 - 0.6\frac{y_{wr}}{b_{\phi}}. \tag{9.26}$$

where y_{wg} is the distance between the plane of the wing chord and the fuselage longitudinal axis. If the wing is above that axis, $y_{wg} > 0$; h_f is the height of the fuselage (or its diameter) at the wing 1/4 b_a level.

We note that determination of the coefficient K_{f+wg} from (9.26) gives reliable results for aircraft configurations in which $d_f/l = 0.1-0.3$ and the coefficient c_y does not exceed 0.4.

The value of the airplane's lateral stability m_x^β with the wing landing flaps down can be determined on the assumption that $m_{x_{wg}}^\beta$ and $m_{x_{v.t}}^\beta$ do not depend directly on flap deflection, but only on c_y. Since lowering of the wing landing flaps changes c_y, this means that it will also affect the airplane's lateral stability m_x^β.

Having determined the airplane's lateral stability for small M, we can then convert it to other M > 0.5 by the formula

$$(m_x^\beta)_M = (m_x^\beta)_{M<0.5} K_{m_x^\beta}, \tag{9.27}$$

where $(m_x^\beta)_{M\leq 0.5}$ is the airplane's lateral stability at $M \leq 0.5$. The procedure for determining it was given above; $K_{m_x^\beta}$ is a correction factor. Table 9.7 shows how it depends on M for conventionally configurated airplanes; these data can also be used in calculating m_x^β for "tailless" designs.

b) Calculation of Airplane's Directional Stability

The directional stability of the airplane can be determined in approximation as a sum consisting of the directional stabilities of the fuselage, fuselage-mounted vertical tailplane, and powerplant, i.e.,

$$m_y^\beta = m_{y_\phi}^\beta + m_{y_{v.t}}^\beta + m_{y_{p.p}}^\beta. \tag{9.28}$$

The fraction of the directional stability created by the fuselage at a given M depends on the shape and dimensions of the fuselage and the overhang of its forward end relative to the airplane's center of gravity. Assuming that the fuselage has

aerodynamic characteristics similar to those of axisymmetric solids of revolution, we can write $m^{\beta}_{y_f} = m^{\beta}_{y_{s.r}}$. For fuselages with shapes closely approaching those of axisymmetric solids of resolution with parabolic nose and tail sections and having slenderness ratios $\lambda_f = 6\text{-}12$, directional stability can be determined from the empirical formula

$$m^{\beta}_{y_\phi} = (c^{\beta}_{z_\phi})_1 \frac{S_{\phi 1}}{S} \frac{L_\phi}{l} \left(\frac{x_{\text{ц.т}}}{L_\phi} - \frac{\bar{x}_{F\phi}}{L_\phi} \right). \tag{9.29}$$

where $(c^{\beta}_{z_f})_1$ is the derivative of the fuselage lateral-force coefficient referred to its lateral-projection area S_{f1}, β is expressed in degrees, L_f is the total fuselage length, $x_{c.g}/L_f$ is the distance from the airplane's center of gravity to the nose of the fuselage, expressed in fractions of its length, $\bar{x}_{F_f}/L_f$ is the distance of the fuselage aerodynamic center from the nose of the fuselage, expressed as a function of its length, $\lambda_f = F_f/d_f$ is the fuselage slenderness ratio, d_f is the midships-section diameter, S is the wing area, and l is the wingspan.

For $M \leq 0.5$, $(c^{\beta}_{z_f})_1$ and $\bar{x}_{F_f} = x_{F_f}/L_f$ can be determined from the formulas

$$(c^{\beta}_{z_\phi})_1 = -0{,}0063 + 0{,}00021\lambda_\phi, \tag{9.30}$$

$$\bar{x}_{F_\phi} = 0.021\lambda_\phi - 0{,}092. \tag{9.31}$$

The fraction of the directional stability due to the vertical tailplane, $m^{\beta}_{y_{v.t}}$, depends on its area, aspect ratio, sweep, and arm, as well as on the relative positioning of the vertical and horizontal tailplanes and the crosswash at the vertical tail.

The quantity $m^{\beta}_{y_{v.t}}$ can be determined from the formula

$$m^{\beta}_{y_{\text{в.о}}} = c^{\beta}_{z_{\text{в.о}}} \bar{S}_{\text{в.о}} \bar{L}_{\text{в.о}} K_{\phi+\text{кр}}, \tag{9.32}$$

where $\bar{L}_{v.t} = L_{v.t}/l$ is the arm of the vertical tail, expressed

as a fraction of wingspan.

The procedure for determining the derivative $c^{\beta}_{z_{v.t}}$ and the coefficient K_{f+wg} was set forth above (see §9.4a).

The influence of the powerplant on the directional stability of a turbojet-engined airplane can be determined approximately from the relation

$$\Delta m^{\beta}_{y_{c.v}} \approx \frac{1}{57.3} c_{P1} \frac{x_{in}}{l},$$

where $c_{P1} = \frac{P}{qS} \frac{1}{\frac{V_c}{V} - 1}$ [see (9.3)], x_{in} is the distance between the air intake and the airplane's center of gravity. For air intakes ahead of the center of gravity, x_{in} is positive; l is the wingspan, and q is the ram pressure.

For M > 0.5 and c_y = 0-0.2, the airplane's directional stability can be determined approximately from the formula

$$m^{\beta}_{y} = (m^{\beta}_{y})_{M \leq 0.5} K_{m^{\beta}_{y}}, \tag{9.33}$$

where $(m^{\beta}_{y})_{M \leq 0.5}$ is the airplane's directional stability at M $\leq$ 055 and $K_{m^{\beta}_{y}}$ is a correction factor that depends on M. The value of this coefficient can be taken from Table 9.7.

c) Determining the Derivative c^{β}_{z} of the Airplane's Lateral-Force Coefficient with Respect to Slip Angle

The derivative of the airplane's lateral-force coefficient with respect to slip angle can be determined approximately as the sum of two derivatives:

$$c^{\beta}_{z} \approx (c^{\beta}_{z_{v.t}})^{*} + c^{\beta}_{z_{fw}}, \tag{9.34}$$

where $(c^{\beta}_{z_{v.t}})^{*}$ is the fraction of the slip-angle derivative of the airplane's lateral-force coefficient that is due to the vertical tailplane. It is referred to the wing area; $c^{\beta}_{z_{fw}}$ is the fraction of the slip-angle derivative of the airplane's lateral force due to

Table 9.7

Variation of Correction Factors with M

M	0,7	0,9	1,0	1,1	1,25	1,5	2,0	2,5	3,0	Notes
$K_{m_x^\beta}$	1	1,07	1,08	1,085	1,09	1,03	0,87	0,77	0,72	for $c_y=0-0,2$
$K_{m_y^\beta}$	1	1,1	1,12	1,13	1,14	1,05	0,68	0,38	0,18	for $c_y=0-0,2$
$K_{c_z^\beta}$	1	1,06	1,1	1,12	1,15	1,12	1,0	0,84	0,74	for $c_y=0-0,2$
$K_{m_x^{\omega_y}}$	1	0,98	0,94	0,89	0,78	0,54	0,3	0,2	0,15	for $c_y=0-0,2$
$K_{c_z^{\delta_H}}$	1	1,05	1,03	0,98	0,82	0,62	0,4	0,25	0,19	for $c_y=0-0,1$
$K_{m_x^{\omega_x}}$	1	1,06	1,10	1,12	1,14	1,0	0,75	0,62	0,54	for $c_y=0-0,4$

the fuselage. It is referred to the area of the airplane's wing.

At $M \leq 0.5$, $(c^\beta_{z_{v.t}})^*$ and $c^\beta_{z_f}$ can be determined from the formulas

$$(c^\beta_{z_{n.o}})^* = c^\beta_{z_{n.o}} \bar{S}_{n.o} K_{\phi+кр}; \tag{9.35}$$

$$c^\beta_{z_\phi} = (c^\beta_{z_\phi})_1 \frac{S_{\phi_1}}{S}. \tag{9.36}$$

The determination of $c^\beta_{z_{v.t}}$, $(c^\beta_{z_f})_1$, and K_{f+wg} was given above.

The airplane's derivative c^β_z can be determined for $M > 0.5$ and $c_y = 0-0.4$ from the expression

$$(c^\beta_z)_M = (c^\beta_z)_{M<0,5} K_{c^\beta_z}. \tag{9.37}$$

Table 9.7 shows the dependence of the correction factor $K_{c^\beta_z}$ on M.

d) <u>Determination of the Airplane's Derivatives</u> $m_x^{\delta_a}$, $c_z^{\delta_r}$, $m_x^{\delta_r}$, $m_y^{\delta_r}$

The approximate effectiveness of conventional ailerons, $m_x^{\delta_a}$ for $M \leq 0.5$ and $c_y \leq 0.4$ can be determined from the formula

$$m_x^{\delta_a} = -2\frac{z_a}{l}(c^{\beta}_{y_{wg}})^{**}\sqrt{\frac{z_a}{b}}\frac{S_1}{S}, \qquad (9.38)$$

where S_1 is the wing area serviced by the aileron. It is determined as indicated in Fig. 9.21. b_a is the aileron mean geometric chord, b is the mean wing geometric chord on the segment serviced by the aileron, z_a is the coordinate of the center of gravity of the wing area S_1 (see Fig. 9.21), and $(c^{\beta}_{y_{wg}})^{**}$ is the derivative characterizing the lifting properties of the wing with consideration of its interference with the fuselage and engine nacelles; its determination was given in §9.2b.

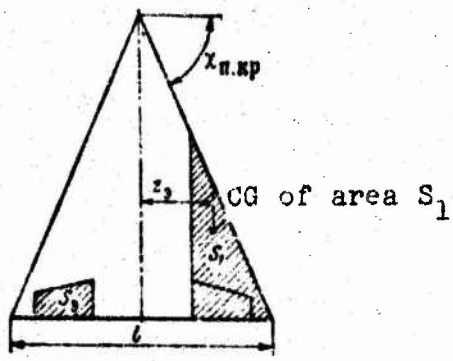

Figure 9.21. Illustrating determination of wing area S_1 serviced by aileron for $M \leq 0.5$.

It follows from formula (9.38) that the effectiveness of the aileron can be varied by varying its geometry: S_1/S, b_a/b, and z_a/l. The effectiveness of the ailerons at $M > 0.5$ can be estimated by the formula

$$(m_x^{\delta_a})_M = (m_x^{\delta_a})_{M\leq 0.5} K_{m_x^{\delta_a}}, \qquad (9.39)$$

where $(m_x^{\delta_a})_{M\leq 0.5}$ is the effectiveness of the ailerons for $M \leq 0.5$, and $K_{m_x^{\delta_a}}$ is a correction factor that depends on M; its values are given in Table 9.7.

The airplane's derivative $c_z^{\delta_r}$ for $M \leq 0.5$ can be determined from the expression

$$c_z^{\delta_r} = (c^{\beta}_{z_{v.t}})^{*}\sqrt{\frac{b_r}{b_{v.t}}} \qquad (9.40)$$

where b_r is the mean geometric chord of the rudder, $b_{v.t}$ is the mean geometric chord of the entire vertical tail, and $(c^{\beta}_{z_{v.t}})^{*}$ is determined in accordance with (9.35). It can be assumed in the preliminary-design stage that for small $M \leq 0.5$, the derivative

$c_z^{\delta_r}$ is independent of the lift coefficient x_y in the range c_y = = 0-0.5.

For M > 0.5, the derivative $c_z^{\delta_r}$ can be determined from the formula

$$(c_z^{\delta_r})_M = (c_z^{\delta_r})_{M \leq 0.5} K_{c_z^{\delta_r}}, \tag{9.41}$$

where $(c_z^{\delta_r})_{M \leq 0.5}$ is the value of the derivative $c_z^{\delta_r}$ at $M \leq 0.5$ and $K_{c_z^{\delta_r}}$ is a correction coefficient that depends on M (see Table 9.7).

Having the airplane's derivative $c_z^{\delta_r}$ for any M and the arm ratios $L_{v.t}/l$ and $y_{v.t}/l$ of the vertical tail, it is easy to determine the derivatives $m_y^{\delta_r}$ and $m_x^{\delta_r}$ from the formulas

$$m_y^{\delta_r} = c_z^{\delta_r} \frac{L_{v.t}}{l}, \tag{9.42}$$

$$m_x^{\delta_r} = c_z^{\delta_r} \frac{y_{v.t}}{l}, \tag{9.43}$$

where $c_z^{\delta_r}$ is the derivative of the lateral-force coefficient with respect to rudder deflection angle, referred to the wing area, $L_{v.t}$ is the distance between the center of gravity and the center of the mean geometric chord of the vertical tailplane, $y_{v.t}$ is the distance from the x axis to the center of pressure of the vertical tail with the rudder deflected, and l is the wingspan.

e) Determining the Rotary Derivative $m_x^{\bar{\omega}_x}$ of the Airplane

The derivative $m_x^{\bar{\omega}_x}$ characterizes the damping properties of the airplane in rotation about the longitudinal axis x. In approximate calculations it is quite admissible to assume that this derivative of the airplane is numerically equal to the sum of the damping coefficients of the wing $m_{x_{wg}}^{\bar{\omega}_x}$, the vertical tailplane $m_{x_{v.t}}^{\bar{\omega}_x}$, and the horizontal tailplane $m_{x_{h.t}}^{\bar{\omega}_x}$, i.e.,

$$m_x^{\bar{\omega}_x} = m_{x_{wg}}^{\bar{\omega}_x} + m_{x_{v.t}}^{\bar{\omega}_x} + m_{x_{h.t}}^{\bar{\omega}_x}. \tag{9.44}$$

Roll damping arises when the wing is rotated about the airplane's longitudinal axis x as a result of redistribution of the normal load over the wingspan. This redistribution takes place owing to the appearance of additional normal velocities ΔV_y that increase from zero at the axis of the airplane to $\omega_x l/2$ at the wing tip. At a given M, the derivative $m_{x_{wg}}^{\bar{\omega}_x}$ depends basically on the aspect ratio, sweep, and taper of the wing. At $M \leq 0.5$ and $c_y = 0$-0.8, the derivative $m_{x_{wg}}^{\bar{\omega}_x}$ can be determined from the diagrams shown in Fig. 9.22. This figure shows the variation of the derivative $m_{x_{wg}}^{\bar{\omega}_x}$ as a function of the aspect ratio λ_{wg} for various 1/4-chord sweep angles and three values of wing taper. These data apply for swept, delta, and straight wings.

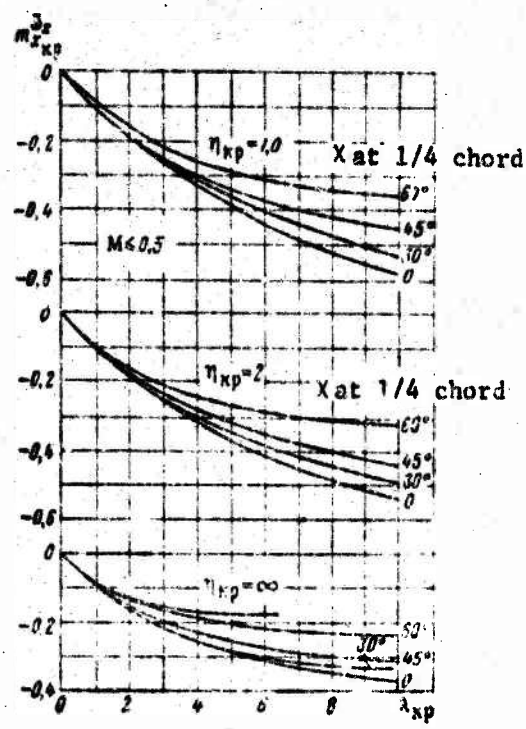

Figure 9.22. Derivatives $m_{x_{wg}}^{\bar{\omega}_x}$ of isolated wings as functions of their aspect ratio λ_{wg} at $M \leq 0.5$.

To determine the roll damping moment of the vertical tailplane, its motion on rotation of the airplane about the longitudinal axis x can be resolved into a translational motion at a rate $V_z = \omega_x y_{v.t}$ ($y_{v.t}$ is the distance from the x axis to the center of pressure of the vertical tailplane) and a rotational motion about the axis passing through the center of pressure of the vertical tailplane parallel to the x axis. At $M \leq 0.5$, the vertical-tailplane center of pressure is then situated near the 1/4 point of the vertical-tailplane mean aerodynamic chord.

The self-damping of the vertical tailplane is it

rotates about an axis passing through the center of pressure can be disregarded, i.e., it can be assumed that the vertical tail has only translational motion at rate $V_z = \omega_x y_{h.t}$. As a result, the averaged value of the slip-angle increment appears over the entire span of the vertical tailplane:

$$\Delta\beta = \frac{\omega_x y_{в.о}}{V} = 2\bar{\omega}_x \bar{y}_{в.о},$$

where

$$\bar{\omega}_x = \omega_x \frac{l}{2V}; \qquad \bar{y}_{в.о} = \frac{y_{в.о}}{l}.$$

The slip-angle increment $\Delta\beta$ causes an increase in the force and moment about the x axis whose coefficient is given by

$$m_{x_{в.о}} = m^{\beta}_{x_{в.о}} \Delta\beta = m^{\beta}_{x_{в.о}} 2\bar{\omega}_x \bar{y}_{в.о}.$$

It follows from this expression that

$$m^{\bar{\omega}_x}_{x_{в.о}} = 2 m^{\beta}_{x_{в.о}} \bar{y}_{в.о}. \tag{9.45}$$

The determination of the derivative $m^{\beta}_{x_{v.t}}$ was given above (see §9.4a).

The following procedure should be used in determining the fraction of the horizontal-tailplane roll damping at small $M \leq 0.5$:

– given the sweep $\chi_{b/4}$, the aspect ratio $\lambda_{h.t}$, the horizontal-tailplane taper $\eta_{h.t}$, and the diagram shown in Fig. 9.22, determine $m^{\bar{\omega}_x}_{x_{wg}}$;

– multiply the value obtained for $m^{\bar{\omega}_x}_{x_{wg}}$ by the coefficient $c = \bar{S}_{h.t} K_{h.t} (l_{h.t}/l)^2$. The result will be $m^{\bar{\omega}_x}_{x_{h.t}}$.

The airplane's derivative $m^{\bar{\omega}_x}_{x}$ for $M > 0.5$ can be determined by the formula

$$(m^{\bar{\omega}_x}_{x})_M = (m^{\bar{\omega}_x}_{x})_{M \leq 0.5} K_{m^{\bar{\omega}_x}_{x}}, \tag{9.46}$$

where $(m_x^{\bar{\omega}_x})_{M \leq 0.5}$ is the roll-damping derivative of the airplane at $M \leq 0.5$ and $K_{\bar{\omega}_x}$ is a correction factor that depends on M.

The values of this coefficient are given in Table 9.7.

f) Influence of Ground-Proximity Effect on Lateral Stability and Controllability Derivatives

The proximity of the ground has a noticeable influence on the lateral stability m_x^β, directional stability m_y^β, and aileron $m_x^{\delta a}$ and rudder $m_y^{\delta r}$ effectiveness.

The influence of the ground at the landing angles of attack on the derivatives m_x^β, m_y^β, $m_x^{\delta a}$, and $m_x^{\delta r}$ depends on the distance to the ground, the wing aspect ratio, wing planform, and the configuration of the airplane. For modern transonic and supersonic aircraft of conventional configuration, the ground effect at landing angles of attack (with the flaps down) results in an increase of m_x^β and a decrease in m_y^β, $m_y^{\delta r}$, and $m_y^{\delta a}$. The increase in the derivative m_x^β near the ground is explained by the unequal effects of the ground on the lift from the left and right sides of the wing at a slip angle.

It has been established that the larger the wing aspect ratio, the greater the amount by which the proximity of the ground increases the derivative m_x^β, and the more sharply does it thereby reduce the derivative $m_x^{\delta a}$. This applies especially to swept-wing aircraft.

For aircraft having swept wings with aspect ratios $\lambda_{wg} \approx 2-3$, the increase in the lateral stability m_x^β near the ground during landing with the flaps down amounts to 8-15%. The smaller figure pertains to aircraft with smaller-aspect-ratio wings and the larger to aircraft with larger-aspect-ratio wings. For these aircraft, the proximity of the ground lowers aileron effectiveness $m_x^{\delta a}$ at the landing attack angles by about 8-16%. The larger figure pertains to large wing aspect ratios. The derivatives m_y^β and $m_y^{\delta r}$ are then lowered by approximately 6-12%.

For delta-winged aircraft with aspect ratios λ_{wg} = 2-3, the proximity of the ground results:

– in an 18-25% decrease in m_y^{β} and $m_y^{\delta r}$ at the landing attack angles;

– in a 6-12% decrease in $m_x^{\delta a}$;

– in a 5-10% increase in the airplane's lateral stability m_x^{β}.

The substantial decrease in the directional stability of the delta-winged aircraft near the ground is evidently caused by the vertical tailplane entering a strongly stagnated flow at large angles of attack near the ground, since the wake zone behind the delta wing is shifted upward by the ground effect.

For airplanes having trapezoidal wings with aspect ratios λ_{wg} = 2-3, the proximity of the ground causes an increase of about 4-8% in the airplane's lateral stability m_x^{β} and an 8-16% decrease in the aileron effectiveness $m_x^{\delta a}$. In this case, there is practically no change in the derivatives m_y and $m_y^{\delta r}$.

We see from the above data that the proximity of the ground makes lateral balancing of the airplane difficult in slip and is detrimental to lateral stability characteristics. This applies in particular to swept- and delta-wing aircraft.

g) Approximate Determination of the Airplane's Axial Moments of Inertia

To determine the dynamic stability and controllability characteristics of the airplane, it is necessary to know its axial moments of inertia I_x, I_y, and I_z.

Table 9.8

Coefficients	K_x	K_y	K_z
Turbojet aircraft weighing up to 20,000 kg	0.10-0.12	0.26	0.18-0.1[illegible]
Turbojet aircraft weighing more than 20,000 kg	0.13-0.15	0.27	0.1[illegible]-[illegible]

The moments of inertia of a conventionally configurated airplane with normally loaded wing about the main central axes can be calculated approximately by the empirical formulas

$$I_{x_0}=\frac{G}{g}(K_x l)^2; \tag{9.47}$$

$$I_{y_0}=\frac{G}{g}\left(K_y \frac{L+l}{2}\right)^2; \tag{9.48}$$

$$I_{z_0}=\frac{G}{g}(K_z L)^2, \tag{9.49}$$

where G is the weight of the airplane in kg, l is the wingspan in meters, L is the length of the airplane in meters, and K_x, K_y, and K_z are coefficients taken from statistical data.

Table 9.8 gives values of these coefficients for aircraft with normal specific wing loads.

The moments of inertia of the airplane about coordinate axes that deviate by an angle ϕ from the main central axes of inertia can be calculated by the formulas

$$I_x=I_{x_0}\cos^2\varphi+I_{y_0}\sin^2\varphi; \tag{9.50}$$

$$I_y=I_{y_0}\cos^2\varphi+I_{x_0}\sin^2\varphi; \tag{9.51}$$

$$I_{xy}=\frac{I_{y_0}-I_{x_0}}{2}\sin 2\varphi. \tag{9.52}$$

§9.5. VERIFYING SELECTION OF VERTICAL-TAIL-PLANE DIMENSIONS, WING DIHEDRAL, AND AILERON DIMENSIONS

In a first approximation, the selection of the dimensions and position of the vertical tail and the wing dihedral can be checked against the parameter $\kappa = \omega_{x_{max}}/\omega_{y_{max}}$, which indicates the ratio of the maximum roll angular rate to the maximum angular rate of yawing motion. The following expression applies for the parameter κ:

$$\kappa=\frac{m_x^{\beta}}{m_y^{\beta}}\frac{I_y}{I_x}\frac{\quad}{\left[\quad-\left(\frac{m_x^{\omega_x}}{I_x}\right)^2\frac{I_y}{m_y^{\beta}}qSl\right.}. \tag{9.53}$$

where m_x^β and m_y^β are the airplane's transverse and directional stabilities, respectively; I_x and I_y are the airplane's moments of inertia about the axes x and y, respectively; $m_x^{\omega_x} = m_x^{\bar{\omega}_x}\frac{l}{2V}$ is the roll damping derivative, q is the ram pressure, S is the wing area, and l is the wingspan.

Practice has shown that airplanes with good lateral stability and controllability characteristics have $\kappa = 0-3.0$. In particular, it is desirable to have $\kappa < 3.0$ for fast maneuverable airplanes and $\kappa \leq 1.0$ for heavy airplanes. The value of κ must be checked for takeoff and landing situations and for flight of the airplane near its ceiling at its speed or Mach-number limit.

It is advisable to check the choice of aileron and rudder parameters for steady slip at an angle $\beta = W_z/V$ (where $W_z = 15$ m/s) during the landing glide and landing of a single-engined airplane. For multiengined airplanes, these parameters must be checked for lateral balancing of the airplane without slip ($\beta = 0$) in two cases:

– failure of one outboard engine during takeoff at $c_y = c_{y_{1/0}}$ Wing flaps not deflected;

– failure of two engines on the same side in the flight situation most characteristic for the particular airplane.

The conditions for lateral balancing of the airplane can be written

$$\left.\begin{aligned} \sum M_y &= 0, \\ \sum M_x &= 0, \\ \sum Z &= 0. \end{aligned}\right\} \qquad (5.54)$$

Here M_y is the projection of the moment onto the y axis, M_x is the projection of the moment onto the x axis, and Z is the projection of the force onto the z axis, or the airplane's lateral force component.

Assuming that the aerodynamic forces and moments are linear functions of the slip angle β and the aileron and rudder deflections, we can write the system of equations (9.54) in expanded form with $\omega_x = \omega_y = 0$:

$$\left.\begin{aligned} &M_y^{\delta_a}\delta_a + M_y^{\beta}\beta + M_y^{\delta_r}\delta_r + M_{y_{en}} = 0;\\ &M_x^{\delta_a}\delta_a + M_x^{\beta}\beta + M_x^{\delta_r}\delta_r + M_{x_G} = 0;\\ &Z^{\delta_a}\delta_a + Z^{\beta}\beta + Z^{\delta_r}\delta_r + G\cos\theta\cdot\sin\gamma = 0, \end{aligned}\right\} \qquad (9.55)$$

where

$$M_y^{\delta_a} = m_y^{\delta_a} qSl;$$
$$M_y^{\beta} = m_y^{\beta} qSl;$$
$$M_y^{\delta_r} = m_y^{\delta_r} qSl;$$
$$M_{y_{en}} = \sum (P_{en} + Q_{en}) z_{en} = m_{y_{en}} qSl;$$

$M_{y_{en}}$ is the sum of the moments about the y axis due to the unbalanced thrust and additional frontal drag of the nonfunctioning engines.

$$m_{y_{en}} = \frac{\sum (P_{en} + Q_{en}) z_{en}}{qSl};$$
$$M_x^{\delta_a} = m_x^{\delta_a} qSl;$$
$$M_x^{\beta} = m_x^{\beta} qSl;$$
$$M_x^{\delta_r} = m_x^{\delta_r} qSl;$$
$$M_{x_G} = \sum G_{rp} z_{rp} = m_{x_G} qSl;$$

M_{x_G} is the total rolling moment due to unbalanced positioning of the loads (with respect to the x axis) under the wing, δ_a and δ_r are the aileron and rudder deflection angles, respectively, β is the slip angle;

$$Z^{\delta_a} = c_z^{\delta_a} qS;$$
$$Z^{\beta} = c_z^{\beta} qS;$$
$$Z^{\delta_r} = c_z^{\delta_r} qS;$$
$$G\cos\theta\sin\gamma \approx qS\sin\gamma.$$

At small roll angles γ, we have $\tan\gamma \approx \gamma$. To obtain the trimming rudder and aileron deflection angles and the roll angle,

it is convenient to write the system of equations of the airplane's lateral steady-state motion in dimensionless form:

$$\left.\begin{aligned} m_y^{\delta_н}\delta_н + m_y^{\delta_э}\delta_э &= -(m_y^{\beta}\beta + m_{y_{зн}}); \\ m_x^{\delta_н}\delta_н + m_x^{\delta_э}\delta_э &= -(m_x^{\beta}\beta + m_{x_Q}); \\ c_z^{\delta_н}\delta_н + c_z^{\delta_э}\delta_э + c_y\gamma &= -c_z^{\beta}\beta. \end{aligned}\right\} \tag{9.56}$$

Assuming in a first approximation that $c_z^{\delta a} = m_y^{\delta a} = 0$, we obtain the following expressions for the rudder and aileron deflections and the roll angle that are required to balance the airplane:

$$\delta_{н_{бал}} = -\frac{m_y^{\beta}}{m_y^{\delta_н}}\beta - \frac{m_{y_{зн}}}{m_y^{\delta_н}}; \tag{9.57}$$

$$\delta_{э_{бал}} = -\left(\frac{m_x^{\beta}}{m_x^{\delta_э}} - \frac{m_x^{\delta_н} m_y^{\beta}}{m_x^{\delta_э} m_y^{\delta_н}}\right)\beta + \frac{m_x^{\delta_н} m_{y_{зн}}}{m_x^{\delta_э} m_y^{\delta_н}} - \frac{m_{xQ}}{m_x^{\delta_э}}; \tag{9.58}$$

$$\gamma = -\left(\frac{c_z^{\beta}}{c_y} - \frac{c_z^{\delta_н} m_y^{\beta}}{c_y m_y^{\delta_н}}\right)\beta + \frac{c_z^{\delta_н} m_{y_{зн}}}{c_y m_y^{\delta_н}}, \tag{9.59}$$

where γ is in radians.

It is clear from these expressions that the balancing values of the control-surface deflections and the roll angle consist of two parts:

<u>the first part</u> is composed of the control-surface deflections and roll angle necessary to balance the airplane in steady slip at a constant slip angle β in the absence of moments produced by unbalanced engine thrust and stores that are not symmetrically arranged with respect to the x axis;

<u>the second part</u> is composed of the control-surface deflections and roll angle needed to fly the aircraft without slip ($\beta = 0$) when the airplane is being acted upon by moments due to unbalanced engine thrust and wing stores that are positioned asymmetrically relative to the x axis.

The aileron and rudder deflection angles determined from (9.58) and (9.57) should be 3°-5° smaller than their maximum

deflection angles. If it is found in the checking process that the aileron and rudder deflection angles needed to balance the airplane are larger than the permissible values, it will be necessary to change the control-surface parameters to values that satisfy the stated requirement.

If this measure does not produce the desired result, it will also be necessary to adjust the parameters of the vertical tail and the wing dihedral.

We note that it is advisable to reduce the balancing deflection $\delta_{r_{bal}}$ of the rudder by increasing its effectiveness $m_y^{\delta_r}$. It is best to reduce the balancing deflection $\delta_{a_{bal}}$ of the ailerons by increasing their effectiveness $m_x^{\delta_a}$ and by reducing the airplane's lateral stability m_x^{β}. §9.4 discusses these parameters as functions of the vertical-tail and aileron parameters and the wing dihedral.

Footnote

Page No.	
206	(1) This distance is measured from the free streamline passing through the trailing edge of the wing.

Part III

DETERMINATION OF THE BASIC WEIGHT, GEOMETRICAL, AND STRUCTURAL CHARACTERISTICS OF THE NEW AIRCRAFT DESIGN

Chapter 10

SELECTION OF THE AIRPLANE'S CONFIGURATION

§10.1. CONFIGURATION AS AFFECTED BY THE INTENDED USE OF THE AIRPLANE

The external configuration of an airplane is characterized by the shapes of its airframe components and their relative positions and by the type, number, and placement of the engines, as well as their air intakes.

The intended use of an airplane influences its configuration both directly and through the required flight-technical and takeoff/landing properties.

The direct influence of the airplane's purpose on specific features of its configuration can be traced in the decision as to the number of engines to be used on a passenger aircraft. One of the basic requirements made of the passenger airplane is safety, and this is provided, among other measures, by making the airplane capable of taking off and flying after failure of one or more engines.

Since flight accidents caused by in-flight engine failure involve forced landings, the probability of a forced landing due to engine failure may be considered instead of the accident probability. If the airplane has z engines, the probability that one

of them will fail is greater the larger the number z, and for small p, this probability equals z · p with sufficient accuracy, where p is the probability of engine failure. If the total thrust of the engines is such that failure of one of them does not leave enough thrust to continue flight, the probability z · p of failure of one of the z engines will also be the forced-landing probability.

If, on the other hand, the remaining thrust is sufficient to sustain flight, flight may be continued. Then the probability of failure of one of the remaining (z - 1) engines equals (z - 1)p. The probability of the first and second engines on the same flight equals the product of the failure probabilities of the two, i.e.,

$$z \cdot p(z-1)p = z(z-1)p^2.$$

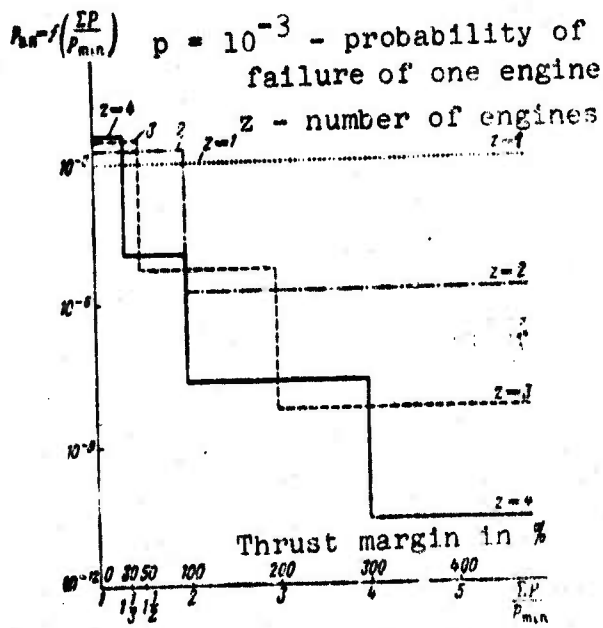

Figure 10.1. Influence of thrust margin and number of engines on forced-landing probability.

This probability becomes the forced-landing probability if the thrust remaining after failure of the second engine is not

enough for continuation of flight. Thus, given enough total thrust in a multiengined airplane, it becomes possible to continue flight after failure of the first, second, etc. engine. This is accompanied by a stepwise decrease in the forced-landing probability until one engine remains in operation, at which point we obtain the minimal forced-landing probability.

Figure 10.1 shows the forced-landing probability in the event of engine failures as a function of the total thrust of all engines for z = 1, 2, 3, and 4 engines. The probability is plotted logarithmically, with $p = 10^{-3}$ taken as the probability of engine failure. The total thrust is given in relative form $\bar{P} = \Sigma P/P_{min}$, where P_{min} is the minimum thrust required to continue flight. We see from the diagram that when the total thrust is small, an increase in the number of engines increases the forced-landing probability.

For a single-engined airplane, the forced-landing probability equals the probability p of engine failure and remains at this value regardless of thrust. For a twin-engined airplane, there is one step on the forced-landing probability decrease curve at $\bar{P} = 2$ (thrust margin 100%); for a three-engined airplane, there are two such steps, and three for a four-engined airplane. The larger the number of engines, the greater the degree of safety that can be attained, provided that there is a sufficiently large increase in the thrust margin.

Thus, the optimum number of engines for a passenger airplane from the standpoint of maximum flight safety in the event of engine failure is determined by the thrust excess required of the airplane as compared with the minimum thrust required for flight. In the event of engine failure during the takeoff run at a speed below V_{trim}, safety is ensured by aborting the takeoff and stopping the airplane before the end of the runway; in the event of engine failure at a speed above V_{trim}, the takeoff is completed and the question of safety and the number of engines is resolved on the basis of the diagram (see Fig. 10.1), but P_{min} is

determined on the basis of the thrust excess that ensures an "engine-out takeoff" on the particular runway and not on the basis of level flight at zero altitude.

It should be noted that making a passenger airplane safer by increasing the number of engines and their relative thrust as compared to the minimum requirement results in heavier powerplants.

In addition to the specific requirements as to the airplane's configuration that proceed from its purpose, it must also satisfy general requirements that are mandatory for airplanes of its particular purpose. Such requirements are drawn up, for example, by the State Scientific Research Institute of Civil Aeronautics for Soviet civil aircraft.

Our passenger airplanes must now also conform to ICAO (International Civil Aeronautical Organization) requirements.

There are also general requirements for other types of aircraft.

§10.2. INFLUENCE OF REQUIRED SPEED ON CONFIGURATION, ENGINE TYPE, AND ENGINE LOCATION

The basic property that has the strongest influence on selection of the airplane's configuration is its speed. The changes in aircraft layout that took place during the development of aviation were at all times prompted by the desire to obtain increased speeds. At the same time, the configuration had to guarantee the necessary stability and controllability characteristics in the airplane.

The braced biplane has major advantages when speed requirements are minimal and emphasis is placed on load capacity, takeoff and landing properties, light weight, small dimensions, and low cost. In this biplane, the additional drag of the ribbon bracing is accepted as the price of the great weight reduction resulting from the fact that the entire height of the biplane cell becomes the base that takes the cell bending forces.

This has been confirmed in practical work with such aircraft as the U-2 (PO-2) designed by N.N. Polikarpov and the An-2 of designer O.K. Antonov. Wheel fairings are mandatory for a modern biplane.

As speed requirements were raised, the biplane yielded to the monoplane. The flight speed at which the biplane loses its advantages can be stated only in a given particular case after comparing the cost figures for the same job done by the biplane and the monoplane. The semicantilever monoplane may be found superior in a comparatively narrow range of required speeds. In this case, the high-wing type will be best, since the struts work in tension during flight, the upper surface of the wing is free of superstructures, and the downward visibility is good. As in the case of the biplane, the rectangular wing is found to be simpler and cheaper for the semicantilever monoplane, and much weight is saved by virtue of the same lengthening of the base that takes the half-wing bending load; this can be regarded as a principle in which lift is transferred from the wing half to the fuselage by the shortest possible route (the strut). Nonretractable landing gear with wheel fairings is preferred to save useful space in the fuselage.

The thick-profile cantilever monoplane will be advantageous with a further increase in the required flight speed. Specific calculations are again performed to establish the preference of this configuration in accordance with the required speed. In specifying the profile thickness ratio, it is necessary to resolve a contradiction between the desire to reduce wing weight and increase its rigidity on the one hand, and, on the other, to reduce its induced and profile drag. The first two conditions dictate a small span-to-maximum-thickness ratio for the wing, a quantity expressed as follows in terms of the wing's parameters:

$$\frac{l}{f_{max}} = \frac{l}{c}\,\frac{\eta_c + 1}{2\eta_c} = \frac{\lambda}{\bar{c}}\,\frac{\eta_c + 1}{2\eta_c},$$

where

$$\eta_c = \frac{c_{max}}{c_{min}}, \text{ and } \bar{c} = \frac{S_{mid}}{S}.$$

This makes it clear that to reduce wing weight, it is necessary to reduce λ and increase $\bar{c}$, but reducing λ and increasing $\bar{c} = S_{mid}/S$ increases both wing-drag components. In first approximation, the problem is resolved by taking $l/c = \lambda/\bar{c}$ from statistical data on good airplanes of the same type, and then more precisely to minimize the aviation weight of the wing at a given flight speed; the general method of optimum-parameter selection might also be used.

The demand for higher flight speeds influences the airplane's configuration especially strongly with the approach to the speed of sound. First, the compressibility of the air begins to make itself felt, and when local velocities become supersonic, compression shocks appear, primarily on the wing, so that wave drag must be dealt with. Thinner and M-stable profiles and small aspect ratio swept wings are used to reduce wave drag. If shocks appear and develop primarily on the thickest profile and the fuselage effect promotes their development, it is advantageous to use the so-called "crescent wing," which has a larger sweep angle at the root and a smaller one toward the tips. To simplify the design of extension flaps and increase their effectiveness on the swept wing, it is helpful to reduce the sweep of the trailing edge at the root, offsetting this with a larger sweep angle at the root of the leading edge (a leading-edge "buildup"). All of these measures, which shift the wave-drag point to higher speeds (with the exception of the reduced aspect ratio), make the wing more complicated and heavier. Measures that shift the appearance of wave drag to larger Mach numbers also lower the maximum wave drag at the transition to the speed of sound.

Thus, to break the sound barrier it is necessary to use a wing with even smaller profile thickness ratio and aspect ratio and stronger sweepback.

These requirements are met by the delta wing or similar wings with short tip chords and wings with increased sweep at the root of the leading edge. Such wings are lighter, have larger internal capacities, and make flap design easier. The designer is guided by the same configurations in specifying the shapes of the horizontal and vertical tails.

The fuselage and canopy are made as slender as possible to reduce wave drag. Observance of the "area rule" helps reduce wave drag in the region of the speed of sound. This rule states that the curve of the over-all cross-sectional areas perpendicular to the airplane's longitudinal axis must be as smooth as possible. It implies that hollows and bumps on this curve must be smoothed out by moving various components of the airplane along this axis and slimming down and filling in the corresponding cross sections.

Configuration requirements and wing-fuselage interference influence the heightwise placement of the wing on the fuselage.

A low wing reduces structural weight and simplifies retraction of the landing gear into the wing, but it also increases parasite interference. The midwing position produces less interference between the wing and a round-section fuselage, but clutters the interior space of the fuselage.

The high wing gives little interference but complicates retraction of the landing gear into the wing.

Here it must be remembered that the undesirable interference of the low wing can be corrected by shaping the fuselage cross section and providing wing fillets.

As concerns the relative positions of the wing and the horizontal tailplane, the prevalent configuration will be the conventional one with the tailplane aft of the wing as long as the airplane's speed does not exceed that of sound. Such long-known configurations as the "flying wing," the "tailless" airplane, and the "canard" have been built and flown many times, but they were found inferior to aircraft with the normal tail design and have

not come into extensive use.

The main reason for failure of the "canard" to gain acceptance is that it is not as safe in flight owing to the "sticking" that occurs when the attack angle is increased to critical. The influence of stability and controllability requirements on the relative positions of the wing and stabilizer was discussed in detail in Chapter 8.

Flight speed influences not only selection of layout, but also selection of engine type. Since the development of the aviation engine paralleled the development of configurations basically under the pressure for increased speeds, it is natural that there is a relation between the speed of the airplane and the type of engine. At low subsonic speeds, $0 < M < \sim 0.6$, the air-cooled piston engine is the optimum, while the propjet becomes more advantageous at higher speeds ($\sim 0.6 \leq M < \sim 0.8$). At trans- and supersonic speeds, $0.8 < M < \sim 3$, various types of turbojet engines are used.

In turn, the type and number of the engines influence the configuration of the airplane. Engines may be placed in the fuselage, on the fuselage, or on the wing.

Placing the engines in the fuselage reduces the drag on the airplane, but it also complicates the structure of the fuselage and makes it heavier. If there are an odd number of engines, one of them must be placed in or on the fuselage; the best place for a propeller engine is the nose of the fuselage, but this is inevitably detrimental to the pilot's forward vision. For turbojet engines, the optimum placement is the tail section of the fuselage because of the short exhaust-gas path that this gives. As for the air intake, it can be either frontal or lateral. With the intake in the nose of the fuselage, the air passage must be split to accommodate the retracted nose wheel and the cockpit.

This explains the advantage of having an even rather than an odd number of engines. In the case of propeller engines, the

nose of the fuselage is left free and the pilot can see better; with turbojets, the tail of the fuselage is unburdened and in both cases the fire hazard is reduced and the nose level is lowered for passengers. An even number of propeller engines is best placed on the wing in such a way that the propwash increases lift at takeoff. An even number of jets can be placed either on the wing or on the fuselage tail section. Placing the engines on the wing gives a distinct weight advantage over the tail mounts on the fuselage, because wing weight is lowered by engine "unloading" of the wing and fuselage weight is increased by the additional load imposed by the engines.

Landing gear can be retracted into the engine nacelles without greatly increasing their midships area.

When the engines are mounted on the wings, it is necessary to consider reciprocal effects between the nacelles and the wings. This makes it desirable to place the nacelle under the wing, as can be done when the wing is high.

When the airplane has a high wing, retraction of the gear into the wing or engine nacelles is not advisable; it is better to retract it into the fuselage, with track increased by rigging the supporting arms out on the sides of the fuselage and covering them with fairings, as was done in the An-14 airplane of designer O.K. Antonov.

Combining turbojet engines with the wing may be advantageous whether the engines are placed under the wing (on pylons or without pylons) or behind the wing. To reduce parasite interference and improve observance of the area rule when the engines are suspended on pylons, it is necessary to move them as far forward as possible; when pylons are not used, they must be moved forward or aft so that the maximum thicknesses of the profile and the engine nacelles will not coincide.

Placing the engines behind the wing spars lowers drag appreciably. In this case, the air-intake passage must be run

through the spars, and this increases their weight. The passage is run under the wing if the latter's profile is thin. In placing turbojets on the span of the wing, they can be placed close to one another and to the fuselage. The possibility of placing turbojet engines close to the fuselage makes it possible to reduce the moment that causes the airplane to yaw on failure of an engine on one side. It also becomes possible to hang a pair of engines on a single underwing pylon or mount a whole "package" of engines flush under the wing. Turbojet engines can also be mounted on the tail section of the fuselage on horizontal pylons. This sets up a favorable interference with the fuselage, reduces the fire hazard, and lowers the noise level in the passenger cabin.

Turbojets mounted on the fuselage tail section must not blanket the horizontal tailplane at large attack angles. If there are an odd number of engines, one of them can be placed in the root section of the vertical fin or in the tail section of the fuselage. In addition to the weight penalty, placing a heavy engine on the tail section of the fuselage makes it difficult to trim the airplane, so that it is necessary to lengthen the nose section and accept the associated deterioration of longitudinal and directional stability.

§10.3. INFLUENCE OF TAKEOFF AND LANDING REQUIREMENTS ON CONFIGURATION

The configuration selected for the airplane on the basis of the required flight speed is often inconsistent with good takeoff and landing characteristics.

In specifying the configuration for the airplane, therefore, it is also necessary to take takeoff and landing properties into consideration.

Three basic trends are now emerging in the aircraft industry in regard to selection of configuration with allowance for takeoff and landing behavior:

1. Use of the conventional airplane configuration with the

relative geometrical parameters selected to ensure the required flight speed and takeoff/landing characteristics, with use of efficient high-lift devices on the wing.

2. Varying the geometry of the airplane in flight, e.g., using a wing with sweep angle variable in flight.

3. Use of the engines (sustainer or special) to develop lift.

Chapter 11

DETERMINING THE AIRPLANE'S WEIGHT AND BASIC DIMENSIONS

§11.1. THE METHOD OF RELATIVE WEIGHTS

This method is of great importance in preliminary aircraft design. It enables us, without imposing additional requirements, to determine the takeoff weight and dimensions of the airplane quite quickly and accurately, to establish whether all items of the Technical Specifications are realistic, and to analyze the influence of various factors on takeoff weight and, consequently, on the cost of the airplane and the technical-economic criteria used as a basis for determining the optimum version of the design.

This method consists essentially in the following.

The takeoff weight G is broken up into four groups of weights:

1) $G_{p.l}$, the weight of the payload, which consists of the weights of the crew, equipment, armament, and cargo;

2) G_s, the structural weight;

3) $G_{p.p}$, the weight of the powerplant;

4) $G_{f.s}$, the weight of the fuel and fuel system.

The weight-balance equation is obtained in the form

$$G = G_{пл} + G_{к} + G_{дв} + G_{т.с}.$$

The same equation written in fractions of takeoff weight will be

$$1=\bar{G}_{p.n}+\bar{G}_{s}+\bar{G}_{n.y}+\bar{G}_{p.l} \tag{11.1}$$

This equation might be called the "equation of interreaction of the properties of the airplane," because, as we shall see below, it links the flight properties of the airplane with one another, with the payload, and with other properties and parameters of the airplane and its engine.

The weight $G_{p.l}$ (in kilograms) depends on the purpose of the airplane; it can be established at the very start of the design work and assumed constant for a given class of airplanes:

$$G_{p.l} = \text{const.}$$

The relative structural weight $\bar{G}_s$ depends on the design overloads, configuration, dimensions, etc. In first approximation, it can be assumed constant ($\bar{G}_s$ = const) and taken from statistical data for aircraft of the same purpose and similar configuration. Working formulas are used for more accurate determinations.

The relative weight of the powerplant is determined from the formulas:

for propjet engines

$$\bar{G}_{n.y}=(1+K_a)\frac{N_{en}N}{G}, \tag{11.2}$$

for turbojet engines

$$\bar{G}_{n.y}=(1+K_a)\frac{N_{en}P}{G}, \tag{11.3}$$

where $K_a = G_a/G_{en}$ is the relative weight of powerplant accessories expressed as a function of engine weight. The power/weight ratio N/G of a propjet airplane and the thrust/weight ratio P/G of a turbojet airplane are determined in accordance with flight data, i.e., on the basis of top speed and flight altitude, ceiling, rate of climb, or takeoff distance.

The largest value of $\bar{G}_{p.p}$ from among those determined for each flight property is to be substituted into (11.1). The

requirements for the rest of the properties will then be more than satisfied. The weight of the fuel system is determined from the formula

$$\bar{G}_{т.с}=(1+K_c)\bar{G}_т, \qquad (11.4)$$

where $K_{sy} = G_{sy}/G_f$ is the relative weight of the fuel-system machinery and tanks expressed as a fraction of fuel weight and the relative weight of the fuel $\bar{G}_f = G_f/G$ is determined from the desired flight range or endurance. To this end, it is necessary to know the engine's fuel-consumption curve and the aerodynamic characteristics of the airplane.

If the relative weights $\bar{G}_s$, $\bar{G}_{p.p}$, and $\bar{G}_{f.s}$ are known, the relative payload weight can be determined from (11.1):

$$\bar{G}_{п.н}=1-(\bar{G}_к+\bar{G}_{і.у}+\bar{G}_{т.с}).$$

Knowing the absolute and relative payload weights, we can determine the takeoff weight:

$$G=\frac{G_{п.н}}{\bar{G}_{п.н}}=\frac{G_{п.н}}{1-(\bar{G}_к+\bar{G}_{і.у}+\bar{G}_{т.с})}. \qquad (11.5)$$

Equation (11.5) clearly shows that the higher the strength and flight-performance requirements, i.e., the larger $\bar{G}_s$, $\bar{G}_{p.p}$, and $\bar{G}_{f.s}$, the smaller is the fraction remaining for $\bar{G}_{p.l}$ and the larger the airplane's takeoff weight.

A near-zero remainder from the unity, and the more so a negative remainder, indicates that the design is unrealistic because the flight-performance requirements are too high.

Thus, the equation interrelating the properties of the airplane enables us to determine the feasibility of meeting the set of property requirements and to determine (or approximate) the optimum combination of these requirements on the basis of minimum takeoff weight.

We see from (11.5) that a relative error in the determination of the payload $G_{p.l}$ results in an identical relative error in the

takeoff-weight determination, but the absolute error in the latter will be larger by a factor $1/\bar{G}_{p.1}$ than the absolute error in $\bar{G}_{p.1}$; consequently, the payload must be determined as accurately as possible the first time to avoid the need to recompute it repeatedly.

§11.2. DETERMINATION OF PAYLOAD

The payload consists of the crew, equipment, and cargo. Proceeding from the intended use of the airplane, it is necessary to determine the composition and weight of the crew, draw up a detailed list of equipment, and calculate its weight, including fasteners, wiring, and plumbing. The special cargo of a military aircraft consists of armament, launchers, ammunition, and special equipment. For a cargo aircraft, the maximum cargo weight can be determined as the weight of a single heaviest transportable object or even the weight of several such objects. The maximum cargo dimensions determine the dimensions of the cargo bay.

The situation becomes more complex when the payload of a passenger airplane is to be determined. This is because a given traffic load on a given line can be handled during a given period by a small number of hauls by larger airplanes or a larger number of hauls by small airplanes. In the former case, the intervals between hauls may be longer, which is inconvenient for passengers, but in the latter the airport may be overloaded and the cost of compensating the crews may rise. For how many passengers should the airplane be designed?

The optimum payload can be determined from the minimum value of a general criterion. A tentative answer can be obtained from such considerations.

In the finished airplane, the maximum sum of payload and fuel weights is determined by takeoff conditions and strength, and can be assumed constant:

$$G_{пл}+G_{т}=\text{const.} \tag{11.6}$$

The optimum range L will be that at which the payable "work" $G_{p.l}L$ done by the airplane is maximized. Since L is approximately proportional to G_f, we can write in approximation that

$$G_{пл}G_{т}=\max. \tag{11.7}$$

corresponds to the condition $(G_{p.l}L)_{max}$.

It follows from (11.6) and (11.7) that the airplane will be optimal if

$$G_{пл}=G_{т}.$$

The new aircraft design will be near-optimum if

$$G_{пл}=G_{т.р},$$

where $G_{f.c}$ is the weight of the fuel consumed.

Since the weight $G_{p.e}$ of the passenger equipment stands in about the same relation to the payload weight as the weight of the navigational fuel reserve and the weight of the dry fuel system have to the weight of the fuel consumed (~25-30%), the last equation can be replaced by

$$G_{пл}+G_{п.э}=G_{т.с},$$

where $G_{f.s}$ is the weight of the fuel system with a full fuel load G_f, as determined from the technical range L_t. In this case, takeoff weight is determined as follows:

$$G=\frac{G_{э.п}}{1-(\bar{G}_{к}+\bar{G}_{п.у}+2\bar{G}_{г.с})}, \tag{11.8}$$

where $G_{c.e}$ is the weight of the crew and equipment (without the passenger equipment).

§11.3. DETERMINATION OF RELATIVE STRUCTURAL WEIGHT

The structural weight is composed of the weights of the wing, fuselage, landing gear, and control systems. Weight formulas must be used to determine the weights of these parts of the airplane with satisfactory accuracy as functions of their parameters.

a) Theoretical Formula for the Weight of a Trapezoidal Wing with Empirical Coefficients [21]

The weight G_{wg} of the wing consists of the weight of the spar flanges (or the carry-through structure in general) $G_{s.f}$, the weight of the spar webs $G_{s.w}$, the weight of the rib flanges $G_{r.f}$, the weight of the rib webs $G_{r.w}$, the weight of the skin on the leading and trailing parts of the wing G_{sk}, and the weight of the ailerons and flaps $G_{a.f}$:

$$G_{кр}=G_{п.л}+G_{с.л}+G_{п.пер}+G_{ст.пер}+G_{об}+G_{а.м}. \tag{11.9}$$

The weight of the spar flanges is [12]:

$$G_{п.л}=\frac{C_{п.л}n_A G\gamma}{12\cdot 1000\sigma f\varphi\cos^2\chi}\,\frac{\lambda}{\bar{c}}\,lK_{п.л}. \tag{11.10}$$

Here $C_{s.f}$ is an empirical coefficient, n_A is the computed ultimate overload for case A, G is the takeoff weight of the airplane in kg, γ is the specific gravity of the material in g/cm^3, f = = 0.82 is the ratio of the average stress in the flange to the maximum stress in the same cross section, ϕ is the ratio of the arm of the force couple acting on the upper and lower flanges (panels) to the wing profile thickness, σ is the stress at an intact point on the flange at the moment of failure, i.e., without consideration of stress concentration in the weakened cross section, in kgf/cm^2, χ is the sweep angle of the wing on the line of maximum profile thickness, λ is the wing aspect ratio, $\bar{c}$ is the wing mean profile thickness ratio, and l is the wingspan in meters. The numeral 1000 takes account of the dimensions indicated above for the quantities G, γ, σ, and l.

The coefficient $K_{s.f}$ allows for the lighter weight of the spar flanges in the trapezoidal wing due to unloading as compared with the flange weight in the rectangular wing with spanwise-constant thickness and load per unit length and without consideration of unloading. It is determined from the formula

$$K_{п.л}=k_1k_{1г}-k_{1кр}\bar{G}_{кр}-k_{1т}\bar{G}_{т}-k_{1гр}\bar{G}_{гр}. \tag{11.11}$$

Here the coefficient k_1 depends on the wing tapers $\eta_b = b_{max}/b_{min}$

in plan and $\eta_c = c_{max}/c_{min}$ midships, and expresses the decrease in the flange weight of the unrelieved trapezoidal wing as compared with the constant-profile rectangular wing; $k_{1\Gamma}$ is a correction factor that reflects the influence of the spanwise distribution of the circulation Γ as compared with the distribution according to the law of chords.

The remaining coefficients express the influence of unloading due to the weight G_{wg} of the wing itself, the weight G_f of the fuel, which is distributed over the entire span of the wing, and the weight of concentrated loads G_{1d}. These concentrated loads may be engine nacelles with engines, landing-gear housings with landing gear, tanks with fuel if they occupy a small fraction of the span, etc.

These coefficients are determined from the following formulas:

$$k_1 = \frac{(\eta_c+1)[3(\eta_c-1)-(\eta_n-1)]}{(\eta_n+1)(\eta_c-1)^2}\left[\frac{(\eta_n-1)(\eta_c-1)}{3(\eta_c-1)-(\eta_n-1)}\,\frac{1}{3}+\right.$$

$$\left.+\frac{1}{2}-\frac{1}{\eta_c-1}+\frac{1}{(\eta_c-1)^2}\ln\eta_c\right]; \qquad (11.12)$$

$$k_{1\Gamma} = 1{,}04-0{,}02(4-\eta_v)^2, \qquad (11.13)$$

when $\eta_v \geq 4$, $k_{1\Gamma} = 1.04$; k_{1wg} is determined from (11.12), where η_b is replaced by $\eta_G = \infty$ or $\eta_G = \eta_b\eta_c$; k_{1f} can also be determined from (11.12), where η_b is replaced by

$$\eta_\tau = \frac{(b_t c_t)_{max}}{(b_t c_t)_{min}},$$

where $(b_t c_t)_{max}$ and $(b_t c_t)_{min}$ are the cross-sectional areas of the fuel tanks at the root and tip of the wing;

$$k_{1rp} = 3\frac{\eta_c+1}{(\eta_c-1)^2}\left\{\bar{e}(\eta_c-1)-[1+(\eta_c-1)\times\right.$$

$$\left.\times(1-\bar{e})]\ln\frac{\eta_c}{1+(\eta_c-1)(1-\bar{e})}\right\}, \qquad (11.14)$$

where $\bar{e} = e/(l/2)$ and e is the arm of the load measured from the airplane's plane of symmetry.

For $\eta_c = 1$, $k_{1ld} = 3\bar{e}^2$.

We calculate the weight of the spar webs from the formula

$$G_{ст.л} = \frac{c_{ст.л} n_A G \gamma l}{4 \cdot 1000 \tau \cos \gamma} K_{ст.л}, \qquad (11.15)$$

where $c_{s.w}$ is an empirical coefficient, G is taken in kg, γ in g/cm^3, and τ in kgf/mm^2.

Here the coefficient $K_{s.w}$ takes account of the decrease in web weight in the trapezoidal wing due to unloading as compared with web weight in a rectangular wing with spanwise constant thickness and load per unit length.

It is determined from the formula

$$K_{ст.л} = k_3 k_{3г} - k_{3кр} \bar{G}_{кр} - k_{3г} \bar{G}_г - k_{3гр} \bar{G}_{гр} - \frac{c}{\cos \chi} K_{п.л}. \qquad (11.16)$$

Here the coefficients k_3, $k_{3г}$, k_{3wg}, k_{3f}, and k_{3ld} are analogous to the coefficients k_1, $k_{1г}$, k_{1wg}, k_{1f}, and k_{1ld}. The term $(c/\cos \chi)K_{s.f}$ takes account of the unloading of the webs by forces acting along the spar flanges.

$$k_3 = \frac{2}{3} \frac{\eta_b + 2}{\eta_b + 1}, \qquad (11.17)$$

$$k_{3г} = 1.03 - 0.013(4 - \eta_b)^2. \qquad (11.18)$$

If $\eta_b \geq 4$, we have $k_{3г} = 1.03$.

k_{3wg} is determined from (11.17) after replacing η_b by $\eta_G = \infty$ or $\eta_G = \eta_b \eta_c$; k_{3f} is determined from (11.17), taking instead of η_b

$$\eta_\tau = \frac{(\sigma_б \cdot c_б)_{max}}{(\sigma_б \cdot c_б)_{min}};$$

$$k_{3гр} = 2\bar{e};$$

$$C = \frac{2}{3\varphi} \frac{\eta_c + 1}{\eta_c + 1}, \qquad (11.19)$$

$K_{s.f}$ is determined from (11.11). The weight of the rib flanges:

$$G_{п.пер} = c_{п.пер} \frac{n_A G}{1000} \frac{\gamma}{\tau} \frac{1}{\cos \chi} l. \qquad (11.20)$$

The weight of the rib webs:

$$G_{\text{ст.пер}} = c_{\text{ст.пер}} \frac{n_A G}{1000} \frac{1}{\tau} \frac{1}{\lambda} l. \tag{11.21}$$

The weight of the skin on the leading and trailing parts of the wing:

$$G_{\text{об}} = c_{\text{об}} \cdot S. \tag{11.22}$$

The weight of the ailerons and takeoff/landing flaps:

$$G_{\text{з.м}} = c_{\text{з.м}} (\bar{S}_{\text{з}} + \bar{S}_{\text{м}}) G. \tag{11.23}$$

Substituting all of these weights into (11.9) and dividing both sides of the equation by the takeoff weight G, we obtain an equation for determination of the wing relative weight $\bar{G}_{wg} = G_{wg}/G$.

Solving this equation for $\bar{G}_{wg}$, we obtain a formula for the relative weight of the wing:

$$\bar{G}_{\text{кр}} = \left\{ \left[\frac{A \frac{\lambda}{\bar{c}} - BC}{\cos^2 \chi} (k_1 k_{11} - k_{1\text{т}} \bar{G}_{\text{т}} - k_{1\text{гр}} \bar{G}_{\text{гр}}) + \frac{B}{\cos \chi} (k_3 k_{3\text{г}} - k_{3\text{т}} \bar{G}_{\text{т}} - k_{3\text{гр}} \bar{G}_{\text{гр}}) + \frac{c_{\text{п.пер}}}{a \lambda \bar{c}} + \frac{c_{\text{ст.пер}}}{\tau \lambda} \right] \frac{n_A \gamma l}{1000} + \frac{c_{\text{об}}}{p} + c_{\text{з.м}} (\bar{S}_{\text{з}} + \bar{S}_{\text{м}}) \right\} \times$$

$$\times \left[1 + \left(\frac{A \frac{\lambda}{\bar{c}} - BC}{\cos^2 \chi} k_{1\text{кр}} + \frac{B}{\cos \chi} k_{3\text{кр}} \right) \frac{n_A \gamma l}{1000} \right]^{-1}. \tag{11.24}$$

Here a denominator larger than 1 reflects the decrease in wing weight due to self-unloading.

$$A = \frac{c_{\text{п.л}}}{a 12 f \varphi}; \tag{11.25}$$

$$B = \frac{c_{\text{ст.л}}}{4\tau}; \tag{11.26}$$

$$C = \frac{2}{3\varphi} \frac{\eta_c - 1}{\eta_c + 1}. \tag{11.27}$$

The following numerical values of the coefficients can be taken for the calculation:

$c_{s.f} = 1.3-1.4;$

$c_{s.w} = 3.3-3.4;$

$c_{r.f} = 0.75-0.90;$ $\gamma = 2.85\ g/cm^3;$

$c_{r.w} = 1.5-1.9;$ $\sigma = 45\ kgf/mm^2;$ For duralumin

$c_{sk} = 0.013;$ $\tau = 20\ kgf/mm^2.$

$c_{a.f} = 0.086-0.088;$

$f = \phi = 0.82.$

If all available space inside the wing is used to hold fuel, the weight of the fuel in the wing can be assumed proportional to the external volume of the wing:

$$G_{T.tp} = 1000\bar{w}_f w\gamma_T, \tag{11.28}$$

where γ_f is the specific gravity of the fuel, $\bar{w}_f$ is the ratio of fuel volume to wing volume, w is the volume of the wing in m^3 and is determined by the formula

$$w = 0.44K\frac{\bar{c}}{\sqrt{\lambda}}S^{3/2}, \tag{11.29}$$

where

$$K = \frac{\eta_b + \eta_c + 2\eta_b\eta_c + 2}{(\eta_b + 1)(\eta_c + 1)}. \tag{11.30}$$

If $\eta_b = \eta_c = \eta$, we have $K = 2\frac{\eta + \eta^2 + 1}{(\eta + 1)^2}$ and if $\eta = \infty$, we have $K = 2$.

Formula (11.24) holds for wings with aspect ratios $\lambda \geq 4$; the same formula can be used for wings of smaller aspect ratio if the influence of that part of the wing area and span taken up by the fuselage is allowed for. This can be done in approximation by reducing the coefficients $c_{s.f}$ and $c_{s.w}$ in the ratio $(l - D_f)/l$ and the coefficients $c_{r.f}$ and $c_{r.w}$ in the ratio $(S - S_{wg.f})/S$.

For a variable-sweep wing, the wing weight calculated by (11.24) at minimum sweep must be increased by the weight of the swing-wing mechanism and hinges, which makes up about 35% of the weight of the wing

There are also other formulas for wing weight.

Table 11.1

Material	Temperature, °C		
	100	150	200
Duralumin (D16)	1.03	1.06	1.14
Refractory duralumin	1.015	1.03	1.10

For a small-aspect-ratio delta wing for a supersonic airplane, A.A. Badyagin [22] proposes the formula

$$\bar{G}_{кр} = K_t \left[\frac{7 n_{\varphi} p}{\bar{\sigma} \cdot 10^6} l \left(\lambda + \frac{4.6}{\lambda} \right) + \frac{7}{p} + 0.015 \right], \qquad (11.31)$$

where ϕ is the unloading factor; ϕ = 0.55-0.75, n_c is the calculated unloading factor, K_t is a coefficient that takes account of aerodynamic heating and is taken from Table 11.1, l is the wingspan and p is the specific load on the wing.

The approximate formulas of Driggs can be used for the wing weights of subsonic airplanes.

These formulas are much simpler than (11.24) but less exact. They appear for the first time in this book and are converted to the metric system, with the $\sigma = f(G)$ and $\sigma = f(\alpha)$ graphs replaced by formulas. To bring out more clearly the analogy between the Driggs formula and formula (11.24), we replace the ratio l/c_{max} by the expression $\frac{l}{\bar{c}} \frac{\eta_c + 1}{2\eta_c}$, which is equal to it. Then we have for the straight wing

$$\bar{G}_{кр} = 1.77 \frac{n_A l}{10^3 \sigma} \left[5 + \frac{\lambda}{\bar{c}} \frac{\eta_c + 1}{2\eta_c} F(\alpha, \beta) \right]. \qquad (11.32)$$

For a swept wing

$$\bar{G}_{кр} = 1.86 \frac{n_A l}{10^3 \sigma \cos\chi} \left[5 + \frac{\lambda}{\bar{c}} \frac{\eta_c + 1}{2\eta_c \cos\chi} F(\alpha, \beta) \right]. \qquad (11.33)$$

Here

$$\sigma = KG^{0.22} \text{ is in kgf/mm}^2 \qquad (11.34)$$

and G is expressed in tons.

Given good design, small cutouts, and extensive unloading, K = 13.

Under average conditions, K = 10.

In the case of poor design, numerous cutouts, and little unloading, K = 8;

$$F(\alpha,\beta)=\frac{\alpha f(\alpha)-\beta f(\beta)}{\alpha-\beta}; \tag{11.35}$$

$$f(\alpha)=0{,}0567+\frac{1}{10+2{,}9\sqrt{\alpha}}; \tag{11.36}$$

$$f(\beta)=0{,}0567+\frac{1}{10+2{,}9\sqrt{\beta}};$$

$$\alpha=1-\frac{\eta_n}{\eta_c};$$

$$\beta=\frac{1}{\eta_n}.$$

If $\eta_b = \eta_c = \eta$, $\alpha = 0$;

$$F(\alpha,\beta)=f(\beta)=0{,}0567+\frac{1}{10+\frac{2{,}9}{\sqrt{\eta}}}.$$

b) Relative Weight of Fuselage

The weight of the fuselage is composed of the weight of the stringers, skin, bulkheads, flooring, canopy, windows and glazing, doors and doorframes, and assembly hardware.

1. Weight of stringers and attached skin

Taking case A' or E' as the design case for the fuselage in accordance with the larger of the design overloads $n_{A'}$ of $n_{E'}$, we shall consider the fuselage as a beam resting on two supports — the front and rear wing spars. We shall disregard the aerodynamic forces and the inertial forces due to angular acceleration. The fuselage is replaced by a cylinder with wall thickness δ constant around the cross-sectional contour and a radius R. The section moment of inertia of such a cylinder is

$$I=\pi R^3\delta$$

and its wall thickness

$$\delta = \frac{Mn_{A'E'}}{\pi R^2 \sigma_c},$$

where $n_{A'E'}$ is the larger of the overloads $n_{A'}$ and $n_{E'}$ and only the moment due to weight forces is considered.

The annular-section area

$$f = 2\pi R\delta = \frac{2Mn_{A'E'}}{R\sigma_c}.$$

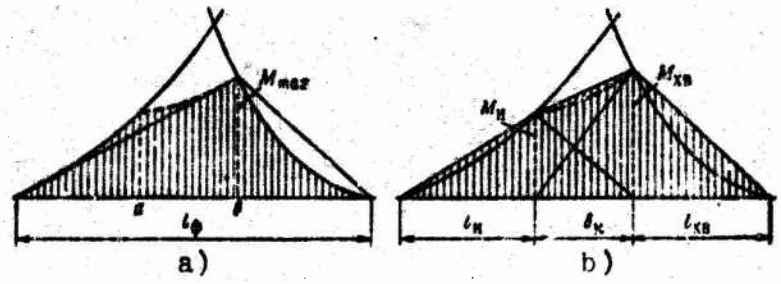

Figure 11.1. Two methods of simplifying moment diagram.

The weight of the carry-through structure is

$$G_{\text{пр.ш}} = \frac{c_{\text{пр.ш}}\gamma 4n_{A'E'}}{\sigma_{\text{кр}} D} \int_0^{l_\phi} M dx. \tag{11.37}$$

Here $c_{cts} = 1.2$ is a correction factor that reflects the conversion from the theoretical weight of the carry-through structure to its real weight and is obtained from weight statistics and $\sigma_{cr} = 25$ kgf/mm^2. The diameter D of the fuselage is taken out of the integrand, since we disregard the variation of diameter over the length of the fuselage. However, this circumstance can be taken into account by an appropriate increase in the moments with respect to the ends of the fuselage. $\int_0^{l_\phi} M dx$ — is the area of the bending-moment diagram over the fuselage length (Fig. 11.1a). The wing spars are located at points a and b. By drawing straight lines from the apex of the moment diagram to the front and rear

points of the fuselage axis, we obtain a triangle of area larger than the area of the moment diagram:

$$\int_0^{l_\Phi} M dx \approx \frac{M_{max} l_\Phi}{2}. \tag{11.38}$$

If the locations of the wing loads and spars are not known, M_{max} can be used, as in the case of a beam under uniform load $(G_{ld.f} + G_f)$ and supported at the center:

$$M_{max} \approx \frac{(G_{rp.\Phi} + G_\Phi) l_\Phi}{8}; \tag{11.39}$$

$$\int_0^{l_\Phi} M dx \approx \frac{G_{rp.\Phi}(1 + K_\Phi) l_\Phi^2}{16}. \tag{11.40}$$

If the load and spar positions are known, the resulting moment diagram can be simplified by substituting a broken line drawn through the moment points at the front and rear spar (see Fig. 11.1b).

This results in a slight increase in the area of the moment diagram, but does not exaggerate the weight, since the formula is corrected by the factor c_{cts}.

In this case

$$\int_0^{l_\Phi} M dx = \frac{1}{2} [M_n(l_n + e_n) + M_{xn}(l_{xn} + e_n)]. \tag{11.41}$$

The nose moment M_n about the front spar is determined as the sum of the moments from loads that can be regarded as lumped and from distributed loads, which are assumed uniform:

$$M_n = \sum (G_n x_n) + \sum \left(\frac{q_n}{2} x_n^2\right).$$

Here G_n and x_n are the concentrated forces from the wing front spar and their arms and q_n and x_n are the distributed loads per unit length and the arms of the forward ends. The moment of the tail section at the rear spar is determined similarly.

2. Weight of bulkheads

The framing bulkheads are designed to maintain the sectional

shape of the fuselage when it bends and twists, and unless an additional local force is applied to a bulkhead, the design case corresponding to it is bending of the fuselage.

In this case, the bulkhead is compressed by opposing forces and the maximum moment in two opposite bulkhead sections is determined from the formula

$$M_{\max \text{ шп}} = 0.25 q_{\max} R^2, \tag{11.42}$$

where R is the radius of the bulkhead, which can be assumed equal to the fuselage cross-section redius and q_{max} is the maximum load per unit length, compressing the bulkhead as a result of fuselage bending; it is determined from the formula

$$q_{\max} = 8a \frac{M^2 R}{EI^2}. \tag{11.43}$$

Here δ is the relative thickness of the skin in the annular fuselage section, M is the bending moment in the particular fuselage cross section, I is the moment of inertia of the fuselage cross section, E is the elastic modulus, and a is the distance between bulkheads. Substituting the expressions

$$\frac{M}{I} R = \sigma_{\text{кр}}, \quad I = \frac{\pi D^3}{8} \delta.$$

into (11.43), we get

$$q_{\max} = 8a\sigma_{\text{кр}} \frac{M}{\pi D^3 E \delta} = 8a\sigma_{\text{кр}} \frac{M}{\pi D^3 E}. \tag{11.44}$$

We substitute the resulting expression for q_{max} into (11.42) and obtain

$$M_{\max \text{ шп}} = \frac{a\sigma_{\text{кр}}}{2} \frac{M}{ED\pi}.$$

Assuming that the bulkhead has a Z- or channel cross section with height h, we determine the cross-sectional area of its two flanges:

$$2f = 2 \frac{M_{\max}}{h\sigma_{\text{шп}}} = \frac{\sigma_{\text{кр}} M_{\text{ф}} a}{\sigma_{\text{шп}} \bar{h} DE\pi},$$

where

$$\bar{h} = \frac{h}{D}.$$

The weight of one bulkhead, not counting its vertical members, is

$$G_{1\text{шп}} = \gamma \pi D \cdot 2f = \frac{\gamma^2 n_{кр} M_\phi a}{\sigma_{\text{шп}} E \bar{h} D}.$$

Substituting the element dx of fuselage length for a, we obtain the weight of the bulkheads on each element dx of fuselage length; integrating over the entire length, we obtain the weight of all bulkheads:

$$G_{\text{шп}} = c_{\text{шп}} \frac{n_{A'E} \gamma^2 n_{кр} (1 + 4\bar{h})}{10^3 E \sigma_{\text{шп}} \bar{h} D} \int_0^{l_\phi} M dx. \qquad (11.45)$$

Here the multiplier $(1 + 4\bar{h})$ takes account of the fact that the stress from the compressive force $P = q_{max}D$ is added to the stress from the moment $M_{max} = q_{max}D^2/16$ in the bulkhead cross section; $\sigma_{cr} = 26$ kgf/mm^2 is the critical stress in the carry-through structure, and $\sigma_{cr} = \sigma_{bh} = 26$ kgf/mm^2 are the stresses in the carry-through structure and bulkheads.

The statistical coefficient $c_{bh} = 23$ takes account of the weight of the bulkhead vertical members and the conversion to the real weights.

This large c_{bh} is explained by the fact that it also includes the weight of the reinforced bulkheads, which is three times the weight of the standard bulkheads. The integral expresses the area of the fuselage-bending moment diagram considered earlier.

Combining the weights of the stringers, the attached skin, and the bulkheads [see (11.37) and (11.45)], we get

$$G_{\text{стр+обш+шп}} = \left[\frac{4.8}{\sigma_{кр}} + \frac{23(1 + 4\bar{h})}{E\bar{h}}\right] \frac{n_{A'E} \gamma^2}{10^3 \cdot D} \int_0^{l_\phi} M dx. \qquad (11.46)$$

In formulas (11.37) and (11.45), $c_{cts} = 1.2$ and $c_{bh} = 23$. In addition, it was assumed that $\sigma_{cr} = 26$ kgf/mm^2, $\sigma_{bh} = 26$ kgf/mm^2, $h = 0.03$, and $E = 7000$ kgf/mm^2.

The coefficient 10^3 is introduced so that γ can be substituted into the formula in g/cm^3, σ and E in kgf/mm^2, and the

remaining quantities in meters and kilograms.

The large value of the coefficient c_{bh} indicates that there is considerable room for reducing the weight of the bulkheads and a need for an individualized approach to the design of each bulkhead with accurate allowance for its effective forces.

Formula (11.46) shows that the area of the bending-moment diagram appears as a common multiplier in the weights of the carry-through structure and the bulkheads. Let us now examine how the wing sweep angle will influence the area of the moment diagram and this weight.

If the wing sweep angle is changed, the aerodynamic center of the wing and its mean aerodynamic chord must remain in the same positions to preserve the trim of the airplane; if the wingtips are shifted aft, the wing root chords and the wing spars in the fuselage will be shifted forward.

We plot the stationary wing aerodynamic center, i.e., the point at 25% of mean aerodynamic chord (Fig. 11.2) from the wing leading edge, on the fuselage axis. If it is assumed that the forward spar runs through the line of centers, then for a given sweep angle χ, the forward spar passes through the fuselage at a distance (see Fig. 11.2)

$$x=\left(z_{\text{ц.т}}-\frac{D_{\text{ф}}}{2}\right)\text{tg}\,\chi,$$

where z is the coordinate of the wing area center of gravity and D_f is the width of the fuselage.

Having plotted the diagrams of the nose and tail bending moments to the point at which they intersect, we lay off the distance x from the aerodynamic center in the direction of the nose for the particular angle χ, obtain the position of the front spar, and obtain the position of the rear spar by laying off the width b_r of the wing box from the front spar in the direction to the tail.

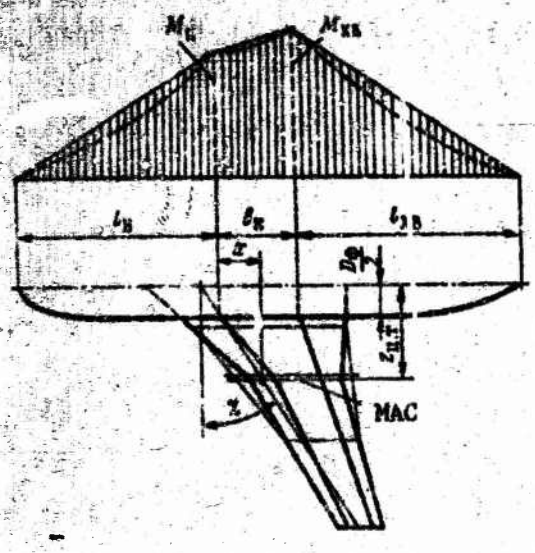

Figure 11.2. Influence of wing sweep on fuselage moment diagram.

Thus, we have obtained all data for calculation of the moment-diagram area from (11.41) as a function of χ.

If the nose- and tail-moment curves are extended to the point where they meet, the intersection will indicate the position of the fuselage-load center of gravity and, in approximation, that of the fuselage itself. We see from this construction of the moment diagram that the smallest value of M_{max} will hold when $M_n = M_{tl} = M_{max}$ and these values of the moments M_n and M_{tl} will be the smaller the greater the distance between the wing spars. Consequently, the minimum weight will be obtained for the carry-through structure and bulkheads when the fuselage and its loads are suspended at their center of gravity approximately midway between the spars and the weight of the fuselage framing will be smaller the larger the distance between the wing spars at the fuselage.

3. Weight of skin on pressurized section of fuselage

Part of the weight of this skin was included, as its attached width, in the weight of the carry-through structure. The remainder is determined as the weight of the wall of a cylindrical container with an excess pressure p_{exc} inside it. The maximum stress in the skin is a section along the generatrix of the cylinder is

$$\sigma_p = \frac{p_{max} D_f}{2\delta_f},$$

whence the thickness of the skin is

$$\delta = \frac{p_{max} D_f}{2\sigma_p}.$$

The weight of the pressurized part of the skin is

$$G_{г.об}=0{,}8\frac{p_{изб}\cdot 10{,}33\pi\gamma D^2 l_г}{2\sigma_p}, \qquad (11.47)$$

where the number 10.33 has been introduced so that γ can be substituted in g/cm^3 and p_{exc} and σ_b in kgf/mm^2. Here γ = 2.85 g/cm^3, p_{exc} = 0.25-0.6 atm depending on the altitude capability of the airplane, and σ_b = 8 kgf/mm^2 (taken from the fatigue calculation).

The coefficient 0.8 allows only for that part of the skin not included in the width attached to the stringers.

4. Weight of pressurized end wall

If the end wall has the form of a spherical segment, it will work under tension when the excess pressure is applied, and the bulkhead bracing it will be compressed by a uniform load directed toward the center of the bulkhead. The weight of these two parts of the end wall can be expressed by the formula

$$G_{дн.шп}=c_{дн.шп}\frac{10{,}33\gamma p_{изб}\pi D^3}{16}\left[\frac{(1+\bar{f}^2)^2}{2\bar{f}\sigma_p}+\frac{(1-\bar{f}^2)}{\bar{f}\sigma_c}\right]. \qquad (11.48)$$

Here $\bar{f}$ = f/R = 2f/D is the relative depth of the end wall. The first term in the square brackets takes account of the weight of the shell and the second the weight of the framing bulkhead. It is easily shown that the minimum of the expression in the brackets and, consequently, the weight minimum of the end wall and bulkhead will occur at

$$\bar{f}_{опт}=\sqrt{\frac{1}{3}\left(\frac{2\sigma_p}{\sigma_c}+1\right)}. \qquad (11.49)$$

Even if we assume $\sigma_b = \sigma_s$, we have $\bar{f}_{opt}$ = 1, which is not acceptable in practice.

We convert (11.48) to the form

$$G_{дн.шп}=c_{дн.шп}\frac{10{,}33p_{изб}\gamma\pi D^4}{16\sigma_p}a. \qquad (11.50)$$

Here $c_{ew.bh} \approx 2.5$ and

$$a = \left[\frac{(1+\bar{f}^2)^2}{2\bar{f}} + \frac{\sigma_b}{\sigma_s}\left(\frac{1-\bar{f}^2}{\bar{f}}\right)\right].$$

For a lattice-reinforced flat end wall, we can assume a = 4, σ_b = 8 kgf/mm^2, and σ_s = 16 kgf/mm^2.

5. Weight of skin on unpressurized section of fuselage

With the exception of the part already considered with the carry-through structure, this skin works in shear under the fuselage shearing and twisting forces.

The maximum tangential stress in the fuselage section at the base of its unpressurized part due to the shearing force Q is determined from the formula

$$\tau_{cp} = \frac{Q2R^2}{\pi R^3} \cdot \frac{1}{2\delta} = \frac{Q}{\pi R\delta}.$$

If, in addition to the vertical shearing force Q, the vertical tailplane is also acted upon by a horizontal force $Y_{v.t}$, these forces must be replaced by their resultant $\sqrt{Q^2 + Y^2_{v.t}}$ and increased by the stress τ_{tors} from the torsional moment $M = Y_{v.t} \cdot h'$, where h' is the arm of the force $Y_{v.t}$ with respect to the fuselage axis. Then

$$\tau_{круч} = \frac{M}{2F\delta} = \frac{Y_{в.о}h'}{2\pi R^2} \cdot \frac{1}{\delta}.$$

The total stress

$$\tau_{крит} = \tau_{ср} + \tau_{круч} = \left(\sqrt{Q^2 + Y^2_{в.о}} + Y_{в.о}\frac{h'}{D_{кр}}\right)\frac{1}{\pi R_{кр}\delta}.$$

From this we determine the skin thickness:

$$\delta = \left(\sqrt{Q^2 + Y^2_{в.о}} + Y_{в.о}\frac{h'}{D_{кр}}\right)\frac{2}{\pi D_{кр}\tau}. \qquad (11.51)$$

Practice gives us the following simple dependence of the critical stress on the thickness of the sheet metal:

$$\tau_{crit} = \delta \ [\text{kgf/mm}^2].$$

From this we obtain

$$\delta = \sqrt{\left(\sqrt{Q^2 + Y^2_{в.о}} + Y_{в.о}\frac{h'}{D_{кр}}\right)\frac{2}{10\pi D_{кр}}} \text{ mm}. \qquad (11.52)$$

Instead of the fuselage diameter, the diameter of the pressurized end wall appears in this formula because the end of the pressurized section of the fuselage may be aft of the end of its cylindrical section.

Knowing the thickness of the skin, we determine its weight:

$$G_{об.нг} = C_{об.нг}\gamma\pi D_{ср} l_{нг} \cdot 10^3 \cdot \delta,$$

where γ is in g/cm^3 and the remaining dimensions are in meters. The coefficient $C_{sk.up} = 1.05$. D_{av} is the average diameter of the unpressurized section.

For aircraft in which the pressurized part occupies less than half the length of the fuselage,

$$Q \approx n_{A'E} \frac{G_{гр.ф}}{2}.$$

For passenger aircraft with short unpressurized tail sections, it can be considered only for the forces $Y_{v.t}$ and $G_{tl} n_{A'}$.

We combine the weights of the entire skin and the pressurized end wall in the single formula

$$G_{об.г} + G_{ан} + G_{об.нг} = \left(0.8 l_г + \frac{2.5}{8} Da\right) \frac{10.33 p_{ов} \gamma \pi D^2}{2\sigma_p} + \\ + 1.05 \pi D_{ср} l_{нг} 10^3 \delta.$$

Here

$$a = \left[\frac{(1+\bar{f}^2)^2}{2\bar{f}} + \frac{\sigma_p}{\sigma_c} \frac{1-\bar{f}^2}{\bar{f}}\right]; \quad \bar{f} = \frac{f}{R}.$$

for δ, see (11.52).

The sum of all loads in the unpressurized part of the fuselage with overloading $n_{A'}$ should be taken as the shearing force Q:

for military aircraft

$$Q \approx n_{A'} \frac{G_{гр.ф}}{2},$$

for passenger aircraft

$$Q \approx n_A \cdot G_{оп}.$$

The weights of the remaining parts of the fuselage are computed by the empirical formulas derived by V.A. Kiselev by processing weight statistics (they reflect the theoretical relationships approximately).

6. Weight of canopy

$$G_{фон} = 53\sqrt{D}K_{фон}(1 + p_{изб}), \tag{11.53}$$

$K_{can} = 1$ for a pilot's canopy, $K_{can} = 1.5$ for pilot and navigator canopies, and $(1 + p_{exc})$ signifies that the canopy has a weight at $p_{exc} = 0$.

7. Weights of windows and glazing

This weight is proportional to the length l_{wd} of the part of the fuselage with windows and depends on the moments bending the tail section of the fuselage and the excess pressure p_{exc} in the cabin:

$$G_{ок} = 0{,}59 l_{ок} l_{хв}(1 + p_{изб}). \tag{11.54}$$

If the length of the row of windows and the length of the fuselage tail section are still unknown, it can be assumed for passenger aircraft that

$$l_{ок} l_{хв} \approx \frac{l_ф^2}{4}.$$

8. Weight of doors and doorframes

$$G_{дв} = 14{,}9D^2(1 + p_{изб}). \tag{11.55}$$

9. Weight of floor

This weight is proportional to the length l_p of the pressurized part of the fuselage and to its diameter:

$$G_{пол} = 0.73Dl_p. \tag{11.56}$$

10. Weight of assembly components

This includes the weights of the components used to join the fuselage to the wing, tail, undercarriage, and engines, counting the weights of the elements themselves and the reinforcements

applied to the corresponding fuselage-framing elements:

$$G_{сош}=10^{-2}(k_1G_{гр.л+ф}+k_2G_{оп}+ \\ +k_3G_{л.у}+k_4G+k_5G), \tag{11.57}$$

Here $k_1 = 4$ for a low-wing monoplane and $k_1 = 7$ for a high-wing monoplane; $G_{ld.f+f}$ is the weight of the loads in the fuselage plus the fuselage itself; $k_2 = 5$, G_{tl} is the weight of the tailplanes, $k_3 = 7$, $k_3 = 0$ if the engines are wing-mounted, $G_{p.p}$ is the weight of the powerplant, $k_4 = 0.1$ (counting the nose-wheel attachment), $k_5 = 0.3$ if the main undercarriage is mounted to the fuselage, $k_5 = 0$ if the main undercarriage is mounted to the wing, and G is the takeoff weight.

11. Weight formula for fuselage

We can now write a formula for the fuselage relative weight, having selected its dimensions and the excess pressure p_{exc} in the cabin and knowing the weights of all loads carried in the fuselage with the weight of those parts of the airplane mounted on the fuselage given as fractions of takeoff weight. We adopt the following simplifying assumptions for this purpose. The weights of the pressurized skin, end wall, canopies, windows, doors, and fl[illegible] can be computed from (11.47) and (11.50)-(11.56) in kilograms and compose a constant sum $G_{f\ const}$ in kilograms.

To determine the thickness δ of the unpressurized skin, we assume $Y_{v.t} = 0$ in (11.52) and substitute a lin[illegible] tion for the parabolic one. We then obtain the approximate formula

$$\delta=1{,}7+\frac{n_{A'E'}K_{об.нг}}{\pi R14\cdot10^3}(G_{гр.ф}+G_ф),$$

where $K_{sk.up} = 1$ for a military airplane and $K_{sk.up} =$ [illegible] passenger airplane.

Now the weight of the unpressurized part of the s[illegible] broken up into two terms:

$$G_{об.кг} = 1{,}785\pi D l_{кг} \gamma + \frac{150}{100} n_{A'E'} l_{кг} K_{об.кг} \gamma (G_{гр.ф} + G_{ф}) = G_{об.кг.const} + B(G_{гр.ф} + G_{ф}). \quad (11.58)$$

The first term of this expression appears in the sum $G_{f\ const}$. We substitute formula (11.39) into (11.46) for the weight of the carry-through structure and bulkheads:

$$G_{пр.п.шп} = \left[\frac{4{,}8}{\sigma_{кр}} + \frac{23(1+4\bar{h})}{E\bar{h}}\right] \frac{n_{A'E'} \gamma l_{ф}^2}{10^3 \cdot 16 \cdot D} (G_{гр.ф} + G_{ф}) = A(G_{гр.ф} + G_{ф}). \quad (11.59)$$

The relative weight of the fuselage is now connected by the equation

$$\bar{G}_{ф} = A(\bar{G}_{гр.ф} + \bar{G}_{ф}) + B(\bar{G}_{гр.ф} + \bar{G}_{ф}) + \frac{k_1}{100}(\bar{G}_{гр.ф} + \bar{G}_{ф}) + \bar{G}_{ф\ const} + 10^{-2}(k_2 \bar{G}_{оп} + k_3 \bar{G}_{л.у} + k_4 + k_5). \quad (11.60)$$

Here, for military and civil aircraft

$$A = \left[\frac{4{,}8}{\sigma_{кр}} + \frac{23(1+4\bar{h})}{E\bar{h}}\right] \frac{n_{A'E'} \gamma l_{ф}^2}{10^3 \cdot 4D},$$

for military aircraft

$$B = 0{,}15 n_{A'E'} l_{кг} \gamma \frac{D_1}{D_{зн}} \frac{1}{10^3},$$

for civil aircraft B = 0 and

$$\bar{G}_{ф\ const} = \frac{G_{ф\ const}}{G},$$

where $G_{f\ const}$ is the sum of the constant weights.

The values taken for the coefficient k_1-k_5 are the same as for formula (11.57).

The weight of the fuselage appears in the first three terms of (11.60). We might derive from this a formula for the weight of the fuselage as an explicit function of all the other quantities, as we did for the weight of the wing. Remembering, however, that simplifying assumptions have already been made, we introduce yet another. We substitute the expression

$$\bar{G}_{\text{гр.ф}}+\bar{G}_{\phi}=(1+K_{\phi})\bar{G}_{\text{гр.ф}}$$

into (11.60) and obtain

$$\bar{G}_{\phi}=(1+K_{\phi})(A+B+k_1)\bar{G}_{\text{гр.ф}}+\bar{G}_{\phi\,\text{const}}+k_2\bar{G}_{\text{оп}}+k_3\bar{G}_{x,y}+ \\ +k_4+k_5. \qquad (11.61)$$

Here $\bar{G}_{ld.f}$ is composed of the relative weights of the crew, equipment, payload, tailplanes, powerplant, and landing gear if the latter are attached to the fuselage.

If the main undercarriage struts are secured to the wings, we have $k_5 = 0$.

If the engines are mounted on the wings, the terms with $\bar{G}_{p.p}$ are dropped.

As we see from (11.61), the relative weight of the fuselage has been distributed over the weights of the fuselage loads in such a way that each part of the fuselage weight represents a certain fraction of the load carried in it. This distribution of the fuselage weight and the weight formula can be derived more accurately if the area of the moment diagram is determined from the two moments M_n and M_{tl} [see (11.41)]; this will take account not only of the influence of each load, but also of its position along the length of the fuselage.

The weight of the fuselage can be determined approximately from the formula

$$G_{\phi}=K_{\phi}G_{\text{гр.ф}}, \qquad (11.62)$$

where $G_{ld.f}$ is the sum of all fuselage loads.

Such loads are the crew, equipment, commercial or bomb cargo and the equipment necessary to handle it, the tailplanes, most of the controls and possibly the fuel, landing gear, and engines if these loads are accommodated in whole or in part in the fuselage.

Statistical data indicate the following average values for the coefficient K_f expressed as a fraction of the weight of

fuselage loads: the heaviest fuselages are obtained for subsonic passenger aircraft with the engines on the wings:

$$K_f = 0.33.$$

If the engine of a passenger aircraft is mounted on the fuselage, $K_f = 0.23$.

This decrease is explained not only by the fact that the weight of the fuselage is referred to the weight of the loads increased by the weight of the engines, but also by the fact that an increase in the longitudinal forces from bending of the fuselage makes it necessary to thicken the skin, stringers, and spars, with the result that the critical buckling stresses are larger.

If the fuselages are to accommodate loads of the same weight as passengers, but these loads are less bulky, as is the case, for example, for military aircraft, the fuselage diameter can be reduced considerably, and then the stresses in the material may be increased even further.

This fact, together with the reduction of the fuselage's surface area, makes the K_f of a military aircraft even smaller, and the coefficients assume the following values:

For aircraft with engines in the wing $K_f = 0.20$.

For aircraft with engines on the fuselage tail section, $K_f = 0.16$.

There may be deviations in either direction from these average values, by ±0.04.

For supersonic airplanes, K_f should be selected on the basis of the upper limit.

Applying (11.62), we can distribute the fuselage weight approximately in proportion to the fuselage loads, multiplying the weight of each load by $(1 + K_f)$, i.e., adding the appropriate fraction of fuselage weight to each load.

c) Weight of Landing Gear

The weight of the landing gear is proportional to the takeoff weight:

$$G_{ш} = \bar{G}_{ш} G,$$

where

$$\bar{G}_{ш} = 0{,}04 \div 0{,}06.$$

More precisely, this coefficient decreases slightly with increasing takeoff weight.

V.M. Sheynin [24] gives the statistical dependence of $\bar{G}_g$ on takeoff weight in diagram form. This dependence can also be expressed by the following formulas:

For passenger aircraft

$$\bar{G}_{ш} = 2{,}2 \frac{G + 204}{G + 79}, \tag{11.63}$$

for military aircraft

$$\bar{G}_{ш} = 3{,}2 \frac{G + 352}{G + 240}, \tag{11.64}$$

where G is the takeoff weight in tons and $\bar{G}_g$ is in %.

d) Weight of Tailplanes

The weight formula for the wing can be used to compute the absolute weight of the horizontal tail, but the calculation is simpler because there is no unloading at the tail and we can assume $k_{1г} = k_{3г} = 1$ and $\eta_b = \eta_c = \eta$.

The largest value from among all the cases listed by the Strength Norms is taken as the design load. The same procedure can also be used to compute the weight of the vertical tailplane, regarding it as half of a wing with span $l = 2l_{v.t}$ and aspect ration $\lambda = 2\lambda_{v.t}$. Since the weight of the tail represents a small fraction of the takeoff weight (~2%), its weight can be considered in simpler fashion, although major errors are undesirable even in this calculation owing to the possibility of substantial trim deviations.

The approximate weights of the horizontal and vertical tailplanes can be determined thus:

$$\left.\begin{aligned} G_{г.о} &= p_{г.о} S_{г.о}, \\ G_{в.о} &= p_{в.о} S_{в.о}. \end{aligned}\right\} \qquad (11.65)$$

where $p_{h.t}$ and $p_{v.t}$ are the weights of one square meter of horizontal and vertical tailplane. For subsonic airplanes, these weights are determined as functions of the area of the corresponding tailplane, using the formula

$$p_{г.о} = 7 + 0{,}22 S_{г.о} \qquad (11.66)$$

with $p_{v.t}$ defined by the corresponding formula. For supersonic aircraft, the weight per square meter of tail surfaces must be taken from statistical data on similar aircraft types.

e) Weight of Controls

The weight of the airplane's control consists of the weight of the control station with all its auxiliary devices and the control lines in the fuselage and wing; also, the hydraulic boosters in the control systems of fast aircraft. The weight of the control lines in the fuselage is proportional to their length, and the weight of those in the wing to its span. The weight of the control station can be assumed constant. The weight of the entire control system can be determined thus:

$$G_{упр} = G_{л.упр} + 8 l_{ф} + 2 l, \qquad (11.67)$$

where the weight of the control station $G_{ctl.s}$ = 125 kg for one pilot and $G_{ctl.s}$ = 200 kg for two pilots.

If boosters are used, their weight must be included in the first term of (11.67).

§11.4. DETERMINATION OF RELATIVE WEIGHT OF FUEL SYSTEM AND POWERPLANE

a) Relative Weight of Fuel

For turbojet aircraft of which long range is required, the relative weight of the fuel can be obtained from the familiar

logarithmic formula for flight range:

$$L=\frac{3{,}6VK}{C_{yx}}\ln\frac{G}{G_{кон}}. \qquad (11.68)$$

This formula can be written

$$\frac{1}{A}=\ln\frac{1}{\bar{G}_{кон}}, \qquad (11.69)$$

where $\bar{G}_{fin}$ is the relative final weight and

$$A=\frac{3{,}6VK}{LC_{yx}}=\frac{G}{TC_{yx}P_{нач}}. \qquad (11.70)$$

Here T = L/3.6V is the flight time in hours and the aerodynamic efficiency K is expressed as the ratio of the initial weight G to the initial thrust P_{ini}. Formula (11.70) brings out the physical significance of 1/A: it is the relative weight of fuel that would be needed if the thrust remained equal to P_{ini} for T hours. Formula (11.71) can also be written

$$\frac{1}{1-\bar{G}_{т}}=e^{\frac{1}{A}},$$

whence

$$\bar{G}_{т}=1-e^{-\frac{1}{A}}. \qquad (11.71)$$

Formula (11.71) can be replaced by the simpler formula

$$\bar{G}_{т}=\frac{1{,}03}{A+0{,}025}. \qquad (11.72)$$

Calculations by this formula yield results with errors no greater than 1% in the range $\bar{G}_f$ = 0.5-0.3.

If the amount of fuel is small, it can be determined by considering the consumption rate to be constant and to correspond to the average weight of the airplane:

$$G_{ср}=G-\frac{G_{т}}{2},$$

then

$$\bar{G}_{т}=\frac{1}{A+0{,}5}. \qquad (11.73)$$

The relative weights of the fuel aboard airplanes with piston and propjet engines can be determined by the same formulas [(11.71), (11.72), and (11.73)], but the specific fuel consumption C_{sp} is now referred to 1 hp, requiring inclusion of a factor $75\eta/V$ in the expression for A. The result:

Here $K = K_{max}$, $\eta \cong 0.75$, and C_{sp} is found from the fuel-consumption curve of the particular engine type.

$$A = \frac{75 \cdot 3{,}6 K\eta}{LC_{ya}} = \frac{270\eta K}{LC_{ya}}. \tag{11.74}$$

b) Relative Weight of Powerplant

The following formula can be written for relative powerplant weight:

$$\bar{G}_{x,y} = (1 + K_y)\frac{P}{G}\gamma_{xn} = (1 + K_y)\mu\gamma_{xn}, \tag{11.75}$$

where $\mu = P/G$ is the thrust/weight ratio of the airplane.

In level flight at constant speed, $\mu = 1/K$. For near-ceiling altitudes, $K = K_{max}$, and γ_{en} must be referred to the thrust P at that altitude. Since thrust is proportional to the atmospheric pressure p_a above 11 km, we have

$$\gamma_{xn} = \gamma_{xn11}\frac{p_{a11}}{p_a}$$

and

$$\bar{G}_{x,y} = (1 + K_y)\frac{\gamma_{xn11}}{K_{max}}\frac{p_{a11}}{p_a} \tag{11.76}$$

The thrust/weight ratio must also be determined from other required flight properties, e.g., cruising altitude and speed, takeoff distance, etc., and the relative powerplant weight must be taken for the flight property that requires the largest value.

If the airplane must have a short takeoff run L_{run}, the relative powerplant weight is determined on the basis of the static zero-altitude thrust/weight ratio $\mu_0 = \bar{P}_0/G$:

$$\bar{G}_{x,y} = (1 + K_y)\bar{P}_0\gamma_{xn}$$

$\bar{P}_0$ can be determined with the formula

$$L_{раз}=\frac{8p}{gc_{x_0}}\ln\frac{1}{1-\frac{c_{x_0}}{c_{y_{отр}}(\overline{P}_0-f)}}, \tag{11.77}$$

whence

$$\overline{P}_0=f+\frac{c_{x_0}}{c_{y_{отр}}}\cdot\frac{1}{1-e^{-\frac{gc_{x_0}L_{раз}}{8p}}} \tag{11.78}$$

or, from the series expansion of the natural logarithm

$$\overline{P}_0\approx f+\frac{8p}{gc_{y_{отр}}L_{раз}}\cdot\frac{1}{1-\frac{gc_{x_0}L_{раз}}{16p}}. \tag{11.79}$$

Here f = 0.02 on concrete, f = 0.06 on hard dirt, c_{x_0} is the frontal-drag coefficient during the runup with consideration of the landing-gear and wing-flap effects;

$$c_{y_{отр}}=0{,}8c_{y_{max}}.$$

For piston and prop-jet aircraft, the relative powerplant weight is determined from a similar formula:

$$\overline{G}_{л.у}=(1+K_y)\frac{N}{G}\gamma_{дв}. \tag{11.80}$$

Here γ_{en} is taken for the specific engine and the specific altitude.

As we see, the relative powerplant weight is now determined for the power/weight ratio N/G.

To determine the power/weight ratio for a given top speed, we use the top-speed formula from [28], which is valid for altitudes below the ceiling:

$$V_{max}=\sqrt[3]{\frac{1200\eta}{c_{x_0}\Delta}\frac{N}{G}\frac{G}{S}-\frac{16}{225}\frac{1}{\pi\lambda_{эф}\eta\Delta}\frac{G}{S}\frac{G}{N}}.$$

Raising both sides to the third power, we obtain a quadratic equation in N/G, from which

$$\frac{N}{G}=\frac{c_{x_0}\lambda}{2400\eta}\frac{V^3_{max}}{p}\times$$
$$\times\left[1+\sqrt{1+\frac{480\cdot 16}{225\pi c_{x_0}/\eta}\left(\frac{p}{V^2_{max}\lambda}\right)^2}\right]. \tag{11.81}$$

If the cruising speed V_{cruise} for a given altitude is stated, we substitute V_{cr} into (11.81) to obtain, instead of V_{max}, the cruising power/weight ratio N_{cruise}/G; then

$$\bar{G}_{x.y}=(1+K_y)\frac{N_{крейс}}{\nu G}\eta_{вн}, \tag{11.82}$$

where $\nu \approx 0.7$ is the fraction of the power used in cruising flight.

The following relations are used to determine $\bar{G}_{p.p}$ for a given runup distance:

$N_0/G = \mu_0$ for piston engines;

$N_0/G \approx 1.4\mu_0$ for propjet engines.

§11.5. DETERMINATION OF BASIC DIMENSIONS OF AIRPLANE AND ENGINE

When the airplane's takeoff weight can be determined, its basic dimensions, areas, spans, characteristic wing and tailplane chords, fuselage diameter and length, and engine basic dimensions (diameter and length) can be computed.

The areas are determined from the formulas

$$S=\frac{G}{p},$$

where p is the specific load on the wing,

$$S_{г.о}=\bar{S}_{г.о}S,$$

$$S_{в.о}=\bar{S}_{в.о}S.$$

The wing and tail spans are computed as

$$l=\sqrt{\lambda S},$$

$$l_{г.о}=\sqrt{\lambda_{г.о}S_{г.о}},$$

$$l_{в.о}=\sqrt{\lambda_{в.о}S_{в.о}}.$$

The formulas for determining the root, tip, and mean aerodynamic chords take the form

$$b_{max}=\frac{l}{\frac{\lambda}{2}\left(1+\frac{1}{\eta}\right)},$$

$$b_{конц}=\frac{l}{\frac{\lambda\eta}{2}\left(1+\frac{1}{\eta}\right)},$$

$$b_A=\frac{2}{3}b_{корн}\left[1+\frac{1}{\eta(1+\eta)}\right].$$

The diameter and length of the fuselage can be evaluated from relations of the type

$$D_{\Phi}=\sqrt{\frac{4G}{\pi p_{м.\Phi}}},$$

where $p_{m.f}$ is the specific load on the fuselage midsection, and

$$l_{\Phi}=\lambda_{\Phi}\cdot D_{\Phi},$$

where λ_f is the fuselage slenderness ratio.

Engine diameter is estimated from the formulas:

For turbojet engines

$$D_{дв}=\sqrt{\frac{4P_{дв}}{\pi P_F}},$$

where P_{en} is the thrust of the engine and P_F is its specific frontal thrust.

For propjet engines

$$D_{дв}=\sqrt{\frac{4N_{дв}}{\pi N_F}},$$

where N_{en} is the engine's power output and N_F is its specific frontal power. The engine's thrust or power is determined as follows:

$$P_{дв}=\mu_P G/z,$$
$$N_{дв}=\mu_N G/z,$$

where μ_P is the available thrust/weight ratio, μ_N is the available power/weight ratio, and z is the number of engines on the airplane.

Engine length can be estimated from the relation

$$l_{дв} = D_{дв} \cdot \lambda_{дв},$$

where $\lambda_{дв}$ is the slenderness ratio of the engine.

Chapter 12

PRINCIPLES OF STRUCTURE-DIAGRAM ELABORATION

§12 1. THE PRINCIPLE OF SHORTEST FORCE-FLOW ROUTE

Force flows are transmitted through the elements of a structure.

The shortest path of the basic force flow (shortening the principal structural elements) endows the structure with the lowest weight. The straight rod in tension or compression may serve as an example.

The extreme case is that in which the force is not transmitted anywhere, but is taken up directly at its point of application. Forty years ago, at one of the Central Aerohydrodynamics Institute conferences, A.N. Tupolev put it this way: "A force must be caught where it has appeared." This is the gist of the relieving or unloading principle as a particular case of the shortest-path principle for force-flow transmission. On the airplane, this principle is embodied, for example, in the wing, where part of the aerodynamic load is offset by the weight of the wing and the loads accommodated in it.

The unloading principle was first used by I.I. Sikorskiy in the "Russkiy Vityaz'" airplane (Fig. 12.1), where the engines were carried outboard in the biplane cell, helping make it possible to build a large-aspect-ratio wing. The unloading principle is also

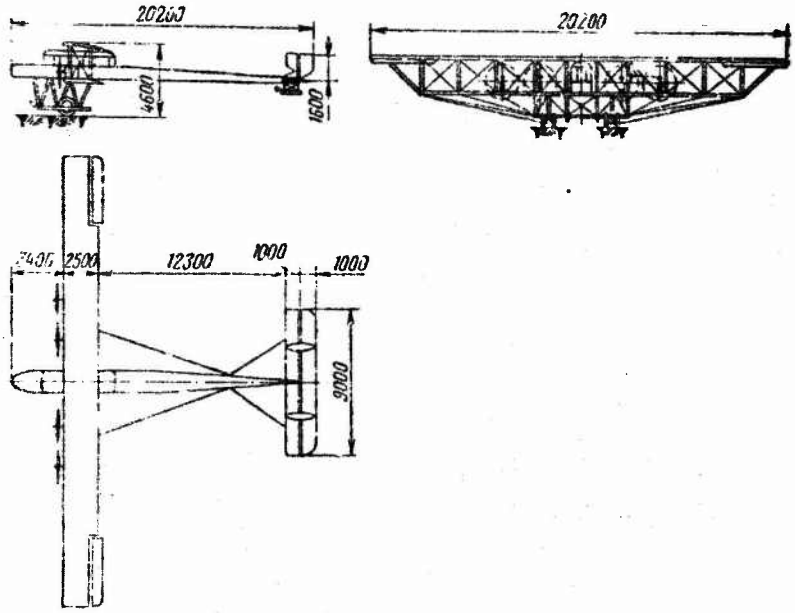

Figure 12.1. I.I. Sikorskiy's "Russkiy Vityaz'" airplane.

used in placing the undercarriage under the engines. It is used in more complete form in large "Flying Wing" aircraft (Fig. 12.2).

Another particular case of the shortest-route principle in the transmission of force flow is found in the principle of closure of the force circuit by means of auxiliary structural elements.

If some auxiliary structure sets up large reaction forces in the main structure, it is advisable in many cases to add closing structural members for complete or partial mutual cancellation of these reactions, thus relieving the main structure. This is illustrated by Fig. 12.3, where rod CD relieves the basic frame completely of the force 2P, and by Fig. 12.4, where rod AB, which joins the upper hinges of the shock absorber and the skid knee action, relieves the airframe of some of the horizontal forces.

It is sometimes necessary to reroute a force flow (forces) or shift them parallel to their original direction. This requires additional structural elements. Examples of elements that change the direction of a force are the roller in the control-cable run

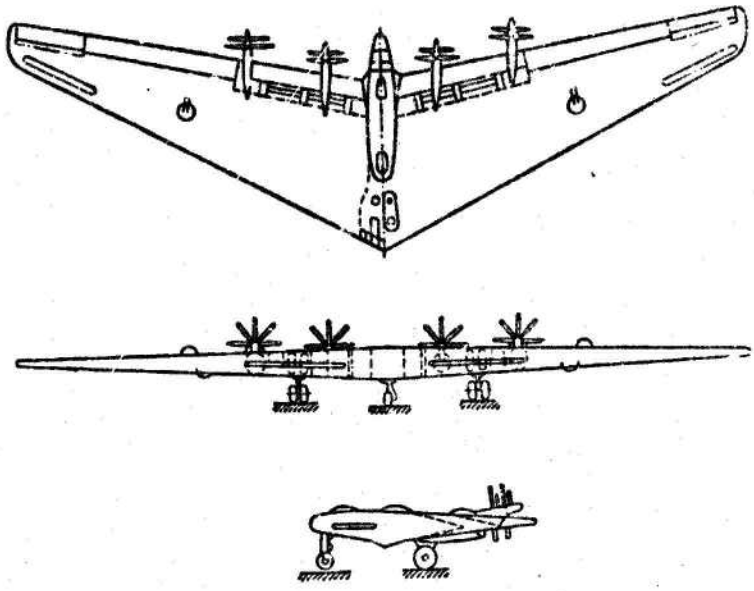

Figure 12.2. "Flying Wing" aircraft.

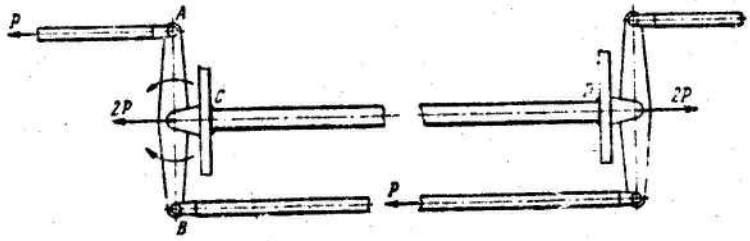

Figure 12.3. Straight twin-arm control rockers.

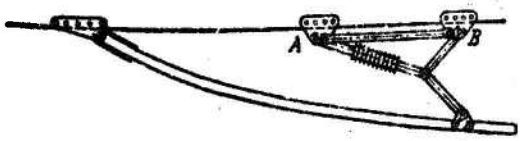

Figure 12.4. Cargo-aircraft skid.

(Fig. 12.5) and the bellcrank in the rigid-rod control run (Fig. 12.6a).

A change in the direction of a force sets up a reaction force, while shifting a force parallel to itself sets up a bending moment and shear.

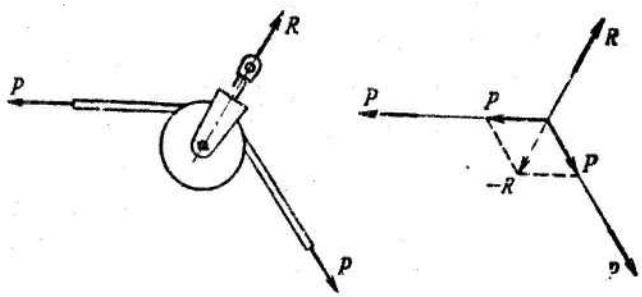

Figure 12.5. Control pulley.

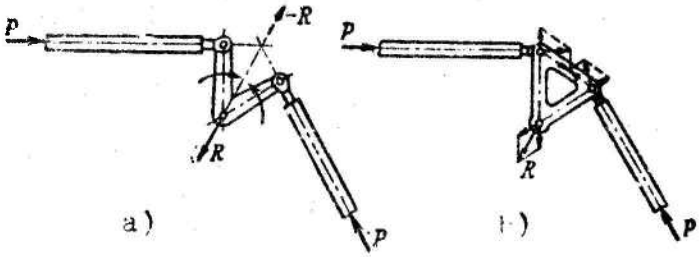

Figure 12.6. Bellcranks.

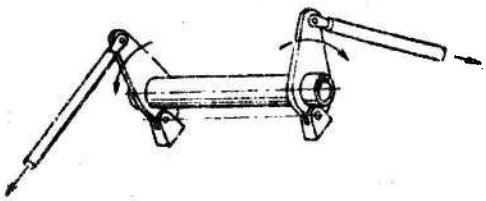

Figure 12.7. Torque tube.

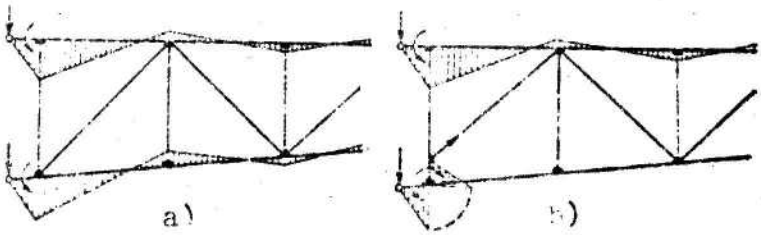

Figure 12.8. Case of favorable influence of eccentricity.

In these cases, it is necessary to give thought to taking up the reaction force, i.e., securing the pulley or bellcrank axle,

and not only from the standpoint of strength, but also from the standpoint of the rigidity of the element to which the pulley or bellcrank is secured; otherwise, additional elastic lash will appear in the control link. All of these measures require an increase in weight; this is the "penalty" for changing the direction of the force. Using the force-closure principle, it is necessary to connect the ends of the bellcrank with a tension rod (see Fig. 12.6b), i.e., to make it triangular and thereby relieve it of bending strains.

An example of shifting a force parallel to itself with reversal of its direction can be found in the straight-armed rocker used in control rods (see Fig. 12.3). The "price" of this shift is still higher, since in this case, in addition to a reaction equal to twice the force P acting through the rods and all of the associated weight penalties, there is also part AB, which works in bending, i.e., with definitely superfluous poorly utilized material.

Shifting a bending moment into another bending plane parallel to the original one calls for a member working in torsion, i.e., it results in additional strain and extra weight. The torsion tube (Fig. 12.7) is an example of such a parallel transfer of a bending moment in a control line.

Eccentricities should be avoided in order to reduce bending moments.

Sometimes the detrimental effect of eccentricities (Fig. 12.8a) can be eliminated by use of another eccentricity, as indicated in Fig. 12.8b, which shows the lower flange of a trussed spar.

§12.2. PRINCIPLE OF FORCE-FLOW SMOOTHNESS

Obstacles may be encountered on the path of a force flow. Elbows, notches, holes, and the like (Fig. 12.9) are obstacles to the flow of forces. Bending moments and stress concentrations arise when the force flow is diverted around such obstacles. To

mitigate this effect, the force flow should be aimed as close as possible to the cutout or hole, i.e., a major part of the material must be placed at the points of stress concentration (Fig. 12.10), and the force flow must be smoothed.

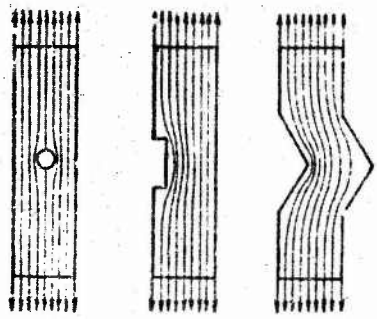

Figure 12.9. Obstacles to force flow.

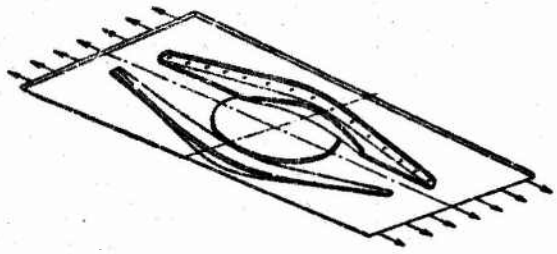

Figure 12.10. Reinforcement around hole.

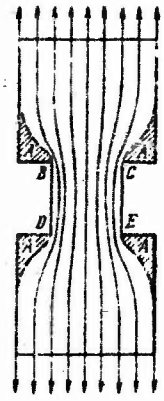

Figure 12.11. Non-smooth force flow.

Violation of this principle in the force flow results in nonuniform distribution of stresses and lowered strength or additional weight. Such a violation is illustrated clearly by Fig. 12.9 and by the plate working in tension with two slots (Fig. 12.11). Using this plate as an example, we shall set forth the procedure for observance of the force-flow smoothness principle.

Stress concentration occurs at the internal angles of the slots at points B, C, D, and E and is responsible for the low strength of this particular specimen. Rounding the corners with small radii reduces this concentration.

After elimination of stress concentration, the maximum stresses occur in the neck region B, C, D, E, and when the specimen fails through the neck, the stresses in its remaining sections are still far below the breaking stress. This nonuniformity is particularly undesirable under impact loading, when the work is

absorbed basically by the material in the volume of the neck and only a small fraction of work falls to the rest of the volume.

The stresses are practically zero in zones A at the external angles of the slots. Such corners, which are useless for handling forces, must always be cut off.

Any nonuniformity in the distribution of stresses lowers the static, impact, and fatigue strengths of the design. When external ends are cut off and internal angles are rounded, the force flow created in the specimen is smoother, with uniform stress distribution in each cross section, but the stresses become nonuniform along the flow. By cutting off all excess material to constant width equal to the neck width, we also obtain uniform stressing over the length of the specimen. This equal-strength ribbon will have static strength equal to that of the previous smooth specimen and its dynamic strength will be higher. The equal-strength ribbon will be lighter than the original component; for this reason, it is always desirable to aim for equal strength in structural members and the design as a whole.

In addition to acute angles, slots, and holes, stress concentration may also result from defects in material and technology – welding nonpenetration, cracks, gouges, and scratches. A contact stress that arises, for example, from the pressure of a structural rivet or bolt on the internal surface of the material in a hole may also amplify or initiate concentration.

Stress concentration should be eliminated by eliminating its causes or by reinforcing the place in question by increasing the thickness of the material or adding a reinforcing plate.

§12.3. ADVANTAGES OF TENSION AND COMPRESSION OVER BENDING

It is known that the distribution of stresses over the cross section of a member working in bending and, consequently, also the utilization of its material, are nonuniform. Figure 12.12a shows the distribution of normal and tangential stresses in a rectangular-section beam, and Fig. 12.12b the distribution of

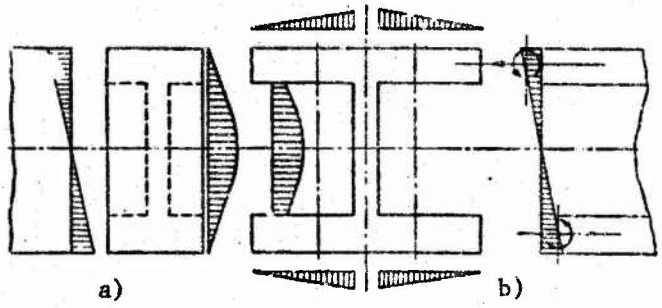

Figure 12.12. Stresses in rectangular (a) and I- (b) beams.

these stresses in an I-beam made from the same material and with the same section height, but with a wider flange. When the two beams are subjected to equal maximum normal stresses, the distribution of the normal stresses over the section height remains the same in the I beam, but stresses close to the maximum act on a larger area (owing to the wider flanges). These stresses can be regarded as heightwise-constant stresses from the pure tension and compression of the flanges and the small bending moments acting on each flange will redistribute the stresses in the heightwise direction.

The tangential-stress distribution obtained in the I-beam is also more advantageous, since the largest stress (at the neutral layer) is larger and, consequently, the wall material is better utilized.

Thus, structures designed to take up bending moments must be made in such a way that the elements of the structure are loaded to the maximum by tension, compression, and shear.

The effort to reduce bending stresses and obtain more uniform stress distribution has led to the practice of covering each "frame" of a frame-type spar with a sheet, thereby converting to a "webbed" structure, or inserting diagonal rods into the frames to obtain a "trussed" construction.

In a strutted wing, the moment bending the spars is reduced by making the strut work in tension or compression.

§12.4. USE OF THE LONGEST BENDING BASELINE

In certain structures, it is necessary to transmit a force P by transferring it parallel to itself over a distance l into a different plane (Fig. 12.13), in which the height h available is substantially shorter than l. This is done using a girder or beam with full advantage taken of the base height. This minimizes the weight of the girder or beam.

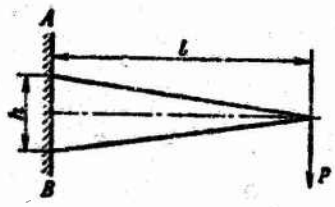

Figure 12.13. Use of the longest bending baseline.

Figure 12.14. Use of the longest bending baseline and longest contour in torsion.

The same principle obliges us to select a spar-flange cross section such that the material is situated as close as possible to the skin of the wing and the spars themselves are as close as possible to the maximum wing cross-sectional thickness (Fig. 12.14) and to design the jointing elements in such a way that they will transmit the forces acting along the flanges as close as possible to the wing surface without projecting from the wing.

§12.5. ADVANTAGES OF A MAXIMUM-AREA CLOSED CONTOUR IN TORSION AND A ROUND TUBE IN LONGITUDINAL BENDING

In some design cases, structural parts of an airplane are loaded by twisting moments.

Solid-section rods work poorly in torsion because the tangential stresses are distributed nonuniformly over the cross section. In a circular cross section, the maximum tangential stresses occur along the entire outer surface (Fig. 12.15a), while in a square cross section (Fig. 12.15b), the maximum stresses are

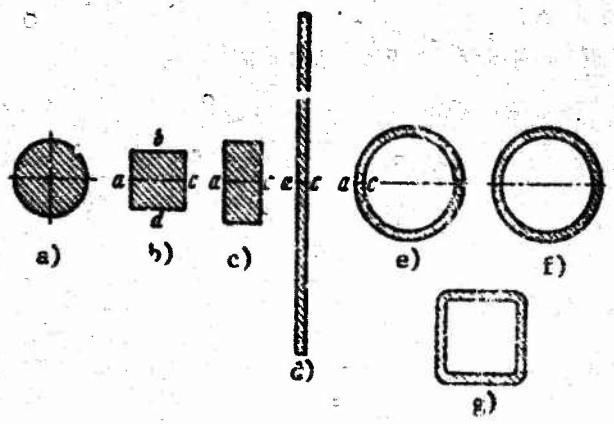

Figure 12.15. Cross sections of rods working in torsion.

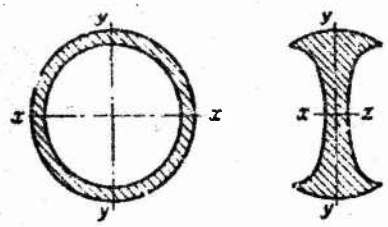

Figure 12.16. Cross section of beam equivalent to section of round tube.

obtained at points a, b, c, and d. These stresses will be larger for a given twisting moment in a square cross section of the same area as the round section. In an oblong rectangular cross section (see Fig. 12.15c), the maximum tangential stresses due to torsion are obtained at points a and c, and, other conditions the same, become even larger, and as the section is lengthened further (see Fig. 12.15d), they continue to increase. The stress does not change if this thin plate (Fig. 12.15d) is rolled up into a tube (see Fig. 12.15e) without joining the contacting edges. However, the picture changes abruptly if the edges are joined to one another, e.g., by welding (see Fig. 12.15f). In this case, the stresses decrease abruptly, are identically directed, and uniform along the contour, and practically constant in the direction across the wall. Tubes f and g can take much larger twisting moments and will twist through smaller angles than the solid rods a and b at the same material cross-sectional area. The round tube will be stronger and more rigid than the square one (Fig. 12.15g), because its contour encompasses a larger area for a given perimeter. In addition, the walls of round tubes

buckle under larger stresses than the flat walls of square tubes.

Round (solid) and annular cross sections are in general the optimum for rods working in torsion. For a given weight, it is expedient to increase the diameter of the pipe and the area inside the cross-section contour up to a certain point, even though the wall thickness will be reduced.

The principle of increased contour-section area holds for any form of closed contour. For example, in designing the structural contour of a wing cross section working in torsion (Fig. 12.14), it is advantageous to utilize the entire wing-profile contour unless it is broken by flaps or leading-edge slats.

The principle of utilizing the longest contour in tors does not apply when the contour is too long for the moment involved, since in this case the walls of the contour become so thin that they lose stability due to warping.

The round tube is the optimum design not only in the case of torsion, but also for longitudinal bending, because the moment of inertia of the round annular cross section is the same for bending in any direction and will be greater than the smallest moment of inertia of any other cross section for a given amount of material, e.g., that of the square tube (Fig. 12.15g). We note in passing that the round annular section will be the optimum for a revolving shaft under a transverse bending load imposed by a force of constant direction. In all other cases of transverse bending, the round tube will no longer be optimal. However, the tube does not work badly in bending: for example, it is stronger and more rigid than a square tube of the same weight. By shifting material along the neutral layer x toward the y axis in the annular section (Fig. 12.16), we obtain a section whose moment of inertia and modulus of strength approach those of the I-beam.

§12.6. CONCENTRATION OF FORCES IN MEMBERS THAT BUCKLE

Structural elements working in shear and compression may buckle.

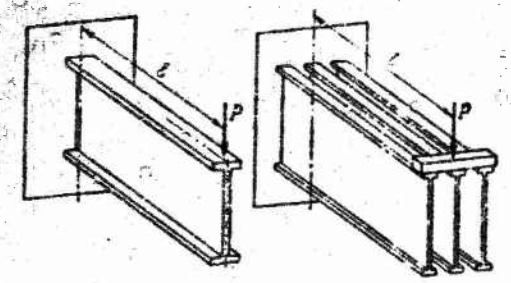

Figure 12.17. Advantage of transmitting bending through a single beam.

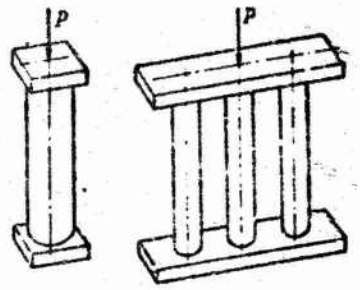

Figure 12.18. Advantage of transmitting compression through a single tube.

In all cases of such loading, it is advantageous to transmit the force through a single structural member rather than distributing it among several members working on parallel. By way of example, the right side of Fig. 12.17 shows three beams working together in bending under the action of a force P. If the tension flanges are strong enough, the compression flanges or the webs, which work in shear, may buckle as the force P is increased. In a single beam of the same height but with cross-sectional dimensions three times larger, the stresses – normal and tangential – will remain the same, but the stability of the flange and web will be more than three times greater. Consequently, the strength of the design is increased at the same weight or its weight has been reduced with no loss of strength.

Transmission of a compressive force through a single round tube (Fig. 12.18) of a given length will be more advantageous than transmitting it through several parallel tubes of the same length made with the same amount of material and with the same ratio of wall thickness to diameter, since the moment of inertia of the tube cross section and, consequently, the critical force are proportional to the fourth power of the diameter, and the cross-sectional area of the tube to the square of diameter. Given equal weights, one tube will carry more, and given equal strength, it will weigh less than several tubes.

§12.7. INCREASING THE LOCAL STABILITY OF THIN WALLS

As we know, thin walls may buckle in compression and shear.

Unsupported edges and flat wall areas buckle most readily; for this reason, the vertical members of an open profile do not

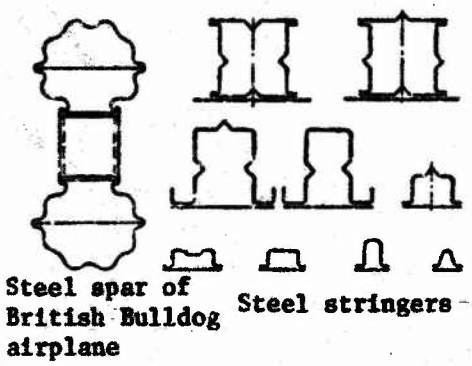

Figure 12.19. Cross sections of steel spar and stringers.

Figure 12.20. Cross section of spar of "Stal'-2" airplane.

perform as well in compression as those of a closed profile. Open profiles in structures that work in compression should be closed by use of an additional member. If unsupported edges remain, they should be reinforced to increase their stability by beading or rolling. Flat areas should be avoided or made as narrow as possible and bounded on both sides with small-radius foldovers. The latter serve as supports for the flat area.

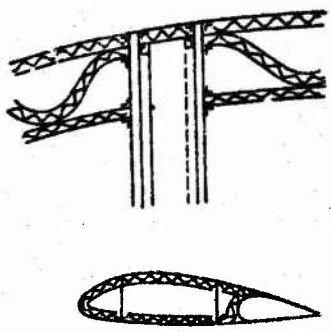

Figure 12.21. Thin-walled construction with corrugated reinforcement.

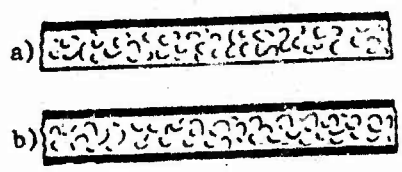

Figure 12.22. Sandwich-panel construction.

The smaller the curvature of the wall, the less stable will it be; compressed walls of small curvature and broad flat areas must therefore be reinforced by rolling grooves ("beads") into them or reinforcing them with section members or corrugated metal. Figure 12.19 shows a cross section through a steel spar and stringers used on the British Bristol Bulldog airplane. Figure 12.20 shows a cross section through the spar of the "Stal'-2" airplane designed by A.I. Putilov, and Fig. 12.21 the cross section of a hypothetical wing in which the entire structural contour is formed by two sheets of skin with corrugated metal between them.

These last two designs, which are built up from a series of adjacent cells, may be referred to as "honeycomb" designs. The spaces between the two sheets are now filled with a honeycomb structure that resembles the combs of bees, except that the axes of the hexahedral cells are directed normal to the skin instead of along the skin.

Finally, there is one more effective way to reinforce a thin wall for stability: reinforcing the sheet of metal with a layer of porous material, e.g., a foamed plastic. Figure 12.22 shows single-laminated (a) and sandwich (b) structures of this type.

§12.8. THE PRINCIPLE OF EQUAL STABILITY

We observed in §12.6 that when the diameter of a tubular strut working in longitudinal compression is increased with no change in length or weight, the thickness of the wall decreases, but the total stability of the strut increases until the wall buckles locally. On further increase in the diameter and decrease in the wall thickness, only local buckling occurs, with a decrease in local staoility (Fig. 12.23). Obviously, a design such that general and local buckling are equally possible will stand up under the largest force. This design will have the lowest weight for a given compressive force.

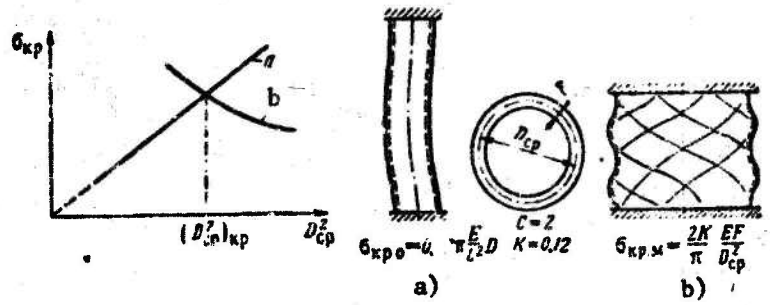

Figure 12.23. Buckling of compressed round tube: general (a) and local (b).

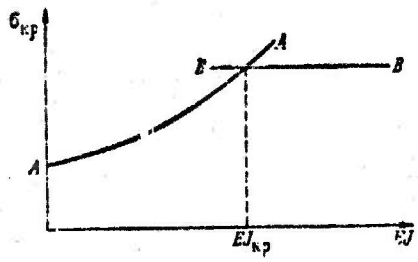

Figure 12.24. Local and general buckling on bending of fuselage.

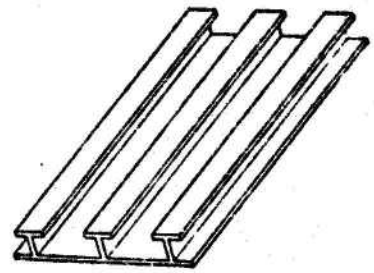

Figure 12.25. Monolithic panel with T-sections.

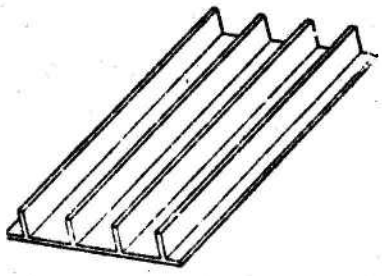

Figure 12.26. Ribbed monolithic panel.

Another illustration of use of the equal-stability principle is the circular-section fuselage working in bending [12]. Let us assume that with a given skin and skin-supporting stringers and with a given interval between bulkheads, the rigidity (EI) of the bulkhead cross section is inadequate and the fuselage loses general stability at a certain bending-moment value, i.e., the skin buckles inward together with the stringers and bulkheads. On an increase in the rigidity EI of the bulkheads, this buckling will occur at a larger bending moment and a larger σ_{cr} in the skin (Fig. 12.24, curve AA). At some critical value of EI, local buckling of the compressed panel between bulkheads will occur,

i.e., the skin will buckle with the stringers, but the bulkheads will remain intact.

On a further increase in bulkhead rigidity, only local buckling of the panel will occur, and the moments and σ_{cr} will stop increasing (line BB); consequently, an increase in EI will only increase the weight of the bulkheads. The value EI_{cr} will be the optimum.

Yet another example of use of the equal-stability principle can be found in the monolithic panel with stiffening ribs in the form of T-sections (Fig. 12.25), working in compression. This panel can be made by extrusion; it may be subject to general loss of stability of the entire panel or local stability loss of the skin between the ribs. The panel shown in Fig. 12.25 is not the optimum and is usually subject to local skin buckling, but it can be optimized by:

1) shortening the spacing between ribs and thereby increasing the stability of the skin;

2) lowering the stability of the ribs by making the T-sections smaller or going over to simple ribs without the T. The latter approach also simplifies manufacture (Fig. 12.26).

§12.9. CONTRADICTIONS BETWEEN PRINCIPLES

Each of the principles set forth above is valid within its own limits, and they may contradict one another. In this case, it is necessary to find a solution such that the weight of the structure is minimized with imperfect satisfaction of each of the mutually contradictory principles.

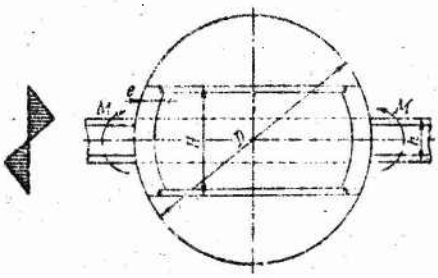

Figure 12.27. Optimum height of spar inside fuselage.

We consider the following problem as an example: it is necessary to run a wing spar through the fuselage of a single-

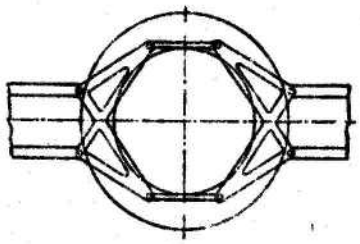

Figure 12.28. Transmission of moment through truss.

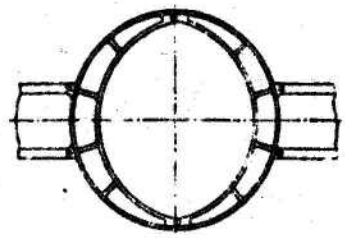

Figure 12.29. Transmission of moment across annular bulkhead.

engined airplane (Fig. 12.27), or, stated differently, it is necessary to compensate the right-wing moment M with an identical moment from the left wing working through a fuselage bulkhead. The principle of shortest force path calls for joining the starboard fasteners of the spar flanges to the port elements with rods working in compression and tension, i.e., inserting into the bulkhead a segment of spar with the same structural height h as in the outer wing sections. On the other hand, the principle of the longest bending base requires that the structural height H of this spar segment be increased to the extent permitted by available space in the fuselage. The problem can be solved approximately as follows: we place vertical members that work in bending and have a constant structural height e along the sides of the bulkhead and join the ends of these members by rods working in compression and tension. The expression for the weight of the entire frame for a given moment M as a function of frame height H is

$$G=2M\frac{\gamma}{\sigma}\left[\frac{\overline{D}}{\overline{H}}+\frac{3}{2}\frac{\overline{H}-1}{\overline{e}}\right], \tag{12.1}$$

where

$$\overline{H}=\frac{H}{h},\ \overline{D}=\frac{D}{h},\ \overline{e}=\frac{e}{h}$$

and is used to find the minimum of the resulting expression with respect to $\overline{H}$.

The minimum weight for the framework as a whole is obtained with

$$\bar{H}_{опт} = \sqrt{\frac{2}{3}\bar{D}\bar{e}} = \frac{1}{h}\sqrt{\frac{2}{3}eD} \geqslant 1, \qquad (12.2)$$

i.e., at a $H \geq h$, despite use of the vertical members that work in bending. This will be the optimum solution for this particular example.(1) It is also necessary to consider the case of unbalanced loads, e.g., from deflected ailerons. It will obviously be necessary to abandon the hinges and make the frame rigid; it will also be necessary to cover the bulkhead with sheetmetal beyond the limits of the frame if a passage must be left in the frame to conduct air to a turbojet engine. Depending on the required area of the cutout in the bulkhead, some other design may be optimal. For small cutouts, for example, it is better to replace the vertical girders by trusses (Fig. 12.28), and, conversely, if a large passage area is required, it is advantageous to use the entire bulkhead as an annular beam working in bending (Fig. 12.29).

§12.10. COMBINATION OF FUNCTIONS

As applied to stressed structural elements, the principle of combined functions consists in using the same structural element

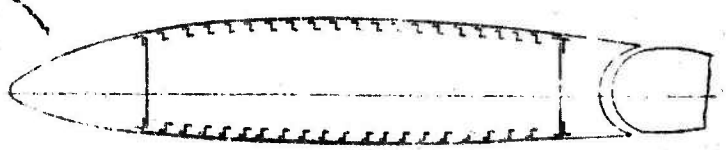

Figure 12.30. Shell wing.

to take several different loads.

An example of combination of functions can be found in a fuselage in which the external structural elements work with bending and torsion of the fuselage in all directions and accept

Footnote (1) appears on page 300.

aerodynamic loads from the external airstream, while the pressurized section of the fuselage is loaded by an internal excess air pressure. Another example is the shell wing section (Fig. 12.30), which, like the fuselage, works in bending and torsion with its panels accepting aerodynamic loads and the shell, if it is made airtight, also serves as a fuel tank. Such designs are widely used in modern aircraft, and if they have not displaced other constructions entirely, this is only because of the need to provide access to the inside of the wing and accommodate various other assemblies in it.

It should be noted that combination of stress-bearing functions usually results in a statically indeterminate structure. Damage to some elements of such a structure will not render it unserviceable, and this is yet another advantage. Like the other principles, the function-combining principle is not universal. There will always be structural elements with narrow special functions.

FOOTNOTE

Page No.	
298	(1) The solution presented here is a typical example of the mathematical design technique.

Chapter 13

BALANCE AND LAYOUT OF THE AIRPLANE

§13.1. GENERAL PRINCIPLES OF LAYOUT AND BALANCE

The layout of an airplane is related to the development of its external configuration and consists in accommodating the crew, equipment, and loads; it is accompanied by repeated determinations of the airplane's center of gravity. Layout culminates in elaboraton of a layout drawing in two projections with explanatory cross sections, with indication of the basic airframe elements and the center-of-gravity positions for characteristic loading cases.

To reduce errors in balancing the aircraft from the very outset, layout should begin with the wing, on which the designer plots the mean aerodynamic chord and marks the required CG position with respect to the airplane's aerodynamic center to obtain the required static stability. The other parts of the airplane and its loads are positioned relative to the wing in such a way that the airplane's center of gravity coincides with the position selected for it. It is desirable to place variable loads and loads produced in flight as close as possible to the airplane's center of gravity to minimize their effects on balance. Then the basic elements of the fuselage, wing, and tailplane frames are entered on the layout drawing, for the time being on axial lines, loads and machinery are accommodated and their centers of gravity marked; to begin, a common center of gravity can be used for

equipment. A table of balances is drawn up and the airplane's center of gravity determined. To bring the CG position into coincidence with the position stated for it on the mean aerodynamic chord, loads, machines, and equipment are at first shifted within the limits of the volumes available inside the airplane, and if this is not enough, the various parts of the airplane are shifted and their volumes adjusted, and the external shapes of the airplane may even be changed.

The heavier the load to be moved, the smaller the shift required to bring the airplane's CG to the required point.

It may be advantageous, for example, to shift the engine installations or the pilot's cabin with all of its weights along the x axis. If this requires lengthening the engine nacelles or the nose of the fuselage, the destabilizing moment is increased and it is necessary to increase the arm or area of the tailplanes. All of this will increase structural weight and require correction of the summary of weights and trims.

In this adjustment process, balancing should be done only with respect to the x axis. So that all arms x will be of the same sign, the nose of the fuselage is taken as the coordinate origin and the CG position $\bar{x}_{cg}$ is recomputed each time with respect to the forward point of the mean aerodynamic chord and as a fraction of its length. Only toward the end of the basic reconciliation is the position of the CG also determined with respect to the vertical ($\bar{y}_{cg}$).

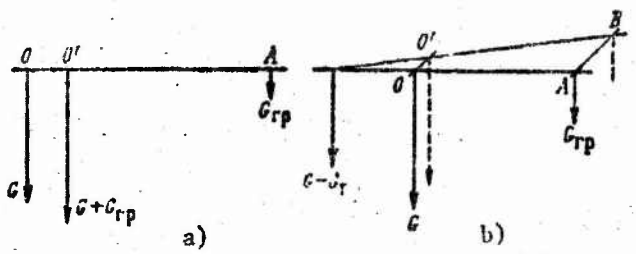

Figure 13.1. Shift of airplane's center of gravity due to a new load (a) and after shifting of a load (b).

The following simple rules are used to determine the CG position:

1. Loading an airplane of weight G with a load G_{ld} applied at point A shifts the airplane's center of gravity O toward point A by a distance (Fig. 13.1a)

$$\overline{OO'} = \overline{OA}\frac{G_{гр}}{G + G_{гр}}.$$

2. Shifting the load G_{ld} from point A to point B on an airplane having a weight G shifts the airplane's center of gravity O parallel to segment AB by a distance (Fig. 13.1b)

$$\overline{OO'} = \overline{AB}\frac{G_{гр}}{G}.$$

An effective method of correcting the balance consists in shifting the mean aerodynamic chord itself by moving the wing along the x axis.

This leaves fuselage layout unchanged, and if the sweep of the wing is changed instead of its attachment point, the structural frames to which the wing spars are attached will retain their positions in the fuselage. However, the mean aerodynamic chord can only be shifted through a small distance, since the aerodynamic centers of the fuselage and tail move with them and the center of the entire airplane is shifted in the same direction. If the center is moved forward, the airplane's stability margin is reduced and may drop below the required level. Furthermore, disposable and variable loads may prove to be too far from the airplane's center of gravity. If, in such cases, the main undercarriage is mounted to the fuselage, there will be a change in its longitudinal arm relative to the airplane's CG, which has been arrived at on the basis of takeoff and landing conditions. Finally, the new wing sweep may differ substantially from the optimum value selected.

Adjustment to the positions of machinery, structures, and loads are inevitable, and the weight and CG position of the airplane must be watched constantly to minimize the time required

for layout and balancing. If possible, any deviation should be corrected immediately by appropriate measures, and the change noted in the tables of weights and trends.

The layout must provide space for compressed-air, hydraulic, electrical, fuel, and gas lines.

§13.2. LAYOUT OF FUSELAGE

The fuselage accommodates the largest numbers of machines, loads, and elements of equipment.

In accommodating loads along the fuselage, it must be remembered that they are three-dimensional forms and that their positions must be considered not only along the length and up the height of the fuselage, but also across its width to give them the optimum positions from the standpoint of their performance, access to them, and passage between them; to this end, transverse sections must be indicated at the appropriate places in addition to the lateral projection.

Fundamental attention must be given to the layout of the flight deck. Good vision for the pilots must be guaranteed primarily forward and downward so that the horizon and the runway in front of the airplane will be visible. The requirement of good visibility is incompatible with aerodynamic requirements, since it is necessary to make a step in the fuselage for the canopy or provide a streamlined superstructure and bend down the upper line of the lateral contour in front of the canopy. As flight speed increases, the superstructural canopy must be made longer and the notch smoother. In modern supersonic aircraft, the long tapered nose may interfere with vision to such an extent that it is necessary to provide for deflecting the nose section downward at takeoff and landing.

Lateral vision is checked on a cross section through the flight deck. The instrument panel and instruments must be positioned so that the pilot can see them and they are well lighted.

The control column and pedals must be in the most convenient positions. All levers and knobs of other controls must be easily reached by the crew member in question and located in their customary positions. The position of the nose gear and its retracting mechanism is adjusted. Here the designer should be guided by the principles of structural-diagram elaboration. It is desirable to place the main nose wheel strut assembly in the plane of a bulkhead and to make certain in the cross section that the moment from the lateral force applied to the wheel is transmitted to the lateral zones of the bulkhead with the minimum weight penalty. The remaining structural components of the nose wheel to fuselage attachment should be placed as close as possible to the fuselage framing components; for this purpose, it is also necessary to adapt the fuselage structure.

For a military aircraft, all utility compartments, the entrance to the cockpit, and the position of the aft pressurized bulkhead must appear on the drawing. There may be a similar bulkhead forward if the nose section of the fuselage is unpressurized, e.g., if it accommodates the antenna and components of a radar. The bay for disposable loads is located near the airplane's center of gravity and various load configurations are laid out. Loads dropped in various flight situations must not strike anything on encountering the slipstream. Equipment that can be installed outside the pressurized cabin is also placed here. The special equipment of the military airplane, which depends on its mission, is accommodated in the unpressurized part of the fuselage, and the small wing volume of the modern military airplane makes it necessary to use the space in the fuselage around the airplane's center of gravity to accommodate much of the fuel as well.

In a passenger airplane, the passenger cabin and all other utility spaces are located aft of the flight deck. The width of the passenger cabin is determined by the number of seats abreast, and by the width of the seats and the aisle; here it can be

assumed that the armrests are on the level of the horizontal diameter of the cross section. Ceiling height should be sufficient to permit a man to stand in the aisle at full height without bumping anything with his head or shoulders.

The length of the passenger cabin is determined by the number of rows of seats and the interval between rows. Here it is necessary to know the maximum number of passengers and the longitudinal spacing that ensures an acceptable minimum of comfort. A smaller number of seats will make it possible to increase this interval; the seats must therefore be removable, with provision for attaching them to the floor at any longitudinal interval. It is desirable to have the window spacing coincide with the seat spacing for the passenger-load version taken as the basic one. The spacing of framers is also determined by the window spacing.

The space under the floor is used for baggage. Its inclusion in the pressurized compartment of the fuselage also simplifies the design and lightens its weight. However, loading and unloading passenger baggage from a long low space through one or even two small pressure-tight hatches will be difficult, and it may be found advantageous, even at the cost of increasing the design weight, to partition off all heavy-baggage compartments from the pressurized section. The optimum solution can be found for each particular case by an economy calculation in which the man-hours saved in loading and unloading and the reduction of passenger waiting time are compared with the loss of commercial load resulting from the increased design weight. The wing shell in the fuselage is usually separated from the pressurized cabin by pressure-tight walls.

Control runs through the pressurized part of the fuselage must be separated from the baggage and passengers by rigid walls, but it is also necessary to provide access to places at which inspection and servicing are required. Space for the stewardesses, wardrobe, hand-baggage compartment, galley, and lavatories must be provided within the pressurized part of

fuselage. Ducts for uniform distribution of conditioned air are run longitudinally through all areas.

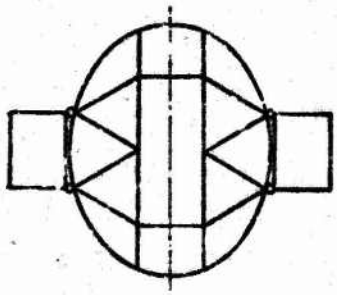

Figure 13.2. Tail bulkhead with aisle and pylons.

The pressurized part of the fuselage is separated from the unpressurized tail section by a pressure-tight bulkhead. This bulkhead will be lighter if it is made in the form of a spherical segment, but if a door is necessary or if engine or tail mounts are secured to the bulkhead's flanges and reinforcing rods and other members are added in the plane of the bulkhead, it is simpler to provide pressurization by covering the bulkhead with flat reinforced sheets. The space in the unpressurized tail section can be used for passenger baggage and other cargo. In arriving at the contours for the fuselage tail section, the designer is again confronted with contradictions, as he was in selecting those of the nose section.

From the aerodynamic standpoint, the tail section should be oriented in the direction of the wing downwash, i.e., it should be moved downward, but in order to obtain a large enough angle of attack at liftoff from the ground and during landing without an excessive increase in undercarriage height, it is necessary to bend the tail section of the fuselage, or at least the bottom line of its lateral contour, upward. The vertical tailplane is mounted on the fuselage tail section aft of the pressure wall, while the horizontal tail may be mounted on either the fin or the fuselage. Engine pylons are also attached here if the engines are carried on the fuselage tail section.

The general principle observed in designing all these attachments is that of transmitting the forces by the shortest possible route through the bulkheads into the skin of the fuselage, and the torque from the vertical tail also through the bulkheads, but into the entire fuselage contour.

If the horizontal tail is to be mounted on the fuselage, the problem is similar to that of the wing attachment. The same problem arises when engines are mounted on horizontal pylons on the fuselage tail section. If, at the same time, a passenger hatch and boarding ramp are to be provided in the tail section, the pylon spars may be made integral with fuselage bulkheads, and the bulkheads may be either annular or with a passageway as shown in Fig. 13.2.

Fuselage layout for modern passenger aircraft is discussed in greater detail in the book by S.M. Yeger' [30].

§13.3. LAYOUT OF ENGINE NACELLES AND LANDING GEAR

The layout drawing of the engine nacelle is made in the form of a lateral projection and a plan view with several cross sections. The outline of the engine and its accessories is indicated on the drawing and its attachment to the wing is developed. We recall that this attachment must transmit the maximum thrust to the wing with consideration of a strength margin, the weight of the engine plus normal acceleration, the engine's lateral inertial forces, and the reaction torque from the propeller in the case of piston and propjet engines. It may be found helpful from the standpoint of weight economy to attach the engine nacelle directly to spars instead of to ribs; this may require special superstructures on the wing. In accommodating the piston engine, the air intake is pointed directly upstream and the exhaust pipes as nearly as possible downstream in order to take advantage of the ram pressure and exhaust-gas reaction. If the elbows of the exhaust pipes are extended and combined into a manifold, it must be remembered that this will increase weight and that the back pressure will lower engine power output.

In laying out a turbojet engine nacelle, special attention must be given to the design of the inlet diffuser and exhaust nozzle. The intake should be designed in such a way as to have the minimal losses in all speed and altitude conditions during flight. During the standing start, air is drawn in by the intake

section from all directions, with some of the filaments even aspirated from the rear; as they round the leading edge of the intake, they may separate from the inlet-diffuser walls and reduce the air throughput through the intake. This must be taken into account in laying out the engine.

The entrance edge of the diffuser must provide smooth separation between the jet entering the engine, which supplies it with the necessary amount of air, and the free stream; obviously, lower altitudes and higher speeds will require smaller intake-stream and intake cross-sectional areas.

Regulation of intake area is unnecessary for subsonic aircraft, since the suction or pressure effect of the intake on the free stream regulates it automatically, causing it to contract or expand with the approach to the intake.

To prevent separation of the inlet stream from the leading edge on either the inside or outside, the edge must be thick and rounded. At supersonic speeds, a normal shock forms in front of a blunt edge, causing large losses at the intake; the edge must therefore be sharpened.

At low speeds, a sharp edge causes flow detachment at the intake, which results in large thrust losses. This contradiction is resolved by installing auxiliary doors behind the intake and opening them during takeoff.

Air must enter the compressor at supersonic speed; in flight at high supersonic speeds, therefore, the velocity of air must be reduced to subsonic with minimal losses. This can be done by setting up a system of shocks ahead of the intake or even inside the diffuser. For this purpose, a specially shaped cone is placed on the axis of a round intake or a wedge in a rectangular-section intake. To control this system of shocks and the intake area in accordance with changes in flight situation, the cone of wedge is relocated in flight along the axis of the intake stream, and in the case of the rectangular diffuser, its leading edges can also

be made to deflect.

As we see, the requirements made of the intake by various flight situations are strongly contradictory and the problem must be solved as follows. The optimum intake is designed for the airplane's basic flight regime and then "spoiled" slightly in favor of the other necessary regimes by changing the dimensions and introducing auxiliary controlling devices.

Still regarding the intake, we should add that it is absolutely necessary to heat a rounded entrance edge to prevent icing.

Contradictions are again encountered in the design and layout of the exhaust nozzle. The nozzle must therefore be variable to obtain maximum efficiency in the various flight situations. Nozzles are made reversible for deceleration during landing; this is a particularly important safety feature for heavy passenger aircraft.

In designing and mounting a reversible nozzle, measures must be taken to prevent structural damage from the high temperature of the reversed gas jet. Finally, heavy passenger aircraft are now required to have noise-abatement devices, which inevitably result in thrust losses. Sound-deadening devices are used on the engine mounts to muffle engine noise penetrating into the passenger cabin through the metallic structure.

Hot zones on the engine surface are cooled by air blown into the space between the skin of the nacelle and the surface of the engine.

The main landing-gear struts may be accommodated in the engine nacelle, in a separate nacelle, or in the fuselage.

Main landing-gear struts are accommodated well in the nacelles of propeller engines whose exhaust gases are diverted laterally.

Here the main hinge of the strut should be located as close as possible to the wing spar. As in the case of the engine installation, the undercarriage suspension may require an auxiliary load-

bearing superstructure to transmit forces from the landing gear to the wing. It is usually more convenient to retract the gear backward. The simplest system results when a strut with one or two wheels must be retracted; in this case, the lowered strut is positioned by its own hydraulic jack or a folding brace. To prevent the brace from folding of itself under compression, the axis of its middle hinge is offset from the axis of the brace. The brace upper hinge must be secured to the wing spar or the structural frame of the nacelle. The gear is usually retracted by a hydraulic jack, whose upper end must be rigidly supported. The lateral force on the wheel is taken up by bending of the strut, and the moment from this force by the force couple at its upper transverse attachment base; the twisting moment from the lateral force is transmitted to the strut through a torque-arm system and taken up by the same transverse base. The gear must be firmly locked in its lowered and retracted positions. The landing-gear doors are either operated by their own jacks or driven off the retracting mechanism.

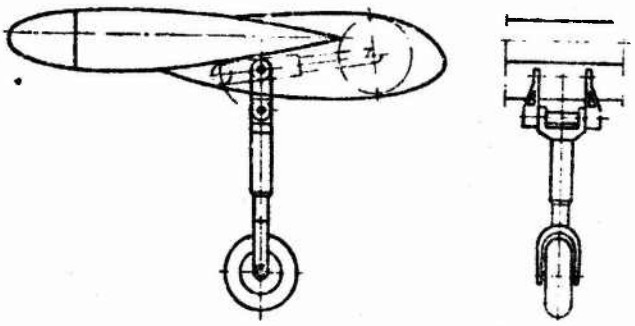

Figure 13.3. Jointed landing-gear strut.

If the landing-gear struts are long, but must be made as short as possible when retracted to reduce the shift of the center of gravity and to shorten the engine nacelle, the struts are made to "fold" by adding an additional element: on retraction, this link is folded forward and the strut itself backward. This scheme requires installation of additional mechanical links or an additional hydraulic jack. The two hinges of the link must

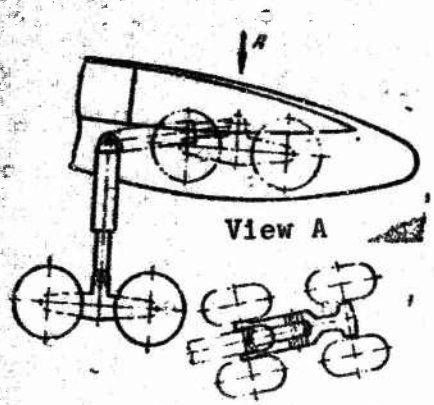

Figure 13.4. Retraction of truck without tilting.

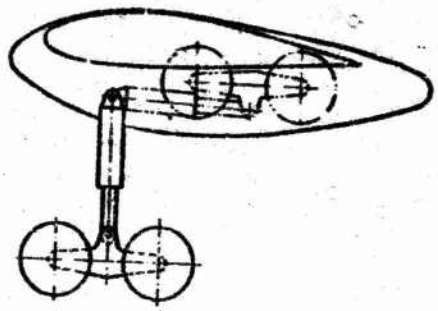

Figure 13.5. Retraction of truck with tilting.

have spatially separated transverse bases, and the link itself must be adapted to transmit the lateral force applied to the wheel (Fig. 13.3).

The undercarriage design is more complicated if it has a two-axle truck, since the truck must be attached to the strut on a hinge because otherwise the front and rear wheels would not touch down simultaneously at landing; the new hinge calls for the addition of new mechanical links or a new jack.

To accommodate the truck easily in the nacelle, it must take a horizontal position. Let us consider two schemes by which a four-wheeled truck can be retracted.

1. During retraction, the truck's motion is translational and it retains its horizontal position. To reduce the height of the landing gear in the retracted position, the truck must be made wider so that the strut can fit into the split forward end of the frame in the retracted position as it is deflected through more than 90° from its initial vertical position (Fig. 13.4).

2. On retraction, the truck is tilted through 180° and pulled into the nacelle wheels-up. Then the retracted strut will occupy a position between the wheels underneath the truck frame, and it will not be necessary to increase the wheel track (Fig. 13.5).

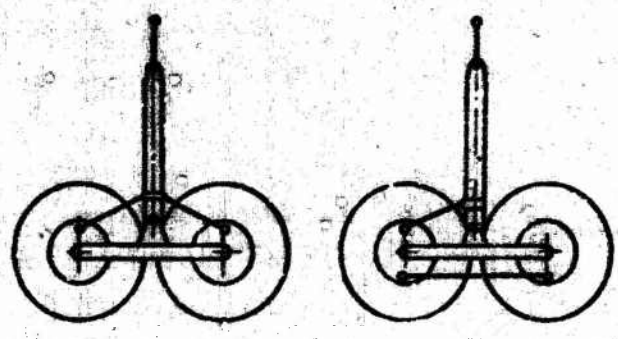

Figure 13.6. Transmission of braking torque to strut.

In either case, the corresponding motion of the truck during retraction can be obtained by use of additional mechanical links or additional hydraulic jacks.

In the second variant, the truck is simpler and lighter, but tilting it complicates the retraction mechanism.

In the first variant, it is also possible to lighten the weight of the truck by lengthening the strut and raising its upper hinge enough to prevent the retracted strut from resting against the truck frame, but the longer strut will require a longer nacelle.

The choice among these three variants can be made on the basis of calculation of the weight of each of them.

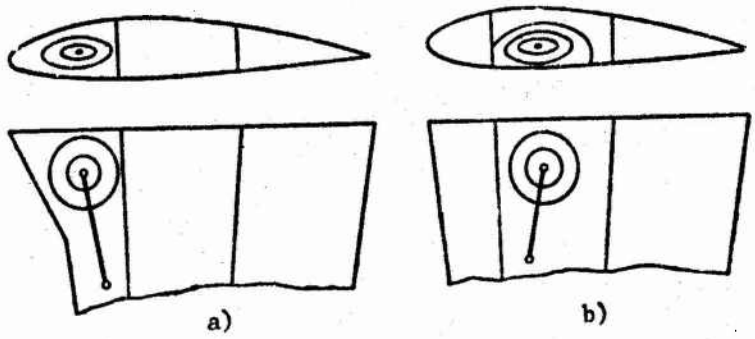

Figure 13.7. Retraction of landing gear into straight wing. a) In leading-edge section; b) in central section.

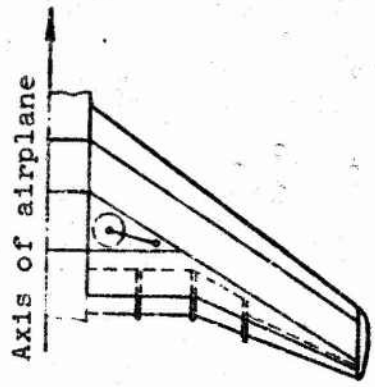

Figure 13.8. Layout of swept wing.

The landing-gear strut with hinged truck presents one more complication involving the operation of the brakes. In a braked wheel, one part of the braking device revolves with the wheels, while the other must be secured in a fixed position. If this part is mounted on the truck, the braking torque from the wheels will be transmitted to the truck and cause it to turn in the direction of wheel rotation. This moment will impose an additional load on the front wheels and take load off the rear wheels, causing uneven tire wear. To prevent this, it is necessary to transmit the braking torque not to the truck, but to the landing-gear strut. This is done by a system of rods that connects the stationary brake disks directly to the strut; these rods must not interfere with retraction of the gear (Fig. 13.6).

The above main-undercarriage-strut designs are also used for retraction into special nacelles placed behind the structural shell of the wing.

If wing dimensions permit, the main gear is retracted into the wing.

Retraction of the main-gear wheel into the root section of the wing or the bottom of the fuselage is convenient if the undercarriage uses a tail wheel (Fig. 13.7). However, if the main undercarriage strut is located aft of the airplane's center of gravity, it can be retracted conveniently only into a swept wing; in this case, the wheel is fitted into the triangle formed by the aft oblique and auxiliary straight spars (Fig. 13.8).

We have been concerned with methods of retracting struts with single wheels. The same methods are also applicable for retraction of multiwheel trucks. Here it must be made certain that the truck is accommodated with maximum convenience in the space allotted for

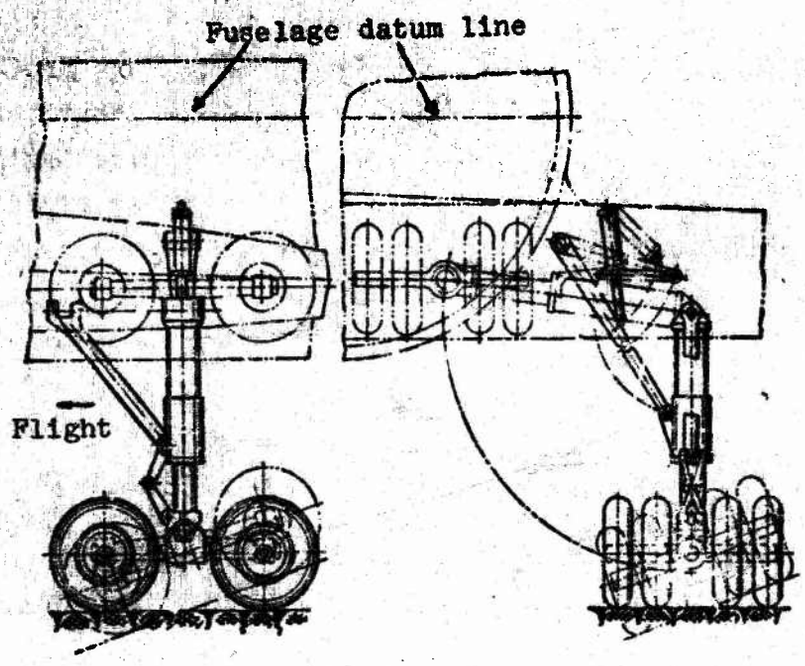

Figure 13.9. Retraction of undercarriage truck into fuselage.

it, if necessary by rotating it around the strut. Figure 13.9 shows one possible way of retracting a multiwheel truck into the fuselage of a subsonic passenger airplane.(1)

This scheme makes it possible to dispense with the landing-gear nacelles at the cost of a slight increase in the diameter and weight of the fuselage. Any advantage of this scheme over those using landing-gear nacelles can be brought out only by comparative calculations of the weights and frontal drags.

§13.4. LAYOUT OF WING

The basic problems involved in laying out the wing are selection of the wing profiles and accommodation of structural elements. As concerns accommodation of loads and machinery in the wing, this problem is solved on the basis of the same principles that prevailed in fuselage layout.

Footnote (1) appears on page 321.

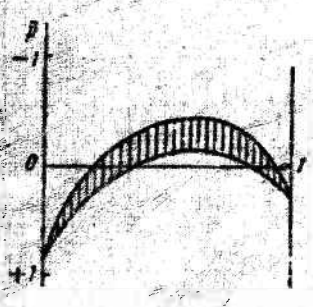

Figure 13.10. Distribution of pressure on a laminar profile.

In selecting the profiles, it must be remembered that there are two modern profile types: laminar and M-stable. The laminar profile has low frictional resistance. This is achieved by moving the point p_{min} (the point of transition from the laminar to the turbulent boundary layer) as far as possible from the profile leading edge (Fig. 13.10), since turbulization of the boundary layer is inevitable aft of this point, in the zone of positive pressure gradient ($d\bar{p}/dx > 0$). The negative gradient forward of the point p_{min}, which helps preserve laminar flow, decreases with increasing c_y, and the value $d\bar{p}/dx = 0$ corresponds to the upper limit in c_y of the laminar segment on the polar curve. At this upper limit of laminar flow, the point $\bar{p}_{min}$ and, consequently, also the transition point $\bar{x}_t$ are located near skin convexities. The same effect results from surface roughness, and for this reason the skin on the laminar segment must be thick and polished until the continuous-roughness high spots are reduced to 3-4 μ. The laminar profile is almost ineffective when the wing is in propwash and when there are sheet-metal joints at the leading edge with chinks and even flush rivets that have not been filled and ground down.

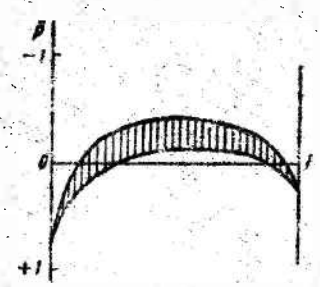

Figure 13.11. Distribution of pressure on M-stable profile.

In the M-stable profile, the onset of wave drag is shifted to a large Mach number. The principle embodied here is that at a given c_y, as expressed by the shaded area (Fig. 13.11), the maximum local velocity should differ as little as possible from the flight speed, i.e., $\bar{p}_{min}$ should be as small as possible.

The basic requirement made of the skin on the M-stable profile is rigidity, since increased rippling in the minimum-vacuum zone increases $\bar{p}_{min}$.

It is not yet possible to use purely supersonic profiles (wedge, rhomboid, trapezoidal, etc.) for supersonic airplanes because they are characterized by small $c_{y_{max}}$. Even the thin symmetrical profiles that are in use have rather sharp leading edges and do not give large c_y. To increase c_y, the detrimental effect of the sharp leading edge is compensated by deflecting it downward at takeoff and landing and by the use of stronger high-lift devices on the trailing edge. In laying out the shape of a supersonic wing, use is also made of what is known as "conical twist" of the leading edge.

This leading-edge form sets up conical supersonic flow over the leading edge, with increasing vacuum toward the wingtips and at the wingtips, forward-directed force components that reduce frontal drag.

Regarding the positioning of the main structural elements of the wing, two possible schemes are of interest:

1) the wing of large aspect ratio and small taper for subsonic speeds and 2) the wing with small aspect ratio and large taper for supersonic speeds. In the first wing layout, there are usually two spars running on either side of the line of maximum thickness and joined by upper and lower panels. They form a structural shell that accepts bending and twisting moments.

For strongly swept and large aspect ratio wings, it is better to place the ribs perpendicular to one of the spars so that the ribs can be shorter. Fuel is usually carried in the shell, and the best utilization of volume and minimum fuel-system weight will be obtained if the fuel is put directly into the pressure-tight shell. If insert tanks are used, part of the lower panel must be made removable.

It is desirable to avoid transverse assembly joints in the wing, and the panels must be made long for this purpose.

Panels are made from thick skin, which is reinforced by the stringers, and, if heavily loaded, they are made monolithic with T- and simple ribs. Deicing heat and slats may be called for at the leading edge; passages for the heating gases and boundary-layer blowing are also accommodated here. The ailerons and main flaps are suspended on the trailing edge; the control runs usually pass in front of and behind the shell.

In the second wing design, the number of spars is increased and the spars are placed perpendicular to the fuselage axis. In this case, the part of the wing between the spars is used to hold fuel, for which purpose some of the compartments are sealed. Skin panels are monolithic without transverse joints and, consequently, for the most part extruded with parallel simple ribs; their thickness can be reduced smoothly toward the wingtips for spanwise-equal strength, e.g., by milling. To place the ribs as close as possible to the straight lines of the ruled surface of the wing, it is better to extrude narrow panels and, for example, lay one narrow panel of constant width along the line of maximum profile thickness and cut one edge, together with the ribs, diagonally off the others; these trapezoidal panels are laid on the wing with their uncut edges closest to the line of maximum profile thicknesses. Narrow panels of this type are easily bent lengthwise and crosswise and can be shaped even to an unruled wing surface.

§13.5. LAYOUT OF TAIL

The relative positions of the horizontal and vertical tailplanes must be such that they blanket one another as little as possible at the various combination of attack angle α and slip angle β, i.e., it is desirable to have them at different longitudinal coordinates on the fuselage, but then one of the tailplanes will have a much shorter arm from the airplane's center of gravity and require an increase in area. If the horizontal tailplane is mounted on the vertical tail or near its top, the sweeps

of the two tails will move them away from one another and, in addition, increase their arms with respect to the airplane's center of gravity. However, when the horizontal tail is mounted this high, the loads on the vertical tail are increased and it becomes heavier. The horizontal tail can also be placed on the tail section of the fuselage if this section does not carry engines.

For flight with sideslip, the flow past the round fuselage may be regarded as composed of two flows: longitudinal and transverse; in the transverse flow around the cylinder, the maximum velocities are obtained on the upper and lower fuselage generatrices. These crossflows increase the local skewness of the filaments and cause premature separation at the leading edge of the fin root section. To blanket this detachment out at large angles β, a fence whose height decreases toward the front of the fuselage is placed in front of the fin. This fence directs the local flow along the fuselage and also puts part of the lateral projection area of the fuselage to work, permitting a slight reduction in the area of the vertical tailplane.

Moving the vertical tailplane back lowers the height of the airplane, which is important for hangar storage of the airplane, reduces the mutual blanketing of the tail surfaces and increases the effectiveness of the horizontal tail, though at the same time increasing its weight.

With increasing speed, the planform of the tail surfaces and their profiles change in the same way as those of the wing. At subsonic speeds, a slightly swept and rounded leading edge may ice up, so that deicing heat must be supplied to the fin and stabilizer leading edges.

The control surfaces of large fast airplanes must have aerodynamic and gravity compensation. Axial aerodynamic compensation has an advantage over the servo tab in that the compensating weights can be distributed uniformly.

There are certain analogies between the structural diagram and design of the tail and those of the wing. For large fast airplanes, extruded, stamped, etched, and milled panels can be used on the stabilizer and fin, with excess weight removed. The control surfaces are required to be very light, so that the weight of the trimmers can be reduced. Honeycomb designs may be found advantageous for these surfaces.

FOOTNOTE

Page No.	
315	(1) This scheme was proposed by Engineer A.I. Gladkov.

Chapter 14

EXAMPLE OF APPLICATION OF THE PRINCIPLES OF PRELIMINARY DESIGN

§14.1. CONTRADICTIONS ENCOUNTERED IN MEETING PERFORMANCE REQUIREMENTS FOR THE AIRPLANE AND METHODS OF OVERCOMING THEM. THE VARIABLE-SWEEP WING

As we noted in Chapter 1, many of the design measures that improve one of the flight characteristics are at the same time detrimental to another. We cite a few typical examples.

To attain high supersonic speeds, use of wings with very thin profiles is mandatory. When the profile becomes very thin, however, the wing cannot be given a large aspect ratio, since it becomes very heavy and sags badly. On the other hand, reducing its aspect ratio lowers the maximum lift/drag ratio at subsonic flight speeds, with the result that the maximum subsonic flight range is shortened.

Reducing the thickness of the profile and increasing the wing's aspect ratio lowers $c_{y_{ldg}}$ and, consequently, increases landing speed and rollout distance. Thus, by taking design measures that increase supersonic top speed, the designer sacrifices maximum range and lowers the takeoff and especially the landing properties of the airplane.

The demand for higher top speeds from subsonic aircraft also shortens maximum range if the requirement is met by increasing

available engine thrust and, consequently, engine weight, since these measures increase the relative weight of the powerplant and lower the relative weight of the fuel if the relative weights of the payload and structure remain constant.

The requirement for higher ceiling, which is met by increasing the thrust/weight ratio P/G or by reducing the load per square meter of wing by increasing its area (see §5.3), also shortens subsonic and supersonic flight ranges, since the relative weight of the fuel is reduced.

If the requirement for a higher ceiling at supersonic speeds is met by increasing aspect ratio, the contradiction vanishes, since the increase in maximum lift-drag ratio is advantageous for both ceiling altitude and subsonic range. At the same time, increasing the wing aspect ratio requires a thicker wing profile, and this results either in a lower top speed or, if V_{max} is unchanged, an increase in engine thrust, engine relative weight, and, in the final analysis, a decrease in the relative weight of the fuel with the consequent shorter flight range. If ceiling altitude is increased by increasing engine thrust, there is an attendant increase in subsonic or transonic top speed. If, on the other hand, the ceiling is raised by increasing the area of the wing, the airplane will have a lower top speed. We stress that increasing M_{lim} and, consequently, the permissible speed limit simultaneously increases ceiling altitude (see §5.3) and supersonic range (see §6.3).

General methods of resolving specification contradictions were set forth in Chapter 1. In this case, the most correct procedures for overcoming the above contradictions are: a) use of improvements and design measures that improve one flight property of the airplane without detriment to the others; b) proper selection of design solutions with which an improvement of one indicator is minimally detrimental to the other; c) use of compromises that satisfy the requirements as to the basic flight qualities at the cost of some impairment of other, less important qualities

of the airplane. For example, by deflecting the wing leading edge and blowing the boundary layer off the leading edge and off the flaps to improve $c_{y_{ldg}}$, we improve the takeoff/landing properties of the airplane at the cost of a small decrease in flight range due to the slight increase in the design weight of the wing.

Obviously, all measures that improve maximum lift/drag ratio are desirable if they are not accompanied by any marked decrease in $c_{y_{ldg}}$ or increase in the structural weight of the wing, as are measures that reduce design weight with no change in strength and rigidity.

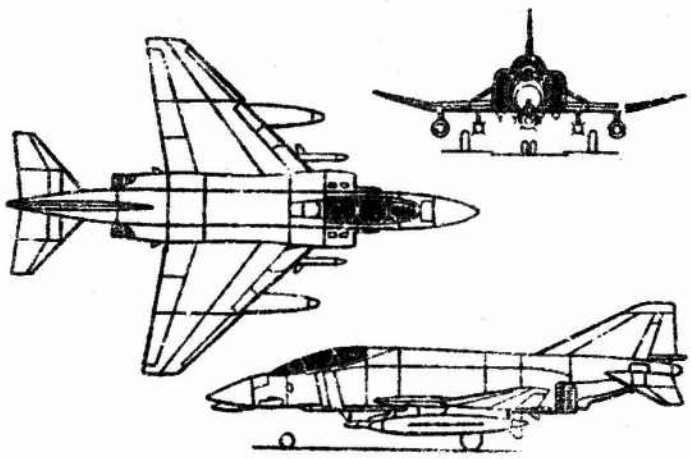

Figure 14.1. McDonnell F-4E Phantom multipurpose fighter-bomber. G = 20,850 kg, S = = 41.2 m^2, P_{11} = 15,400 kgf, M_{11m} = 2.1, H_{clg} = 17,800 m.

Let us present an example of proper selection of a design measure that aids in resolving contradictions among several properties. Let us assume that it is necessary to obtain a higher supersonic ceiling. This can be done by increasing either thrust or wing area. Using high-lift devices on the wing to obtain the large $c_{y_{ldg}}$ that ensures the required landing speed, it is more advantageous to go to increased thrust, since a larger $\bar{P}$ = = $P_{11}/2Q_{011}$ reduces accelerating and climbing fuel consumption

(see §6.5), lowers the per-kilometer fuel consumption rate at supersonic speeds, increases the airplane's throttle response, and makes ceiling less dependent on temperature in the stratosphere.

Another example of a correct solution can be found in establishment of the wing speed angle for modern multipurpose supersonic aircraft. A delta wing with sweep equal to or greater than 60° has the least frontal drag and lightest weight. However, the subsonic maximum lift/drag ratio and $c_{y_{ldg}}$ are lowered when this wing is used. In order to increase K_{max} and $c_{y_{ldg}}$, therefore, the last series-produced American multipurpose airplane, the F-4E Phantom (Fig. 14.1) has a near-delta wing with clipped tips and a sweep of only 45° (at quarter-chord).

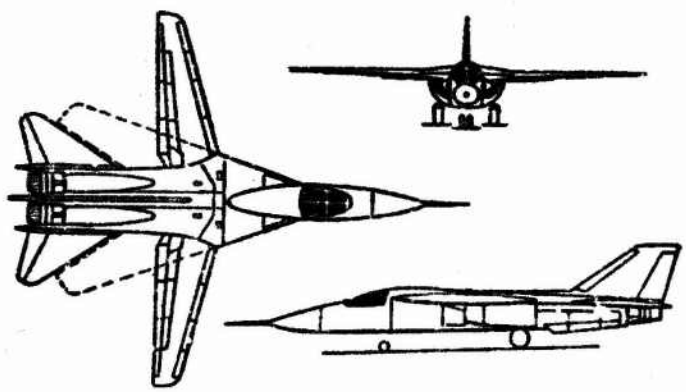

Figure 14.2. Dynamics Grumman F-111A multipurpose fighter-bomber. G = 32,000 kg, S = = 57-64 m^2, P_{11} ≈ 24,400 kgf, M_{lim} = 2.5, H_{clg} = 18,000-19,000 m.

A highly advantageous design measure, and one that eliminates a whole series of the contradictions spoken of above, is the use of the variable-sweep wing on supersonic aircraft.

Figure 14.2 and 14.3 show modifications of the American F-111 multipurpose airplane, which has such a wing. As the sweep is

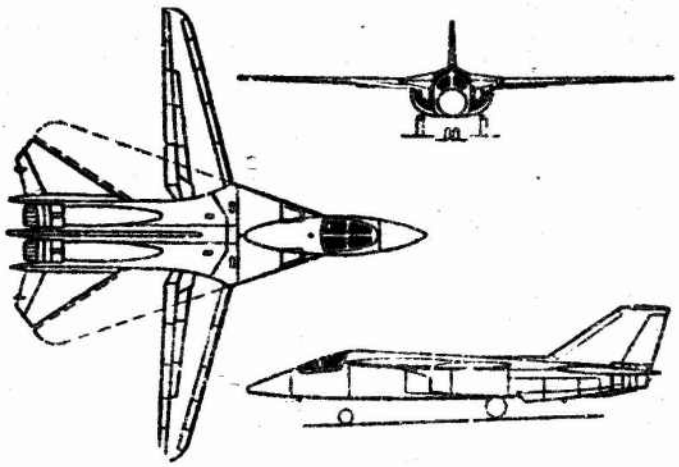

Figure 14.3. Dynamics Grumman F-111B multipurpose fighter-interceptor.

increased, the wing profile thickness ratio parallel to the stream decreases, and this reduces the frontal drag in supersonic flight. The very slight or nonexistent wing sweep at takeoff and landing, together with the use of modern high-lift devices on the wing, makes it possible to increase the $c_{y_{ldg}}$ of such an airplane (see §7.2) by 2-3 times over the $c_{y_{ldg}}$ of an airplane with a strongly swept wing. As a result, the wing area of a swing-wing aircraft can be reduced, with the effect of increasing supersonic range and zero-altitude range at $M \geq 0.8$-0.* with no change in supersonic-ceiling altitude.

When such an airplane flys at $M = 0.85$-0.90 with a 35°-45° wing sweep, the geometrical aspect ratio of the wing is increased over that of a wing swept 60-70°, with the result that the airplane's K_{max} and maximum transonic range increase. The increase in range occurs despite a slight increase in the structural weight of the wing. A disadvantage of the variable-sweep wing is the complication of the wing's design and the resultant higher cost of the airplane. However, a swing-wing airplane is capable of more successful performance of various tactical missions with changes in armament and certain items of equipment. On the other

*Translator's Note: Illegible in foreign text.

hand, supplying the air force with multipurpose aircraft that require only changes in armament and equipment to perform a variety of tactical missions reduces the number of aircraft types in series production and thereby increases the number of aircraft of the same type that are ordered. This increase in the number of similar aircraft sold makes possible a substantial reduction of their cost.

This is why complicating the design of an airplane does not always make it more expensive.

§14.2. SELECTION OF POWERPLANT TYPE AND LAYOUT OF SUPERSONIC AIRCRAFT

At the present stage in the development of aviation engines, it is convenient to power supersonic aircraft either with afterburner-equipped turbojet engines or ducted-fan turbojets with afterburning in the fan and duct streams. The ducted-fan engine with fuel afterburning in both streams has a lower specific weight at $M = M_{lim}$ and is shorter than the turbojet engine. However, it develops much less thrust per unit frontal area of the engine and consequently develops the same thrust as a turbojet only with air-intake ducts of larger frontal area. This increases powerplant weight and, if the engines are housed in nacelles and not in the fuselage, which has a midships section larger than that of the engine, also increases the frontal drag of the airplane. As compared with turbojets, ducted fans have lower specific fuel consumption rates at transonic speeds.

If a supersonic airplane must have a longer transonic flight range (at $M = 0.85$-0.9) and a longer range in zero-altitude flight, the fanjet may obviously have the advantage over the turbojet. If the midships cross section of the engine nacelles or the fuselage is determined by the engine midships section and the airplane will fly basically at high altitudes and $M \approx M_{lim}$, preference must be given to the turbojet.

Looking farther ahead in time, when increases in the temperature ahead of the turbine have made it possible to increase

the thrust of the turbojet without afterburning and to fly at $M = M_{lim}$ without afterburning, use of turbojets with low compressor pressure ratios will be advantageous for aircraft from which it is important to secure longer supersonic flight ranges.

Selecting the airplane's configuration is the first step in preliminary design. The designer selects it even though he does not yet know the weight of the airplane, its dimensions, or, in many cases, even the amount of engine thrust. However, by determining the payload weight from the technical specifications for the airplane and knowing the range requirement, the designer can always use statistical material for a rough estimate of the airplane's weight. This estimate is necessary because the optimum configuration of the airplane depends on its size.

We shall be concerned primarily with supersonic aircraft whose normal takeoff weights do not exceed 30,000-40,000 kg. Let us stipulate at the outset that by supersonic we mean fully supersonic (see §5.3), i.e., not only the top speed, but also the speed of flight at the ceiling are supersonic.

Thus far, such aircraft have been built only with swept or delta wings and tails situated aft of the wing, or in the form of a flying delta wing with 60° leading-edge sweep (Mirage III, Mirage IV, F-106). An exception is the well-known Lockheed F-104, which has a straight thin-profile trapezoidal wing. Analysis of the flight-performance characteristics of the aircraft that have been built has shown that flying-wing types have very small $c_{y_{ldg}}$. To lower their landing speeds, therefore, the designers were obliged to reduce the load per square meter of wing considerably and lower the values of P_{11}/S and $P = P_{11}/2Q_{011}$. As a result, the performance characteristics of such aircraft came to depend heavily on stratosphere air temperature, their per-kilometer fuel-consumption rates at supersonic speed were found to be very high, and their interception radii shorter.

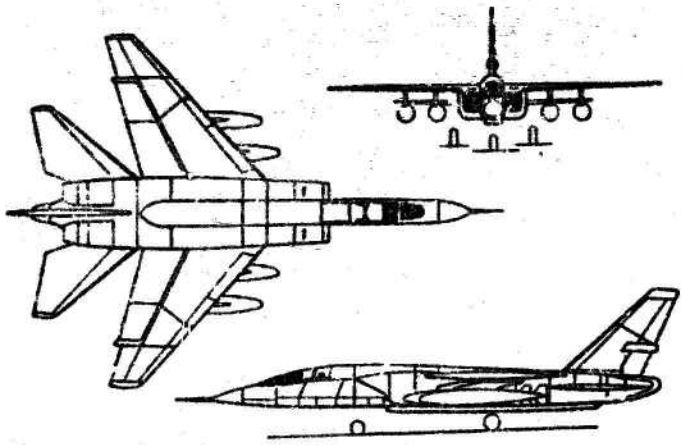

Figure 14.4. Carrier-based North American Vigilant reconnaissance bomber. G = 22,470 kg, S = 65 m^2, P_{11} = 15,400 kgf, M_{lim} = = 2.1, H_{clg} = 18,200 m.

On the whole, comparative flight-performance analyses of aircraft have shown that the flying-wing configuration is not justified for aircraft weighing less than 40-50 tons.

The configuration with trapezoidal unswept wings and conventional horizontal-tail position used in the F-104 has not been repeated. Such a wing must be very thin and will have acceptable weight only with a small aspect ratio (<2.5). Under these conditions, it has no advantages over the 45°-50° swept wing. And the capacity of the straight wing is smaller than that of a delta wing with clipped ends, as used, for example, on the Phantom fighter (Fig. 14.1). Among other things, it becomes impossible to retract the wheels into the wing. The optimum wing for multipurpose aircraft with fixed-sweep wings is the delta with clipped tips and a 40-45° sweep angle, like those of the Phantom and the American Vigilant carrier-based reconnaissance bomber (Fig. 14.4). An aspect ratio of 3-4 can be obtained with such thin-profile wings and this greatly increases the maximum lift/drag ratio at transonic speeds.

If high performance in supersonic flight is all that is important for the airplane, it may be found advantageous to use delta wings with a 60° or greater leading-edge sweep. This in spite of the fact that a wing of this type with an aspect ratio of about two will have a smaller $c_{y_{ldg}}$, even with improved high-lift devices, than the wings of the aircraft shown in Figs. 14.1 and 14.4.

Full-span flaps are used on such foreign aircraft as the F-111A (Fig. 14.2), the Vigilant (Fig. 14.4), and the experimental British TSR-2 in order to increase $c_{y_{ldg}}$, and rolling moments are set up not with ailerons but with the stabilizers, whose halves can be deflected in opposite directions, and with spoilers.

Table 14.1

χ at leading edge	Span, m	S of wing, m^2	Aspect Ratio: With projecting part of wing	Aspect Ratio: Without projecting part of wing	$\bar{c}$ of profile	M = 0,85: c_{x_0}	M = 0,85: A	M = 0,85: K_{max}	M = 2,5: c_{x_0}	M = 2,5: A	M = 2,5: K_{max}	$c_{y_{noc}}$
16°	19,2	64	5,75	7,65	0,072	—	—	—	—	—	—	≈2
50°	14,6	60	3,56	4,85	0,06	0,014—0,016	0,013	3,4—12,5	—	—	—	—
72,5°	9,74	57	1,66	—	0,04	—		—	0,025	0,56	4,22	—

In almost all aircraft in the previously mentioned weight range, the engines are housed in the tail section of the fuselage or beside it. The air intakes usually run along the flank of the

fuselage and are not placed in its nose section; this shortens the air passages and is advantageous from the standpoint of accommodating radar equipment.

As we have noted, the swing-wing airplane is a highly advantageous configuration. Table 14.1 shows how the geometrical and aerodynamic characteristics of the F-111A multipurpose fighter-bomber depend on wing sweep. Some of the figures given in the table were calculated. We see that this combination of figures is clearly unattainable with an aircraft having a fixed-sweep wing. It may be assumed that the variable-sweep wing will soon come into very widespread use.

We turn now to the problem of the relative positioning of the wing and fuselage. Supersonic-aircraft engineering practice shows that the mid-, low-, and high-wing arrangements are used with equal frequency on aircraft with their horizontal empennages behind the wing.

In the low-wing scheme, the wing is closer to the ground, and this increases $c_{y_{ldg}}$, improves lateral stability, and makes it possible to retract the wheels into the wing instead of the fuselage, thus simplifying and lightening landing-gear design. In the high-wing modification, it is easier to use fuselage space to accommodate weapons. This position is also convenient for the variable-sweep wing. Interference between the wing and fuselage is minimal for the mid-fuselage position of the wing, but utilization of fuselage capacity is least convenient.

If high performance at subsonic speeds is not required of the airplane, but a very high supersonic ceiling is needed, a flying delta-wing layout with a small G/S but with the parameters P_{11}/G and $\bar{P} = P_{11}/2Q_{011}$ near or greater than unity without fail may be found rational for this special-purpose high-altitude supersonic airplane. In this case, the flying-wing configuration is expedient because the landing-speed requirements are satisfied by the small G/S and a flying wing of large area has

a small c_{x_0}. The important point is that with the large wing area, all measures that reduce c_{x_0} are vital, since a decrease in the product $c_{x_0}S$ makes it possible to reduce the thrust output of the turbojets and, consequently, powerplant weight.

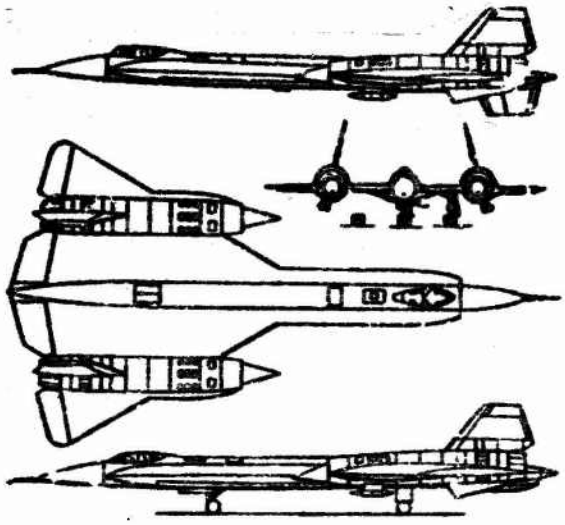

Figure 14.5. Lockheed SR-71 strategic reconnaissance aircraft. $G = 61{,}700$ kg; $S \approx 186$ m^2; $P_{11} \approx$ $\approx 50{,}000$ kgf, $M_{lim} = 3$, $H_{clg} =$ $= 22{,}000$-$23{,}000$ m.

In choosing a configuration for a supersonic airplane with a wing area greater than 100-150 m^2, the designer encounters difficulty in obtaining the necessary wing angle of attack without excessive lengthening of the landing gear. When the empennage is aft of the wing, the distance from the airplane's center of gravity to the fuselage tail support becomes so long that a landing angle of 10°-13° can be obtained only with an unacceptably high undercarriage.

Figure 14.5 shows a diagram of the Lockheed SR-71 (A-11) and Fig. 14.6 a diagram of the B-70 experimental strategic reconnaissance aircraft. Figure 14.7 presents diagrams of supersonic transports – A.N. Tupolev's Tu-144 and the designs for the American Lockheed 2000 and the Anglo-French Concorde. We see that of these

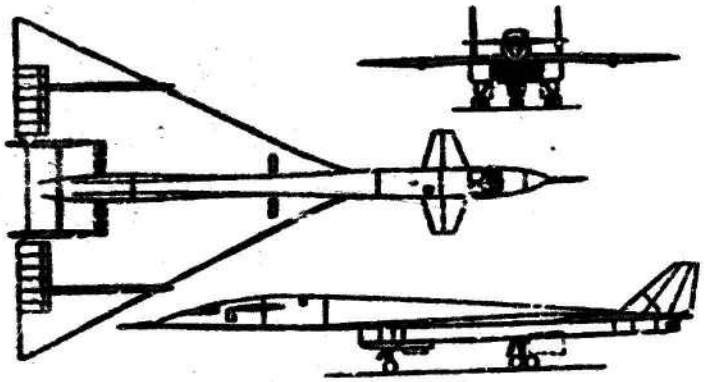

Figure 14.6. North American B-70 Valkyrie strategic reconnaissance aircraft. G = = 230,000 kg, S = 585 m^2, M_{lim} = 3.

aircraft, four are of the flying-wing configuration and one (the B-70) is a canard.

This points up the aforementioned difficulties of designing landing gear for heavy supersonic aircraft with the conventional tail-behind-wing position. In addition, it is important to have high values of such performance characteristics as range and ceiling at $M = M_{lim}$ for the single-regime supersonic aircraft of the types shown in Fig. 14.7. As we pointed out earlier, the flying-wing configuration, which lowers c_{y_0} and increases the supersonic K_{max}, is advantageous in this case. The aircraft under discussion were designed for takeoff and landing from long runways; high landing speeds are therefore acceptable.

All of the flying-wing aircraft have the sweep of the wing variable long the span. In the A-11, the fuselage behind the pilot's cabin is designed as a lifting wing of very small aspect ratio. Like varying the wing sweep along the span, this measure reduces the aft shift of the aerodynamic center on the transition to supersonic flight, as was pointed out in §8.3. We note that the flat bottom of the fuselage on such aircraft as the F-111 and Vigilant serves the same purpose (Figs. 14.2 and 14.4).

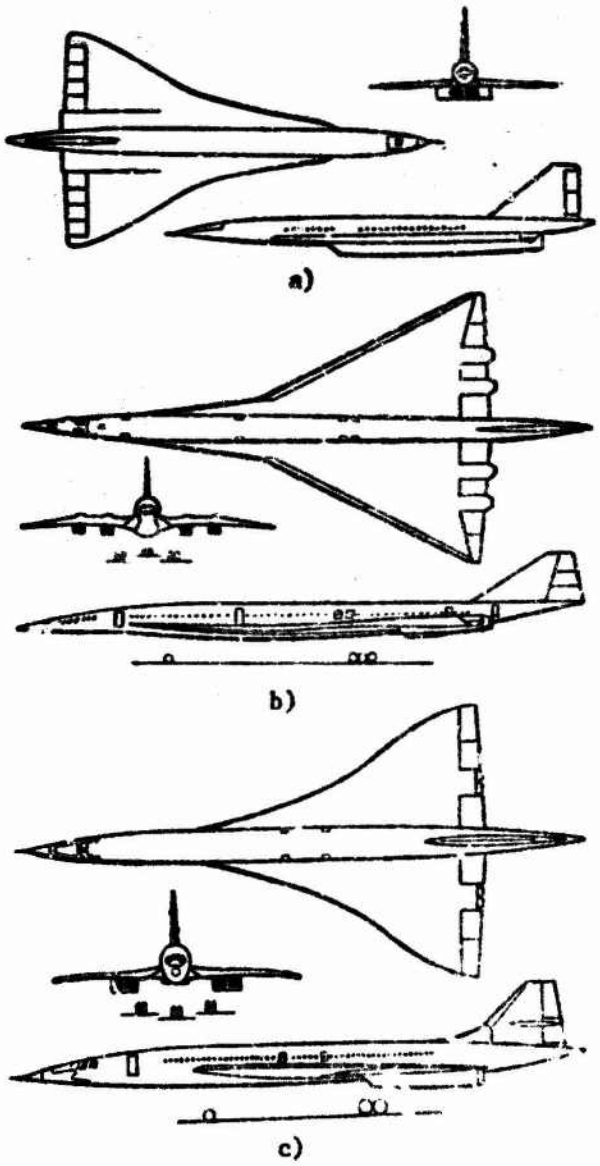

Figure 14.7. Diagrams of supersonic transports. a) The Tupolev Tu-144 (USSR); b) the Lockheed 2000 (USA); c) the Concorde (France, England).

The flying-wing configuration has been thoroughly mastered for supersonic aircraft. If we compare the canard with the flying wing, it becomes obvious that the flying wing must have a smaller $c_{y_{ldg}}$ than the canard, in which a pitchup moment is developed not

only by the elevons, but also by the rotating forward tail. On the other hand, the flying wing gives a somewhat smaller c_{y_0}. The canard's fuselage is loaded by aerodynamic forces from the empennage and will therefore be heavier than the fuselage of an airplane with no horizontal tail surface.

With the rather wide variety of powerplant positions, it is typical that the engines are mounted closer to the airplane's tail in all cases to shorten the distance from the center of gravity to the tip of the fuselage tail section, although this lengthens the passages supplying air to the engines. It is also characteristic that in most cases the engines are mounted in pairs and not in nacelles (with one engine in each nacelle). All heavy supersonic aircraft are designed as low-wing monoplanes.

§14.3. SELECTION OF POWERPLANE TYPE AND LAYOUT FOR TRANS- AND SUB-SONIC AIRPLANES

At the present stage in engine development, the ducted-fan and turboprop engines, which are more economical than turbojet, are most advantageous for the majority of subsonic and transonic airplanes. Only for aircraft that must reach speeds just below Mach one and need only moderate range will the turbojet and ducted fan compete with one another.

The ducted-fan engine with high compounding ratio is nearly as economical as the propjet. It is simpler in design than the propjet, but gives no increase in $c_{y_{1/o}}$ owing to the absence of propwash over the wing.

If the airplane is transonic and must cruise at M = 0.8-0.9, preference must be given to the ducted fan. Lower cruising speeds require a more profound comparative analysis of the advantages and disadvantages of the ducted fan and propjet based on the specific characteristics of the engines being compared.

The basic transonic and subsonic military aircraft types, leading trainer and liaison aircraft aside, are now ground- and carrier-based, asault aircraft, transports, which are also used

by airborne troops, and special-purpose aircraft.

Transonic attack aircraft are still built, not only in series production, but also as prototypes, despite the fact that multipurpose supersonic aircraft can operate successfully against ground targets. The reason for this is as follows.

As a rule, attack missions are carried out from low altitudes. Low-altitude flight is highly desirable from the standpoint of avoiding antiaircraft fire. For this reason, the attainment of high flight performance at high altitudes is not particularly important for the attack plane.

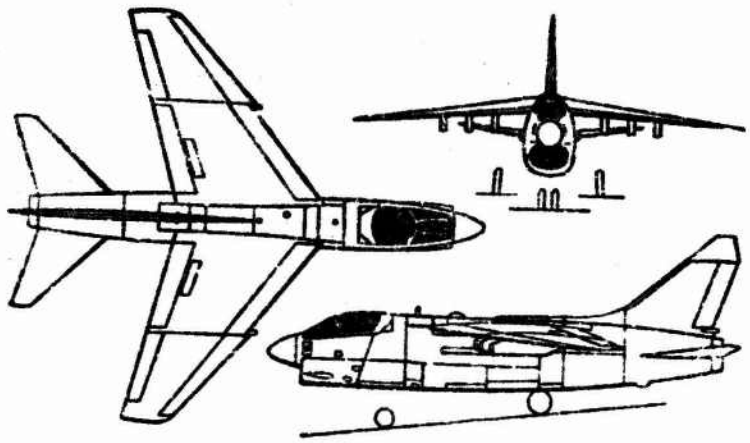

Figure 14.8. A-7A Corsair attack bomber, which is both carrier-based and used by the USAF. G = 14,750 kg, S = 34.8 m^2, V_{max} = 930 km/h.

In flight with afterburners, modern supersonic multipurpose aircraft are capable of reaching M ≈ 1.2 at the ground. However, their fuel consumption rates are very high at this speed. Flight at M ≈ 1.2 shortens range to about one-third of the range available at M ≈ 0.9. Flying very fast near the ground makes it difficult to find and attack targets. At the same time, if the attack airplane does not need to fly at a maximum M greater than 0-85-0.9 (i.e., V_{max} > 1,040-1,100 kg/h) at zero altitude, this Mach number can be attained even without afterburning and,

consequently, will not be accompanied by excessive fuel consumption. The transonic attack airplane must be designed with the object of minimizing the cost of building both the airplane and its equipment. For an airplane of this type, low cost is the most important factor and that which justifies building it. For a given range and payload weight, it is desirable to minimize the weight of the airplane, since lower weight means lower cost. Increasing the sweep of the wing beyond 35°-40° does not greatly increase M^*_{cr}, but it does shorten range drastically. It is therefore not advantageous to use a strongly swept wing on a transonic attack aircraft. It is desirable to keep the wing aspect ratio at three or more. Strong high-lift devices on the wing are important for the attack plane, since it must have high takeoff and landing characteristics, and these should not be obtained at the cost of a small load per square meter of wing, since increasing the wing area increases per-kilometer fuel consumption sharply at speeds near the top. The Ling-Temco-Vought A-7A Corsair II attack airplane shown in Fig. 14.8 is the most recent aircraft of this type to go into production. We see that the airplane has the conventional configuration for transonic fighters. The high wing was apparently chosen to facilitate accommodation of armaments.

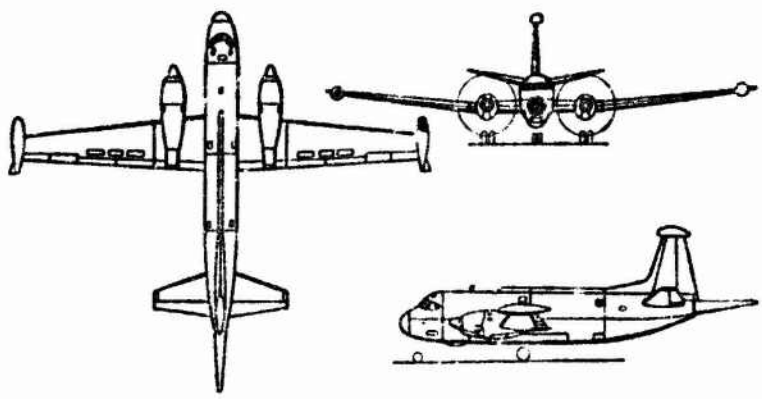

Figure 14.9. Breguet Atlantique antisubmarine airplane. G = 43,500 kg, S = 120 m^2, H_{clg} = = 9,100 m. Maximum endurance 18 h.

In designing a military transport, the designer will be concerned primarily with:

a) low fuel consumption, since the lower the minimum per-kilometer fuel consumption, the lower will be the airplane's takeoff weight;

b) convenience in loading and unloading ordnance and personnel and accommodating them in the fuselage;

c) good takeoff and landing characteristics.

We turn now to the configuration of two subsonic special-purpose military aircraft. As we pointed out in §5.3, reducing the load per square meter of wing, combined with the highest possible thrust/weight ratio, is an important measure toward increasing subsonic ceiling. On such an airplane, a large-area trapezoidal wing must have a rather large aspect ratio, since an increase in aspect ratio increases $c_{y_{opt}}$ and lowers the optimum speed, and to raise the ceiling of such an airplane it is important that flight at near-optimum speeds occur without wave drag at high altitudes. The fuselage of the airplane must be designed to accommodate reconnaissance equipment.

Antisubmarine warfare calls for airplanes capable of patrolling for many hours at a time. Use of propjet engines is advantageous.

Since patrolling is done at a speed near the economy speed and, consequently, with a large c_y, it is important to provide the wing with devices that prevent flow separation.

Figure 14.9 shows a diagram of a Breguet antisubmarine aircraft.

§14.4. FIRST-APPROXIMATION DETERMINATION OF TAKEOFF WEIGHT, WING AREA, AND ENGINE THRUST FOR A SUPERSONIC AIRPLANE

Having elaborated the airplane's configuration and selected the type of engine in the preliminary-design process, the designer proceeds to determine rational values of the airplane's takeoff

weight, wing area, and engine thrust, values with which the flight-performance data of the airplane will conform to the requirements made of it. It was pointed out above that for a given payload G_{pay} determined by the specifications for the airplane, the weight of the airplane will be minimized if the sum of the relative structural weight of the airplane, powerplant weight, and fuel weight ($\bar{G}_s + \bar{G}_{p.p} + \bar{G}_f$) is minimized.

The specifications for a supersonic airplane, and for a transport in particular, always state the highest flight Mach number, and for fully supersonic aircraft this is the maximum permissible M (M_{lim}) (see §5.2). The specifications also indicate the maximum supersonic flight range or, for an interceptor, the radius of interception. In determining the takeoff weight of an airplane, it is highly inconvenient to proceed from the interception radius, since the airplane may be flown to the interception point at various speeds and various engine settings. If the afterburner is used on an interception up to the time of attack and attack is from the rear hemisphere, it can be assumed in approximation that the supersonic range L is related to the interception radius as $R_{int} = KL$, where, as the calculations show, K = 0.45-0.55 for attack from the rear hemisphere. If the attack is head-on, we have K = 0.55-0.65. For $M_{lim} = 2$, the larger value of K pertains to R = 200 km, and the smaller value to R = = 400 km. For $M_{lim} = 2.5$ and 3, the larger K corresponds to R = = 500 km and the smaller to R = 1,000 km. These relationships can be used to change over from the interception-radius requirement to supersonic range.

In most cases, the specifications for a supersonic airplane indicate its ceiling or state a requirement as to cruising altitude.

For a supersonic airplane, takeoff and landing performance is characterized primarily by the length of the airplane's landing roll, because in most cases the takeoff run is shorter than the rollout and can always be shortened by use of booster rockets

Using the relationships given in §7.2, it is always possible to convert from rollout requirements to landing-speed requirements. We shall therefore assume that the specification as to the airplane's takeoff and landing performance is determined by the speed at which the airplane must land.

To summarize, we shall assume that the tactical-technical specifications are stated: payload weight, M_{lim}, maximum supersonic flight range L, ceiling altitude H_{clg}, and landing speed V_{ldg}. We are required to determine wing area and engine thrust, the latter characterized by its value at an altitude of 11,000 m and $M = M_{lim}$, with which the takeoff weight of the airplane will be minimized.

Even before engine thrust is determined, it is necessary to consider a family of engines that have the same C_{sp} and differ only in midships area, which is proportional to the thrust of a turbojet engine and approximately proportional to its weight.

The following quantities must be obtained as starting data from the characteristics of the engine family:

a) the specific weight γ_{en} of the engine at $M = M_{lim}$, $H = 11{,}000$ m, and maximum afterburning:

$$\gamma_{AB} = \frac{G_{AB}}{P_{11}};$$

b) the specific fuel consumption C'_{sp} at 11,000-m altitude and $M = M_{lim}$ with full-flow fuel delivery;

c) the value of $\bar{C}_{sp} = C_{sp}/C'_{sp}$ at $M = M_{lim}$ and 0.6 of maximum thrust ($P/P' = 0.6$).

All of these characteristics are to be determined for the effective thrust of the engine on the airplane with consideration of losses in the intake defuser, air passages, and exhaust nozzle.

It can be assumed in first approximation that at $M = M_{lim}$ and with a correctly determined defuser pressure recovery factor, the thrust P_{ef} will be 2-4% smaller than P and $C'_{sp_{ef}}$ will be larger by the same percentage. In addition to the above quantities, it

is necessary to find from statistical data

$$K_{\text{л.у}}=\frac{G_{\text{л.у}}}{G_{\text{ко}}} \quad \text{and} \quad K_{\text{т.с}}=\frac{G_{\text{т.с}}}{G_{\text{т}}},$$

where $G_{p.p}$ is the weight of the engine, accessories, mounts, etc., and $G_{f.s}$ is the weight of the fuel, tanks, and fuel system.

We shall consider first the procedure for solution of the problem when the wing high-lift devices and, consequently, $c_{y_{ldg}}$ have not yet been selected. In this case, $c_{y_{ldg}}$, like the weight G of the airplane, its wing area S, and the thrust P_{11} of its turbojet engines, will be unknowns.

To solve the problem in first approximation, it is necessary to assign, on the basis of statistical data, the airplane's relative structural weight ($\bar{G}_s = G_s/G$), the maximum lift/drag ratio (K_{max}) in flight at $M = M_{lim}$, and the quantity A, which is characterized by $c_{x_i}\left(A\approx\frac{\sqrt{M^2-1}}{4}\right)$ and $K_{f.s}$ in addition to the characteristics indicated above, which are engine-related (γ_{en}, $K_{p.p}$, C'_{sp}, $\bar{C}_{sp}$).

We first discuss determination of the relative powerplant weight $\bar{G}_{p.p} = G_{p.p}/G$. For this purpose, we introduce K_{max} into the expression for the pressure at the ceiling altitude. If we denote the ratio of K_{clg} to K_{max} by $\bar{K}_{clg}$, we have

$$p_{H_{\text{пот}}}=\frac{p_{11}G}{P_{11}K_{\text{пот}}}=\frac{p_{11}G}{P_{11}\bar{K}_{\text{пот}}K_{\max}}. \tag{14.1}$$

Since $G_{en} = \gamma_{en}P_{11}$ and $G_{p.p} = K_{p.p}G_{en}$,

$$P_{11}=\frac{G_{\text{л.у}}}{K_{\text{л.у}}\gamma_{\text{дв}}} \quad \text{and} \quad p_{H_{\text{пот}}}=\frac{p_{11}GK_{\text{л.у}}\gamma_{\text{дв}}}{\bar{K}_{\text{пот}}K_{\max}G_{\text{л.у}}},$$

whence we obtain

$$\bar{G}_{\text{л.у}}=\frac{G_{\text{л.у}}}{G}=\frac{K_{\text{л.у}}}{\bar{K}_{\text{пот}}}\cdot\frac{\gamma_{\text{дв}}p_{11}}{K_{\max}p_{H_{\text{пот}}}}. \tag{14.2}$$

In this expression, $p_{H_{clg}}$ is the pressure at the airplane's

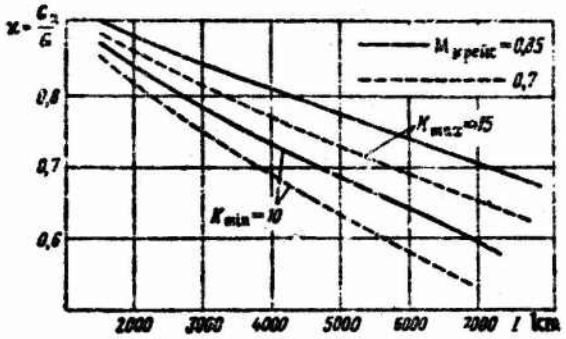

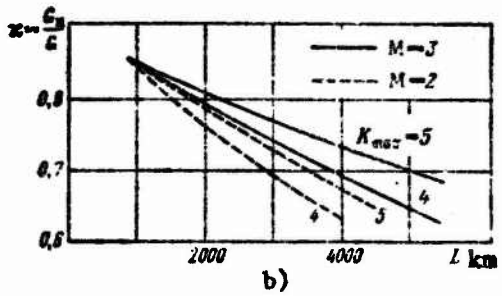

Figure 14.10. a) Ratio of weight of airplane at target to takeoff weight as a function of subsonic flight range; b) ratio of weight of aircraft at target to takeoff weight as a function of supersonic flight range.

ceiling altitude for the takeoff weight G. When the influence of the decrease in the airplane's weight that results from burning of fuel is taken into account, $\bar{G}_{p.p}$ will be expressed as follows for the ceiling altitude:

$$\bar{G}_{\text{п.у}} = \frac{(1-\bar{G}_{\text{пол}})K_{\text{п.у}}\gamma_{\text{пр}}p_{H}}{\bar{K}_{\text{пол}}K_{\max}p_{H_{\text{пот}}}}. \tag{14.3}$$

If the ceiling altitude is stated for a distance equal to half the range, the $1-\bar{G}_{f_{clb}}$ in (14.3) must be replaced by the coefficient κ (Fig. 14.10). Since $p_{H_{clg}}$ is stated by the tactical-technical requirements, the only unknown remaining in (14.3) is $\bar{K}_{clg}$.

As we showed in §6.6, the "cruising climb" range is

$$L_{\text{гор}}=\frac{3{,}6aM_{\text{крез}}K_{\max}}{C'_{\text{ya}}(\bar{C}_{\text{ya}}/\bar{K}_q)_{\min}}\ln\frac{1}{1-\dfrac{G_{\text{гор}}}{(1-\bar{G}_{\text{пол}})G}}. \tag{14.4}$$

Consequently,

$$e^{\frac{L_{\text{гор}}C'_{\text{ya}}(\bar{C}_{\text{ya}}/\bar{K}_q)_{\min}}{3{,}6aM_{\text{крез}}K_{\max}}}=\frac{1}{1-\dfrac{\bar{G}_{\text{гор}}}{(1-\bar{G}_{\text{пол}})}}, \tag{14.5}$$

whence we obtain

$$\bar{G}_{\text{гор}}=(1-\bar{G}_{\text{пол}})\left[1-\frac{1}{e^{\frac{L_{\text{гор}}C'_{\text{ya}}(\bar{C}_{\text{ya}}/\bar{K}_q)_{\min}}{3{,}6aM_{\text{крез}}K_{\max}}}}\right]. \tag{14.6}$$

The tactical-technical requirements state the total flight range L including the climbing, accelerating, and descent paths. Thus the range L_{lvl} that appears in (14.6) is related to the range L given by the tactical-technical requirements by $L_{lvl} = L - (L_{clb} + L_{bs})$. According to (6.12),

$$L_{\text{пол}}=2{,}2H_{\text{экон}}K_4K_5.$$

The descent distance

$$L_{\text{сн}}=H_{\text{экон}}K_{\text{пик}\,\text{ср}}. \tag{14.7}$$

K_4 is a function of $\bar{P} = P_{11}/2Q_{011}$ and is taken from the diagram of Fig. 6.16 (see §6.5); we obtain K_5 from Fig. 6.17, assuming as a convention that $P_{11}/G = 1$.

The relative amount of fuel burned in climbing, $\bar{G}_{f_{clb}}$, will be determined from the expression

$$\bar{G}_{\text{пол}}=\bar{G}_{\text{пол.исх}}K_1K_2K_3 \tag{14.8}$$

and the diagrams of Figs. 6.13-6.15. Let us assume that P_{11}/G equals unity. We ultimately obtain the following expression for $\bar{G}_{f_{lvl}}$:

$$\bar{G}_{\text{т гор}} = (1 - \bar{G}_{\text{т пол.нск}} K_1 K_2 K_3) \times$$

$$\times \left[1 - \frac{1}{e^{\frac{(L - 2{,}2 H_{\text{э кон}} K_4 K_5 - H_{\text{э кон}} K_{\max}) C'_{\text{ya}} \left(\frac{\bar{C}_{\text{ya}}}{\bar{K}_q} \right)_{\min}}{3{,}6 a M_{\text{прел}} K_{\max}}}} \right]. \tag{14.9}$$

In (14.9), L and M_{lim} and specified by the tactical-technical specifications and

$$H_{\text{э кон}} = \frac{V^2_{\text{кон}}}{2g} + H_{\text{кон}}; \; V_{\text{кон}} = a M_{\text{прел}}.$$

H_{fin} is 2-3 km higher than the altitude at the beginning of the flight. $G_{f_{clb.ini}}$ is a function of $H_{e_{fin}}$ (see Fig. 6.13).

The quantity $(\bar{C}_{sp}/K_q)_{min}$, $\bar{K}_{clg}$ and the coefficients K_1 and K_4 are functions of $\bar{P} = P_{11}/2Q_{011}$ (see Figs. 5.10, 6.9, 6.14, and 6.16). Thus, if $\bar{P}$ is given, we can determine $\bar{G}_{p.p}$, $\bar{G}_{f_{clb}}$, and $\bar{G}_{f_{lvl}}$.

The relative weight of the fuel consumed in descent, $\bar{G}_{f_{ds}}$, can be assumed equal to 0.01. Since the weight of the fuel and fuel system is larger by a factor $K_{f.s}$ than the weight of the fuel, we obviously have

$$\bar{G}_{\text{т.с}} = K_{\text{т.с}} G_{\text{т}} = K_{\text{т.с}} (\bar{G}_{\text{т гор}} + \bar{G}_{\text{т пол}} + \bar{G}_{\text{т ск}}). \tag{14.10}$$

Knowing the payload weight and the relative weights $\bar{G}_s$, $\bar{G}_{p.p}$, and $\bar{G}_{f.s}$, we can find the weight G of the airplane. We find from (5.7) that

$$P_{11} = \frac{(1 - \bar{G}_{\text{т пол}}) G p_{11}}{\bar{K}_{\text{пот}} K_{\max} p_{H_{\text{пот}}}}. \tag{14.11}$$

As in (14.3) and (14.9), the only unknown in expression (14.11) for P_{11} is $\bar{K}_{clg}$, which depends on $\bar{P}$.

Since $P_{11} = 2Q_{011}\bar{P} = 1.4 c_{x_0} S p_{11} M^2_{lim} \bar{P}$, the wing area S will be

$$S = \frac{P_{11}}{1{,}4 c_{x_0} \cdot p_{11} M^2_{\text{прел}} \bar{P}}.$$

Since $K_{max}=0.5\sqrt{1/c_{x_0}A}$, we have $c_{x_0}=\frac{1}{4K_{max}A}$. Taking this into consideration,

$$S=\frac{AK_{max}P_{11}}{0.35p_{11}M^2_{пред}\bar{P}}. \qquad (14.12)$$

Assuming on the basis of expression (7.12) for V_{ldg} that 80% of the fuel has been burned when the airplane lands and that $G_{ldg} = (1 - 0.8\bar{G}_T)G$, we find that

$$c_{y_{пос}}=\frac{16\cdot 0.9(1-0.8\bar{G}_T)G}{SV^2_{пос}}. \qquad (14.13)$$

Ultimately, we obtain the following system of nine equations for determination of G, S, P_{11}, and $c_{y_{ldg}}$ for the given M_{lim}, H_{clg}, L, and V_{ldg}:

$$\bar{K}_{пот}=\bar{K}_{пот}(\bar{P});\ (\text{см. рис. 5.10}) \qquad \text{I}$$

$$(\bar{C}_{y2}/\bar{K}_q)_{min}=(\bar{C}_{y2}/\bar{K}_q)_{min}(\bar{P});\ (\text{см. рис. 6.9}) \qquad \text{II}$$

$$\bar{G}_{T_{пол}}=\bar{G}_{T_{пол.исх}}K_2K_3; \qquad \text{III}$$

$$\bar{G}_{T_{гор}}=(1-\bar{G}_{T_{пол}})\left[1-\frac{1}{e^{\frac{(L-0.2H_{э_{кон}}K_6K_8-H_{э_{кон}}K_{max})C'_{y2}(\bar{C}_{y2}/\bar{K}_q)_{min}}{3.6aM_{пред}K_{max}}}}\right] \qquad \text{IV}$$

$$G_{л.у}=\frac{(1-\bar{G}_{T_{пол}})K_{л.у}\gamma_{11}p_{11}}{\bar{K}_{пот}K_{max}p_{H_{пот}}}; \qquad \text{V}$$

$$G=\frac{G_{п.н}}{1-[\bar{G}_н+\bar{G}_{л.у}+K_{т.с}(\bar{G}_{T_{гор}}+\bar{G}_{T_{пол}}+\bar{G}_{T_{сн}})]}; \qquad \text{VI}$$

$$P_{11}=\frac{(1-\bar{G}_{T_{пол}})Gp_{11}}{\bar{K}_{пот}K_{max}p_{H_{пот}}}; \qquad \text{VII}$$

$$S=\frac{K^2_{max}AP_{11}}{0.35p_{11}M^2_{пред}\bar{P}}; \qquad \text{VIII}$$

$$c_{y_{пос}}=\frac{16\cdot 0.9(1-0.8\bar{G}_T)G}{SV^2_{пос}}. \qquad \text{IX}$$

It is convenient to determine the G, S, P_{11}, and $c_{y_{ldg}}$ in which we are interested by using equation system (I-IX) because it is evident at once whether values can be found for them that will

satisfy all of the requirements stated and whether the number of unknowns corresponds to the number of equations.

Since we have assigned the quantities $K_{p.p}$, γ_{en}, C'_{sp}, K_{max}, $\bar{G}_s$, $K_{f.s}$, and $\bar{G}_{f_{as}}$, ten unknowns remain in the nine equations given above, namely: $\bar{K}_{clg}$, $(\bar{C}_{sp}/\bar{K}_q)_{min}$, $\bar{G}_{p.p}$, $\bar{G}_{f_{clb}}$, G, $c_{f_{lvl}}$, $\bar{P}$, P_{11}, S, and $c_{y_{ldg}}$. The coefficients K_1, K_2, K_4, K_5, and $G_{f_{clb.ini}}$ are determined from the graphs. We can therefore assign one unknown arbitrarily. It is convenient to assign $\bar{P}$, since it determines K/K_{max} in cruising-climb flight and $(\bar{C}_{sp}/\bar{K}_q)_{min}$. Not knowing $\bar{P}$, we cannot find P_{11} for a given ceiling, or find $\bar{G}_{f_{lvl}}$ and, consequently, the airplane's takeoff weight for a given range. Modern series-produced supersonic aircraft have $\bar{P}$ in the range from 0.6 to 0.95, while for prototypes it ranges from 0.9 to 1.35. In the first-approximation calculation, it is recommended that $\bar{P}$ be taken in the range from 0.9 to 1.3. The larger $\bar{P}$, the smaller the wing area obtained and the larger the required $c_{y_{ldg}}$. In most cases, an increase in $\bar{P}$ will be accompanied by a decrease in the airplane's takeoff weight. In this case, if the resulting required $c_{y_{ldg}}$ is attainable, it is recommended that $\bar{P}$ be taken equal to 1.1-1.2 (we shall discuss $\bar{P}_{max}$ below).

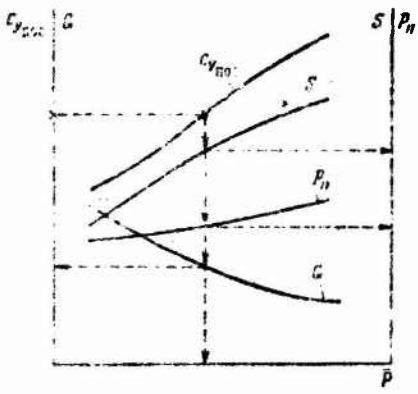

Figure 14.11. Nature of the dependence of $c_{y_{ldg}}$, G, S, and P_{11} on $\bar{P}$ for given M_{lim}, H_{clg}, $G_{f_{clb}}$, and V_{ldg}.

The decrease in K_{max} with decreasing wing area is left out of account in the first approximation. As a result, the decrease in the airplane's takeoff weight with increasing $\bar{P}$ is slightly exaggerated.

It is convenient to solve the system of equations (I-IX) in the order in which the equations are listed.

If the designer has determined the available $c_{y_{ldg}}$ before calculating

G, nine unknowns remains in the above nine equations. In this case, it is expedient to assign three values to $\bar{P}$, to find G, P_{11}, S, and $c_{y_{ldg}}$ for each of them, and plot their dependence on $\bar{P}$. Having determined which $\bar{P}$ corresponds to the required $c_{y_{ldg}}$, we find the unknown G, P_{11} and S for this $\bar{P}$ (Fig. 14.11).

In certain cases, M_{lim}, G_s, L, and V_{ldg}, but not the ceiling, may be stated in the specifications for the airplane. With these initial data, it is necessary to determine the ceiling altitude as a function of $\bar{P}$.

We obtain from Eqs. (14.11)

$$\frac{P_{11}}{G}=\frac{(1-\bar{G}_{T_{пол}})p_{11}}{\bar{K}K_{max}p_{H_{пот}}};\qquad \frac{P_{11}}{S}=\frac{0{,}35p_{11}M^2_{прех}\bar{P}}{K_{max}A}.$$

Consequently,

$$\frac{P_{11}}{S}:\frac{P_{11}}{G}=\frac{G}{S}=\frac{0{,}35M^2_{прех}\bar{P}\bar{K}_{пот}p_{H_{пот}}}{(1-\bar{G}_{T_{пол}}A)}. \tag{14.14}$$

On the other hand, according to (14.13)

$$G/S=\frac{c_{y_{пос}}V^2_{пос}}{16\cdot 0{,}9(1-0{,}8\bar{G}_T)}.$$

Equating the resulting expressions for G/S to one another, we find that

$$p_{H_{пот}}=\frac{c_{y_{пос}}V^2_{пос}A(1-\bar{G}_{T_{пол}})}{16\cdot 0{,}9\cdot 0{,}35(1-0{,}8\bar{G}_T)M^2_{прех}\bar{P}\bar{K}}. \tag{14.15}$$

To determine $p_{H_{clg}}$, it is necessary to assign $\bar{P}$ and the quantity $(1 - 0.8G_f)$. Equation (14.15) is the tenth equation in the system given above, in which, if the tactical-specifications do not state the ceiling but state only M_{lim}, $G_{p.l}$, L, and V_{ldg}, there are 11 unknowns. Assigning $\bar{P}$, we find K_{clg}, compute $G_{f_{clb}}$, determine $p_{H_{clg}}$ from (14.15), and then, solving the equation system as described above, we find the unknowns G, S, and P_{11}.

Assigning several $\bar{P}$ and plotting G, S, P_{11}, and H_{elg} as functions of $\bar{P}$, we find the $\bar{P}$ with which the required flight range is attained at minimal aircraft weight.

We regard the above calculation as a first approximation for the following reasons. It did not take account of the dependence of K_{max} and the airplane's structural weight on wing area. At the same time, the larger the wing area, the larger must be the airplane's maximum lift/drag ratio and, at the same time, the heavier must be the wing; this results in increased relative structural weight of the airplane.

The larger the $\bar{P}$ that we have assigned, the smaller is the wing area that we obtain. We must therefore slightly reduce K_{max} by increasing $\bar{P}$ and at the same time also reduce the relative structural weight. This is why the first approximation results in only a tentative determination of wing area.

However, such a calculation must be performed, since, without knowing the dimensions of the wing at least roughly, we cannot compute the airplane's c_{x_0}. Rough knowledge of the weight of the airplane and the wing area S also makes it easier to determine the fuselage area and midships section, which are needed to calculate its frontal drag.

§14.5. SECOND-APPROXIMATION DETERMINATION OF TAKEOFF WEIGHT, WING AREA, AND ENGINE THRUST FOR A SUPERSONIC AIRPLANE

In the second-approximation calculation of the supersonic airplane's weight, wing area, TJE thrust, and required $c_{y_{ldg}}$, the influence of wing area on the airplane's maximum L/D and its relative structural weight will be taken into account. This requires derivation of an equation system that differs from (I-IX) given above, in solution of which the wing area was determined last. When the dependence of K_{max} and $\bar{G}_s$ on the wing S is taken into account, this cannot be done.

The coefficient of the airplane's profile and parasitic drag c_{y_0} can be written

$$c_{x_{0_{wg}}} = c_{x_{0_{wg.on}}} + \frac{\sum c_x S_m}{S}. \qquad (14.16)$$

In (14.16), $c_{x_{0_{wg.tl}}}$ is the profile drag coefficient of the wing with the profile drag coefficient of the tail referred to it:

$$c_{x_{0_{wg.on}}} = c_{x_{0_{wg}}} + \frac{c_{x_{0_{on}}} S_{on}}{S} \qquad (14.17)$$

and $\Sigma c_x S_m$ is the sum of the products of the frontal-drag coefficients of the fuselage, fuselage canopy, and unretracted landing gear by their midships-section areas. Below we shall indicate how the drag of the engine nacelles is to be taken into account if they are situated on the wing.

In preparing to perform the second-approximation calculation, the designer must assign the profile thicknesses, aspect ratios, sweeps, and tapers of the wing and tail and the ratio of their areas. This enaoles him to calculate $c_{x_{0_{wg.tl}}}$ for $M = M_{lim}$ and $H = 11{,}000$ m and to determine the quantity A, which characterizes induced drag.

The fuselage midships area can be estimated and $\Sigma c_x S_m$ calculated on the basis of the tactical-technical specifications for the airplane and the results of the first-approximation calculations.

Knowing $c_{x_{0_{wg.tl}}}$ and $\sum c_x S_m$ and applying (14.16), we can find c_{x_0} for any wing-area value and then compute the maximum L/D:

$$K_{max} = \frac{1}{2}\sqrt{\frac{1}{c_{x_0} A}}.$$

According to (5.6), the pressure $p_{H_{clg}}$ at ceiling altitude in flight at $M = M_{lim}$ is

$$p_{H_{пот}} = \frac{G_{пот} p_{11}}{P_{11} K_{пот}} = \frac{(1 - \bar{G}_{топ}) G p_{11}}{2 \bar{K}_{пот} K_{max} \bar{P} Q_{011}}. \qquad (14.18)$$

Here G_{clg} is the weight of the airplane at its ceiling and $\bar{G}_{f_{clb}}$ is the relative amount of fuel consumed during climbing and acceleration;

$$\bar{K}_{пот}=\frac{K_{пот}}{K_{max}};\quad \bar{P}=\frac{P_{11}}{2Q_{011}}=\frac{P_{11}}{2\cdot 0,7p_{11}M^2_{прел}c_{x_0}S}.$$

From (14.18), we obtain an expression for the airplane's takeoff weight:

$$G_{max}=\frac{\bar{K}\,\bar{P}\cdot 2Q_{011}K_{max}p_{H_{пот}}}{(1-\bar{G}_{f_{пол}})p_{11}}. \qquad (14.19)$$

We see from (14.19) that $G_{t/o}$ depends on flight altitude, Q_0, K_{max} and P. If the ceiling altitude is stated for the halfway point of the flight range, then the coefficient κ (see Fig. 14.10) should be substituted for ($1 = \bar{G}_{f_{clb}}$). The thrust of the TJE can be assigned in terms of $\bar{P}$ and Q_{011}:

$$P_{11}=\bar{P}2Q_{011},$$

whence proceeds the following expression for powerplant weight:

$$G_{д.у}=K_{д.у}G_{дв}=K_{д.у}\gamma_{дв}P_{11}=K_{д.у}\gamma_{дв}\bar{P}2Q_{011}.$$

Consequently,

$$G_{д.у}=1,4p_{11}M^2_{прел}c_{x_0}SK_{д.у}\gamma_{дв}\bar{P}. \qquad (14.20)$$

Expression (14.20) implies that $G_{p.p}$ is a function of c_{x_0} and depends on the wing S and the value of $\bar{P}$. Determining the weight of the powerplant, we go on to determine the structural weight of the airplane.

As will be pointed out below, we shall assign a number of wing-area value in determining the weight of the airplane, the wing area, and TJE thrust. Using the formulas given in §11.3 or others preferred by the designer, the weight of the wing can be calculated for each wing area and the weight of the tail can also be determined. The weight of the fuselage can be determined from

the weights of the loads carried in the fuselage, including fuel (see §11.3), or as a fraction of the airplane's takeoff weight. Undercarriage and control-system weights are taken from statistical data as a certain percentage of the takeoff weight: $G_{g.ctl} = G_{g.ctl}G$. The relative weight of the fuel consumed in climbing and accelerating, $\bar{G}_{f_{clb}}$, is calculated by the method of §6.5:

$$\bar{G}_{\text{топл}} = \bar{G}_{\text{топл.нсх}} K_1 K_2 K_3.$$

The coefficient K_1 is a function of $\bar{T}$, the coefficient K_2 of P_{11}/G, and K_3 of C'_{sp}.

The relative weight of the fuel used in bringing the airplane down and landing it, $\bar{G}_{f_{ds}}$, is small and can be put at one percent of the airplane's takeoff weight.

If all of the fuel (G_f) is used during the airplane's flight, the weight of the fuel used in level flight, $G_{f_{lvl}}$, will then obviously be

$$G_{\text{топ}} = G_{\text{т}} - (G_{\text{топл}} + G_{\text{тсн}}) = G_{\text{т}} - (\bar{G}_{\text{топл}} + \bar{G}_{\text{тсн}})G.$$

$G_{f_{lvl}}$ must be known to calculate the range of "cruising climb" flight, L_{lvl}.

The weight of all fuel, tanks, and the fuel system is

$$G_{\text{т.с}} = G - (G_{\text{к}} + G_{\text{д.у}} + G_{\text{п.н}}).$$

Since $G_{f.s} = K_{f.s}G_f$, we have

$$G_{\text{т}} = \frac{1}{K_{\text{т.с}}}[G - (G_{\text{к}} + G_{\text{д.у}} + G_{\text{п.н}})].$$

Taking this into account, we get

$$G_{\text{топ}} = \frac{1}{K_{\text{т.с}}}[G - (G_{\text{к}} + G_{\text{д.у}} + G_{\text{п.н}})] - (\bar{G}_{\text{топл}} + \bar{G}_{\text{тсн}})G. \qquad (14.21)$$

In (14.21),

$$G_{\text{к}} = G_{\text{кр.оп}} + G_{\text{ф}} + G_{\text{шуп}}.$$

According to (6.5), it is necessary to know the minimum value of the ratio $(\bar{C}_{sp}/K_q)_{min}$, in which

$$\bar{C}_{уд}=\frac{C_{уд}}{C'_{уд}}, \quad \bar{K}_q=\frac{K_{q_{min}}}{K_{max}}.$$

to obtain the minimum per-kilometer fuel consumption. It was shown in §6.3 that the minimum value of this ratio is a function only of $\bar{P} = P_{11}/2Q_{011}$ and the decrease in C_{sp} on reduction of fuel delivery to the afterburner, which is characterized by the value of C_{sp} at $P/P' = 0.6$. Figure 6.9 shows $(\bar{C}_{sp}/K_q)_{min}$ as a function of $\bar{P}$. According to (6.17), the level-flight range for an initial weight $G(1 - \bar{G}_{f_{clb}})$ will be

$$L_{гор}=\frac{3{,}6\cdot 2{,}3aM_{прел}K_{max}}{C'_{уд}\left(\frac{\bar{C}_{уд}}{\bar{K}_q}\right)_{min}}\lg\frac{1}{1-\frac{G_{т_{гор}}}{(1-\bar{G}_{т_{пол}})G}}. \qquad (14.22)$$

Using (6.12) to determine

$$L_{пол}=2{,}2H_{экон}K_4K_5$$

and

$$L_{сн}=K_{max_{ср}}H_{экон}=K_{max_{ср}}\left(\frac{a^2M^2_{прел}}{2g}+H_{пот}\right),$$

we can find the total technical flight range

$$L=L_{пол}+L_{гор}+L_{сн}.$$

We find from the landing-speed expression (7.12) that if the airplane lands with 20% of its fuel left,

$$c_{y_{пос}}=\frac{2\cdot 0{,}9(G-0{,}8\bar{G}_т)}{0{,}125SV^2_{пос}}.$$

It follows from all of the above that in order to determine G, S, and $c_{y_{ldg}}$ for the airplane and P_{11} for the engine for given values of M_{lim}, $G_{p.l}$, H_{clg}, L, and V_{ldg}, it is necessary to solve simultaneously a system of ten equations:

$$c_{x_0}=c_{x_{0кр.оп}}+\frac{\sum c_xF}{S}; \qquad (I)$$

$$\bar{K}_{пот} = \bar{K}_{пот}(\bar{P}); \qquad \text{II}$$

$$G = \frac{2\bar{K}_{пот}\bar{P}Q_{011}K_{max}P_{H\,пот}}{(1-\bar{G}_{т_{пол}})\,p_{11}}; \qquad \text{III}$$

$$G_{л.у} = 2Q_{011}K_{л.у}\gamma_{лв}\bar{P}; \qquad \text{IV}$$

$$G_{кр.оп} = G_{кр.оп}(S); \qquad \text{V}$$

$$\bar{G}_{т_{пол}} = \bar{G}_{т_{пол.исх}}K_1K_2K_3; \qquad \text{VI}$$

$$G_{т_{гор}} = \frac{1}{K_{т.г}}\,[G - (G_{кр.оп} + G_{ф} + G_{м.упр} + G_{л.у} + G_{в.н})] - (\bar{G}_{т_{пол}} + \bar{G}_{т_{см}})\,G; \qquad \text{VII}$$

$$\left(\frac{\bar{C}_{yx}}{\bar{K}_q}\right)_{min} = \left(\frac{\bar{C}_{yx}}{\bar{K}_q}\right)_{min}(\bar{P}); \qquad \text{VIII}$$

$$L = \frac{3{,}6 \cdot 2{,}3aM_{крст}K_{max}}{C_{yx}\left(\frac{\bar{C}_{yx}}{\bar{K}_q}\right)_{min}}\lg\frac{1}{1-\frac{G_{т_{гор}}}{(1-\bar{G}_{т_{пол}})\,G}} + 2{,}2H_{з_{кон}}K_4K_5 + K_{max}H_{з_{кон}}; \qquad \text{IX}$$

$$C_{y_{пос}} = \frac{2 \cdot 0{,}9(G - 0{,}8G_{т})}{0{,}125SV^2_{пос}}. \qquad \text{X}$$

In this equation system, the dependence of $\bar{K}_{clg}$ on $\bar{P}$ (Eq. II) is that shown in Fig. 5.10, while Fig. 6.9 shows $(\bar{C}_{sp}/\bar{K}_q)_{min}$ as a function of $\bar{P}$ (Eq. VIII). Equation (V) is determined by the weight formula that the designer decided to use to compute wing weight.

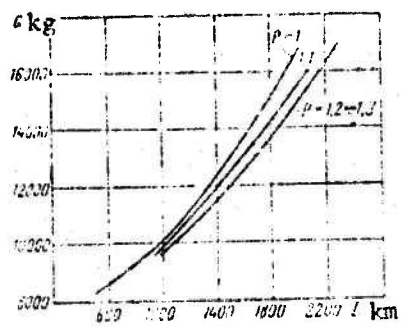

Figure 14.12. Weight of airplane as a function of supersonic range and $\bar{P} = P_{11}/2Q_{011}$. Values are assigned to M_{lim}, H_{clg}, $G_{p.l}$, and V_{ldg}.

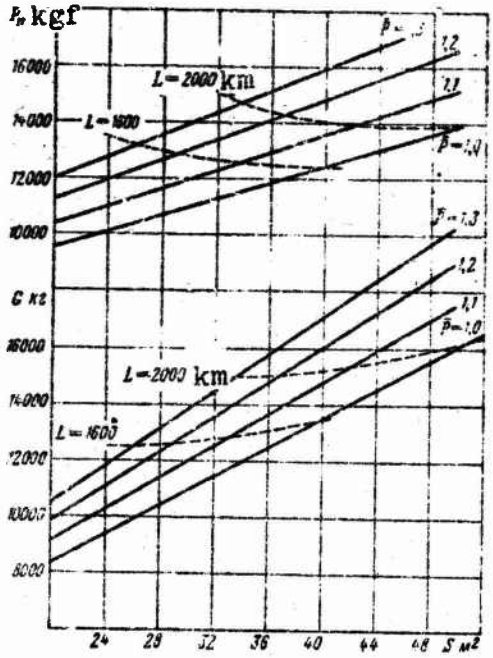

Figure 14.13. Weight of airplane and TJE thrust at 11,000-m altitude as functions of wing area and $\bar{P} = P_{11}/2Q_{011}$. Values are assigned to M_{lim}, H_{clg}, $G_{p.l}$, and V_{ldg}.

Since Q_{011} is a function of S and c_{x_0}, K_{max} is a function of c_{x_0} and A, K_1 and K_4 are functions of $\bar{P}$, K_4 and K_5 are functions of P_{11}/G, and K_3 is a function of G'_{sp}, it becomes obvious that since there are ten equations in the above systems, and M_{lim}, $p_{H_{clg}}$, L, V_{ldg}, and $G_{p.l}$ are assigned by the tactical-technical specifications, eleven unknown quantities remain, and to wit:

$$c_{x_0}, \bar{K}_{пот}, G, G_{п.у}, G_{кр.оп}, G_{г_{пол}}, G_{г_{1.02}},$$
$$\left(\frac{\bar{C}_{уп}}{\bar{K}_q}\right)_{min}, c_{p_{max}}, \bar{P} \text{ and } S.$$

Since there are ten equations and 11 unknowns, one of the latter must be assigned. As in first-approximation calculations, it is recommended that a value be assigned to $\bar{P}$, since it determines the flight regime at the ceiling with minimal per-kilometer fuel

consumption and enables us to find the wing-area-independent quantities K_{clg}, $(\bar{C}_{sp}/\bar{K}_q)_{min}$ and the coefficients K_1, K_4.

The system of equations (I-X) is most conveniently solved as follows. We assign three values to P in the range from 0.8-0.9 to 1.2-1.3. We assign three values of S for each $\bar{P}$.

Knowing $\bar{P}$ and S, we find in succession all values appearing in equation system (I-X) and plot the airplane's takeoff weight G as a function of range L (Fig. 14.12) and also curves of takeoff weight P_{11} as functions of wing area (see Fig. 14.13).

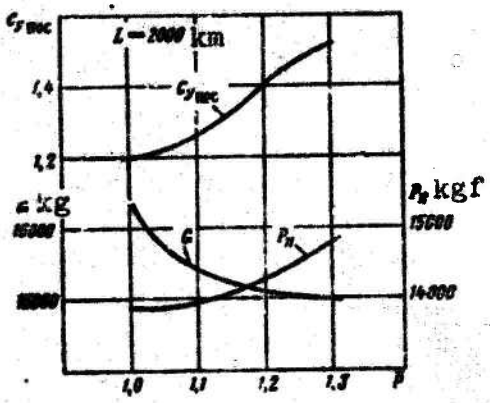

Figure 14.14. Weight of airplane, $c_{y_{ldg}}$, and P_{11} as functions of $\bar{P}$ for assigned M_{lim}, H_{clg}, $G_{p.l}$, L, and V_{ldg}.

The tactical-technical specifications stated a certain range L. Thus the diagram of Fig. 14.12 makes it possible to determine the aircraft weight at which the range and ceiling requirements are satisfied. Having determined the takeoff weight from Fig. 14.12, we consult Figs. 14.13 and 14.14 to find the wing area S, the thrust P_{11}, and $c_{y_{ldg}}$.

In addition, takeoff weight, TJE thrust, and the required $c_{y_{ldg}}$ are plotted against $\bar{P}$ (see Fig. 14.14) for the given flight range.

The diagrams shown in Figs. 14.12, 14.13, and 14.14 not only permit determination of the unknowns G, S, P_{11}, and $c_{y_{ldg}}$, but also indicate the manner in which they depend on the required supersonic range and the value taken for $\bar{P}$. If $c_{y_{ldg}}$ is assigned, we plot the takeoff weight against $\bar{P}$ for the stated range and

Table 14.2

S	S_1	S_2	S_3
$\frac{\sum c_x S_м}{S}$			
$c_{x_{0кр.оп}}$			
$c_{x_0} = c_{x_{0кр.оп}} + \frac{\sum c_x S_м}{S}$			
$c_{x_0} S$			
$2Q_{011} = 1{,}4 p_{11} M^2_{прех} c_{x_0} S$			
$K_{max} = \frac{1}{2}\sqrt{\frac{1}{c_{x_0} S}}$			
$\frac{G}{\overline{P}\overline{K}} = 2Q_{011} K_{max} \frac{p_{H_{пот}}}{p_{11}}$			

Table 14.3

Quantities									
$\overline{P}$	$\overline{P}_1 =$			$\overline{P}_2 =$			$\overline{P}_3 =$		
$\overline{K}$									
$\overline{P}\,\overline{K}$									
$(\overline{C}_{уд}/\overline{K}_d)_{min}$									
K_1									
$\overline{G}_{\tau_{пол}} = G_{\tau_{пол.нех}} K_1 K_2 K_3$									
S (we assign values)	S_1	S_2	S_3	S_1	S_2	S_3	S_1	S_2	S_3
$G = \left(\frac{G}{\overline{P}\overline{K}}\right) \frac{\overline{P}\,\overline{K}}{1 - \overline{G}_{\tau_{пол}}}$									

(continued on next page)

Table 14.3 (cont'd.)

S (we assign values)	S_1	S_2	S_3	S_1	S_2	S_3	S_1	S_2	S_3
$P_{11} = 2Q_{011}\bar{P}$									
$G_{д.у} = K_{д.у}\gamma_{гв}P_{11}$									
$G_{кр.оп}$									
$G_{ф}$									
$G_{ш.упр}$									
$G_{п.м}$									
$\sum G = G_{д.у} + G_{кр.оп} + G_{ф} + G_{ш.упр} + G_{п.м}$									
$\frac{1}{K_{т.с}}\left(G - \sum G\right)$									
$\left(\bar{G}_{т_{пол}} + \bar{G}_{т_{см}}\right) G$									
$G_{т_{гор}} = \frac{1}{K_{т.с}}\left(G - \sum G\right) - \left(\bar{G}_{т_{пол}} + \bar{G}_{т_{см}}\right) G$									
$\frac{G_{т_{гор}}}{\left(1 - \bar{G}_{т_{пол}}\right) G}$									
$\lg \frac{1}{1 - \frac{G_{т_{гор}}}{\left(1 - \bar{G}_{т_{пол}}\right) G}}$									
$\frac{3.6 \cdot 2{,}3 a M_{пред} K_{max}}{C'_{у_1}(\bar{C}_{уд}/\bar{K}_q)_{min}}$									
$L_{гор} = \frac{3.6 \cdot 2{,}3 a M_{пред} K_{max}}{C'_{у_1}(\bar{C}_{уд}/\bar{K}_q)_{min}} \times \lg \frac{1}{1 - \frac{G_{т_{гор}}}{\left(1 - \bar{G}_{т_{пол}}\right) G}}$									
$L_{пол} = 2.2 H_{э_{кон}} K_1 K_5$									
$L_{см} = H_{э_{кон}} K_{max}$									
S (we assign values)	S_1	S_2	S_3	S_1	S_2	S_3	S_1	S_2	S_3
$L = L_{пол} + L_{гор} + L_{см}$									
$c_{\eta_{пос}}$									

(concluded)

required $c_{y_{ldg}}$ (see Fig. 14.14), determine $\bar{P}$ from the available $c_{y_{ldg}}$, and are therefore also able to find G, S, and P_{11}.

It is convenient to form the calculations on tables similar to Tables 14.2 and 14.3.

If the engines are housed in engine nacelles, their frontal area will increase in proportion to an increase in thrust. In this case, the airplane's noninduced frontal drag should be broken up into three components: the drag of the wing and tail, the drag of the fuselage, and the drag of the engine nacelles, which is proportional to P_{11}. In this case, the airplane's c_{x_0} should be calculated with the expression

$$c_{x_0} = \frac{1}{1-2\varepsilon\bar{P}}\left(c_{x_{0\text{кр.оп}}} + \frac{2c_x S_м}{S}\right), \qquad (14.23)$$

where ε is a coefficient that takes account of the engine-nacelle drag and equals 0.1-0.15; $\bar{P} = P_{11}/2Q_{011}$.

A number of calculations of the G, S, P_{11}, and $c_{y_{ldg}}$ of supersonic aircraft for which M_{lim}, H_{clg}, L, $G_{p.l}$, and V_{ldg} were assigned in accordance with tactical-technical specifications indicated that in most cases an increase in $\bar{P}$ results in a definite though not particularly large decrease in the airplane's takeoff weight, an increase in the thrust P_{11}, a substantial decrease in wing area, and an increase in the required $c_{y_{ldg}}$.

If the weight of a square meter of wing is not large, it may be found that an increase in $\bar{P}$ has almost no effect on the airplane's takeoff weight. At the same time, as we have noted, the larger the value of $\bar{P}$, the smaller the wing S and the larger must be $c_{y_{ldg}}$.

The weak dependence of aircraft weight on $\bar{P}$ for a given range and ceiling is explained by the fact that an increase in $\bar{P}$ results in an increase in P_{11} and G/S as a result of the smaller wing area.

A decrease in the area of the wing will reduce its weight. larger value of $\bar{P}$ will lower $\bar{G}_{f_{clb}}$ and $(\bar{C}_{sp}/\bar{K}_q)_{min}$, thus helping increase range, or, if range is held constant, lowers the required $G_{f_{lvl}}$. However, the increase in $\bar{P}$ will increase $G_{p.p}$ and the decrease in wing S will lower K_{max}, with a resulting increase in $G_{f_{lvl}}$. On the whole, it may be found that the sum $G_{f_{lvl}} + G_{f_{clb}} + G_{wg}$ and, consequently, also the aircraft weight G will change little on a change in P.

In such a case, it might appear irrational to settle for a larger $\bar{P}$, since the wing high-lift devices become more complicated owing to the need for a larger $c_{y_{ldg}}$. However, reference should be made, as it was above, to the danger of making $\bar{P}$ and P_{11} too small. At $\bar{P}$ smaller than 0.8 (see §5.3), the ceiling altitude becomes highly sensitive to a decrease in thrust, even one due to a rise in stratosphere temperature, or to an increase in c_{x_0}. The designer must also provide a certain thrust margin in all cases, and the smaller the $\bar{P}$, the smaller will this margin become, both owing to the smaller P_{11} and as a result of the increase in S.

In the final analysis, when $\bar{P}$ has little influence on G, selection of a rational $\bar{P}$ and, consequently, G, S, and P_{11} will governed to a greater degree by landing-speed requirements and the possibility of obtaining large values of $c_{y_{ldg}}$.

If, with increasing $\bar{P}$, the airplane's takeoff weight is lowered and the required $c_{y_{ldg}}$ can be obtained, the question arises as to the largest value of P that should be regarded as rational. As $\bar{P}$ increases, TJE's must be throttled back farther in flight at $(\bar{C}_{sp}/K_q)_{min}$. For many TJE's, however, the linearity of the variation of C_{sp} with decreasing thrust is violated on a more than 40% drop from afterburner thrust ($P/P' < 0.6$), and when the TJE is throttled back further, the decrease in C_{sp} first slows down and then stops altogether. The right-hand limit of the curves given

in Fig. 6.9 corresponds to $P/P' = 0.6$. If we take a P larger than that corresponding to the right-hand limit of the $(\bar{C}_{sp}/\bar{K}_q)_{min} = (\bar{C}_{sp}/\bar{K}_q)_{min}(\bar{P})$ curves, we have no right to extrapolate the $(\bar{C}_{sp}/(\bar{C}_{sp}/K_q)_{min}$ curves shown in Fig. 6.9 without a special check. It is quite possible that under these conditions, a further increase in $\bar{P}$ will greatly retard the decrease in $(\bar{C}_{sp}/\bar{K}_q)_{min}$ and that the decrease in aircraft takeoff weight with increasing $\bar{P}$ will cease. It must also be remembered that the larger $\bar{P}$ for a constant ceiling, the lower is the altitude at which per-kilometer fuel consumption is minimal.

Indeed, according to (5.12)

$$\frac{c_{y_{\text{пот}}}}{c_{y_{\text{нав}}}} = \frac{p_{H_{\text{нав}}}}{p_{H_{\text{пот}}}} = \sqrt{2\bar{P}-1}; \quad \frac{c_{y_{q_{\min}}}}{c_{y_{\text{нав}}}} = \frac{p_{H_{\text{нав}}}}{p_{H_{q_{\min}}}}.$$

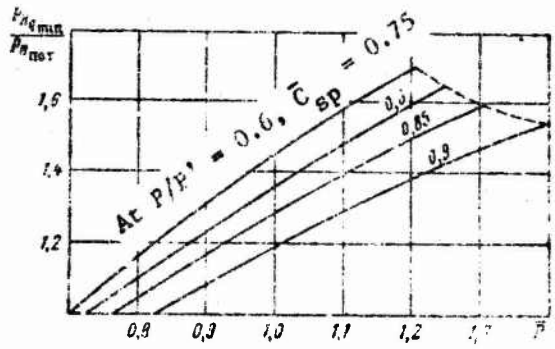

Figure 14.15. Ratio of the pressure at the flight altitude with q_{min} to the pressure at ceiling altitude as a function of $\bar{P} = P_{11}/2Q_{011}$.

Dividing the first equation by the second, we get

$$\frac{p_{H_{q_{\min}}}}{p_{H_{\text{пот}}}} = \frac{\sqrt{2\bar{P}-1}}{c_{y_{q_{\min}}}/c_{y_{\text{нав}}}}. \tag{14.24}$$

Figure 6.10 is a plot of $c_{y_{q_{min}}}/c_{y_{opt}}$ against $\bar{P}$. With increasing $\bar{P}$, the numerator of (14.24) increases much more rapidly than the

denominator. Thus, if $\bar{P} = 1$ and $C_{sp} = 0.15$ at $P/P' = 0.6$, we have $p_{H_{q_{min}}}/P_{h_{clg}} = 1.3$, and at $\bar{P} = 1.3$, this ratio becomes equal to 1.6. For a given ceiling altitude, therefore, the cruising altitude will be about 1,300 m lower at $\bar{P} = 1.3$ than at $\bar{P} = 1$. Figure 14.15 shows $p_{H_{q_{min}}}/p_{H_{clg}}$ as a function of $\bar{P}$ for equal degrees of C_{sp} decrease with decreasing P/P'.

We noted that the larger $\bar{P}$, the smaller is the airplane's wing area and the larger must $c_{y_{ldg}}$ become for V_{ldg} = const. A decrease in area is highly favorable for zero-altitude flight at sonic and transonic speeds (see §14.4), since per-kilometer fuel consumption is much lower for smaller wing S under such conditions. Thus, if the airplane must deliver high performance near the ground, the preference settles on larger values of G/S as well, with good takeoff and landing characteristics obtained by use of wing high-lift devices.

If the ceiling of the airplane is not stated, but only the altitude at which cruising supersonic flight is to begin, the calculating sequence set forth in Tables 14.1 and 14.2 is retained, but it is necessary to assign several values to $\bar{P}$ and to use expression (14.24) or Fig. 14.15 to calculate the pressure in the atmosphere at the ceiling for each of them. In this case, an increase in $\bar{P}$ will be accompanied by a rise of the ceiling, and we should expect the takeoff weight of the airplane to increase or remain constant instead of decreasing with increasing $\bar{P}$.

If the ceiling altitude is stated for the conditions at the target rather than under cruising-flight conditions, $(1 - \bar{G}_{f_{clb}})$ should be replaced by the coefficient κ (see Fig. 14.10) in Eq. (III).

It must be remembered in calculating the climb and descent distances that as a result of the cruising climb, the $H_{e_{fin_2}}$ in in the glide is about 2-3 km higher than the $H_{e_{fin_1}}$ at the

beginning of cruising flight.

In certain cases, the designer determines $c_{y_{ldg}}$ by the act of selecting the airplane's layout. In such cases, there are ten rather than 11 unknowns in the system of ten equations given above.

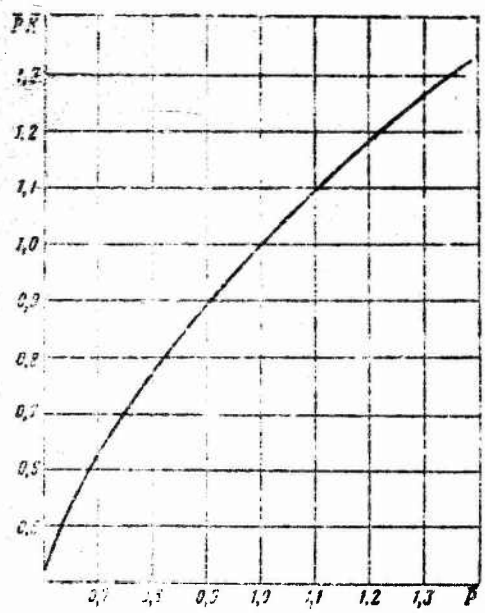

Figure 14.16. $\bar{P}\bar{K}$ as a function of $\bar{P}$.

For given V_{ldg} and $c_{y_{ldg}}$, the procedure for solving the above equation system must be modified as follows.

We denote the ratio G_{ldg}/G by $\bar{G}_{ldg}$. It follows from Eq. (X) that the load per square meter of wing can be found for the given V^2_{ldg} and $c_{y_{ldg}}$:

$$\frac{G}{S} = \frac{0.125 c_{y_{ldg}} V^2_{ldg}}{2 \cdot 0.9 \bar{G}_{ldg}}.$$

In this formula, G_{ldg} is determined from the first-approximation calculation.

Assigning several values to the wing area S, we obtain a series of aircraft takeoff weights $G = GS/S$.

Knowing G, we use Eq. (III) to find $\bar{P}\bar{K}$. Since $\bar{G}_{f_{clb}}$ depends on $\bar{P}$ and its value is still unknown, we perform the calculation of $\bar{P}\bar{K}$ in two approximations. In the first approximation, we assign a value to $\bar{P}$ and use it to find $\bar{G}_{f_{clb}}$. Having computed $\bar{P}\bar{K}$ we determine $\bar{P}$ by consulting the curve of $\bar{P}\bar{K}$ vs. $\bar{P}$ shown in Fig. 14.16. Having found $\bar{P}$, we calculate $\bar{G}_{f_{clb}}$ again and perform the second-approximation calculation of $\bar{P}\bar{K}$.

Assigning a wing area, we can find $Q_0 = 1.4 p_{11} M^2_{lim} c_{x_0} S$, for

each S and, knowing $\bar{P}$, we can determine $P_{11} = 2Q_{011}\bar{P}$.

The rest of the calculation is as described above, in the following procedure. Equation (IX) is used to calculate the range for each wing area. Range is plotted against wing area and the plot used to determine the wing area at which the required range is obtained. Certain values of G, $\bar{P}$, and P_{11} will correspond to the wing area obtained. In the calculating process we can, without completing it, improve G_{ldg} after obtaining the value of $G_{f_{lvl}}$, by assuming that $G_{ldg} = G - 0.8G_f$. Obviously, G will be inversely proportional to $\bar{G}_{ldg}$ for each wing area S.

If M_{lim}, $G_{p.l}$, V_{ldg}, $c_{y_{ldg}}$, and the supersonic range L are stated for a supersonic airplane but there are no ceiling or cruising-altitude requirements, the parameters of the airplane may differ from those obtained for the above version of the requirements.

Equation (III) cannot be used in this case. Solving the problem as before, we assign three values to $\bar{P}$, with the smallest equal to 0.7. We assign three values of S for each $\bar{P}$. Knowing V_{ldg} and $c_{y_{ldg}}$, we find G. We calculate c_{x_0} and Q_0 and find P_{11} for each S. We then use the method described above to compute the distance L and obtain the weight G of the airplane as a function of range. We also plot curves of G and P_{11} against S. We then determine G for the required range and use the G to find the unknowns S and P_{11}. Having obtained the results of this calculation for each $\bar{P}$, we plot G against $\bar{P}$. The smallest value of G enables us to find a certain $\bar{P}$ and hence the S and P_{11} that correspond to it.

The calculations show that a decrease in ceiling altitude, which is accompanied by a decrease in $\bar{P}$, lowers takeoff weight for a given range, but that at small $\bar{P}$ a further decrease results in a sharp increase of $(\bar{C}_{sp}/\bar{K}_q)_{min}$ (see Fig. 6.9), and a further decrease in ceiling altitude is not advantageous.

Table 14.4

S	S_1	S_2	S_3
$\frac{\sum c_{x_0} S_n}{S}$			
$c_{x_0} = c_{x_{0\text{кр.оп}}} + \frac{\sum c_x S_n}{S}$			
$c_{x_0} S$			
$K_{max} = \frac{1}{2}\sqrt{\frac{1}{c_{x_0} A}}$			
$2Q_{\text{м}1} = 1.4 p_{11} M^2_{\text{пред}} c_{x_0} S$			
$\frac{G}{\bar{P}\bar{K}} = 2Q_{011} K_{max} \frac{p_{H_{\text{ст}1}}}{p_{11}}$			
$\bar{P} = \frac{P_{11}}{2Q_{\text{м}1}}$ $\bar{K}$			
$\bar{P}\bar{K}$			
$(\bar{C}_{y\lambda}/\bar{K}_\phi)_{min}$			
$\bar{G}_{\tau_{\text{пол}}} = \bar{G}_{\tau_{\text{пол.нек}}} K_1 K_2 K_3$			
$G = \left(\frac{G}{\bar{P}\bar{K}}\right) \frac{\bar{P}\bar{K}}{1 - \bar{G}_{\tau_{\text{пол}}}}$			
$G_{\text{л.у}} = K_{\text{л.у}} \gamma_{\text{ла}} P_{11}$			
$G_{\text{кр.оп}}$			
G_ϕ			
$G_{\text{ш.упр}}$			
$G_{\text{п.п}}$			
$\sum G = G_{\text{л.у}} + G_{\text{кр.оп}} + G_\phi + G_{\text{ш.упр}} + G_{\text{п.п}}$			

(continued on next page)

Table 14.4 (Cont'd.)

S	S_1	S_2	S_3
$\frac{1}{K_{т.с}}(G-\sum G)$			
$(\bar{G}_{т_{пол}}+\bar{G}_{т_{сн}})G$			
$G_{т_{гор}}=\frac{1}{K_{т.с}}(G-\sum G)-(\bar{G}_{т_{пол}}+\bar{G}_{т_{сн}})G$			
$\lg\frac{1}{1-\frac{G_{т_{гор}}}{(1-\bar{G}_{т_{пол}})G}}$			
$\frac{3{,}6\cdot 2{,}3M_{пред}K_{max}}{C'_{ya}(\bar{C}_{ya}/\bar{K}_q)_{min}}$			
$L_{гор}=\frac{3{,}6\cdot 2{,}3M_{пред}K_{max}}{C'_{ya}(\bar{C}_{ya}/\bar{K}_q)_{min}}\lg\frac{1}{1-\frac{G_{т_{гор}}}{(1-\bar{G}_{т_{пол}})G}}$			
$L_{пол}=2{,}2H_{э.кон}K_4K_5$			
$L_{сн}=H_{э.кон}K$			
$L=L_{пол}+L_{гор}+L_{сн}$			

(concluded)

In many cases, not only M_{lim}, H_{clg}, L, $\theta_{p.l}$, and V_{ldg}, but also the thrust P_{11} may be assigned for a supersonic airplane. In this case, 10 unknowns remain in the system of 10 equations given above.

When the thrust P_{11} is stipulated, the equation system is solved by the following procedure.

We assign three values to S and find c_{x_0}, Q_0, and K_{max} for them. For each S, we determine $\bar{P} = P_{11}/2Q_{011}$. Then, using Eq. (III), we compute the weight of the airplane and the remaining quantities that appear in equation system (I-X). Finding the range L for each S, we determine graphically the S at which the range requirement is satisfied and the associated values of P and $c_{y_{ldg}}$. Our guide should be the calculating procedure given in Table 14.4 rather than that given in Tables 14.1 and 14.2.

The method set forth above for computing the optimum wing area and engine thrust for the supersonic airplane can also be used to select rational values for the wing profile thickness, which codetermines $c_{x_{0_{wg.tl}}}$ and, consequently, also Q_{011} and K_{max} on the one hand and the structural weight of the wing on the other.

In reducing the profile thickness, we also reduce the wave drag of the wing, increase K_{max} and lower Q_{011} and, consequently, also lower P_{11} for given $\bar{P}$ and S. The decrease P_{11} reduces the weight of the powerplant, while the increase in K_{max} lowers the value of $G_{f_{lvl}}$ for a given L_{lvl}. The wing profile thickness with which the increase in wing weight is accompanied by an equal decrease in powerplant and fuel weight will obviously be the optimum.

Reducing the wing profile thickness of a supersonic airplane to an average of 3-5% lowers the takeoff weight of the airplane. The transition to thinner profiles may give rise to a number of structural difficulties, especially for aircraft with aspect ratios larger than two. In specifying the wing profile thickness, account must also be taken of the possibility of using its volume for retraction of wheels and accommodation of tanks. It must be remembered that heavy airplanes with large-area wings permit the use of thinner profiles. The wing will be thicker at a given profile thickness ratio the smaller the aspect ratio of the wing.

Establishing the optimum values of G, P_{11}, S, and $c_{y_{ldg}}$ with the M_{lim}, H_{clg}, L, $G_{p.l}$, and V_{ldg} stated by tactical-technical requirements and the values adopted for $\bar{C}_{wg}$, λ_{wg}, and κ manually by the above method requires no more than one working day. If it is also proposed to vary $\bar{c}$, λ and κ, the number of variants of the calculation increases to the degree that it becomes quite rational to use a high-speed computer to solve the above equation system. In it, $\bar{K}$, $\bar{P}\bar{K}$, $(\bar{C}_{x_0}/\bar{K}_q)_{min}$, and K_1 are functions of $\bar{P}$, whose value we assign. The dependence of these quantities on P should be stored in the machine.

§14.6. DETERMINATION OF TAKEOFF WEIGHT, WING AREA, AND ENGINE THRUST FOR A TRANSONIC AIRPLANE

Transonic aircraft, which have top Mach numbers just below unity, are still in use and production.

In most cases, the top-speed requirement is not the basic one for a transonic airplane.

The basic requirements for cargo and passenger transport aircraft of this type pertain to the loads that the airplanes must haul, their weights and volumes, flight-range and cruising speed for maximum range, and, finally, takeoff and landing characteristics.

The requirement as to the cruising altitude is less important. On the basis of the considerations set forth above, we shall consider a method of determining the weight of the airplane, the area of its wings, and the thrust of its turbojet engines for stated cruising Mach numbers, payload weights and dimensions, including equipment and armament, flight range, and takeoff and landing distances.

Landing speed is determined on the basis of the landing-distance requirements. Thus, we must calculate the weight of the airplane, its wing area, and its engine thrust for given M_{cruise}, payload weight $G_{p.l}$, range L, landing speed V_{ldg}, and takeoff distance.

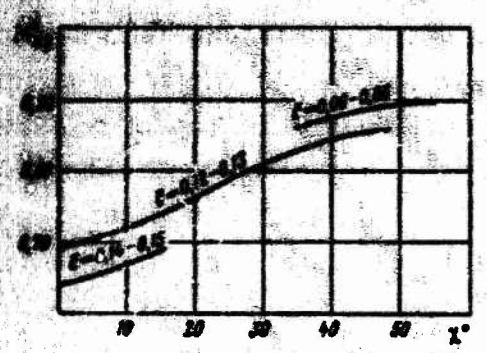

Figure 14.17. M^*_{cr} of airplane wing as a function of sweep angle and wing profile thickness ratio at the fuselage.

We shall first discuss the requirements as to cruising speeds; it is desirable that per-kilometer fuel consumption be lowest at this speed. It was shown above, in §6.2, that the minimum per-kilometer fuel consumption of a transonic airplane is obtained in flight at M^*_{cr}, i.e., at the Mach number at which c_{x_0} begins to increase owing to the appearance of wave drag. As we noted earlier (see §5.1), the use of thinner M-stable wing profiles and sweeping the wing increase M^*_{cr}. However, increasing the sweep beyond 35° increases M^*_{cr} only slightly. For this reason, sweeps greater than 35° are not used on modern series-produced transonic aircraft. With wing root profile thicknesses of 11-13% and 1/4-chord wing sweep angles of 32°-35°, transonic aircraft have M^*_{cr} = 0.82-0.85. With the same wing root profile thickness and a sweep angle of 20°-24°, M^*_{cr} = 0.74-0.78 (Fig. 14.17). It follows from the above that if M_{cruise} is specified for the airplane, the sweep of the wing and its profile thickness are also in effect stated, since $M_{cruise} \approx M^*_{cr}$.

As we noted above (see §14.2), the M_{cruise} requirement also determines powerplant type.

As when G, S, and P_{11} are computed for a supersonic airplane, it is recommended that the problem be solved for the transonic airplane beginning with a first-approximation calculation, followed by a second approximation. In the first-approximation calculation, it is necessary to assign a value to the airplane's maximum lift/drag ratio and its relative structural weight. As concerns flight altitude, the cruising altitude, at which q_{min} [sic], lies in the range from 9,500 to 10,500 m for modern TJE-equipped

aircraft. Since the specific fuel consumption C'_{sp} decreases with increasing altitude (up to 11,000 m), it is advantageous to raise the cruising altitude from the standpoint of per-kilometer consumption. However, the higher the cruising altitude, the greater must be the thrust of the TJE's, and the heavier they become. The increase in TJE weight means a smaller fuel load and hence a shorter range.

Foreign fanjet-equipped aircraft have cruising altitudes slightly lower than those of TJE aircraft.

When he proceeds to the engine-thrust calculations, the designer must select a family of engines whose characteristics are to be used in determining the ratio of maximum engine thrust at cruising altitude and $M = M_{cruise}$ to the static zero-altitude thrust $P_{H_{cruise}}/P_0 = \kappa_2$, the weight of engine per kilogram-force thrust at the ground at $V = 0$, and the specific fuel consumption at the cruising altitude and M_{cruise}, which is equal to 0.95-0.97 of the fuel consumption C'_{sp} at full power, H_{cruise}, and M_{cruise}. It is then necessary to assign a value to the ratio of powerplant weight to engine weight $K_{p.p} = G_{p.p}/G_{en}$ and the ratio of fuel and fuel-system weight to fuel weight, $K_{f.s} = G_{f.s}/G_f$. Proceeding from the requirements for the airplane or from statistical data, we arrive at a value of $\bar{G}_{ldg}$ and the ratio of the airplane's landing and takeoff weights, G_{ldg}/G. Landing speed should be determined from the stated landing distance (see §7.2). The proposed wing high-lift devices should be used as a basis for determining $c_{y_{ldg}}$ and $c_{y_{1/o}}$ and estimation of the reduced friction coefficient f_{red} during the airplane's landing roll (see §7.2).

The summary formulation of the problem is as follows. The specifications for the airplane state: payload weight $G_{p.l}$, cruising Mach number M_{cruise}, range, and takeoff and landing distances (V_{ldg}). It is necessary to determine the weight of the airplane, its wing area, and its engine thrust in first approximation.

To solve the problem, we assign values to the maximum lift/drag ratio K_{max}, the relative structural weight $\bar{G}_s$ of the airplane, $G_{ldg}/G = \bar{G}_{ldg}$, and $c_{y_{ldg}}$, $c_{y_{1/o}}$, and f_{red}. Selecting our family of engines, we determine the ratio of the full-power thrust at H_{cruise} and M_{cruise} to the zero-altitude thrust at V = 0,

$$z_2 = \frac{P'_{H_{крейс}}}{P_0}, \quad \gamma_{en} = \frac{G_{пр}}{P_0}, \quad K_{л.у} = \frac{G_{л.у}}{G_{лн}}, \quad K_{т.с} = \frac{G_{т.с}}{G_т},$$

and C_{sp}, which is equal to 0.95-0.97 of the C'_{sp} at H_{cruise} and M_{cruise}.

We devise a system of equations whose solution will give the unknowns G, S, and P_0 for the airplane. On the basis of Eq. (7.12) for the landing speed, we find that

$$S = \frac{16 \cdot 0{,}9 \bar{G}_{пос} G}{c_{y_{пос}} V^2_{пос}}. \tag{14.25}$$

From (7.5), assuming that $P_{av} = 0.95P_0$, we obtain for the takeoff run

$$\frac{P_0}{G} = \frac{1}{0.95}\left(\frac{V^2_{отр}}{2gL_{раз}} + f_{пр}\right), \tag{14.26}$$

$$V^2_{отр} = \frac{2G}{\varrho S c_{y_{отр}}}. \tag{14.27}$$

Substituting the value of G/S from (14.25) into (14.27), we find that

$$V^2_{отр} = \frac{c_{y_{пос}} V^2_{пос}}{0{,}9 \bar{G}_{пос} c_{y_{отр}}}.$$

Substituting the expression obtained for $V^2_{1/o}$ into (14.26), we find that

$$P_0 = \frac{G}{0{,}95}\left(\frac{c_{y_{пос}} V^2_{пос}}{0{,}9 \cdot 2g c_{y_{отр}} \bar{G}_{пос} L_{раз}} + f_{пр}\right). \tag{14.28}$$

Since $G_{p.p} = K_{p.p}\gamma_{en}P_0$, we have

$$\bar{G}_{л.у} = \frac{G_{л.у}}{G} = \frac{K_{л.у}\gamma_{зп}}{0,95}\left(\frac{V^2_{пос}c_{y_{пос}}}{0,9\cdot 2g\bar{G}_{пос}L_{раз}c_{y_{отр}}} + f_{пр}\right). \qquad (14.29)$$

It is permissible to assume in the first-approximation calculation that in cruising-altitude flight at $M_{cruise} = M^*_{cr}$, c_y is nearly equal to the cruising c_y and $K = 0.86K_{max}$. Then the engine must be throttled back to deliver a thrust $P_{cruise} = G/0.86K_{max}$ at the cruising altitude. We denote the degree of back-throttling of the TJE by κ_3: $(P_{cruise}/P'_{H_{cruise}} = \kappa_3)$. Since

$$P_0 = \frac{P'_{H_{крейс}}}{\varkappa_2} \text{ and } P'_{H_{крейс}} = \frac{P_{крейс}}{\varkappa_3} = \frac{G}{0,86K_{max}\varkappa_3}, \qquad (14.30)$$

we have $P_0 = \frac{G}{0,86K_{max}\varkappa_2\varkappa_3}$. Equating expressions (14.28) and (14.30) for P_0 to one another, we find that the back-throttling κ_3 for the thrust required to obtain the specified takeoff distance will be

$$\varkappa_3 = \frac{0,95}{0,86K_{max}\varkappa_2\left(\frac{V^2_{пос}}{2g0,9\bar{G}_{пос}L_{раз}c_{y_{отр}}} + f_{пр}\right)}. \qquad (14.31)$$

If the calculation of κ_3 gives a value larger than 0.80-0.85, this will mean that with the thrust chosen on the basis of takeoff-run conditions, the airplane will have too small a thrust margin under cruising-flight conditions, and its ceiling will be unacceptably close to the cruising altitude. In this case, the values of P_0 in (14.28) and $\eta_{p.p}$ in (14.29) must be increased by the factor by which the coefficient κ_3 obtained from (14.31) exceeds 0.8-0.85.

If κ_3 is found to be smaller than 0.5-0.6, specific fuel consumption may increase when the TJE is throttled so far back in cruising flight. It is recommended that the cruising altitude be raised in order to increase κ_3.

For transonic aircraft, it is recommended that the relative fuel consumption in climbing to cruising altitude and accelerating

to M_{cruise} be determined in the first-approximation calculation from expression (6.10), which did not take account of the fuel consumed to overcome frontal drag:

$$\bar{G}_{\text{т под}} = \frac{K_{\text{пол}} C_{\text{ух ср}} H_{\text{экон}}}{1800 a M_{\text{крейс}}}, \tag{14.32}$$

where

$$H_{\text{экон}} = \frac{a^2 M^2_{\text{крейс}}}{2g} + H_{\text{крейс}}, \quad K_{\text{пол}} = 0{,}8.$$

After a transformation similar to that made in deriving (14.6), we have

$$\bar{G}_{\text{т гор}} = (1 - G_{\text{т под}}) \left[1 - \frac{1}{e^{\frac{(L - L_{\text{сн}}) C_{\text{ух}}}{3{,}6 \cdot 0{,}86 K_{max} a M_{\text{крейс}}}}} \right], \tag{14.33}$$

where $L_{ds} = H_{e_{fin}} K_{max_{av}}$. In (14.33), $L - L_{ds}$ equals the sum of the distance flown in "cruising climb" and the distance covered in climbing. We disregard the fuel consumed during the descent. Having determined $\bar{G}_{p.p}$, $\bar{G}_{f_{clb}}$, and $\bar{G}_{f_{lvl}}$, we find that

$$G = \frac{G_{\text{п.н}}}{1 - \left[\bar{G}_{\text{к}} + \bar{G}_{\text{л.у}} + K_{\text{т.с}} \left(\bar{G}_{\text{т под}} + \bar{G}_{\text{т гор}}\right)\right]}. \tag{14.34}$$

Equations (14.25), (14.28), (14.29), (14.32), (14.33), and (14.34), form a system of six equations, which are written out below in the order in which they should be solved:

$$\bar{G}_{\text{л.у}} = \frac{K_{\text{л.у}} \gamma_{\text{л.с}}}{0{,}95} \left(\frac{V^2_{\text{пос}} c_{y_{\text{пос}}}}{1{,}8 g \bar{G}_{\text{пос}} L_{\text{раз}} c_{y_{\text{отр}}}} + f_{\text{пр}} \right); \qquad \text{I}$$

$$\bar{G}_{\text{т под}} = \frac{0{,}8 C_{\text{ух ср}} H_{\text{экон}}}{1800 a M_{\text{крейс}}}; \qquad \text{II}$$

$$\bar{G}_{\text{т гор}} = (1 - \bar{G}_{\text{т под}}) \left[1 - \frac{1}{e^{\frac{(L - L_{\text{сн}}) C_{\text{ух}}}{3{,}6 \cdot 0{,}86 K_{max} a M_{\text{крейс}}}}} \right]; \qquad \text{III}$$

$$G = \frac{G_{\text{п.н}}}{1 - \left[\bar{G}_{\text{к}} + \bar{G}_{\text{л.у}} + K_{\text{т.с}} \left(\bar{G}_{\text{т под}} + \bar{G}_{\text{т гор}}\right)\right]}; \qquad \text{IV}$$

$$S = \frac{16 \cdot 0.9 \bar{G}_{пос} G}{V_{пос}^2 c_{y_{пос}}}; \qquad \text{V}$$

$$P_0 = \frac{G}{0.95}\left(\frac{V_{пос}^2 c_{y_{пос}}}{1.8 g \bar{G}_{пос} L_{раз} c_{y_{отр}}} + f_{пр}\right). \qquad \text{VI}$$

The six unknowns in the above system of equations (I-VI) are $G_{p.p}$, $G_{f_{clb}}$, $G_{f_{lvl}}$, G, S, and P_0. The remaining quantities are either defined by the specifications for the airplane or to be assigned. If the engine has been selected prior to determination of the airplane's G and S, and P_0 has been assigned by the same token, Eq. (I) in the system (I-VI) assumes the form $\bar{G}_{p.p} = \gamma_{en} K_{p.p} P_0$, and Eq. (VI) is discarded. Solving the equation system (I-V) in sequence, we obtain the values of G and S; we then use (7.5) to calculate the airplane's takeoff distance. If it is longer than that required, it will be necessary either to increase P or to increase the maximum lift/drag ratio, or to increase $c_{y_{ldg}}$ and $c_{y_{l/o}}$. Given the thrust, it is also necessary to check the amount of back-throttling that will be required at cruising speed, at which the frontal drag is

$$Q_r = \frac{(1 - G_{т_{пос}}) G}{0.86 K_{max}} \text{ и } x_3 = \frac{Q_r}{P_{H_{крейс}}} = \frac{Q_r}{x_2 P_0}.$$

Having made the first-approximation determinations, of weight, wing area, and P_0 for the airplane, we can, assigning the wing aspect ratio and taper and calculating the fuselage dimensions on the basis of the load requirements, arrive at the first rough layout of the airplane and thus obtain starting data for calculation of $c_{x_{0_{wg.tl}}}$, the c_x and S_m of the fuselage and engine nacelles, and the relative weights of the wings, tail, and fuselage.

The first-approximation calculation should also be used to check whether fuel can be accommodated in the wing space, since not even part of the fuel can be accommodated in the fuselages

of many aircraft (cargo and passenger types).

The second-approximation calculation of the G, S, and P_0 of a transonic airplane will differ from the first approximation in the following respects: 1) instead of assigning values to the maximum lift/drag ratio, we shall calculate it. It will depend on wing area and aspect ratio;

2) the structural weight of the airplane will be determined by the weight formulas and will be a function of the wing's area and aspect ratio;

3) the ratio of the cruising-speed L/D to the maximum L/D will be obtained by calculation instead of setting it equal to $0.86K_{max}$.

The dependence of the airplane's $c_{x_{0_{wg.tl}}}$ on wing area can be taken into account with the expression

$$c_{x_0} = c_{x_{0\text{кр.оп}}} + \frac{\sum c_x S_м}{S}, \qquad (14.35)$$

where $\Sigma c_x S_m$ is the sum of the products of c_x by the fuselage and engine-nacelle midships-section areas.

For a transonic airplane,

$$c_{y_{\text{нам}}} = \sqrt{\pi\lambda_{\text{эф}} c_{x_0}}, \quad K_{max} = \frac{1}{2}\sqrt{\frac{\pi\lambda_{\text{эф}}}{c_{x_0}}}.$$

For assigned V_{ldg}, $c_{y_{ldg}}$, and $\bar{G}_{ldg} = G_{ldg}/G$, the weight of the airplane is

$$G = \frac{c_{y_{\text{пос}}} S V^2_{\text{пос}}}{16 \cdot 0{,}9 \bar{G}_{\text{пос}}}. \qquad (14.36)$$

At the beginning of cruising flight, the airplane weighs

$$G = \frac{0{,}5 V^2_{\text{крейс}}}{2} c_y S.$$

We introduce the nomenclature

$$\bar{c}_y = \frac{c_y}{c_{y_{\text{наив}}}},$$

and then find that

$$G = \frac{\varrho_H V^2_{\text{крейс}}}{2} \bar{c}_y c_{y_{\text{наив}}} S = \frac{\varrho_H V^2_{\text{крейс}}}{2} \bar{c}_y (\pi \lambda_{\text{эф}} c_{x_0})^{1/2} S.$$

Equating this expression for G to expression (14.36), we find that

$$\bar{c}_y = \frac{(1 - \bar{G}_{\text{топл}}) \varrho_0}{0{,}9 \bar{G}_{\text{топл}} \varrho_H} \frac{V^2_{\text{пос}}}{V^2_{\text{крейс}}} \frac{c_{y_{\text{пос}}}}{\sqrt{\pi \lambda_{\text{эф}} c_{x_0}}}. \tag{14.37}$$

Previously we obtained

$$\bar{K} = \frac{K}{K_{\max}} = \frac{2}{\bar{c}_y + \frac{1}{\bar{c}_y}}. \tag{14.38}$$

We determine the cruising lift/drag ratio from (14.37) and (14.38).

As in the first-approximation calculation, the relative weight of the powerplant and the engine thrust are determined with expressions (14.29) and (14.30). The relative weight of the fuel consumed in climbing is calculated from (14.32). The relative structural weight $\bar{G}_s$ of the airplane is found with the formulas given in §11.2.

Knowing $\bar{G}_{p.l}$, $\bar{G}_s$, $\bar{G}_{p.p}$, and $\bar{G}_{f_{clb}}$, we find the weight of the fuel consumed in level flight and in overcoming frontal drag during climbing and acceleration from the expression

$$\bar{G}_{\text{тор}} = \frac{1}{K_{\text{т.с}}} \left[1 - (\bar{G}_{\text{п.н}} + \bar{G}_{\text{к}} + \bar{G}_{\text{л.у}} + K_{\text{т.с}} \bar{G}_{\text{топл}})\right]. \tag{14.39}$$

The airplane's range

$$L = \frac{2{,}3 \cdot 3{,}6 a M_{\text{крейс}} \bar{K} (\pi \lambda_{\text{эф}})^{1/2}}{2 \cdot C_{\text{уд}} c_{x_0}^{1/2}} \lg \frac{1}{1 - \frac{\bar{G}_{\text{тор}}}{(1 - \bar{G}_{\text{топл}})}} + H_{\text{экон}} K_{\max}, \tag{14.40}$$

where

$$H_{\text{экон}} = \frac{a^2 M^2_{\text{крейс}}}{2g} + H_{\text{крейс}}.$$

Thus, we obtain the following system of ten equations for determination of G, S, and P_0:

$$c_{x_0} = c_{x_{0\text{кр.оп}}} + \frac{\sum c_x S_{\text{м}}}{S}; \qquad \text{I}$$

$$G = \frac{c_{y_{\text{пос}}} V^2 S}{16 \cdot 0{,}9 \bar{G}_{\text{пос}}}; \qquad \text{II}$$

$$\bar{G}_{\text{к}} = \bar{G}(S\lambda); \qquad \text{III}$$

$$\bar{G}_{\text{топл}} = \frac{0{,}8 C_{y_3} H_{\text{экон}}}{180 \Omega a M_{\text{крейс}}}; \qquad \text{IV}$$

$$\bar{G}_{\text{л.у}} = \frac{K_{\text{л.у}} \gamma_{\text{ан}}}{0{,}95} \left(\frac{V^2_{\text{пос}} c_{y_{\text{пос}}}}{1{,}8 g \bar{G}_{\text{пос}} L_{\text{раз}} c_{y_{\text{отр}}}} + f_{\text{гр}} \right); \qquad \text{V}$$

$$\bar{G}_{\text{топр}} = \frac{1}{K_{\text{т.с}}} \left[1 - (\bar{G}_{\text{п.н}} + \bar{G}_{\text{к}} + \bar{G}_{\text{л.у}} + K_{\text{т.с}} \bar{G}_{\text{топл}}) \right]; \qquad \text{VI}$$

$$\bar{c}_y = \frac{1 - \bar{G}_{\text{топл}}}{0{,}9 \bar{G}_{\text{пос}}} \frac{\varrho_0}{\varrho_H} \frac{V^2_{\text{пос}}}{V^2_{\text{крейс}}} \frac{c_{y_{\text{пос}}}}{\sqrt{\pi \lambda_{\text{эф}} c_{x_0}}}; \qquad \text{VII}$$

$$\bar{K} = \frac{2}{\bar{c}_y + \frac{1}{\bar{c}_y}}; \qquad \text{VIII}$$

$$L = \frac{2.3 \cdot 2{,}6 a M_{\text{крейс}} (\pi \lambda_{\text{эф}})^{1/2} \bar{K}}{2 C_{y_3} c_{x_0}^{1/2}} \lg \frac{1}{1 - \frac{\bar{G}_{\text{топр}}}{1 - \bar{G}_{\text{топл}}}} + H_{\text{экон}} K_{\max}; \qquad \text{IX}$$

$$P_0 = \frac{G}{0{,}95} \left(\frac{V^2_{\text{пос}} c_{y_{\text{пос}}}}{1{,}8 g \bar{G}_{\text{пос}} L_{\text{раз}} c_{y_{\text{отр}}}} + f_{\text{пр}} \right). \qquad \text{X}$$

There are 11 unknowns in the above equation system, namely: c_{x_0}, $\bar{c}_y$, $\bar{K}$, G, $\bar{G}_{p.p}$, $\bar{G}_{f_{lvl}}$, $\bar{G}_{f_{clb}}$, $\bar{G}_s$, P_0, S, and λ. We can therefore assign one unknown. We shall take the wing aspect ratio λ as this unknown.

We shall solve the equation system by assigning several wing areas S and determine the range L for each S. Plotting L, G, and P_0 as functions of S, we find the S, G, and P_0 for the required range. By solving the problem for several wing aspect ratios and plotting the airplane's weight as a function of λ, we find the

optimum wing aspect ratio.

The equation system given above enables us to vary the wing profile thickness and sweep angle. This will result in changes not only in G_s and K_{max}, but also in M^*_{cr} and, consequently, M_{cruise}. However, as we noted above, both the sweep angles and profile thicknesses of transonic aircraft in service vary in narrow ranges, and they can be selected quite reliably on the basis of statistics.

As in the first approximation, expression (14.31) should be used to check for the amount of back-throttling of the engine in flight at cruising speed.

Since the back-throttling in high-altitude flight at M_{cruise} has little influence on C_{sp}, the aspect ratio will approach closer to K_{max} and per-kilometer fuel consumption will decrease as $\bar{c}_y = c_y/c_{y_{opt}}$ moves closer to unity.

By increasing the cruising altitude, we increase $\bar{c}_y$ [see expression (14.37)], and thereby increase the lift/drag ratio. Increasing the cruising altitude to 11,000 meters lowers the value of C'_{sp} and thereby lowers per-kilometer fuel consumption. However, an increase in cruising altitude with no change in the selected P_0 will reduce the amount of back-throttling of the TJE (increase κ_3). Hence the optimum cruising altitude analysis must be performed with simultaneous use of (14.37) and (14.31). On a certain increase in cruising altitude, κ_3 may prove to be larger than 0.80-0.85. In this case, the thrust of the TJE will be determined not by the takeoff-distance requirement, but by the necessary compensation of frontal drag in cruising-altitude flight at M_{cruise}. A further increase in H_{cruise} will cause an increase in P_0 and, consequently, in $\bar{G}_{en}$ as well; this will lower $\bar{G}_f$. This must be taken into account.

It must be recognized that the airplane's ceiling will be raised by increasing wing aspect ratio. At a given cruising altitude, therefore, the larger γ, the smaller will be $\bar{c}_y = \bar{c}_y/c_{y_{opt}}$

in flight at $M = M_{q_{min}}$. This will reduce $\bar{K} = K/K_{max}$ and shorten the airplane's range. In arriving at the optimum wing aspect ratio, therefore, the cruising altitude should be raised when λ is increased. Since $c_{y_{opt}}$ is directly proportional to $\lambda^{1/2}$, the pressure at the cruising altitude must be inversely proportional to $\lambda^{1/2}$. Then an increase in λ with $M_{q_{min}}$ = const will not influence $\bar{c}_y$ (14.37). Since the aircraft weight and engine thrust do not appear in (14.37) and (14.31), the correctness of the cruising-altitude determination can be checked even before the final calculation of the airplane's G, S, and P_0.

For a transport airplane, the range may be stated for a constant altitude rather than for "cruising climb." In this case, the range computed by (IX) will be somewhat on the long side. Flight range is directly proportional to $\bar{K}/C_{sp}$. The fraction in (IX) was calculated for the beginning of cruising flight. At constant altitude and speed, c_y and, consequently, also $\bar{c}_y$ will have changed in proportion to the change in weight at the end of cruising flight. The $\bar{K}$ at the end of the flight is easily computed from (14.38). Knowing $\bar{K}$, we find $K = \bar{K}K_{max}$. We then determine the change in the back-throttling of the TJE at the end of flight. If C_{sp} is known as a function of back-throttling, its value at the end of the flight is easily calculated for determination of the change in the ratio C_{sp}/K during the flight. Taking the average C_{sp}/K and comparing it with the C_{sp}/K for the beginning of the flight, we determine the factor by which the constant-altitude flight range is smaller than the "cruising-climb" range.

§14.7. CONCLUSION

One of the results of preliminary design is the acquisition of initial data for further design work on the parts of the airframe and its subassemblies.

In the design work on the parts of the airplane and the components and subassemblies of the airframe in accordance with the stated requirements, it is necessary to make use of the appropriate

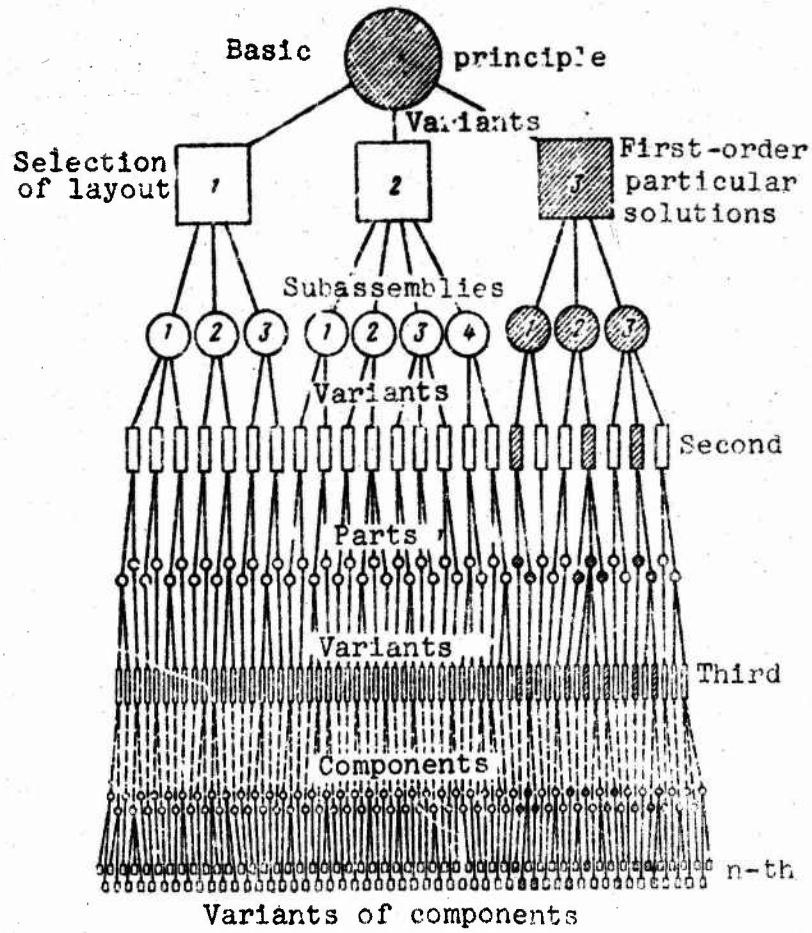

Figure 14.18. Diagram of designing process.

general criterion and to examine several variants.

It is necessary to use a system that reduces the number of variants analyzed. To achieve this, engineering design must also be carried out by the method of successive approximations, proceeding from the general to the particular and doing so in coordinated fashion, i.e., with consideration first of all of the basic factors and then of the secondary ones.

So that the best of the possible variants of the design will be among those analyzed, and so that this variant will be arrived

at by the shortest possible route, it is necessary to systematize the method of successive approximations more rigorously. The system of designs set forth below was proposed by Certified Engineers Bischof and Hansen of the nationalized firm Optik Carl Zeiss Jena [14].

The entire design process is broken up into a series of problems of successively increasing order (Fig. 14.18). The first-order problem is selection of the fundamental principle on which the new product will be based. Quite often, however, the fundamental principle has already been predetermined by the assignment itself.

Solution of this first problem is followed by the solution of second-order problems: selection of the layout, basic structure, and dimensions of each of the basic parts. There will be as many second-order problems as there are basic parts into which the product has been divided.

We then go on to solve third-order problems - selection of the layout, structure, and dimensions of the smaller parts of which the basic parts of the product consist. Then, proceeding in succession from the product as a whole to all of the smaller parts and finally to all elements and their interactions and combinations, we ultimately obtain all of the unknown parameters and the fully elaborated design.

If the variant of the design obtained at the end of this process is to be the best of all possible variants, it is necessary that each of the successively solved problems be solved correctly, or, more precisely, that the best of the possible solutions be found for each problem. To ensure correct solution of each particular problem, the designer must use his creative imagination to envisage and inspect all possible solutions. This is quite feasible for a particular problem, the more so since many solutions are rejected at once as clearly unsuitable. The remaining solutions are subjected to thorough analysis with the object of ascertaining all advantages and disadvantages of each solution.

This analysis is a highly important aspect of the designer's work; it is particularly important that all possible deficiencies of the design be analyzed. The designer must get into the habit of self-criticism, so that he will not become excessively enamored of a new and, at first glance, clever solution that he has thought up and so that all of its deficiencies will be brought out on time. This analytical work done, the synthetic, creative side of the job again comes to the fore. An attempt must be made to improve the solution variants of the particular part of the problem that remain to be compared, i.e., the designer must attempt to enhance desirable properties and eliminate or mitigate undesirable ones. He then proceeds to a selection of the optimum variant from among these improved variants.

The originators of this system propose that this selection be made with consideration of all the basic requirements made of the product, but do not combine them into a single general criterion. However, if there are contradictions inherent in the requirements, the choice will be somewhat subjective, and only the use of a criterion that combines these requirements will result in a fully objective choice of the optimum solution.

It often happens that our knowledge and theoretical calculations do not give a reliable notion of how the particular variant of the structure or element thereof will perform in reality. In these cases, experiment comes to the aid of the designer.

No particular problem can be solved in isolation, without consideration of the solutions of other problems. First of all, it is necessary to recognize the solutions already adopted for problems of earlier order, while solutions to problems of the same order must be arrived at simultaneously and jointly, with establishment of the optimum combinations of these solutions, i.e., the interaction and reciprocal effects of all elements of the design must be taken into account.

A $(k + 1)$-th-order problem is always related to the earlier k-th-order problem from which it stems, both as a part to its

whole and as an effect to its cause. The solution adopted for the k-th order problem becomes an assigned condition in solution of the problems of orders (k + 1), (k + 2), ... that stem from it. In essence, we shall use the method of reduction to equal conditions here, but in this case it is fully justified and does not divert the designer from the past to the optimum solution if the solutions obtained in the preceding steps were correct. As concerns the relation between problems of the same order: it may, in some cases, be very close, depending on the design and the design field, and may be manifested not only in the reciprocal effects between the parts of the design, but also directly at their contacts and in their combinations, while in other cases this relation may be more distant and may exist only through their totality.

The greater the number of such links for the particular problem, the more complex does its solution usually become.

It is convenient to choose the optimum solution for each problem by successive rejection of the clearly inferior ones, and, if a clearly optimal solution cannot be identified among those that remain, by subjecting them to evaluation with the aid of a criterion; however, this selection is sometimes made difficult by the fact that the remaining variants appear to be equivalent even after numerical evaluation. In these cases, it is necessary to elaborate the design variants more thoroughly, i.e., to move to solution of higher-order problems in all of these variants. This more profound elaboration permits more accurate comparison and a sounder choice. In this case, the solution of the k-th order problems is influenced by the solutions of problems of orders (k + 1), (k + 2), ...

Since not all properties of the product that influence the value of the general criterion, but only some of them, may change during solution of particular design problems of higher order, selection of the optimum solution variant to the particular problem can be based in these cases not on the entire expression for the general criterion, but only on its increment due to the

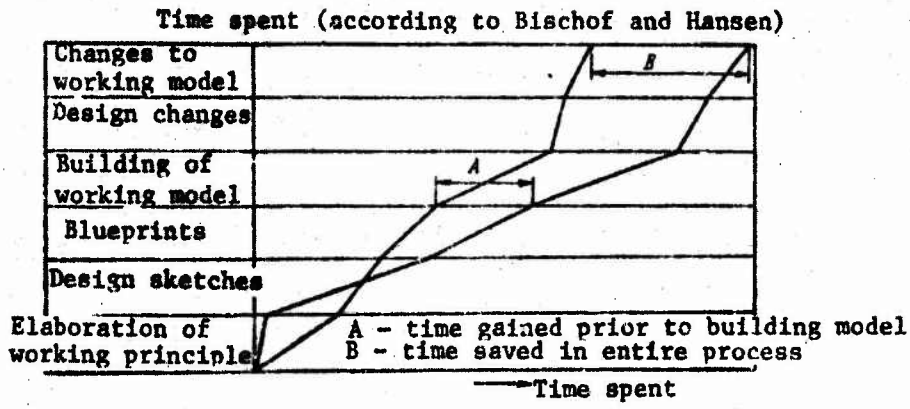

Figure 14.19. Two different design paths.

properties affected.

Thus, a whole system of indicators may be used in design work rather than a single general criterion, but all of them must be obtained from the general criterion and may be used only when they fully reflect the influence of the properties changed in the particular problem on the general criterion. Only in such cases will use of particular indicators be quite sound.

Thus, the need for coordinated solution of a given problem forces the designer to look ahead and inspect the solutions of higher-order problems before the final decision is adopted.

On the other hand, mismatches with solutions adopted previously come to light in solution of a given problem, and it is necessary to introduce certain corrections and refinements, chiefly of dimensional nature, into these previously adopted solutions. However, drastic revision of solutions taken during the early design steps cannot be permitted, since this will severely affect the scheduling and quality of the project. More attention and work should therefore be devoted to solution of first- and second-order problems. Figure 14.19 shows the path of the work on the design and debugging of two products of approximately equal

complexity. More careful elaboration of the design of one product at the initial stage resulted in a saving of time as compared with he other project.

Despite the large number of quantities that are varied during the design work, no major difficulties are encountered in use of a criterion for selection of the optimum variant at each step in the design process. The total value of the criterion is used in the first steps, but many of the quantities that appear in it are constant stated in the technical specifications, and many can be assumed approximately constant.

Supplementary conditions may consist of a series of assigned constant values of certain properties of the future product. However, those basic unknown variable quantities that have the strongest influence on the criterion are examined first. The equation system is used in engineering design to determine these unknown parameters and the value of the criterion itself. One of these equations expresses the criterion in terms of the specified properties and the unknown parameters. The remaining equations will express the required properties in terms of the same parameters. To solve a problem, it is necessary that the number of independent equations containing the unknown parameters not exceed the number of unknown quantities. If the number of unknowns equals the number of equations, we obtain a unique solution. If there are fewer equations than unknowns, we assign a series of successive values to each of the parameters and analyze their practically feasible combinations to find the optimum combination on the basis of the optimum criterion value.

Only some of the quantities are again varied at each of the successive steps, and it is sometimes possible to isolate for use as the criterion only that part of the criterion that depends on the properties varied in the particular case.

REFERENCES

1. Сахоров А. Н., Основные принципы проектирования и конструирования машин, Машгиз, 1929.
2. Кессельринг Ф., Учение о технической композиции, Берлин, изд. Шпрингер, 1934.
3. Стрелецкий Н. С., Гениев Н. А. и Балдин В. А., Курс металлических конструкций. Основы металлических конструкций, Гостехиздат, 1938.
4. Фадеев Н. Н., Изыскание рациональных размеров самолета, Труды ЦАГИ, вып. 461, 1939.
5. Фадеев Н. Н., Авиационный вес, Труды ЦАГИ, вып. 470, 1940.
6. Технологичность конструкции. Сборник статей под ред. С. Л. Ананьева, Москва, 1960.
7. Нечаев А. П., Психология технического изобретательства, М—Л, Госиздат, 1960.
8. Альтшуллер Г. С., Как научиться изобретать, Тамбов, Облгосиздат, 1961.
9. Гюльднер Г., Двигатели внутреннего сгорания, Машгиз, 1957.
10. Соболев Ю. М., Конструктивно-технологическая обработка деталей, Пермь, Облгосиздат, 1952.
11. Крылов А. Н., Мои воспоминания, изд-во АН СССР, 1945.
12. Шэнли Ф. Н., Анализ веса и прочности самолетных конструкций, Оборонгиз, 1957.
13. Экономическая эффективность капитальных вложений и новой техники. Сборник материалов конференции, Соцэгиз, М. 1959, стр. 603
14. Бишоф В. и Хансен Ф., Рациональное конструирование, Берлин, изд. Техника, 1953.
15. Фадеев Н. Н., Скорость и экономичность воздушного транспорта, «Техника воздушного флота», 1936, № 12.
16. Протодьяконов М. М., Условные характеристики топографических условий местности, исчисление эксплуатационных расходов и приложение их в экономике железных дорог, «Техника и экономика путей сообщения», 1924, № 3—10.
17. Бреге Л., Экономика воздушного транспорта, Aeronautical Engineering 5, № 3, 1933.
18. Белов П. А., Вопросы экономики в современной войне, М., Воениздат, 1951.
19. Вентцель Е. С. Введение в исследование операций, изд-во «Советское радио», 1964.
20. Томашевич Д. Л., Конструкция и экономика самолета, Оборонгиз, 1960.
21. Фадеев Н. Н., Теоретическая формула веса трапецевидного крыла, Труды МАИ, вып. 138, Оборонгиз, 1961.
22. Бадягин А. А., Оврицкий Е. А., Проектирование пассажирских самолетов с учетом экономики эксплуатации, «Машиностроение», 1964.
23. Кан С. Н., Свердлов И. А., Расчет самолета на прочность, Оборонгиз, 1958.
24. Шейнин В. М., Весовая и транспортная экономичность пассажирских самолетов, Оборонгиз, 1952.
25. Добровольский В. А., Эрлих Л. Б., Основные принципы конструирования современных машин, Машгиз, 1956.
26. Орлов П. И., Азбука конструирования, Оборонгиз, 1941.
27. Архангельский Г. И., Проектирование элементов конструкции самолетов, Оборонгиз, 1955.
28. Горощенко Б. Т., Аэродинамика скоростного самолета, Оборонгиз, 1948.
29. Горощенко Б. Т., Динамика полета самолета, Оборонгиз, 1951.
30. Егер С. М., Проектирование пассажирских реактивных самолетов, «Машиностроение», 1964.
31. Лебедев А. А., Чернобровкин Л. С., Динамика полета, Оборонгиз, 1962.
32. Склянский Ф. И., Управление сверхзвукового самолета, «Машиностроение», 1964.
33. Остославский И. В., Стражева И. В., Динамика полета, Устойчивость и управляемость летательных аппаратов, «Машиностроение», 1965.
34. Ферри А., Аэродинамика сверхзвуковых течений, М., Гостехиздат, 1953.
35. Шульженко М. Н., Конструкция самолетов, Оборонгиз, 1953

SYMBOL LIST

Russian	Typed	Meaning
ТУ	TS	Tech. Spec
ПОС	ldg	landing
ОТР	tko	takeoff
Р	b	breaking
ЭФ	ef	effective
Р	a	available
а·Д	a.c	aviation, component
ПР	red	reduced
ОПТ	opt	optimum
СР	av	average
ПР	en	enterprise
КОМ	com	commercial
Руб	rbl	rubles
ГОД	ton-yr	ton-year
Т-ЧаС	ton-h	ton-hour
З.П	sal	salary
ПаС	pas	passenger
	yr	year
С.П	a.p	aircraft pool
М-Ц	mo	month
Н.С	g.s	ground structures
Т-КМ	ton-km	ton-km
З	l	load
ПЛ	pl	payload
РеЙС	trip	trip
КРеЙС	cruise	cruise
В.П	t-l	takeoff-to-landing
С	a	aircraft
ДВ	en	engines
Т	f	fuel
ЭК	cw	crew

Russian	Typed	Meaning
Т.О	r.m	routine maintenance
АП	AP	airport
ЧаС / С-Т	h	hours/aircraft
РеМ	o'h	overhaul
КГ	kgf	kgf
ДВ	en	engine
УД	sp	specific
Ф	M	augmented maximum
НОМ	rtd	rated
РеЙС/С-М ГОД	trips/aircraft/yr	trips/a[illegible]c/year
КОП	kop	kopecks
ВР	N.B.	not defined
П	d	dry
ПР	lm	limiting
ТР	bf	buffeting
БАЛ	bal	balance
КР	cr	critical
Щ	f	flaps
КР	wg	wing
ОП	tl	tail
Ф	f	fuselage
М.Г	e.n	engine nacelles
П.Ф	a.f	area, fuselage
НаИБ	opt	optimum
Г	h	horizontal
В	w	wave
П	r	required
ЭК	ec	economy
ПРеД	lim	limiting
беЗ	w/o	without
ИЗб	exc	excess
ПОТ	clg	ceiling

Russian	Typed	Meaning
К	k	kinetic
П	p	potential
Э	e	energy
ПОД	clb	climb
КОН	fin	final
НаЧ	ini	initial
Наб	clb	climb
ИСХ	ini	initial
ГОР	lvl	level
СН	des	descent
ТеХ	tec	technical
ГР	cg	cargo
РаЗ	run	runup
ОТР	l/o	liftoff
Т	t	thrust
ВК	ci	cut-in
УС	bo	booster
ПР	ro	rollout
РеВ	rev	reversal
СеЧ	sec	section
Ц.Т	CG	center of gravity
Ш.Э	h.a	hinge, aileron
Э	a	aileron
Н	l	lower
В	u	upper
Деф	def	deformation
ПРИб	ind	indicated
В.О	v.t	vertical tail
Т	cg	center of gravity
Г.О	h.t	horizontal tail
БезГ.О	w/o h.t	without horizontal tail
З	l	locking
ЭВ	ev	elevon

Russian	Typed	Meaning
СТ	st	stabilizer
Р.В	ele	elevator
ОМыВ	wash	washed
П.Г.О	h.f.p	horizontal foreplane
Э	t	tailheavy
П	n	noseheavy
УД	sp	specific
Г	n	nose
П.КР	l.wg	leading edge, wing
К	e	end
В	el	elevator
МеХ	fl	flaps
ЗеМ	grd	ground
Р.Н	rud	rudder
Н	r	rudder
ИНТ	int	interference
С.У	p.p	powerplant
Т.В	s.r	solid of revolution
ВХ	in	intake
ГР	st	stores
В.П	f.l	forced landing
СбаЛаНС	trim	trim
МИД	mid	midships
П.Н	p.l	payload
К	s	structural
Д.У	p.p	powerplant
Т.С	f.s	fuel system
У	a	accessory
С	sy	system
Т.Р	f.c	fuel consumed
П.О	p.e	passenger equipment
Т	t	technical
Э.О	c.e	crew and equipment
П.Л	s.f	spar flanges

Russian	Typed	Meaning
СТ.Л	s.w	spar webs
П.НвР	r.f	rib flanges
СТ.НвР	r.w	rib webs
Об	sk	skin
Э.М	a.f	ailerons and flaps
ГР	ld	load
В	b	b
С	c	c
б	t	tanks
М	f	flaps
Р	c	calculated
С	st	stringer
ПР.Н	cts	carry-through structure
Н	n	nose
К	r	root
ХВ	tl	tail
ПР.Н.ШП	cts-bh	carry-through structure, bh
ШП	bh	bulkhead
Г.Об	p.sk	pressurized skin
ДН	ew	end wall
СР	sh	shear
КРУЧ	tors	torsional
КРИТ	crit	critical
НГ	up	unpressurized
ГР.Ф	ld.f	loads and fuselage
Об.Г	sk.p	skin, pressurized
Г	p	pressurized
ФОН	can	canopy
ОК	wd	windows
ДВ	dr	door
ПОЛ	flr	floor
СОЧЛ	assy	assembly
Ш	g	gear
УПР	ctl	control
П.УПР	ctl.s	control station

Russian	Typed	Meaning
КОН	fin	final
а	a	atmospheric
у	a	accessories
ПОЛ	pay	payload
КР	cr	cruising
КОНЦ	tip	tip
КОРН	root	root
М.Ф	m.f	midships, fuselage
О	g	general
М	l	local
ГР	ld	load
Т	t	turbulent
ПеР	int	interception
Ц	tg	target
П.Н	p.l	payload
ВЗЛ	t/o	takeoff
Ш	g	(landing) gear